THE DEVELOPMENT OF TRIP COVERAGE MAPS FOR THE MCMASTER NUCLEAR REACTOR

THE DEVELOPMENT OF TRIP COVERAGE MAPS FOR THE MCMASTER NUCLEAR REACTOR

By

K.J.L. STOLL, B.Eng.

A Thesis

Submitted to the School of Graduate Studies

in Partial Fulfillment of the Requirements

for the Degree

Master of Applied Science

McMaster University

MASTER OF APPLIED SCIENCE (2009)
(Engineering Physics)

McMaster University
Hamilton, Ontario, Canada

TITLE: The Development of Trip Coverage Maps for the McMaster Nuclear Reactor.

AUTHOR: K.J.L. Stoll, B.Eng.

SUPERVISORS: Dr. J.C. Luxat, Dr. S.E. Day.

NUMBER OF PAGES: viii, 159

Abstract

Trip coverage maps indicate the reactor conditions under which instrument devices, manual scrams or passive safety systems are capable of arresting reactor transients initiated by specified postulated accidents before reaching safety boundaries. Trip maps are developed by simulating reactor transients with appropriate codes such as the PARET/ANL code. PARET/ANL has been validated against SPERT transient data with favorable results and is particularly suited for research reactor simulation of MTR reactors like the McMaster Nuclear Reactor (MNR).

A conservative PARET/ANL model of MNR has been developed by considering the characteristics and operating limits of the MNR core. Conservative conditions of accident scenarios were adopted and PARET/ANL was used to simulate these conditions in MNR. During these PARET power excursion simulations the MNR engineered safety system responses to loss of regulation rod control, sample handling and fuel handling accident scenarios were assessed and trip coverage maps were developed for each accident category. Forced convection and natural convection reactor conditions were considered.

The PARET/ANL model of MNR predicts at least one engineered safety system is capable of arresting transients initiated from high power conditions ($0.1 - 5.0\,MW$) in all the accident scenarios considered, before the onset of bulk boiling. The model predicts at least one system prevents transients from reaching these thermal limits during transients initiated from low power conditions ($<0.1\,MW$) during loss of regulation rod control events. The withdrawal of SSR from low power conditions induce transients which may progress to bulk boiling in the hottest fuel channel. Fuel handling accident induced transients from a shutdown state are predicted to be arrested by the $<3.8\,s$ period scram and both 125% high flux scram instrument channels before thermal limits are reached.

Table of Contents

Table of Figures

1 Introduction

Operated by McMaster University, the McMaster Nuclear Reactor (MNR) is an open-pool materials testing reactor (MTR type). MNR is used for academic research and instruction, as well as for commercial activities such as the production of radioisotopes, neutron activation analysis and neutron radiography. MTR-type reactors are operated in many countries for purposes almost identical to those of McMaster.

1.1 McMaster Nuclear Reactor

The reactor was designed by AMF Atomics (Canada) Ltd. and first went critical in 1959. MNR was granted its first operating license by the Atomic Energy Control Board (AECB), and has operated continuously since then under licenses granted by either the AECB or its successor the Canadian Nuclear Safety Commission (CNSC).

MNR was originally operated at 1 *MW* until 1964 and generally at 2 *MW* thereafter. During Chalk River's NRU shutdown period in the early seventies, MNR was used as the backup Mo-99 production reactor and operated at 5 *MW* [Sec.01,3]. Currently MNR operates at 3 *MW* Monday through Friday, sixteen hours a day, with the operators on two eight hour shifts [Sec.01,3].

The reactor was originally designed to operate with highly enriched uranium (HEU), however, as part of the global effort to convert research reactors to low enriched uranium (LEU) MNR completed a fuel conversion, and on April 30, 2007 used the last of the HEU fuel assemblies.

1.1.1 Core

MTR fuel can be used in a variety of reactor configurations. The McMaster MTR design is of the pool type, meaning the core is submerged in a pool of de-mineralized light water; the pool water serves as coolant, a biological shield and as a neutron moderator.

The MTR fuel assemblies are shown stylistically in Figure 1. The fuel assemblies stand vertically when assembled in the core on the 9x6 grid plate (as shown in Figure 2). Water from the pool is forced through the top of the assemblies, through the fuel assemblies and over the fuel plates to the outlet; the outlet is the cylindrical bottom end fitting (BEF) (shown on the left in Figure 1).

The fuel assemblies currently used in MNR contain eighteen plates (center Figure 1), the inner sixteen plates contain uranium fuel; the outer two plates are made of only aluminum and are referred to as dummy plates. The control fuel (right Figure 1) assemblies have the same outer dimensions as a standard assembly but also have an allowance in their centre for the penetration of a neutron absorbing control rod. All nine of the plates in a control fuel assembly contain fuel.

The core is assembled by placing the bottom end fittings of the fuel assemblies into mating holes in the rectangular grid plate, as shown on the left in Figure 2. The grid plate contains 54 of these holes which accept either fuel assemblies or other core components such as the graphite reflector blocks or the antimony-beryllium neutron source. Any of these large holes left unused are plugged to prevent pool water flow from bypassing the coolant channels between fuel plates.

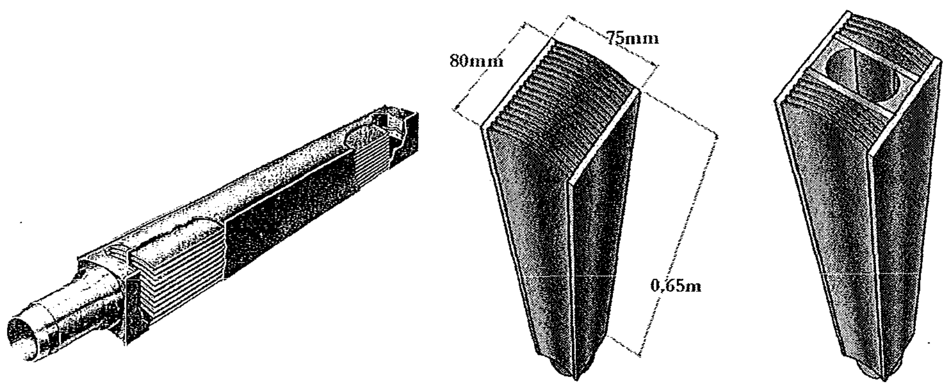

Figure 1. (L) Profile Cutaway View of Fuel Assembly Showing Cylindrical Bottom End Fitting (C) Top View of Standard Fuel Assembly (R) Top View of Control Fuel Assembly

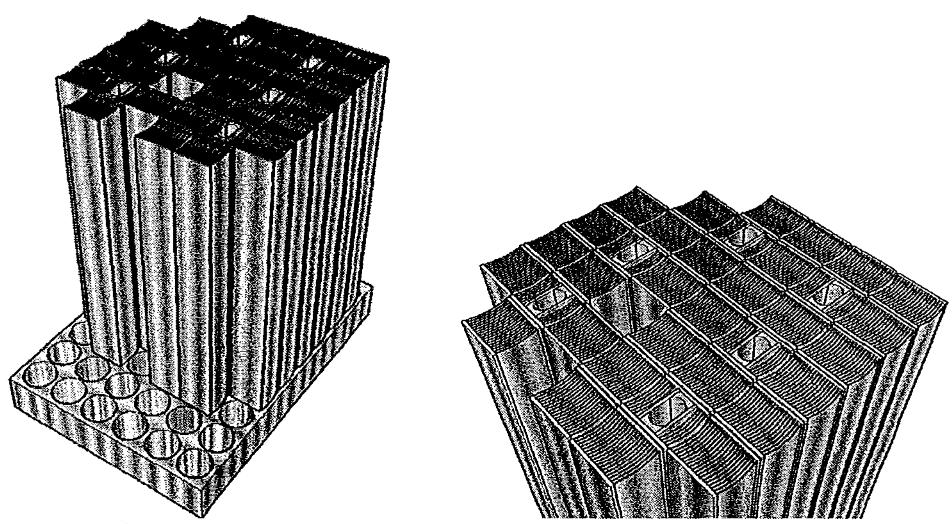

Figure 2. (L) Standard and Control Fuel Assemblies in a Core Arrangement on (R) Top of Core View

MNR is controlled by six metallic neutron absorber rods housed in six control fuel assemblies. These rods protrude into the control assemblies from above the core. The vertical position of all six control rods is set by electric linear actuators. Five manually controlled rods are Cd-In-Ag shim/safety rods (SSR) used for coarse power adjustment and for rapid gravity-drop safety insertions and can be gang operated. The sixth control rod is a stainless steel regulating rod, whose position is actively adjusted by the control system to finely maintain reactor power settings.

During refueling, a small number of fresh fuel assemblies are exchanged for end-of-life assemblies, and the core at any given time is composed of assemblies in various life stages. As fuel assemblies reach their end-of-life they are removed and the remaining assemblies are shuffled to obtain optimum burnup and to satisfy operational requirements. The core arrangement and number of components may change slightly during a fuel change. The manipulation of the fuel assemblies and other core components is done manually with a long tool which allows the operator to reach the core from a bridge spanning the reactor pool, directly above the core.

Each fuel plate in the standard and control fuel assemblies is fabricated by sandwiching the uranium-aluminum fuel meat between two thin aluminum cladding plates. The fuel meat is $0.51\,mm$ thick and composed of U_3Si_2 in an aluminum matrix [Table5-3,3]. The aluminum cladding is $0.38\,mm$ thick, and the assembled fuel plate's total width is $1.27\,mm$. The coolant channel between the plates is nominally $3\,mm$ wide. Each fuel plate is slightly curved to control the direction of thermal expansion. Each LEU standard fuel assembly contains $225\,g$ of U235 [Table5-3,3].

Graphite reflector assemblies are placed in the grid plate holes on the core's south face to reflect neutrons back into the core. Each graphite reflector contains a receptacle for the placement of samples which are to be irradiated with thermalized neutrons. The core also contains a central flux trap (a vacant grid plate location surrounded by fuel assemblies), a Beryllium/Antimony-124 neutron source and a number of vacant grid plate locations on the south side of the core. The east and north sides of the reactor do not have engineered reflection devices but instead have neutron beam tubes adjacent to the core.

1.1.2 Cooling

As discussed above, the coolant flows from the pool, between the fuel plates, along the coolant channel, through the BEF and to below the grid plate. Below the grid plate is a plenum which collects the flow from all the individual core assemblies attached to the grid plate. The plenum is essentially a box with the grid plate as its top. Flow continues from the plenum bottom to a single line through the bottom of the reactor pool to the holdup tank. A schematic of the primary loop is shown in Figure 3.

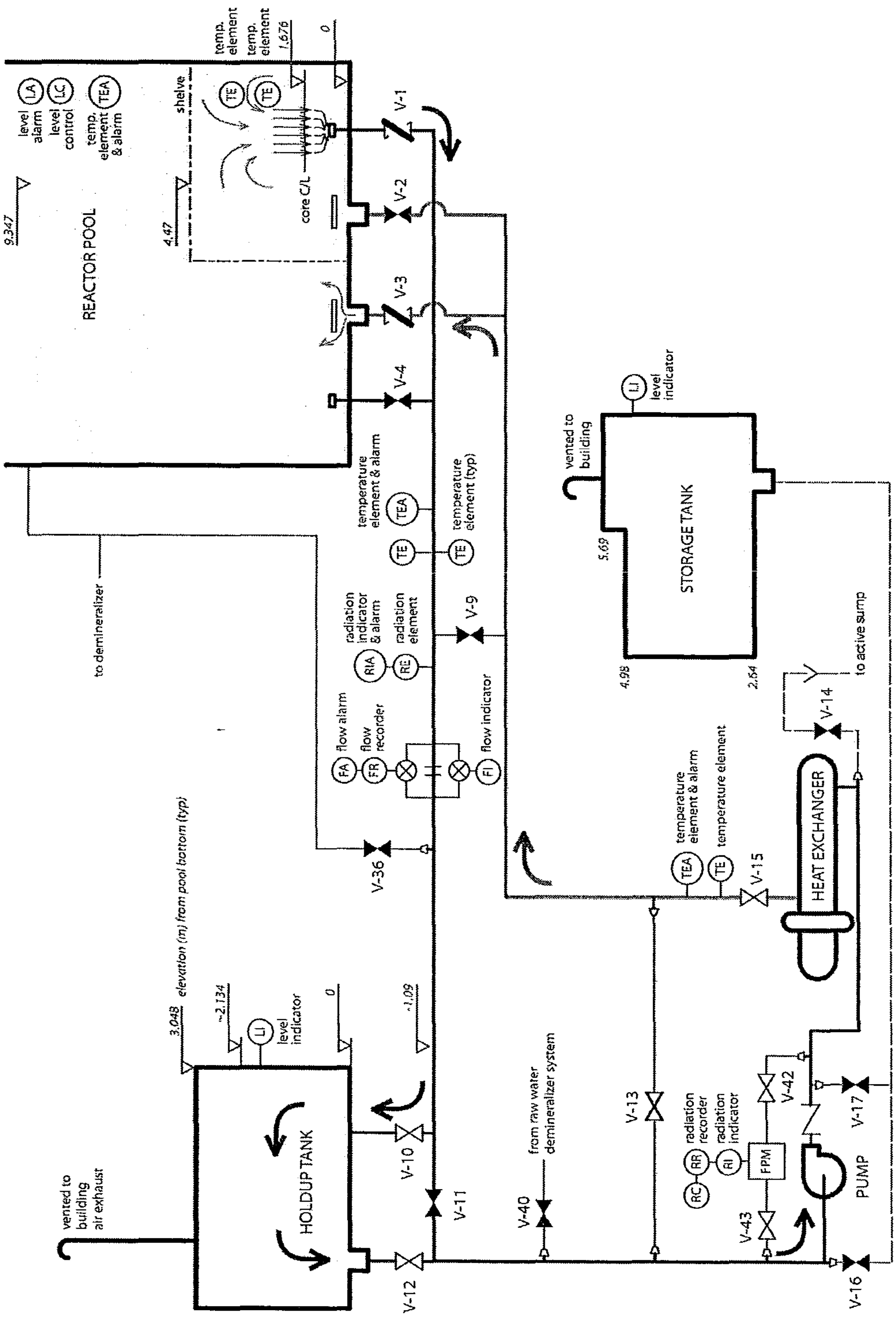

Figure 3. MNR Primary Circuit Cooling System [Fig.3-1,15]

The hold-up tank is a coolant reservoir where the hold-up time is appropriate for the majority of nitrogen-16 (which has a half life of $7.13\,s$) to decay [33]. Nitrogen-16 is produced when an oxygen atom absorbs a neutron while passing through the reactor core.

The coolant is drawn by a pump from the holdup tank, through a water-to-water heat exchanger and a filter before being returned to the reactor pool. The energy removed from the heat exchanger is circulated through a secondary loop to a water-to-air cooling tower, which rejects the heat energy to the reactor's ultimate heat sink, the atmosphere.

Under high power conditions ($>100\,kW$) the pool water flows through the cooling circuit as described above. The pool water flows through the core and into the hold up tank as a result of static head between the reactor pool and hold up tank.

In addition to the 54 large holes in the grid plate, there are also 40 smaller bypass holes (not shown in Figure 2). All 54 large holes are to be either occupied by an assembly of some kind or plugged, but the small holes are allowed to be open to cool the outside surface of control fuel assemblies. The outer plates of a control fuel assembly contain a heat source and opening bypass holes adjacent to the control assemblies produces flow along these outer surfaces.

Under low power operating conditions, the core is allowed to be cooled by natural convection of the pool water. Under natural convection flow, a flapper valve on the side of the plenum is opened. This open valve allows buoyancy induced flow to draw pool water into the plenum and travel up through the coolant channels inside the fuel assemblies, exiting the top of the fuel assemblies.

1.1.3 Engineered Safety Systems

Instrument engineered safety systems refer to a set of electrical instruments designed to monitor a single reactor operating condition and respond to prevent the reactor from operating outside the safe operating envelope. Engineered safety systems usually consist of a measuring device such as a neutron flux monitoring ion chamber or a reactor coolant flow meter, which feeds a signal to an instrument channel capable of initiating a power arresting device such as a shutdown rod. Engineered safety systems are often colloquially named shutdown systems, safety systems or referred to by the reactor condition their instrument channel monitors, such as high power trip, high rate trip, or coolant flow trip.

These safety systems can be designed in the same manner, use the same components and look identical to reactor control systems but are not used for normal reactor operation; safety systems are separate from reactor control systems and are reserved specifically for events which push reactor conditions beyond the capability of the normal control systems (one exception in MNR's case is the SSR bank which is used for both control and for emergency shutdown).

MNR has multiple, separate instrumentation systems which can initiate reverses, scrams and inhibitions [Sec.8,3]. A reverse is the act of driving the SSR bank into the core, a scram is the dropping of the SSR bank into the core and an inhibition disallows the SSR bank drive the ability to withdraw. The following is a summary of MNR's reactor safety instruments pertaining to reactor power transient safety:

Linear Neutron Channel (Lin N)

On automatic control settings, the Lin N channel controls reactor power by constantly adjust the regulating rod position; it is capable of controlling power in all design ranges [Sec.8.4.1,3]. A current signal proportional to neutron flux is supplied by a compensated ion chamber (CIC) located to the north and slightly above the reactor core [Sec.8,3]. The height of the CIC can be moved closer to the core by the operators to obtain a stronger signal; practice is to leave it far from the core in a location capable of generating a useable signal so as to not subject the chamber to huge radiation fields.

In the automatic control setting, the Lin N channel can initiate a reverse at +7% large servo error (LSE); this trip is a power trip, meaning there is a maximum allowable reactor neutron flux (a ceiling, so to speak) above which, the instrument will signal a trip [Sec.8.3.3.1,3].

Startup Channel (SUC)

The startup channel monitors and controls reactor power in the source power range [Sec.8.2.1,3]. It is the only instrument channel other than the Log N channel capable of measuring the magnitude of the neutron flux at extremely low powers. The SUC is able to monitor small fluxes because its signal is generated by a fission chamber using HEU. The fission chamber is positioned near the core during its use, and is removed from the flux once the reactor is at power, and after control has been transferred to the Log N channel [34].

The SUC can signal a $<30\,s$ period inhibition and a $<10\,s$ period reverse but is only effective at extremely low power ranges [Sec.8.2.1,3].

Logarithmic Neutron Channel (Log N)

The Log N channel uses a CIC just as the Lin N channel does, and is also capable of monitoring neutron power in all ranges [Sec.8.2.2,3]. Log N is not used for reactor control, but is capable of initiating four trips: $<30\,s$ period inhibition, $<10\,s$ period reverse, $<3.8\,s$ period scram and a 110% high flux (HF) reverse [Table8-1,3]. The three period trips are considered rate trips, meaning the signal is monitored for large changes in neutron flux, and the HF trip is a power trip.

Safety Channels

There are two uncompensated ion chambers (UIC) suspended above the core providing a neutron flux signal for these channels [Sec.8.2.3,3]. Each channel is identical, and each is set to scram at 125% HF [Table8-1,3]. These channels are not used for control, are effective only at high powers and are power trips [Sec.8.2.3,3].

Manual Scrams and Control

If at any point the reactor operators observe unusual reactor behavior, they are encouraged to induce a manual scram before investigating abnormal events; unlike a power reactor there is little cost associated with an MNR scram, nor are there concerns about electrical grid stability [Sec.16.1.5.1.1,3].

The positions of the five SSR are set manually. The control room has independent position switches for each rod, but all five rods can be driven simultaneously in gang control while the reactor is in either the manual or automatic control [34].

Low Flow Trips

The reactor will scram if total core flow (measured at flow instrument F1 shown Figure 3) is measured to be less than its set point [Sec.8.3.2.3,3]. This scram is not effective when the Log N channel measures less than 2% of set operating power [Sec.8.3.2.3,3].

1.2 PARET Software

To gain understanding of the relationships between various physical processes that occur during a reactor accident and to aid in predicting the course of nondestructive accidents in small cores, the U.S. Atomic Energy Commission conducted the Special Power Excursion Reactor Tests (SPERT) [Pg.iv,5]. The SPERT program investigated transients of various severities in small reactor cores. During the SPERT project, the computer code PARET was developed in an attempt to simulate and predict reactor power transients by summarizing a reactor's physical processes.

PARET is an acronym for: Program for the Analysis of Reactor Transients [8]. The code is a coupled point-kinetics and thermalhydraulics code which now contains a light-water properties library in the appropriate pressure and temperature ranges for simulating MNR operation – originally PARET did not have such a library and was suited to higher pressures and temperatures [4]. The PARET model contains heat transfer, continuous reactivity feedback and hydraulic calculations and employs various empirical convective heat transfer correlations.

PARET represents a core by modeling a small number of representative fuel plates and their adjacent coolant channels. The representative regions are weighted in a manner that predicts the behavior of the entire reactor core. Transients can be dictated by specifying the reactor power at all times throughout the transient or by dictating the reactivity insertion at all times and letting the program calculate the total power itself. Loss of coolant simulations can also be executed.

1.2.1 Point Kinetics

PARET uses the point kinetics equations to determine reactor power, and allows for up to 15 groups of delayed neutron data [20]. If total reactor power is dictated by the PARET user the point kinetics equations are not used, but for most transients the user inserts reactivity from an external source and PARET adds this reactivity to reactivity contributions from feedback effects, and then calculates total power with the following equations [5]:

$$\frac{d\phi(t)}{dt} = \frac{[\rho(t)-\beta]}{\Lambda}\phi(t) + \sum_{i=1}^{I}\lambda_i C_i(t) + S(t)$$ **Equation 1**

$$\frac{dC_i(t)}{dt} = \frac{\beta f_i}{\Lambda}\phi(t) - \lambda_i C_i(t)$$ **Equation 2**

for $i = 1, 2, \ldots, I$

where t = time

$\phi(t)$ = reactor power as a function of time

$\rho(t)$ = reactivity of the system as a function of time

β = effective delayed neutron fraction

Λ = prompt neutron generation time

λ_i = decay constant for group i

C_i = concentration of delayed neutron precursors of group i

f_i = fraction of delayed neutrons of group I, β_i/β

1.2.2 Thermalhydraulics

The hydraulic solution for coolant flow in the coolant channel gap between fuel plates is governed by what is called the modified momentum integrated model. This model makes use of the following conservation of energy, mass and momentum equations [5]:

$$\rho''\frac{\partial E}{\partial t} + G\frac{\partial E}{\partial z} = q$$ **Equation 3**

$$\frac{\partial \bar{\rho}}{\partial t} = -\frac{\partial G}{\partial z}$$ **Equation 4**

$$\frac{\partial G}{\partial t}+\frac{\partial}{\partial z}\left(\frac{G^2}{\rho'}\right)=-\frac{\partial P}{\partial z}-\left(\frac{f}{\rho}\right)\left(\frac{|G|G}{2D_e}\right)-\overline{\rho}g$$ **Equation 5**

where G = mass flow rate
P = pressure
E = enthalpy
f = friction factor
D_e = equivalent hydraulic diameter
g = gravitational acceleration
q = heat source rate per unit volume
L= coolant channel length

PARET evaluates coolant density as a function of local pressure and temperature and all other coolant properties with temperature and a user defined reference pressure; this is a method of the momentum integrated model. The conservation of momentum equation uses a channel averaged coolant mass flow rate [20]:

$$\overline{G}=\frac{1}{L}\int_0^L G\,dz$$ **Equation 6**

And average density, momentum density and slip flow density is given by [20]:

$$\overline{\rho}=\rho_l(1-\alpha)+\rho_v\alpha$$ **Equation 7**

$$\frac{1}{\rho'}=\frac{(1-\chi)^2}{\rho_l(1-\alpha)}+\frac{\chi^2}{(\rho_v\alpha)}$$ **Equation 8**

$$\rho''=[\rho_l\chi+\rho_v(1-\chi)]\frac{\partial\alpha}{\partial\chi}$$ **Equation 9**

where $\overline{\rho}$ = average density
ρ' = momentum density
ρ'' = slip flow density
χ = vapor weight fraction (quality)
α = vapor volume fraction (void fraction)

The PARET heat transfer model is based upon a one-dimensional conduction solution which restricts heat conduction to only through the cladding and into the coolant channel; axial heat conduction along the fuel plate length is not considered. Since all the heat generated in the PARET model is assumed to travel across the clad/coolant interface, an essential part of the heat conduction solution is the determination of the convective heat transfer coefficient.

PARET has been equipped with thermalhydraulic correlations for determining the heat transfer coefficients in each heat transfer regime: natural convection, single phase forced convection, nucleate boiling and transient film boiling. The specific correlations will be discussed later, but the scheme used for determining which type of boiling heat transfer regime prevails at any given time and axial node is as follows [5]:

i) If clad surface is at temperatures less than the fluid saturation temperature, it is assumed the non-boiling regime exists.

ii) When the clad surface temperature, as calculated on the basis of non-boiling conditions, exceeds the fluid saturation temperature, surface heat fluxes are calculated for both the non-boiling and nucleate boiling boundary conditions. If the nucleate boiling heat flux is greater than the forced convection heat flux, nucleate boiling is assumed to prevail; if vice versa, forced convection is assumed to prevail.

iii) If the nucleate boiling heat flux exceeds the departure from nucleate boiling (DNB) heat flux, the possibility of being in either transition or stable film boiling is considered. A clad surface temperature at departure from transition boiling is then calculated by equating the film boiling and transition boiling surface heat fluxes and solving for the surface temperature. If the surface temperature calculated on the basis of the film boiling boundary condition is greater than the one first calculated, film boiling is assumed to prevail. Otherwise, it is assumed that transition boiling exists.

iv) Saturated boiling can occur only for fluid enthalpies greater than the saturated liquid enthalpy.

v) The vapor regime exists only for fluid enthalpies equal to, or greater than the saturated vapor enthalpy.

The above algorithm requires boundary conditions to be used in conjunction with the correlations, the PARET logic is as follows [5]:

i) Nucleate boiling boundary conditions:

$$T_s > T_{sat}$$

$$q''_{DNB} > q''_{NB} > q''_{FC}$$

ii) Transition boiling boundary conditions:

$$q''_{TB} = q''_{DNB} - K_{TB}[T_s - (T_s)_{DNB}]$$
$$q''_{TB} < q''_{DNB}$$
$$T_s < (T_s)_{DTB}$$

iii) Film boiling boundary conditions:

$$q''_{FB} = h[T_s - T_{sat}]$$
$$T_s > (T_s)_{DTB}$$

iv) Superheat boundary conditions:

$$q''_{SH} = h[T_s - T_b]$$
$$H > H_g$$

where T_s = clad surface temperature

T_b = bulk coolant temperature

T_{sat} = fluid saturation temperature

$(T_s)_{sat}$ = clad surface temperature at saturation coolant conditions

$(T_s)_{DNB}$ = clad surface temperature at departure from nucleate boiling

$(T_s)_{DTB}$ = clad surface temperature at departure from transition boiling

H_g = enthalpy of the saturated vapor

K_{TB} = a constant

q'' = heat flux at clad coolant interface

Originally PARET was equipped with a limited number of correlations. To make PARET more capable, research reactor appropriate correlations were added by Woodruff; these updated correlations, used for MNR simulations, are discussed later [20]. However, the original DNB correlation is still appropriate for MNR use and has two forms depending upon the regime about to be departed. For departure from subcooled nucleate boiling it is of the form [Pg.22,5]:

$$q_{DNB} = \left(0.23x10^6 + 0.094G\right)\left[3.0 + 0.01\left(T_{sat} - T_b\right)\right]\left[0.435 + 1.23\exp(-0.0093\, L/D_e)\right]$$

$$\left[1.7 - 1.4\exp(-a)\right] \qquad \textbf{Equation 10}$$

where

$$a = 0.532\left[\frac{H_f - H_i}{H_{fg}}\right]^{3/4}\left(\frac{\rho_f}{\rho_g}\right)^{1/3} \qquad \textbf{Equation 11}$$

For departure from saturated boiling conditions it is of the form [Pg.22,5]:

$$\Delta H_{DNB} = 0.529\left(H_f - H_I\right) + \left(0.825 + 2.36\exp\left(-204 \cdot D_e\right)\right)\left(H_{fg}\right)\exp\left[\frac{-1.5G}{10^6}\right]$$
$$-0.41H_{fg}\exp\left[-0.0048\frac{L}{D_e}\right] - 1.12H_{fg}\left(\frac{\rho_g}{\rho_f}\right) + 0.548H_{fg} \qquad \textbf{Equation 12}$$

where H_f = enthalpy of the saturated fluid

ρ_f = density of saturated fluid

H_g = enthalpy of the saturated vapor

ρ_g = density of saturated vapor

H_I = enthalpy of the inlet fluid

$H_{fg} = H_g - H_f$

G = mass flow rate

L = total coolant channel length (sum of the fuelled and non-fuelled lengths)

1.3 Literature Review

1.3.1 Woodruff, A Kinetic and Thermal-Hydraulics Capability for the Analysis of Research Reactors

The Reduced Enrichment for Research and Test Reactor (RERTR) program was started by the US Department of Energy to develop technology helpful for the conversion of civilian reactors from HEU to LEU in 1978 [37]. Argonne National Laboratories (ANL) modified PARET and made it capable of simulating research reactors; the RERTR program now supplies PARET to those who conduct analysis of research reactors.

Woodruff published a paper which discusses the modifications made to PARET, compares PARET simulations with SPERT-I transients and discusses the results of PARET transient simulations based upon models of the International Atomic Energy Agency 10 *MW* benchmark LEU and HEU cores [20]. A summary of this publication is described below along with a discussion of the correlations Woodruff recommends for use with PARET simulations; the appropriate correlations are adopted for PARET analysis of MNR.

The modifications ANL made to PARET include a number of flow instability and departure from nucleate boiling (DNB) correlations which are more suitable to pressures and temperatures found in many research reactors than were the original PARET correlations.

PARET's voiding model, updated for subcooled boiling capacity, is of the form [Pg.200,20]:

$$\frac{\partial \alpha}{\partial t} = \lambda K(q'')^n - \frac{\alpha}{\tau} - Cv\frac{\partial \alpha}{\partial z} \qquad \textbf{Equation 13}$$

where α = void fraction at axial location z and time t

λ = fraction of the surface heat flux producing voids

K = constant at a given operating pressure

q'' = heat flux at axial location z and time t

n = source exponent

τ = bubble lifetime, s

C = flow distribution parameter

v = flow velocity of the coolant, m/s

The local fluid density contained within the coolant channel is affected by the creation of vapor at the clad surface. Woodruff obtained this voiding model from an internal Idaho National Lab (INL) document and evaluates the sensitivity of parameters λ, n, τ and C [39,20].

Woodruff found these parameters to affect the fuel energy release to the coolant. The bubble lifetime, τ, for nucleate boiling is recommended to be $0.0005\,s$ [Pg.202,20]. Alternatively, the manual for PARET V7.4 recommends using $0.001\,s$ but bases this recommendation upon the higher pressure and temperatures of SPERT-III tests [Pg.200,20]. The transition boiling bubble lifetime is recommended to be $0.001\,s$ [Pg.202,20]. Notice the recommended transition boiling bubble lifetime is larger than is recommended for nucleate boiling; bubble lifetime "should range from $100\,\mu s$ for highly subcooled regions where bubble collapse is rapid to an infinite value with bubbly flow [Pg.200,20]."

The parameter C is recommended to be 0.8 "for highly subcooled regions where bubbles do not detach from the surface but move at ~80% of the coolant velocity along the clad surface [20]." Woodruff later states the model is insensitive to varying C values [Pg.201,20].

PARET users need to estimate the fraction of the surface heat flux producing voids, λ, for both nucleate and transition boiling; this is a parameter which was found to affect clad temperatures [20]. The higher pressure and temperature SPERT-III tests recommended values of 0.05 which Woodruff found appropriate for transition boiling and decided upon 0.03 for nucleate boiling [Pg.202,20].

Woodruff suspected PARET's original single phase heat transfer model was inadequate, so Rosenthal and Miller's correlation was added as an option to the original [Pg.200,20]:

$$h = \sqrt{\frac{k\rho c_p}{T}}$$ **Equation 14**

where T = period of the power rise or e-folding time.

This correlation was developed specifically for MTR transient analysis and is based upon empirical data obtained by heating vertical metal ribbons electrically in a pool of water [38]. The heat generated in the ribbons simulated reactor excursions with periods between 5 and 75 *ms* and the pool temperature, under atmospheric pressure, was varied between $90\,^oF$ and boiling, simulating normal MTR pool conditions; the oxygen concentration of the water was varied between 0.2 and 5.0 *ppm* [38].

PARET uses Rosenthal and Miller's correlation to determine the heat transfer coefficient whenever Re<2000 and the heat transfer correlation computed by Equation 14 is larger than PARET's original correlation [20]. This correlation is also used in the forced convection regime when Re>2000 and h calculated is larger than that calculated for the chosen forced convection correlation [P.200,20].

For subcooled forced convection, the Sieder and Tate correlation was added as an option to the Dittus and Boelter correlation used originally by PARET. The Seider and Tate correlation is [Pg.75,8]:

$$Nu = 0.027\,\mathrm{Re}^{0.8}\,\mathrm{Pr}^{1/3}\left[\mu_b/\mu_w\right]^{0.14}$$ **Equation 15**

And the form of Dittus and Boelter correlation as implemented in PARET is [Pg.75,8]:

$$Nu = 0.023\,\mathrm{Re}^{0.8}\,\mathrm{Pr}^{0.4}$$ **Equation 16**

where Re = Reynolds number

Pr = Prandtl number

μ_b = dynamic viscosity of the coolant at the bulk liquid temperature, m^2/s

μ_w = dynamic viscosity of the coolant at the wall temperature, m^2/s

Literature lists both these correlations as being valid for Re>10,000, however, it should be noted that all the natural convection cooled SPERT-I tests would not have Reynolds numbers anywhere close to 10,000 [Pg.185,40].

Woodruff doesn't discuss the fact these formulas are technically inappropriate for SPERT-I core Reynolds number ranges; he is apparently satisfied with their results, the ultimate measure of suitability.

Another two correlations for the onset of nucleate boiling (ONB), one by McAdams and another by Bergels and Rohsenow, were added to the original PARET correlation by Jens and Lottes. The Jens and Lottes correlation is [P.18,8]:

$$T_w - T_{sat} = 25 q_{ONB}{}^{0.25} \exp\left(-P/_{62}\right)$$ **Equation 17**

where T_w = temperature of clad wall, ^oC

T_{sat} = coolant saturation temperature, ^oC

P = local coolant channel pressure, MPa

q_{ONB} = local heat flux at clad surface, MW/m^2

Jens and Lottes developed this correlation on subcooled boiling experiments of upwards flowing water, in vertical tubes with inside diameters between 3.63 and 5.74 mm, system pressures between 7 and 172 bar, water temperatures from 115 to 340 ^oC, mass velocities from 11 to $1.05 \times 10^4 \, kg/m^2 s$ and heat fluxes up to 12.5 MW/m^2 [Pg.205,40].

The Imperial Units version of McAdams' correlation is [P.18,8]:

$$q_{ONB} = 0.074(T_w - T_{sat})^{3.86}$$ **Equation 18**

where q_{ONB} = local heat flux at clad surface, BTU/ft^2hr

The PARET manual does not list the exact source of this version of McAdam's correlation, however, Collier does discuss other forms of fully developed subcooled boiling work by McAdams at length [Pg.206,40].

Bergels and Rohsenow's correlation [P.18,8]:

$$q_{ONB} = 1.8029x10^{-3} P^{1.156} (1.8 \Delta T_{sat})^{2.16} / P^{0.0234}$$ **Equation 19**

where q_{ONB} = local heat flux at clad surface, MW/m^2

Literature discusses the Imperial version of this correlation being valid between 15 and 2000 $psia$ for water [Pg.190,40].

To calculate the heat transfer coefficient in the boiling regime beyond the onset of nucleate boiling but before fully developed nucleate boiling, in the transition to fully developed subcooled boiling regime, a two-phase heat transfer empirical solution suggested by Bergles and Rohsenhow was added as an option to the PARET original two phase model; the original model is discussed in the Obenchain manual [5].

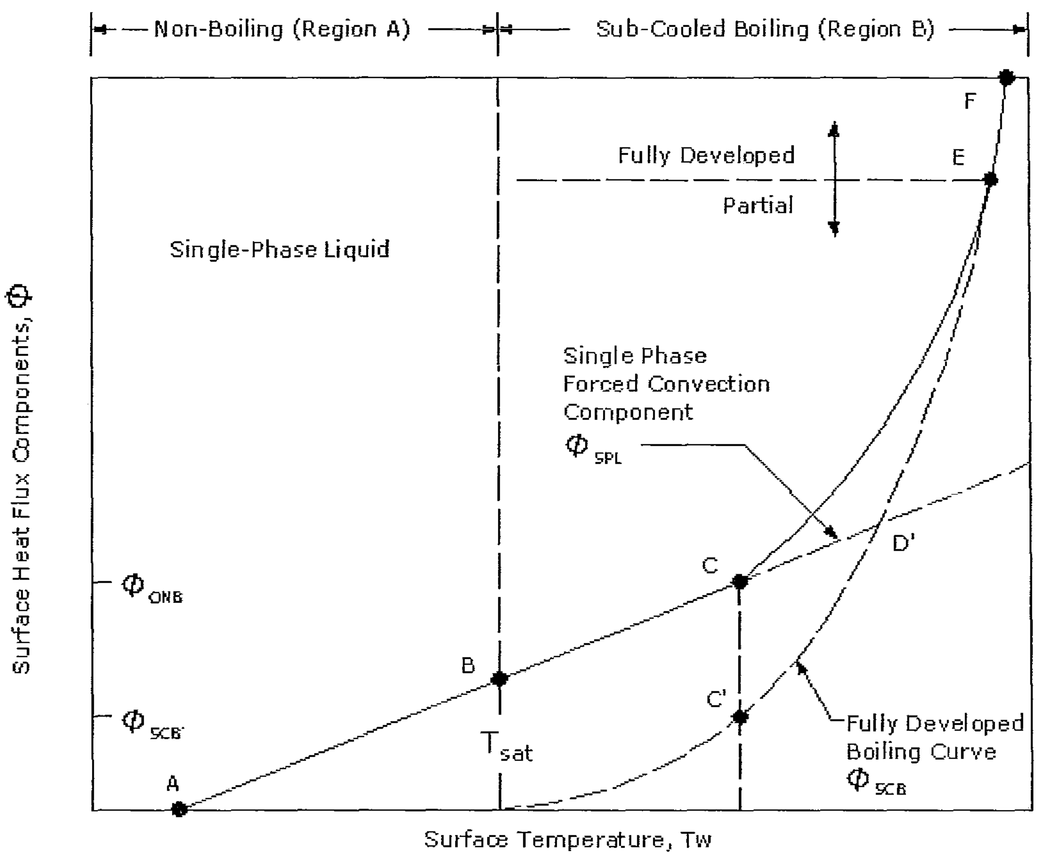

Figure 4. Bergles and Rohsenhow Method of Calculating Heat Flux [40]

Figure 4 shows this progression to fully developed boiling between points C and E. This model is referred to as the "transient two-phase scheme" by the PARET manual, and should not be confused with transition boiling (the unstable boiling regime between CHF and film boiling).

The Bergles and Rohsenhow formula estimates the heat transfer coefficient by interpolating between the single phase forced convection component and the extrapolated fully developed nucleate boiling curve in the following manner [P.201,40]:

$$q = q_{SPL}\left[1+\left(\frac{q_{SCB}}{q_{SPL}}\left(1-\frac{q_{SCB'}}{q_{SCB}}\right)\right)^2\right]^{1/2}$$ **Equation 20**

where q_{SPL} = single phase liquid local heat flux, obtained with either the Sieder and Tate or Dittus and Boelter correlations

q_{SCB} = subcooled boiling local heat flux, obtained with either the Jens and Lottes, McAdams or Bergles and Rohsenhow correlations

q_{SCB}' = subcooled boiling local heat flux, obtained as is q_{SCB}, except with wall temperature set to the moment of ONB, as given by the reworked Bergles and Rohsenhow ONB correlation [Pg.21,8]:

$$T_w^{ONB} = (q_{ONB}/15.6P^{1.156}) \wedge (P^{0.0234}/2.30) + T_{sat}$$ **Equation 21**

Woodruff found changing the thermalhydraulic correlation selections greatly effect the ability of PARET to accurately duplicate SPERT-I transient results. The "best" PARET model uses the updated voiding model, the Rosenthal and Miller single phase heat transfer coefficient correlation, the McAdams correlation for fully developed two-phase flow, the Bergles and Rohsenow method for transition to fully developed nucleate boiling and the original PARET DNB correlation for predicting CHF [Pg.201,20].

Parameter	SPERT-I B-24/32	SPERT-I B-12/64	SPERT-I D-12/25	MNR Reference Core
Plates/element, standard (control)	24	12	12 (6)	16 (9)
Number of elements, standard (control)	32	64	20 (5)	28 (6)
Fuel thickness (cm)	0.051	0.051	0.051	0.051
Clad thickness (cm)	0.051	0.051	0.051	0.038
Water channel (cm)	0.165	0.483	0.455	0.3
^{235}U/plate (g)	7.0	7.0	14.0	14.06
Temperature (spectrum) coefficient ($/°C)	-0.02528	-0.04157	-0.02801	-0.01314
Void coefficient ($/% void)	-0.3571	-0.15	-0.4214	-0.222
Neutron generation time (mico s)	50	77	60	65.1
Beta effective	0.007	0.007	0.007	0.00767
Peak/avg power	2.5	2.2	2.4	~ 3.8

Figure 5. Core Characteristics and Parameters for SPERT-I Cores [20]

The SPERT-I program immersed HEU plate-type cores in an open tank of light water, cooling was solely due to natural convection and each core was subjected to 61 *cm* of static head [20]. The experiments induced a large range of reactor periods by inserting reactivity in a step manner while measuring reactor power and plate temperatures. Woodruff compared the experimental results of the B and D series SPERT-I cores to PARET simulations because their core designs are similar to many plate-type research reactors [Pg.198,20]. A description of the SPERT-I and MNR core parameters are shown for comparison in Figure 5.

Figure 6 and Figure 7 show the comparisons between the SPERT-I experimental data and the PARET simulations of the same cores. In his paper, Woodruff offers a number of qualitative statements regarding PARET's ability to model SPERT-I transients. He states that significant transition boiling is predicted for the most energetic transients and suggests the CHF correlation is too conservative, presumably because the same transient in experiments didn't result in DNB [Pg.202,20]. Also, somewhat poor agreement for clad temperature and energy release where no void is predicted suggests the single-phase correlations may be overly conservative [Pg.202,20].

PARET's limitations are discussed not only by Woodruff but also in the original manual [5]. The incompressible hydrodynamic equations fail to model coolant flows with high steam content and the accuracy of void-induced hydraulic instabilities is questionable [Pg.5]. Modeling transients up to the production of significant voiding should minimize the influence of these weak modeling areas.

While Woodruff does not offer a formulaic summary of PARET's abilities, the following paragraph from the conclusion section of his paper is worth showing in its entirety to illustrate his thoughts [Pg.205,20]:

> The results of this comparison of the PARET code with the SPERT-I cores are generally quite favorable...These results have demonstrated that the voiding model in the code can successfully describe the behavior of transients with subcooled boiling, and that certain choices of methods and correlations are preferred. It would appear that many steady-state CHF correlations are too conservative for use in the analysis of transients. The largest disagreement with experiment occurs in a range where no subcooled boiling is predicted. This would suggest that either the single-phase correlation for heat transfer is inadequate or some important feedback mechanism is being overlooked. The need for improved correlations for transient heat transfer applications remains high and is a fault shared by all transient thermalhydraulic codes. Finally, the code seems to provide conservative estimates for the peak clad temperature with the more energetic transients, and the limiting reactivity insertion cases (clad melting) can be determined.

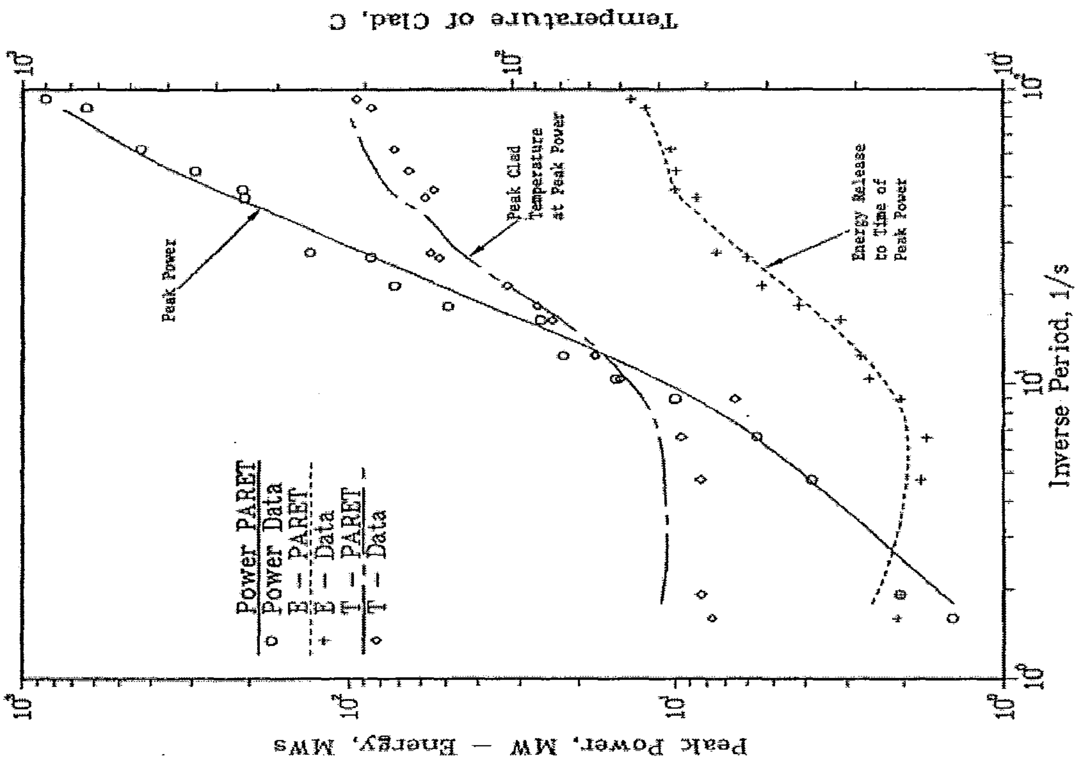

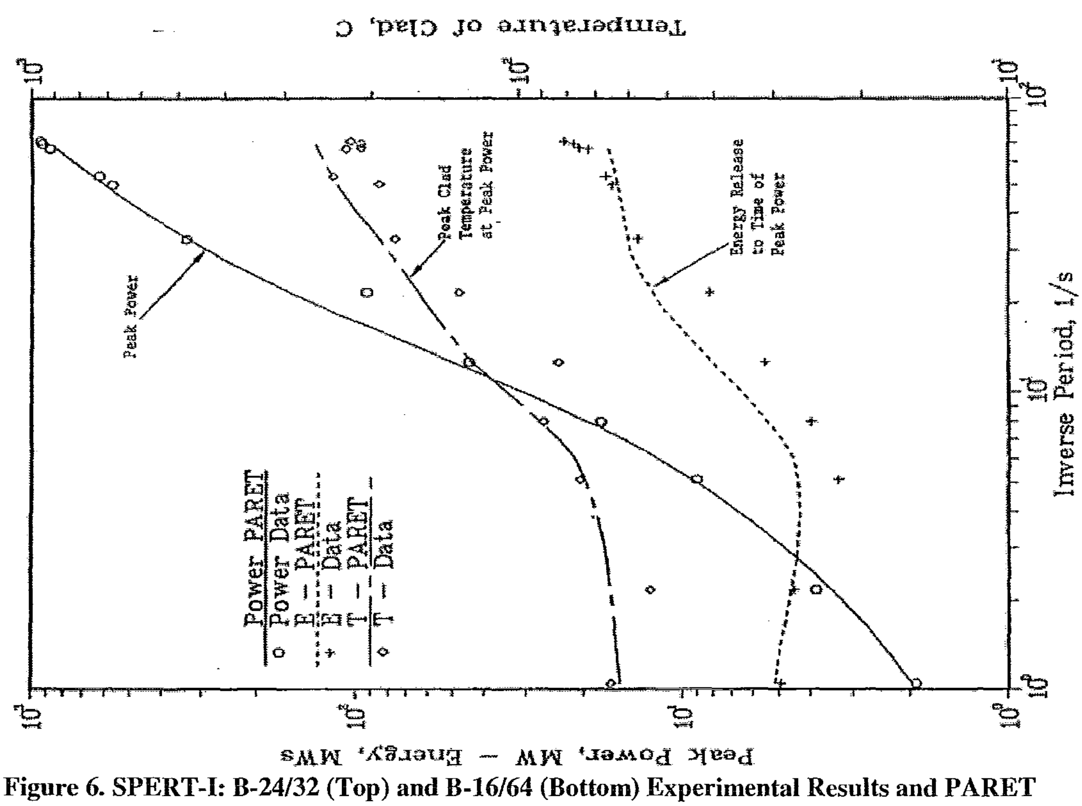

Figure 6. SPERT-I: B-24/32 (Top) and B-16/64 (Bottom) Experimental Results and PARET Simulation Comparisons [20]

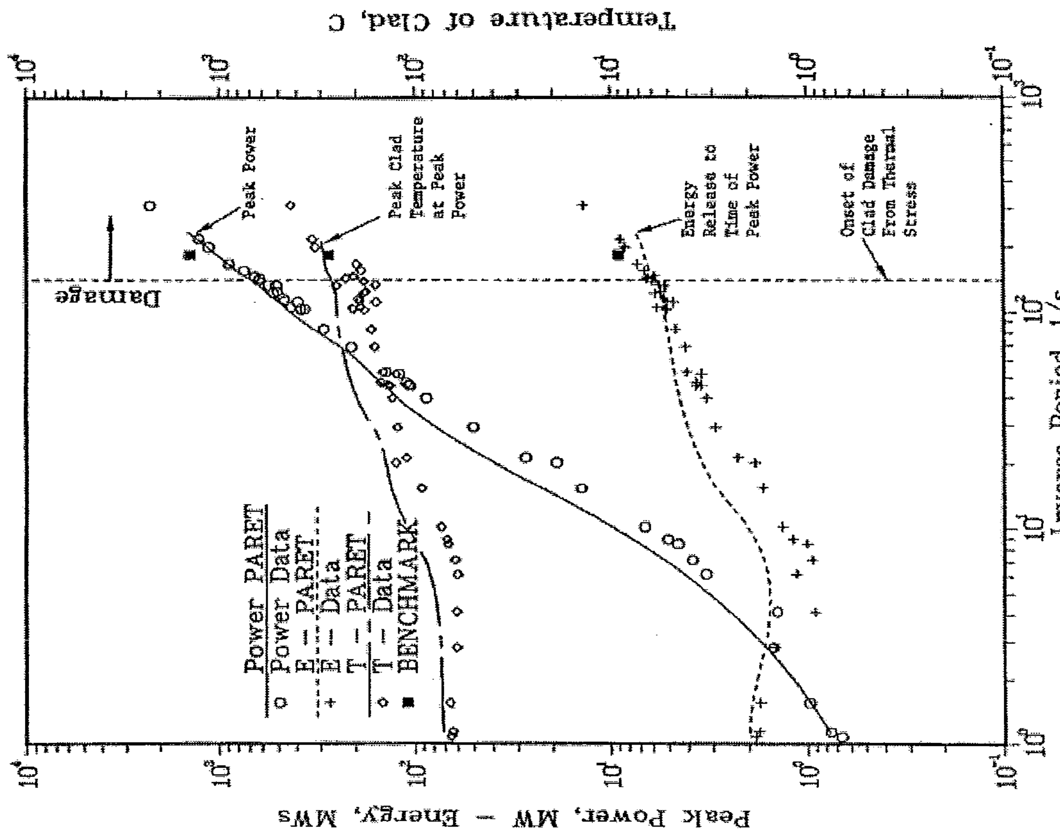

Figure 7. SPERT-I: D-12/25 Experimental Results and PARET Simulation Comparisons [20]

1.3.2 Rosenthal & Miller, An Experimental Study of Transient Boiling

During reactivity insertion accidents, reactor power may rise very quickly, especially if enough external positive reactivity has been inserted to make the reactor prompt critical. Under these conditions large amounts of energy will be deposited in the fuel in very short amounts of time, and the validity of modeling such transients with thermalhydraulic correlations developed upon steady-state experimental data is questionable.

Upon the addition of reactivity, power excursions continue until power becomes high enough to induce changes in the reactor which result in the reduction in reactivity [38]. Boiling induced coolant voiding in MTRs generates a significant amount of negative reactivity, and the behavior of energy transfer from the fuel to the coolant is

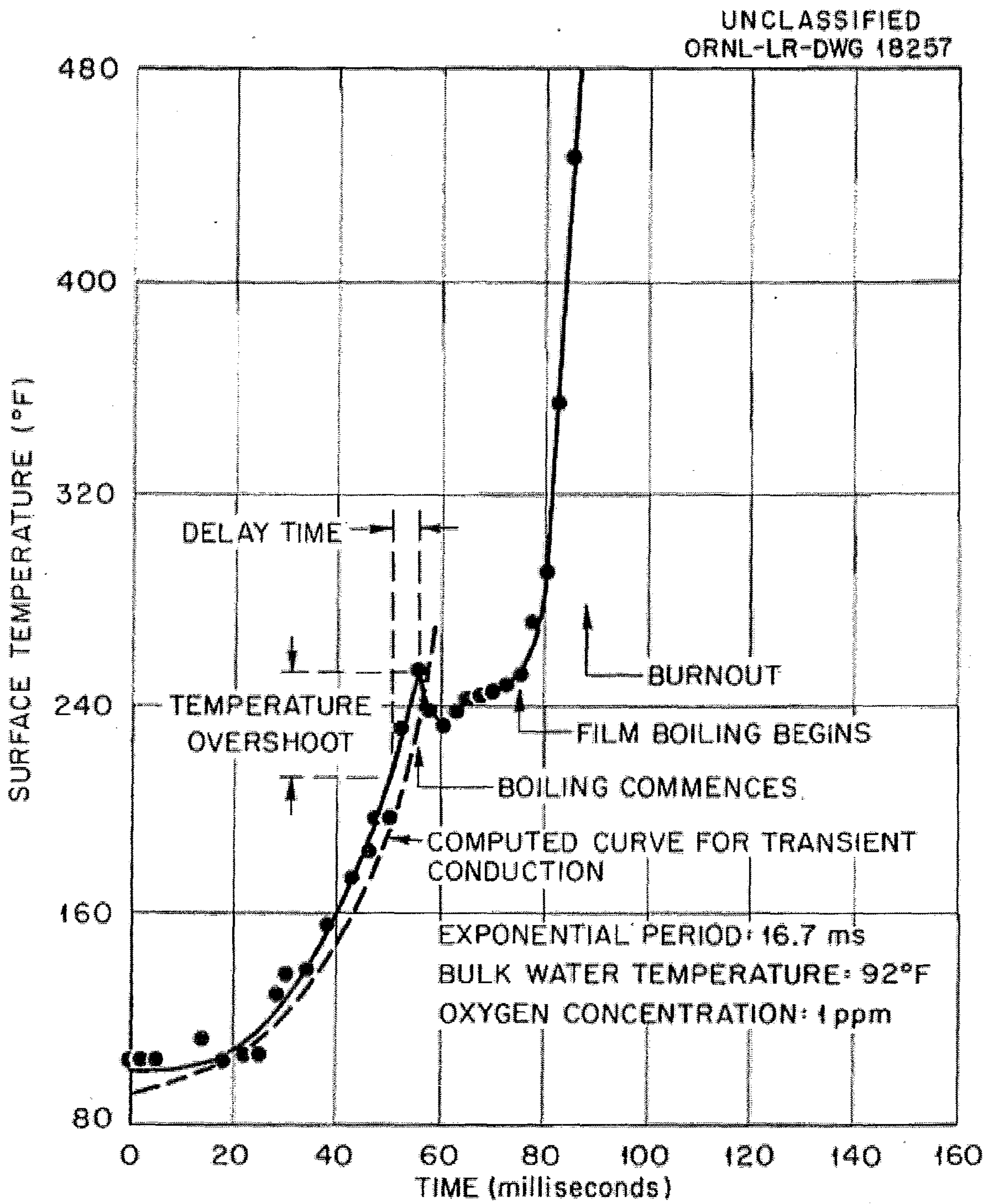

Figure 8. A Typical Temperature-Time Record For Platinum Ribbon in Subcooled Water [38]

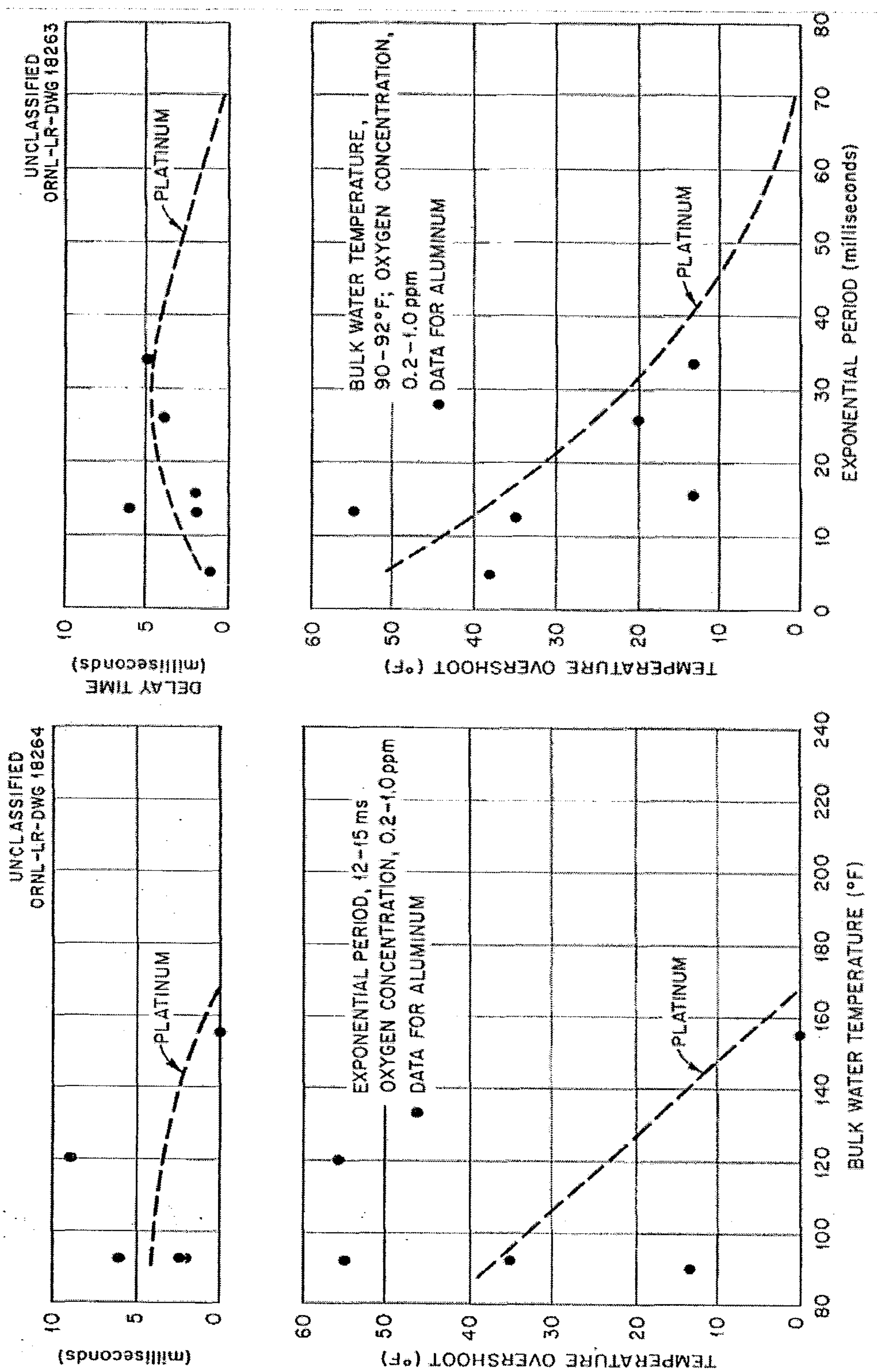

Figure 9. Effect of Period & Water Temp. on Delay Time and Overshoot for Aluminum Ribbons [38]

therefore important to understand. The faster the energy moves into the coolant, the sooner the coolant may void and mitigate the power transient.

As reactor power grows the fuel temperature rises more quickly than that of the coolant. The cladding surface temperature exceeds the boiling point of water while the bulk coolant temperature is still below saturation. The clad surface temperature may far exceed the boiling temperature before boiling commences at the clad surface [Pg.2,38]. When reactor periods are small, a delay between the high clad surface temperature and boiling can allow reactor power to reach large values; these large power levels may be prevented by slower power growth rates which could induce boiling (self limiting behavior) earlier.

Rosenthal and Miller experimentally developed a natural convection heat transfer correlation under transient conditions, which was discussed previously, and during the course of their work developed information which illustrates well the time delay between high clad temperatures and boiling under extremely small power period conditions.

By heating metal ribbons in water pools under transient applied power conditions, temperature plots like the one shown in Figure 8 are developed and show the boiling crisis which develops at DNB as well as the boiling delay time. The metal ribbon surface exceeded boiling temperature by a value equal to the temperature overshoot before boiling occurs on the ribbon surface. The ribbon surface is eventually covered in bubbles and film boiling is the result; burnout occurs when the ribbon temperature spikes as a result of the inability of the liquid phase coolant to make contact with the heated surface [38].

Figure 9 quantifies the magnitude of the temperature overshoot as a function of power period and pool temperature. For aluminum ribbons, the largest temperature overshoot relative to the saturation temperature is ~$55\,^{o}F$ in the range tested. This is of interest when considering transients in aluminum MNR fuel plates; although, most postulated MNR accidents considered in this report do not come close to the small periods tested by Rosenthal and Miller. It should be noted that the experimental data for platinum ribbons imply that at periods larger than ~$70\,ms$ there is little or no temperature overshoot; presumably aluminum has a similar threshold.

Woodruff calls the common practice of applying steady-state correlations to simulation programs "an open question" and simply states "more experimental data are needed in this area [Pg.202,20]."

2 Thermal Limits and Trip Map Methodology

2.1 Introduction

Trip maps are used extensively in Canada by power generating reactor owners to demonstrate that a reactor's shutdown systems are capable of detecting and mitigating a power transient. Trip map reports are frequently developed for power reactors during a licensing process, and as a result, the CNSC has become accustomed to using trip maps as a reactor safety assessment and analysis tool. The CNSC has requested MNR develop trip maps to compliment and expand upon existing MNR trip assessment studies. The development of trip maps for MNR adds additional depth to existing safety analysis.

Trip maps are graphical reports plotted with reactivity insertion rate as the abscissa and initial reactor power as the ordinate, as shown in Figure 10. Hatched areas on the map indicate the associated engineered safety system is capable of detecting and arresting a power transient. A capable shutdown system is defined as a system which can effectively halt a power excursion before a selected point of accident progression has been reached, such as fuel centerline melting, clad melting or burnout. The boundaries of

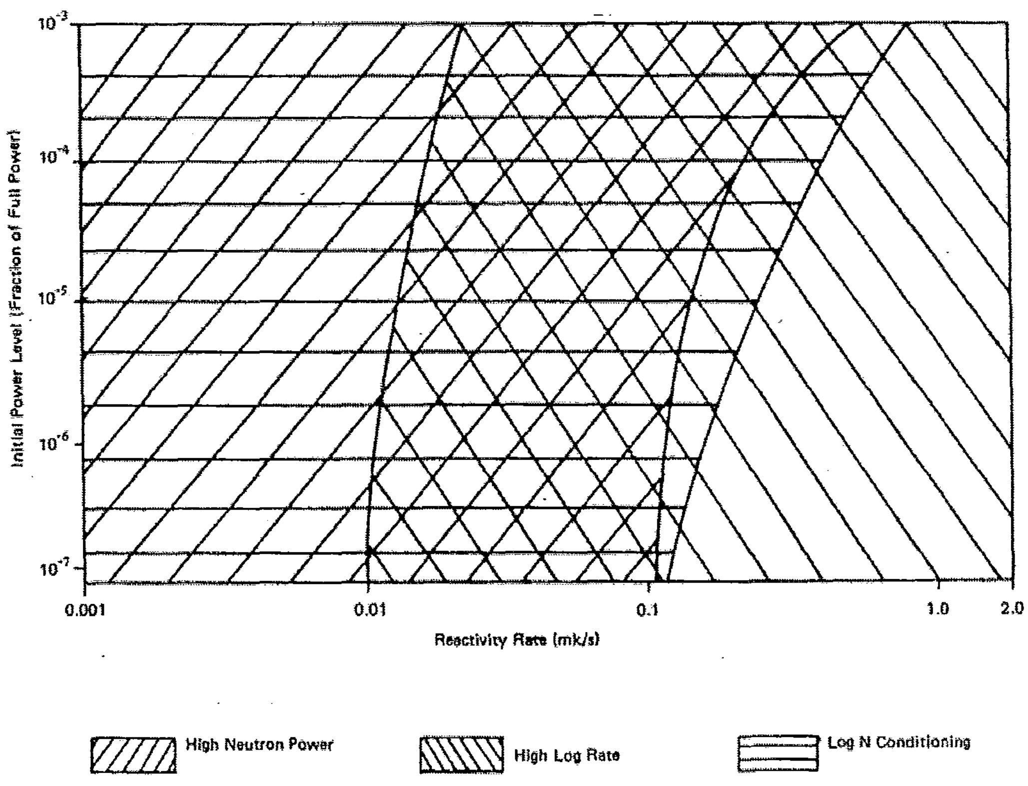

Figure 10. Sample Trip Map

hatched areas on a trip map plot demarcate between where a particular engineered safety system is capable of detecting and arresting a power transient and where it may be ineffective at doing so.

Trip maps are typically developed by postulating reactor accidents, resolving the accident scenario into an equivalent reactivity insertion rate, and using a simulation software package to predict the associated response of both the reactor and the engineered safety systems.

Nuclear engineers and the CNSC are guided by the defense in depth theory which requires that more than a single safety system be capable of arresting reactor power transients initiated from normal operating conditions; this ensures reactor transient prevention doesn't depend upon a single mechanism [Sec.1.2.2,35]. The sample trip map shown in Figure 1 displays the capability of three different instruments, as shown in the map legend. It is important to note that none of the instruments is capable over the entire sample map range shown, and that some areas of the map are effectively covered by all three instruments.

Displaying the effectiveness of all the shutdown systems on a single trip map demonstrates under which initial powers and which reactivity insertion rates and to what degree the reactor is protected in the case of an event; conversely, it shows where the reactor is not adequately protected. In the latter case the reactor operating limits, instrumentation alarm/action set points or safety system design changes can be made to increase the safety systems' domain.

2.2 MNR Safety Limits and SOE Report

The current MNR Safety Analysis Report (SAR) was developed according to the IAEA document Safety Assessment of Research Reactors and Preparation of the Safety Analysis Report and supports the Reactor's current operating license [30]. The fuel matrix and cladding are the primary and secondary barriers to fission product release and avoiding fuel melting ensures fission products are contained within the fuel [35]. In this context the MNR SAR uses the onset of fuel blistering, associated with a $450^{o}C$ clad temperature in irradiated fuel, as a conservative limit for avoidance of irradiated fuel failure [Sec.16.1.6.1,Pg.16.1-5,3].

An even further conservative administrative limit is used in association with MNR operation. McMaster University is required by law to operate MNR according to the document MNR Operating Limits and Conditions (OLC) [Sec.1.1,6]. The OLC defines the operating boundaries for safe operation of the reactor and changes to the document are to be approved by the CNSC [Sec.1.2,6]. The OLC dictates the minimum allowable core coolant flow and has taken these flow limits directly from the conclusions of the approved thermalhydraulic study Safe Operating Envelope of MNR (SOE) [9]. The SOE document uses bulk boiling as a limit in its development of recommended flow rates for MNR since bulk boiling is easily predicted and is an early and conservative precursor to potential fuel damage in slow to medium rate power transients [Sec.2,9].

2.3 PARET Limitations

Since the objective of developing trip maps is to establish which safety systems are capable of arresting transients, it would be interesting if MNR transients could be simulated all the way to the administrative thermal safety limit of fuel melting, but all simulations are limited by the capabilities of the simulation software itself.

As with other programs utilizing incompressible thermalhydraulic models, PARET is not capable of modeling transients which induce the generation of moderate steam volumes; PARET simulations crash upon the generation of this steam. Transients which induce 450 ^{o}C fuel temperatures can be simulated, provided reactor power reaches correspondingly high power levels in a fast manner, otherwise slow transients to high power levels induce boiling [P.197-8,20]. PARET is capable of determining the onset of bulk or film boiling, and of operating into temperature ranges where a small amount of vapor generation occurs [20].

2.4 Boundaries of MNR Trip Map

Given the capability and limitations of transient simulation tools like PARET, out of necessity, this MNR trip map analysis defines an effective trip as that which can prevent the onset of bulk or film boiling (while simultaneously preventing 450^{o}C fuel clad surface temperatures) in all portions of the simulated reactor. Subsequently, an ineffective trip is defined as one that cannot prevent the onset of either bulk or film boiling or 450^{o}C fuel clad surface temperatures.

As will be shown later in the report, all the postulated accidents considered for this study proceed slow enough bulk or film boiling is induced before the MNR thermal safety limit of 450^{o}C clad temperatures is reached. Therefore, the onset of bulk or film boiling is the first undesirable consequence to occur and is the practical thermal limit in this trip map analysis.

The trip maps presented herein are then considered boiling maps rather than safety maps since boiling is not a boundary which has fission product release consequences if surpassed. As such, trip maps generated upon this criterion represent an extremely conservative evaluation of MNR safety systems and are not necessarily indicative of trip coverage with respect to safety limits. In this sense, safety analysis and results presented herein must be used in conjunction with further accident safety analysis.

If another transient simulation software package becomes available or an alternative analysis methodology is identified that is capable of accurately modeling two phase coolant flow, transient simulations into late stages approaching the thermal safety limit of 450 ^{o}C clad temperatures could be conducted. However, a study of MNR safety systems based upon PARET transient simulations still provides a highly conservative analysis of early stage MNR transients.

2.5 Boiling Within an MNR Transient Progression

Given that the power in a reactor can be made almost arbitrarily high, the key to maintaining core geometry and staying within fuel thermal limits is keeping power within the cooling system's capacity to remove the energy generated [Pg.467,12].

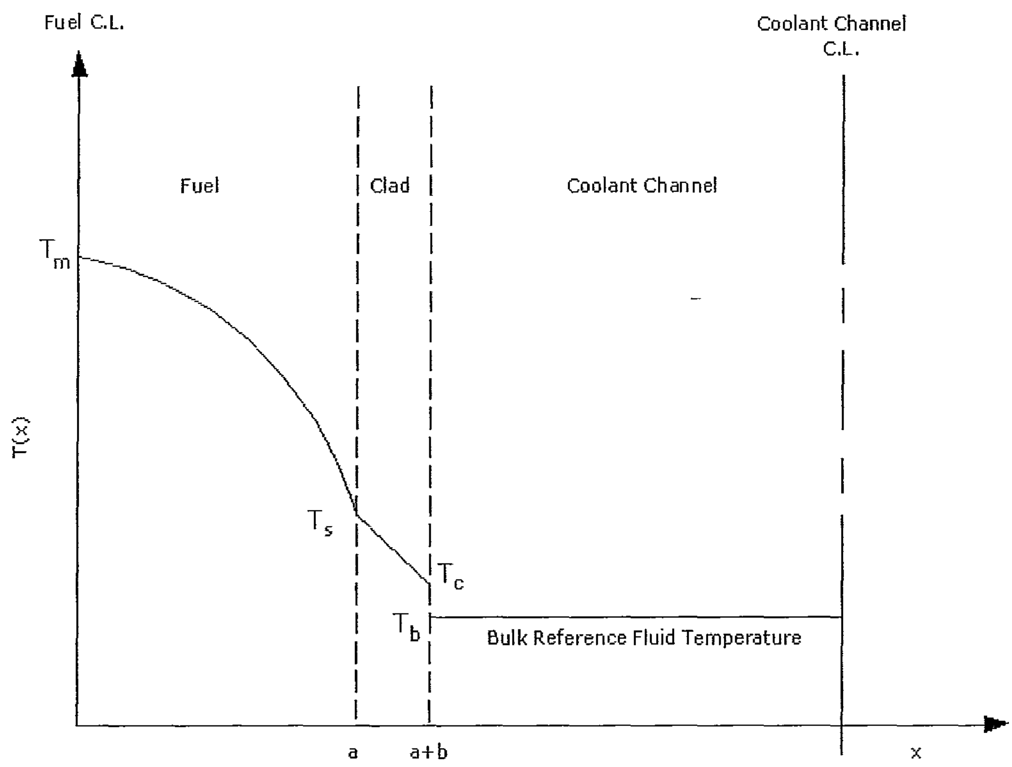

Figure 11. Temperature Profile in Plate Fuel and Associated Coolant Channel as Modeled in PARET

The one dimensional temperature profile for a plate type fuel element is shown in Figure 11. The figure simplistically assumes (as does PARET) the coolant temperature profile across the channel lacks a temperature gradient and is instead equal to the bulk fluid temperature. The heat flux q through either the fuel meat or cladding can be calculated with Fourier's familiar law of conduction [31]:

$$q = -k\frac{dT}{dx}$$ **Equation 22**

and the heat flux transferred from the heated surface to the fluid stream cooling its surface is determined with Newton's law of cooling [31]:

$$q = h(T_c - T_b)$$ **Equation 23**

where q = rate of heat transfer, W/m^2

k = thermal conductivity, W/mK

h = heat transfer coefficient, W/m^2K

In this simplistic, one dimensional heat transfer model of a heat generating fuel plate, Equation 22 and Equation 23 can be used with the conservation of energy equation to obtain the total heat flow through one side of the fuel plate element to the fluid [Pg.430,32]:

$$q = \frac{T_m - T_b}{\frac{a}{2k_f} + \frac{b}{k_c} + \frac{1}{h}}$$ **Equation 24**

Using the common electrical circuit analogy for heat transfer, the denominator is considered the thermal resistance in units of mK/W [32]:

$$R_{th} = \frac{a}{2k_f} + \frac{b}{k_c} + \frac{1}{h}$$ **Equation 25**

$$R_{th} = \frac{a}{2k_f} + \frac{b}{k_c} + \frac{1}{h}$$ Equation 25Equation 25 shows that R_{th} can be made randomly large by reducing the magnitude of h. The same could be said of the thermal conductivity values, but h has been singled out here because engineers spend significant amounts of time attempting to evaluate the heat transfer coefficient under various thermalhydraulic regimes.

If the coolant flow cannot make contact with the clad surface, h becomes unstable and can shrink dramatically, leading to an increase in clad and fuel temperatures. The rate of heat transfer at which this coolant-clad separation occurs is called the critical heat flux (CHF), and it occurs in one of two ways [Chap.5,Part3,36]:

1) The reactor may be running at powers high enough to raise the bulk fluid temperature from its subcooled inlet temperatures to saturation early in the coolant channel flow path. As the coolant continues to move through the channel, vapor is generated and eventually the steam quality becomes high enough that liquid phase coolant is rare and dry patches begin to appear on the clad wall, locally dropping the heat transfer coefficient.
2) The reactor may be running at extremely high powers and induce large amounts of steam generation at the coolant-clad interface. The volume of steam production may be so large that it effectively insulates the clad surface from the liquid phase coolant. This may occur either when the coolant is still subcooled or when the coolant is at saturated temperatures.

The first case can be completely avoided if the bulk coolant temperature is not allowed to reach saturation, since boiling is a required to produce high quality flows. The second case describes the phenomenon called film boiling. In all but the most extreme positive reactivity insertions in MNR, film boiling is completely avoided and reactor power density remains small enough that the reactor coolant progresses from highly subcooled to saturated enthalpies along the coolant channel length. As discussed previously, simulations completed with PARET need to be watched for the onset of bulk boiling and film boiling.

The thin fuel plate thickness and high conductivity of the MTR fuel plate materials in MNR cause the cladding material to maintain temperatures very close to that of the fuel centerline under normal operating conditions. For example, at $5\ MW$ operation the average fuel plate power is $9.96\ kW$ [Sec.5.6,3]. Not knowing the fuel plate centerline temperature but knowing the fuel plate dimensions and the values for k_f and k_c the clad surface temperature can be calculated relatively. Equation 24 without the convection term is:

$$q = \frac{T_m - T_c}{\dfrac{a}{2k_f} + \dfrac{b}{k_c}}$$ **Equation 26**

rearranging to solve for T_c shows very little variation from the centerline temperature:

$$T_c = T_m - q\left(\frac{a}{2k_f} + \frac{b}{k_c}\right) = T_m - 0.61^oC$$ **Equation 27**

At local pressures typical of MNR coolant channels, saturated boiling occurs at approximately 117^oC, far away from the temperatures required to melt or blister the cladding [7]. To illustrate, if bulk boiling were to occur adjacent to the 9960 W fuel plate discussed above, assuming a very small heat transfer coefficient of $3000\,W/m^2K$, Equation 27 says the fuel centerline temperature would be a benign:

$$T_m = T_b + q\left(\frac{a}{2k_f} + \frac{b}{k_c} + \frac{1}{h}\right) = 162^oC \qquad \textbf{Equation 28}$$

This shows that even if the reactor coolant reaches saturation temperature, fuel temperatures are still far away from 450^oC clad surface temperatures.

Although the onset of film or bulk boiling is used as a maximum thermal limit for this trip map analysis, boiling in MTR reactors is itself a major source of negative reactivity feedback and a mechanism which is likely to significantly slow transient progression. A very rough sample calculation can illustrate the large amount of negative reactivity boiling can create. Figure 13 shows the coolant voiding coefficient for MNR, and gives a linear equation linking voiding and negative reactivity feedback. If boiling were to be induced in MNR to the point of creating the cumulative equivalent of pure vapor in only half a coolant channel of each fuel assembly, the negative feedback reactivity would be as follows:

$$(0.5 \text{ channel}/17 \text{ channels per assembly}) \cdot 100 = 2.94\% \text{ void}$$
$$\rho = (-2.2x10^{-1}) \cdot (2.94) = -0.647\$ = -4.96mk$$

Voiding only approximately 3% of the core induces a very strong feedback. Clearly, although boiling is being used as a thermal boundary in this study, boiling itself is a self-limiting behavior and one that need not be avoided for safety reasons.

2.6 Trip Map Methodology

The effect certain postulated initiating events (accident scenarios) have on MNR is investigated by imposing the accident's characteristics upon the PARET model. Most postulated accidents can be resolved into reactivity insertion accidents or loss of coolant accidents and such phenomenon are simulated in the PARET MNR model. For example, loss of reactivity control accidents insert positive reactivity and loss of coolant accidents reduce the coolant flow through the core; a corresponding value of reactivity or loss of coolant is added to the PARET model. The resulting transient is monitored for bulk boiling, film boiling or clad temperatures above 450^oC; the latter is done to confirm that the onset of bulk coolant boiling remains a conservative indicator. If any of these thermal limits occur at any fuel node at any time during the transient, the engineered safety system being tested is deemed incapable.

Developing trip coverage maps for each accident scenario is a parametric process requiring many transient simulations. Each accident scenario is likely to be resolved into a range of reactivity insertion rates rather than a single rate. For example, an analysis of a postulated operator error event may find it is plausible a maximum of $3\,mk$ will be inserted at a rate somewhere between 0.1 and $2\,mk\,/\,s$. The trip coverage map for this operator error event would then require running many PARET simulations which insert $3\,mk$ at insertion rates between 0.1 and $2\,mk\,/\,s$ while a single safety system presides over the transient.

Each safety system is simulated independently, requiring each insertion rate to be simulated while each one of the safety systems is individually active. A judicious number of simulations need to be run within the reactivity insertion rate range estimated for each accident category. The boundaries between where a safety system is effective and not effective may change dramatically between different insertion rates, and in this case more simulations will be required to make sure a clear understanding of the safety systems capabilities is developed.

If one of the overpower safety systems is being tested, such as the +7% large servo error (LSE), 110% high flux (HF) or 125% HF instruments, the PARET model is told to signal SSR movement at 107% of initial power, 110% of initial power, or 125% of initial power, respectively.

Depending upon a reactor's design and kinetic behavior the early stages of a reactivity initiated transient, with an overpower trip active, may behave in a number of ways:

1) The amount of positive reactivity inserted may be small enough that reactor power rises a small amount and then stabilizes under negative feedback effects to steady state without reaching the overpower scram or reverse settings, also without reaching thermal limits.
2) The amount of positive reactivity inserted may be large enough the reactor power raises enough to induce bulk boiling but manages to stay below power levels which induce a scram or a reverse.
3) The amount of positive reactivity inserted may be large enough to induce reactor power to reach scram or reverse levels, and the SSR insert enough negative reactivity to lower reactor power before thermal limits are reached.
4) The amount of positive reactivity inserted may be large enough to push reactor power to scram or reverse levels, inducing the SSR to insert negative reactivity; the inserted positive reactivity may be inserted so quickly though that the SSR do not insert negative reactivity fast enough and still fail to prevent boiling before returning reactor power to low levels.
5) The amount of positive reactivity inserted may be large enough that even though the SSR are signaled to drive into the core, the SSR are not worth enough negative reactivity to prevent reactor power from rising or to lower reactor power.

An active overpower instrument channel which presides over a transient run on the PARET MNR model in the third manner, is deemed capable of preventing bulk boiling. An instrument channel which allows the transient to run as in the second and fourth scenario is obviously incapable of preventing bulk boiling. A transient of the fifth kind indicates a fundamental problem with the capability of the reactivity control rods.

MNR instrument safety systems which monitor reactor power rates, such as the $<3.8\,s$ and $<10\,s$ period trips are simulated differently than the overpower trips. The output file for the first $30\,s$ of the transients are inspected with a text file parsing program to examine if the reactor period is less than that of the instrument's setting. If during this $30\,s$ the period is indeed low, the reactor power at the time of the low period is recorded, and the transient is simulated a second time with the overpower trip set to the said power. As discussed in Appendix B, this is done to compensate for PARET's spurious period trip feature. By giving credit to the period trip only during the initial clean and discreet power ramp of the transient, the trip isn't credited when sharp power oscillations due to strong feedback effects are induced in the later transient times.

A transient initiated with a rate trip instrument channel active will have one of the following outcomes:

1) The positive reactivity may be inserted slow enough that reactor power builds with a period that is less than the trip set point, and neither a scram nor a reverse will be initiated. The reactor power continues to grow until negative feedback effects are strong enough to counteract the small magnitude of positive reactivity inserted and induce steady state power at levels below those that reach thermal limits.
2) The positive reactivity will be inserted in a slow enough rate that reactor power grows slower than those which induce scrams and reverses, but the magnitude of positive reactivity inserted is large enough to induce boiling or reach some other thermal limit.
3) The positive reactivity is inserted fast enough to create short reactor periods, the instrument trips either a scram or reverse and the rods reduce reactor power before thermal limits are reached.
4) The rate of the reactivity inserted is large enough that although its rate of insertion is high enough to cause a rate trip, the transient induces boiling before the SSR can act and return reactor power to low levels.
5) The magnitude of the reactivity inserted is large enough that although its rate of insertion is high enough to cause a rate trip, the SSR are not worth enough negative reactivity to prevent power from rising or to lower reactor power.

Again, the third case is the desirable outcome of an active engineered safety system monitoring reactor power rate. Notice that all the scenario descriptions of overpower trips and rate trips distinguish between rate of positive reactivity insertion and magnitude of positive reactivity insertion.

Redundancy is enough of a need to warrant having more than a single engineered safety system, but the above descriptions show that even multiple engineered safety systems based upon either just overpower or just reactor power rate logic, would not necessarily constitute a sound design. A number of instrument channels set to trip on overpower may not be effective at mitigating a fast acting transient, whereby in the time the scram takes to insert negative reactivity, the quickly growing power has moved from scram-triggering power levels to fuel damaging power levels. Conversely, the slow building power transient may fail to activate a number of rate monitoring instrument channels and raise the power to coolant boiling levels. The MNR design which utilizes an array of each type of instrument is theoretically ideal.

When assessing the manual trips "The operator is credited with manually shutting down the reactor within five minutes of the first unambiguous annunciation of the accident [Sec.16.1.5,3]." Audible alarms (rather than some sort of visual cue) are capable of giving "unambiguous annunciation" even if the operator is out of the control room. Therefore, to simulate a trip on manual scram, MNR PARET transients must be watched for set points where audible alarms would sound: <10s period, 110% HF and +7% LSE [Table2,9]. Once the simulation has passed one of these marks, the simulation is allowed to continue for $300\,s$ (five minutes) before a scram is forced – simulating the operator taking action. If no thermal limit is reached between time zero and shutdown, the manual trip is credited as successful.

Practically, to simulate a manual scram, two simulations need to be run for each reactivity insertion rate. The first run tests if boiling occurs before $300\,s$ since that is a primary requirement. The second run uses a text file parsing program to scan the output file and determine the time one of the audible alarms would have sounded, and if at least $300\,s$ lapses before boiling is indicated on the output file the manual scram is credible.

Although there are three MNR instrument channels which signal audible alarms, the $<10\,s$ period audible alarm is not useful since a transient with periods $<10\,s$ will progress to coolant boiling far before $300\,s$ has lapsed. To illustrate, from an initial power of $1\,W$, a reactor with a $10\,s$ period after $300\,s$ has a power of $e^{300/10} = 1.1x10^{13}W$. The useful alarms are the power trips which can detect transients moving slow enough so that the operators have time to react, the +7% LSE and 110% HF. Because the +7% LSE alarm will always occur before the 110% HF alarm, it is credited for alerting the operators in all the manual scram analyses.

3 - PARET Model of MNR

To simulate transients PARET requires the fuel geometry, thermalhydraulic and neutronic systems of MNR to be described in the input file. Between the descriptions found in this section and those in Appendix B, an extensive explanation of a PARET model of MNR is included in this report.

This section discusses the MNR model features which are used for all transient simulations. Model changes specific to individual accident categories are discussed in detail later in the report.

The assumptions made in developing the general PARET MNR model affect the mechanics of transient analysis, thus it is important that these assumptions be understood.

3.1 Reference Core

Unlike a power reactor core which stays dimensionally constant throughout its lifetime, the MNR core changes physically in size. MNR has no set fuelling pattern and fresh fuel assemblies, irradiated fuel assemblies, control assemblies and graphite irradiation assemblies are arranged on the grid plate during refueling and the resulting core arrangement is likely to be different than the one which preceded the refueling. This variability makes conservative analysis difficult. Luckily, as part of the MNR SAR licensing analysis, a core arrangement identifying and estimating the highest local power densities was developed and called the Reference Core (RC) [1]. To stay consistent with the SAR all PARET based trip map work also describes the physical configuration of the Reference Core.

At any nominal reactor power level, the average fuel assembly power is equal to the nominal core power divided by the total number of fuel assemblies. For any given power level, the fewer the number of fuel assemblies in the core the higher the average fuel assembly power will be. The RC has a fewer number of assemblies in its core than is typical of the actual MNR core loading and thus the thermalhydraulic margin to boiling of the RC is then smaller than will be observed in any other practical MNR core arrangement. The RC incorporates sensitivity analysis of local power density to proximity to absorber rod positions, irradiation side positions and individual assembly depletion. It also approximates core burnup by representing beginning of life (BOL), mid life (ML) and end of life (EOL) fuel stages. The support analysis used in the definition of the RC is documented in the Power Peaking Factor Report (PPFR) [11].

The general arrangement of the Reference Core is shown in Figure 12, and lists the percentage of lifetime burnup for each assembly. The fuel loading pattern and reflector/experiment locations have all been considered in the RC development to ensure these parameters enable the RC to remain conservative; the lowest typical core average fuel burnup is used for the same reason [Sec.3.4-3.6,1]. The RC uses thc same number and type of control assemblies and rods as every other core arrangement.

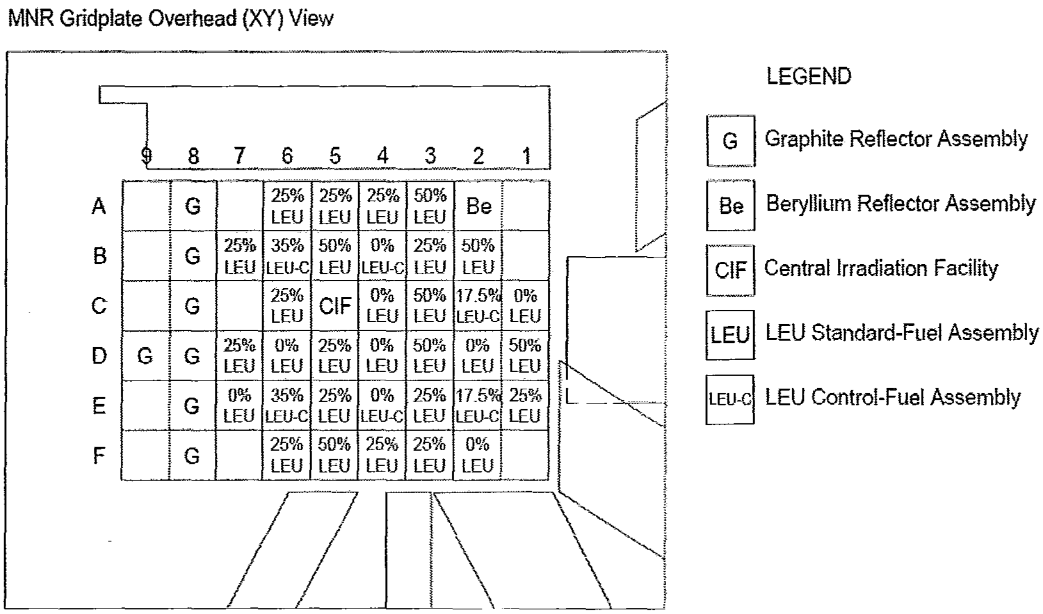

Figure 12. Reference Core General Arrangement [Fig.5, 1]

3.2 Reactivity Feedback Coefficients

MNR, like other light water MTRs has negative coolant voiding and temperature feedback coefficients [20]. These two coefficients are summarized in Figure 13 and Figure 14. The coolant density is dependent upon coolant temperature; therefore distinguishing between the two feedback effects is done artificially only for analysis purposes and has been completed with a WIMS-ANL/REBUS simulation [14]. The PARET input requires both of these effects to be separated.

The fuel temperature feedback of the MNR RC is shown in Figure 15 for two cases, one case with the rods fully withdrawn and another with the rods inserted. Regardless of the manner in which the PARET model places the rods, the fully withdrawn feedback polynomial is used in the PARET MNR model because it provides the least amount of negative reactivity. This curve selection makes the PARET MNR model the most conservative regarding transient simulations.

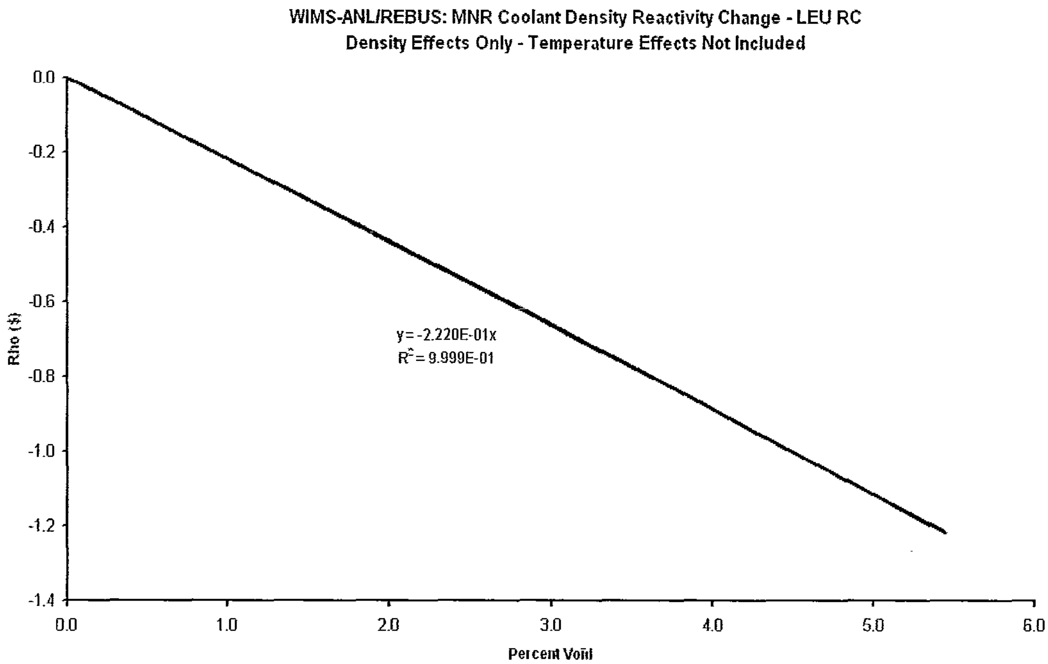

Figure 13. Coolant Density (Voiding) Reactivity Feedback [14]

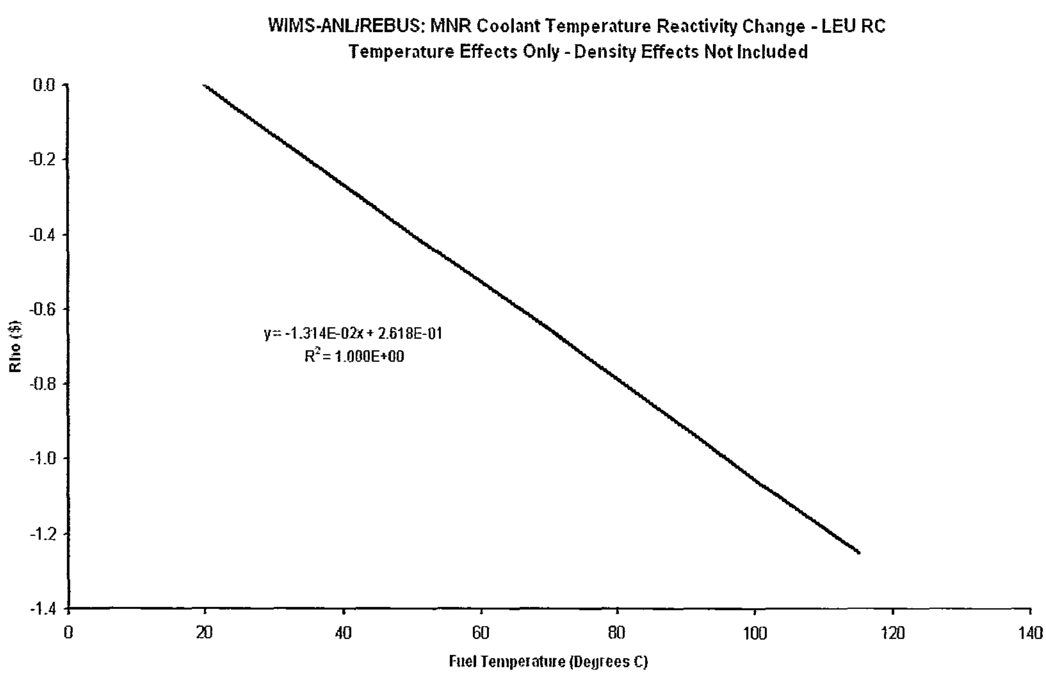

Figure 14. Coolant Temperature Feedback [14]

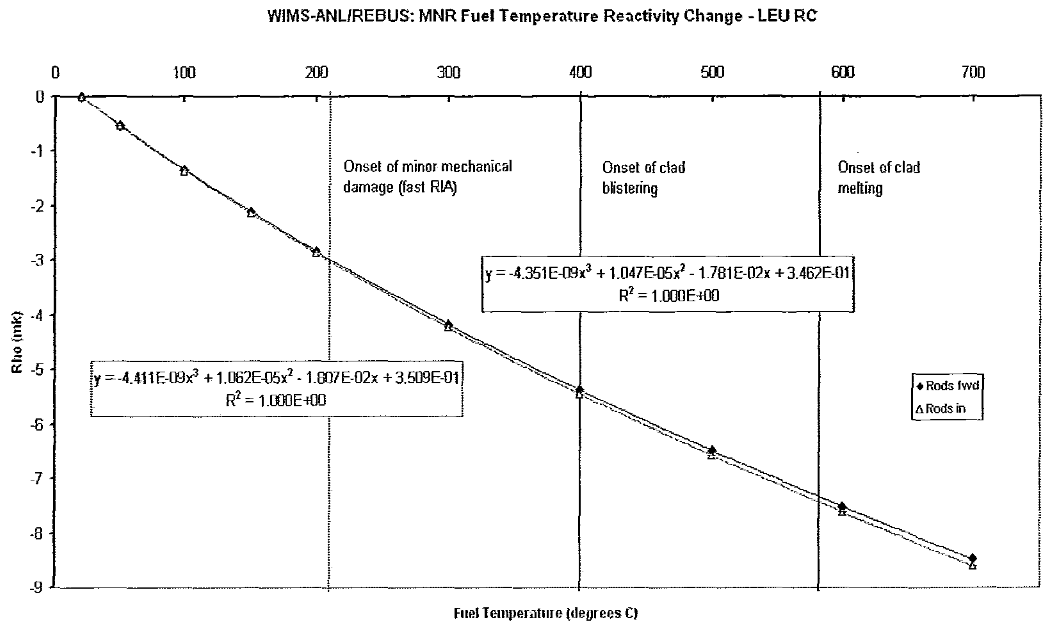

Figure 15. Fuel Temperature (Doppler) Reactivity Feedback [22]

3.3 Shim/Safey and Regulating Rods

MNR has five SSR used for coarse power adjustment and one regulating rod for active power control. To develop a conservatively bounded rod position for the MNR PARET model, all possible rod positions and possible reactivity rod worth must be considered.

The reactivity worth of the regulating rod is administratively limited to between 3.5 and 6 *mk* [Sec.17.3.2.2,3]. The SSR, however, do not have an explicit worth limit, but rather are tied to limits on available excess reactivity.

Because the SSR are used both for changing power levels as well as for shutdown, it is important the reactor not go critical when the rods are barely removed from the bottom of the core, otherwise only small amounts of negative reactivity would be inserted during a short fall to core bottom upon scram. As a result, the reactor is administratively restricted from going critical before the SSR have been withdrawn 50% (meaning the rods have withdrawn 50% of their travel, from the bottom of the active core height) [Sec.10.2,2]. As well, in the case of a scram all five SSR are supposed to fall into the core, however, the worth of the rods must be sufficient that the full insertion of any three rods will maintain the reactor sub-critical at any time [Sec.7.2.1,6].

Historically the SSR have been estimated by measurement and calculations to be worth between -75 and -100 *mk* [Sec.05,3]. The conservative assumption which must be made for modeling purposes, is for the least amount of negative reactivity to be available upon shutdown. The modeled SSR bank is therefore worth a total of $-75\,mk$. This is the case with PARET model runs of MNR in all categories, unless noted otherwise.

The other most conservative assumption one can make about the state of the SSR during operation is to assume their position is 50% withdrawn during all normal operation. Given that the reactor is not allowed to reach criticality anytime before this rod position, this is the location where the most amount of rod reactivity worth will already be inside the reactor, thus leaving the smallest amount of negative reactivity worth poised ready above the core for shutdown uses. If one was to assume the SSR bank were positioned at say 75% withdrawn, more negative reactivity would be available for insertion during a scram, compared to the 50% withdrawn position. Therefore, the shim/safety bank is always assumed to be at 50% withdrawn position in the PARET MNR model, unless otherwise noted.

The regulating rod is historically worth between 3-8% of the SSR bank, and is limited in its travel between 20% and 80% withdrawn from the core [Sec.05,3]. PARET does not model the action or even the presence of the regulating rod, and slow positive reactivity insertions modeled in PARET will therefore be extremely conservative since the corrective control of the regulating rod which would normally compensate under automatic control, is not credited.

In the case of modeling very fast reactivity insertion rates in PARET, neglecting the power control reaction of the regulating rod control system may be close to accurate. The regulating rod is driven at a speed of $1.13\,cm/s$, and quick reactivity insertion rates may overcome the capability of the regulating rod to insert negative reactivity at this drive speed [Sec.05,3].

3.4 Flux Profiles and Power Peaking Factors

The PARET model developed for MNR has two Channels, where Channel in this context refers to a region of the core represented by an individual RC fuel plate and its adjacent coolant channel. Channel One is modeled as the highest expected fuel plate power in the RC and Channel Two as the expected core average fuel plate power density. Modeling a reactor core with the expected hottest and expected average representative fuel elements is a simple analysis technique common in reactor analysis [Pg.472,12]; it is also typical of benchmarked PARET runs [Pg.40,4]. Channel Two being at a lower power density, will never reach boiling before Channel One and is never the limiting Channel; however, it is still included in the transient analysis because it represents the average fuel plate performance within the RC.

An idealized bare parallelpiped core would have a truncated cosine flux profile in all Cartesian directions, as described by the equation in Figure 16.

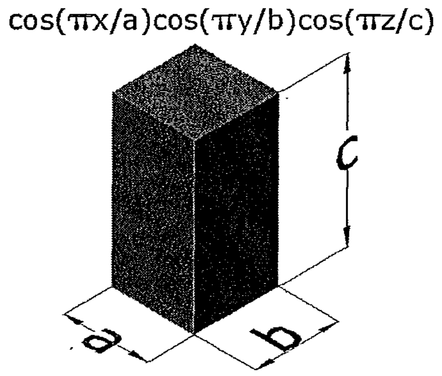

Figure 16. Flux Profile for Parallelepiped Geometry [Pg.209,12]

Unlike a physically large reactor core which requires local flux absorbers to prevent high or low regional fluxes, the compact MNR core does not require local flux control. However, the fuel plates in the MNR core are still far from uniform in power, the fuel plates within each assembly have different power levels, and the plates themselves even have varying power densities along their length and width.

As is shown in Figure 16, the flux varies in every direction of the core. To determine which of the 502 RC fuel plates and its associated coolant channel should be designated as the hottest PARET channel, the MNR Power Peaking Factor Report needs to be consulted [11]. The report expresses the power in all locations of all fuel plates in the reference core with an overall power peaking factor, OPPF. An overall power peaking factor is the product of the following factors [Pg.4-6,11]:

$$OPPF = LPPF_{plate-to-plate} \cdot APPF \cdot RPPF \qquad \textbf{Equation 29}$$

$LPPF_{plate\text{-}to\text{-}plate}$ quantifies the power density between the fuel plates. As is shown in Figure 17, the outer fuel plates in any fuel assembly have significantly higher powers than the inner plates. This is due to assembly self shielding of neutrons and the proximity to the moderating water outside of the fuel assembly to the outer fuel plates. This effect is even more pronounced when the fuel assembly is adjacent to an open water site rather than another fuel assembly because the water site supplies an abundance of thermal neutrons to the closest fuel plates. The formal definition is:

$$LPPF_{plate-to-plate} = \frac{\text{average power density in subject fuel plate}}{\text{average plate power density in subject fuel assembly}}$$

Equation 30

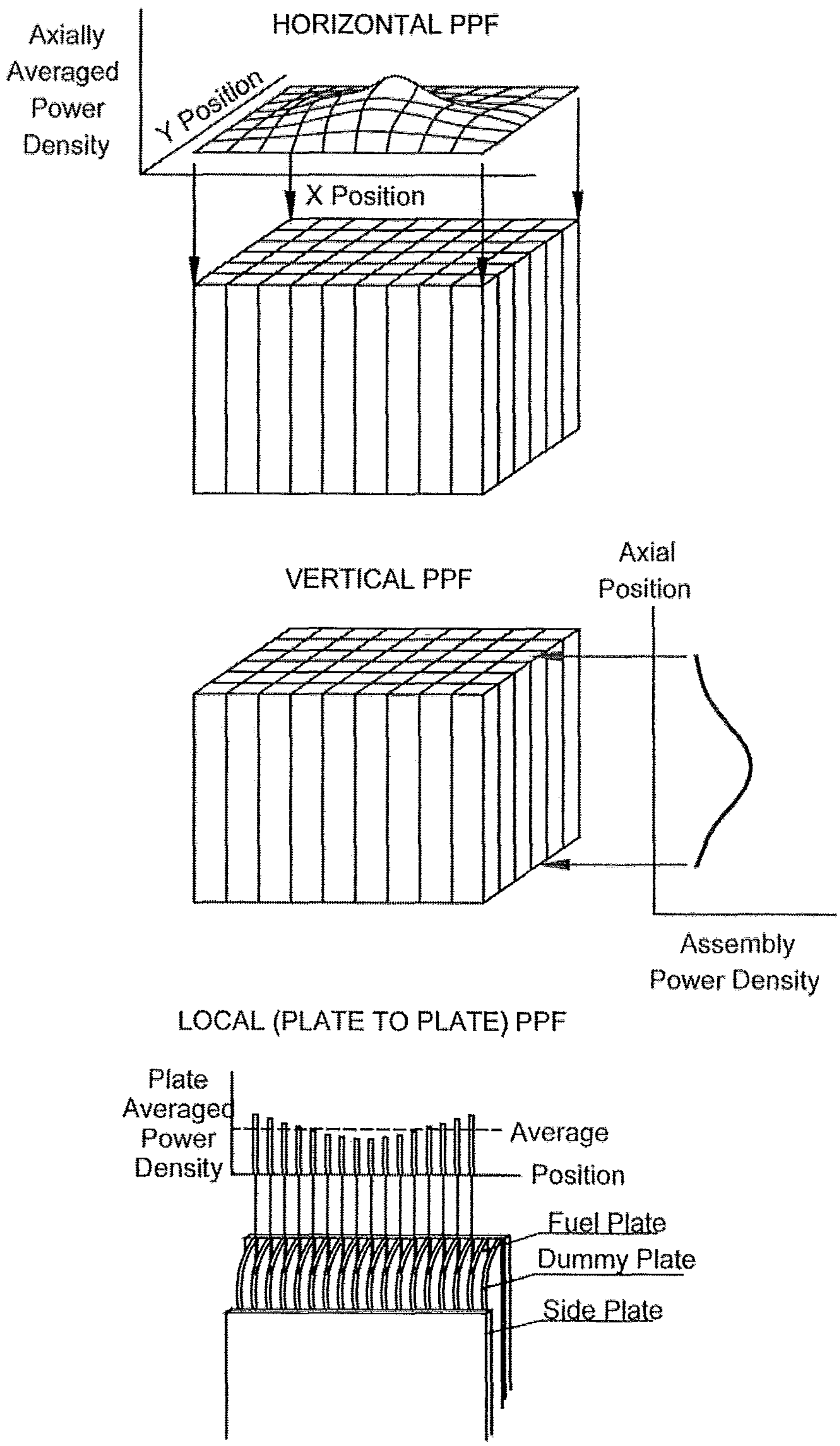

Figure 17. Power Peaking in 3 Dimensions [Pg.39,11]

Individual fuel plates also vary in power along their width due to self shielding and the proximity to moderating water. However, PARET does not place nodes along the width of the fuel plate and can't distinguish between higher and lower power regions in this direction. This does not diminish the conservative nature of the modeled fuel plate in PARET since the total average fuel plate power is still accurate; the model simply assumes that the fuel plate power density is uniform across its width as calculated by its vertical axial node.

The APPF describes the power distribution along the vertical axial length of each fuel assembly, as shown in Figure 17 and the RPPF describes how the power differs between fuel assemblies in the core. Each is formally defined as:

$$APPF = \frac{\text{average power density of the horizontal plane in the subject assembly}}{\text{average power density in the fuel plates of the subject assembly}}$$

Equation 31

$$RPPF = \frac{\text{average power density in the fuel plate of the subject assembly}}{\text{average power density in the core fuel plates}}$$

Equation 32

The APPF profile in an actual MNR core is not a true cosine. Structural core components, samples present in the core and most importantly the control rod bank change the shape of the vertical flux profile. The reactivity worth of five control rods which penetrate the top of the core pushes the axial flux profile peak into the lower half of the core, away from the vertical center of the core. To illustrate, Figure 18 shows the normalized flux profile of the reference core from a simulation with the SSR bank in the position 100% withdrawn, and Figure 19 shows the normalized flux profile of the reference core when the SSR bank is 50% withdrawn.

Based upon the definition of RPPF (called horizontal power peaking factor in Figure 17), if all fuel assemblies in the core had the same power, each assembly's RPPF would be 1. However, even an idealized reactor of this shape would not have a constant RPPF. Idealized bare cores have cosine flux peaking in both horizontal directions as Figure 16 shows, but the uniformity of the RPPF is distorted because some assemblies have adjacent water sites supplying more thermal neutrons than other assemblies may have, or adjacent control rods depressing neutron flux. The burnup of each assembly also distorts the flux distribution.

RC values for $LPPF_{plate\text{-}to\text{-}plate}$, APPF and RPPF can be determined since previous discussions have established the most conservative SSR position is 50% withdrawn. The APPF is strongly dependent upon rod position, and rod position is therefore a prerequisite for APPF definition. The results of a MCNP simulation determining the fuel plates axial power profile with the SSR at 50% withdrawn was previously shown in Figure 18. The normalized curve shown in Figure 18 is the APPF for every point along the 60 *cm* fuel assembly's length.

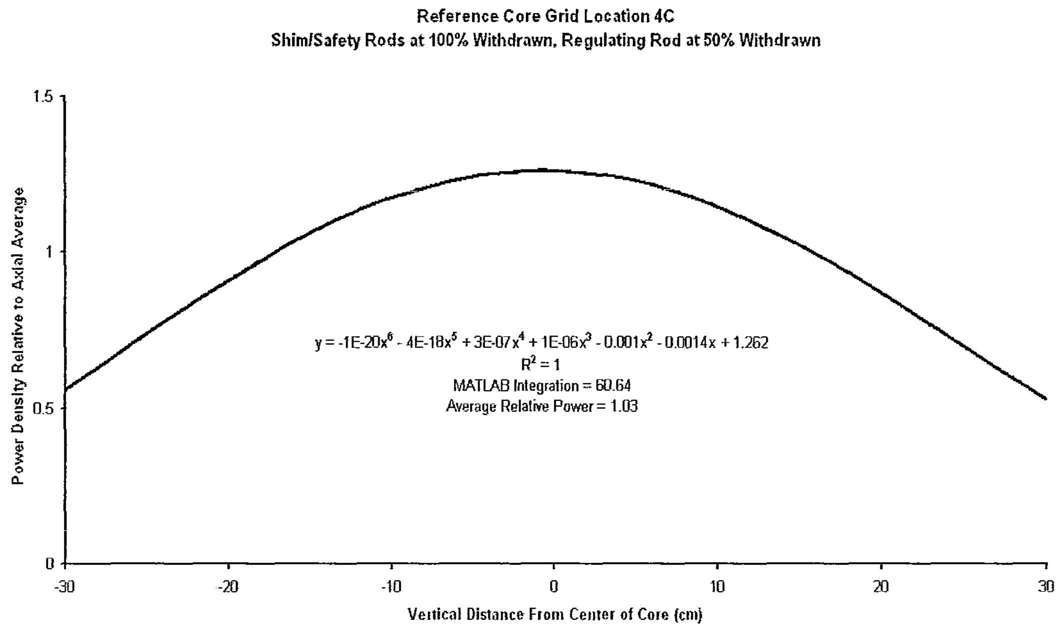

Figure 18. 4C Fuel Assembly Normalized Flux Profile from REBUS Model [24]

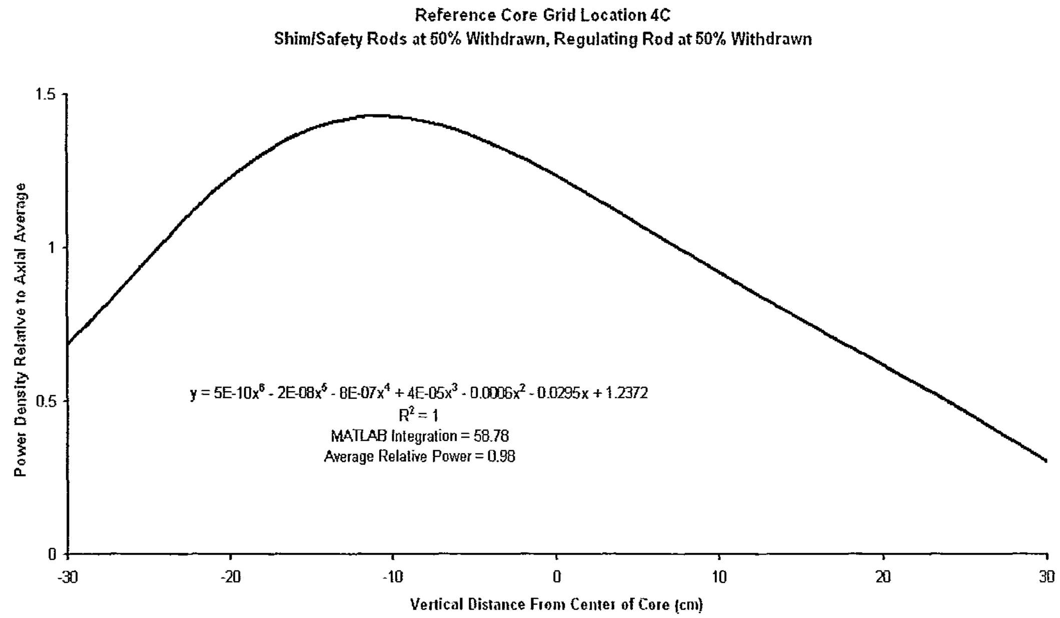

Figure 19. 4C Fuel Assembly Normalized Flux Profile from MCNP Model [25]

m800-rc28-leu-afps-cold-75wd_3ddt.res

22-Jan-2001 16:04:40

A	W	G	W	MNR-L 1.26 1.32 0.63 1.38 1.45	MNR-L 1.26 1.11 0.76 1.36 1.44	MNR-L 1.26 1.11 0.85 1.37 1.63	MNR-L 1.12 1.13 0.67 1.35 1.15	Be	W
B	W	G	MNR-L 1.32 1.31 0.64 1.39 1.54	CTL-L 1.05 1.08 0.79 1.43 1.29	MNR-L 1.18 1.04 0.94 1.40 1.62	CTL-L 1.09 1.17 1.49 1.43 2.72	MNR-L 1.06 1.11 1.10 1.38 1.79	MNR-L 1.13 1.18 0.78 1.38 1.43	W
C	W	G	W	MNR-L 1.06 1.32 1.16 1.38 2.23	W	MNR-L 1.09 1.44 1.80 1.38 3.90	MNR-L 1.02 1.04 1.07 1.38 1.57	CTL-L 1.07 1.13 1.17 1.43 2.02	MNR-L 1.44 1.44 0.85 1.36 2.39
D	G	G	MNR-L 1.32 1.31 0.80 1.36 1.86	MNR-L 1.09 1.16 1.25 1.38 2.18	MNR-L 1.32 1.11 1.44 1.37 2.90	MNR-L 1.09 1.16 1.73 1.38 3.02	MNR-L 1.02 1.04 1.11 1.37 1.60	MNR-L 1.09 1.16 1.30 1.38 2.25	MNR-L 1.02 1.18 0.56 1.34 0.90
E	W	G	MNR-L 1.44 1.43 0.83 1.39 2.38	CTL-L 1.05 1.08 0.90 1.44 1.47	MNR-L 1.06 1.11 1.17 1.40 1.93	CTL-L 1.09 1.17 1.61 1.43 2.95	MNR-L 1.06 1.11 1.21 1.38 1.97	CTL-L 1.07 1.13 1.09 1.37 1.81	MNR-L 1.32 1.32 0.66 1.39 1.59
F	W	G	W	MNR-L 1.32 1.32 0.74 1.42 1.83	MNR-L 1.18 1.04 0.69 1.42 1.20	MNR-L 1.32 1.11 0.94 1.39 1.92	MNR-L 1.32 1.11 0.85 1.37 1.71	MNR-L 1.44 1.44 0.86 1.41 2.53	W
	9	8	7	6	5	4	3	2	1

LEGEND

Fuel Type	
Local Side-to-Side PPF	Local Plate-to-Plate PPF
Radial PPF	Axial PPF
Overall PPF	

Power Peaking Factors (PPFs) are Peak : Average Power Densities

Figure 20. MNR Reference Core Power Peaking Factors [Fig.7,1]

Additionally, the MCNP simulation was completed on a fuel assembly located in grid location 4C. According to the reference core in Figure 20, the assembly in 4C is near the core's center, is a fresh fuel assembly and is adjacent to a water site; these are all factors which increase the power in the fuel assembly. RPPF is 1.8 at this location. For an assembly close to a water site, $LPPF_{plate\text{-}to\text{-}plate}$ is 1.44, this is also practically the highest possible value $LPPF_{plate\text{-}to\text{-}plate}$ can be, since nothing but an adjacent water site provides such a large peaking value to a fuel assembly [Table 3,11]. Note that this $LPPF_{plate\text{-}to\text{-}plate}$ applies to the outermost fuel plate of the 4C assembly because as is shown in Figure 17, an assembly's inner fuel plates operate at lower powers.

The product of RPPF and $LPPF_{plate\text{-}to\text{-}plate}$, 2.592, is included as a factor in the axial flux profile of Channel One shown in Figure 21. The multiplying factor for the average Channel One is by definition 1.0, and its profile as modeled in PARET is shown in Figure 22 - note it is the same as the original MCNP profile.

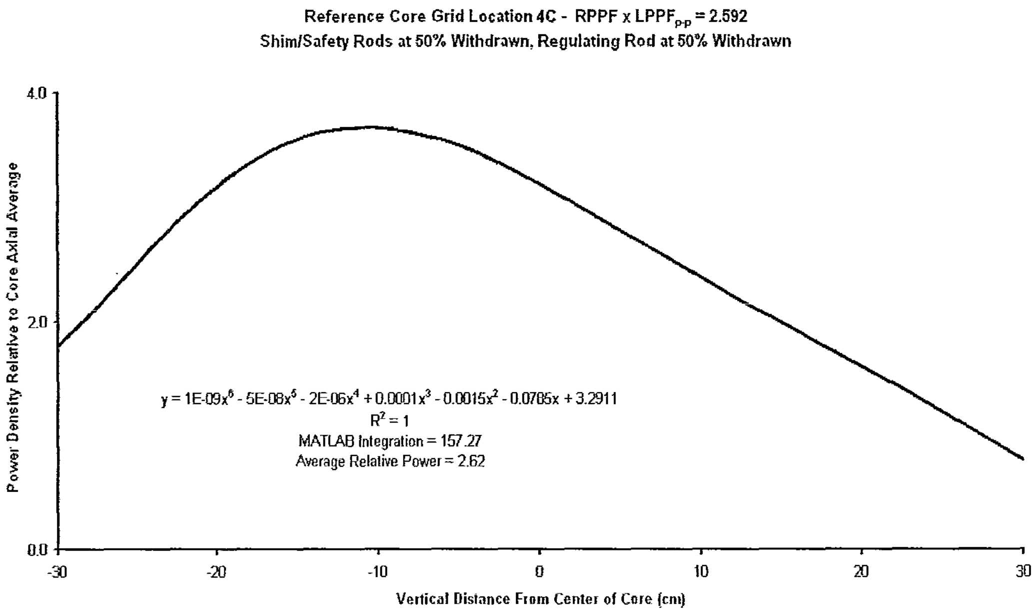

Figure 21. PARET Channel One (Hot Channel) Axial Flux Profile

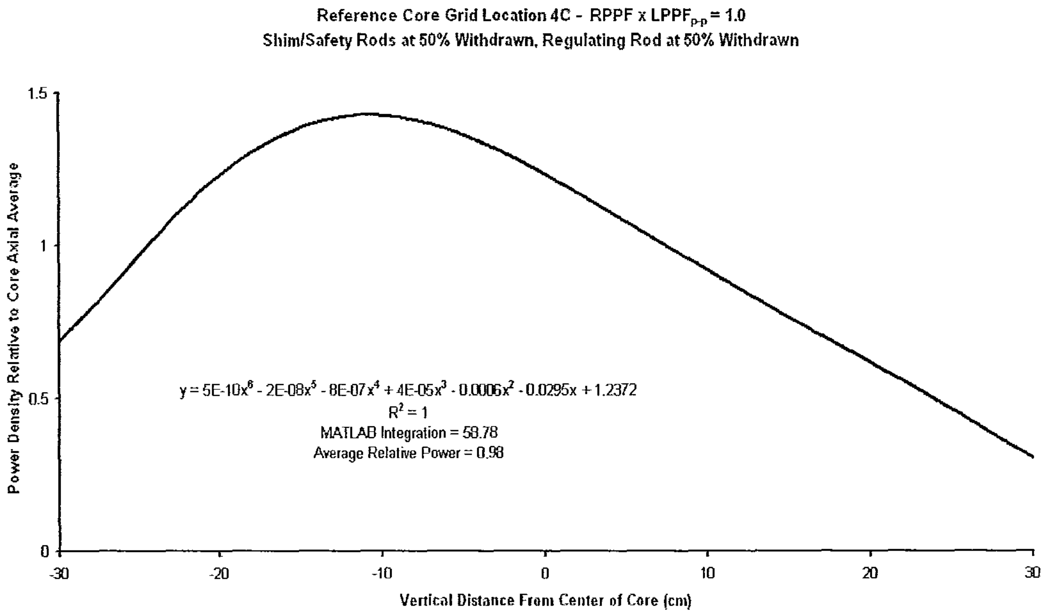

Figure 22. PARET Channel Two (Average Channel) Axial Flux Profile

3.5 Trip Mechanics

If at any point, a monitoring instrument reaches set point, it can reduce reactor power by inducing either a reverse or a scram of the SSR. A reverse occurs when the electric drives engage to move the five SSR into the core. A scram occurs in MNR when the electromagnets holding the five SSR in position are de-energized and the rods drop under gravity into the core.

In all PARET analysis, as in the SAR, a time delay of 0.025 s passes between the instrument signal and movement of the rods in both trips and reverses [Sec.08,Pg.8-10,3].

As discussed in the Shim/Safey and Regulating Rods section, all simulations assume the SSR to be worth a total of -75 mk and positioned at 50% withdrawn during the simulated reactor operation. Thus, at the instant a reverse or trip is initiated the SSR are positioned at 50% withdrawn, meaning the rod tips are 30 cm above the bottom of active core and 30 cm below the top of the active core. The fuelled (active) height of the core is 60 cm [Table5-2,3].

No neutron absorbing rod has a uniform reactivity incremental worth, that is to say, for each cm the rod is inserted into the core, a different amount of negative reactivity will be added to the reactor than the last cm. This non-uniformity occurs despite the rod's dimensional and compositional uniformity because the flux in the core is not uniform; one cm of rod length inserted into the center of the core will absorb more neutrons in that high flux area than the same rod section being inserted into the very top of the reactor where neutron flux is lower. Therefore, when simulating a reactor trip in PARET, the user cannot simply insert the worth of the rods above the core in a linear manner over the insertion time duration – unless an approximation was all that was required.

The total bank value of the SSR rods from historical core arrangement 54A is -93 mk [17]. Since the shape of rod profiles have been found to remain constant and no incremental rod worth profile of rods worth a total of -75 mk for MNR is available, the 54A rod profile has been scaled by a factor of 75/93=0.806 to obtain a reasonable approximation. The resulting scaled rod bank worth is shown in Figure 23.

The rate of a reverse insertion dictated in the PARET simulations is equal to the drive speed of the SSR rods, 0.113 cm/s [Sec.05,3]. PARET users can dictate the reactivity worth and insertion speed of the SSR rods upon a trip or reverse.

3.6 Coolant Flow

When the reactor operators set the total core flow rate, the butterfly valve V1 is adjusted and the flow is measured by flow instrument F1 of Figure 3. This flow rate is the only flow rate the operators actively adjust and is set to meet minimum flow values per reactor power in the OLC document [Sec.6.1,6]. In practice, MNR operators typically set the flow at a single high flow rate appropriate for top allowable power, rather than incrementally increasing flow rates as power is ramped; the cooling circuit is stable at high flow rates.

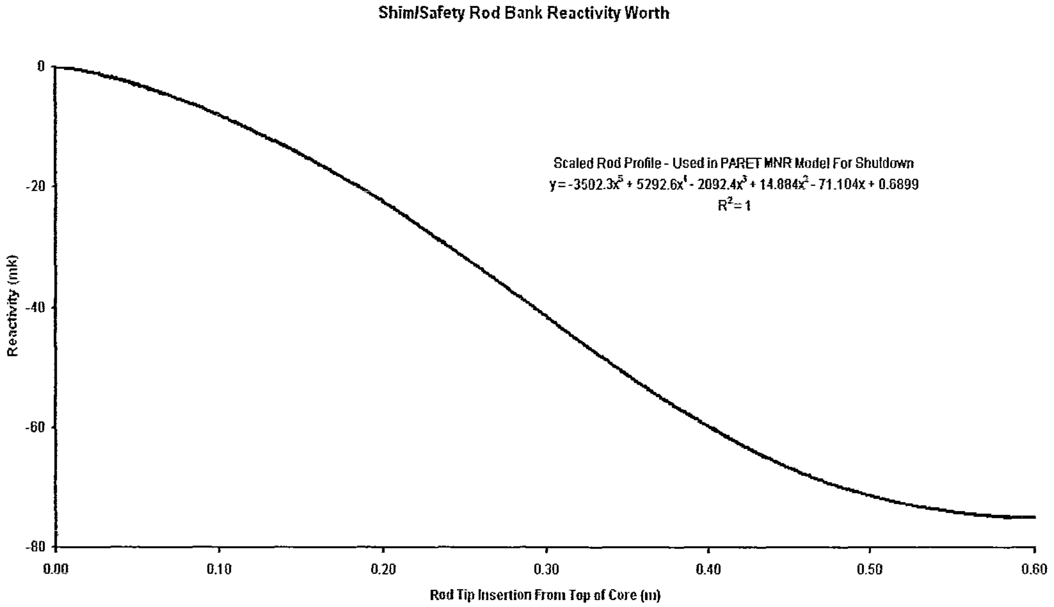

Figure 23. Shim/Safety Rod Bank Reactivity Profile Used in PARET MNR Model – Created by Scaling Rod Worth of Core 54A [17]

This total core flow includes the flow which passes through fuel assemblies, control assemblies, graphite irradiation assemblies, the fission chamber, bypass holes and any other leakage that may find its way into the plenum from the pool. Therefore, the average flow through the fuel assemblies is not simply equal to the total core flow divided by the number of fuel assemblies, but is distributed according to assembly flow resistances.

Over the life of MNR a number of studies have attempted to quantify the flow characteristics of the different types of core components; the ultimate goal of these studies is to determine the fraction of total core flow which passes through the fuel assemblies, and the fraction of flow which bypass the coolant channels adjacent to the fuel plates. Appendix A discusses the methods and findings of these reports in more detail. The useful findings of these reports have been used in the document which studies MNR thermalhydraulics, the Safe Operating Envelope of MNR (SOE) [9].

Using the electrical circuit analogy of fluid flow, the core itself is a parallel flow circuit of the core components. No direct flow measurements have been made on the core flow paths through all the different components, nor has a full scale core mockup been flow tested. However, conservative analytical estimates of the core flow paths were made in the SOE document [9]. The SOE document presents recommendations for minimum core flow to avoid bulk boiling, and these recommendations are adopted directly into the OLC document [Pg.6,9]. The same methods used to develop the analytical flow estimates in the

SOE report and adopted by the OLC document are used in the PARET model of MNR to dictate model flow through cooling channels.

Although the OLC document dictates the minimum allowable total core flows, this value cannot be used directly in the PARET MNR model. The user cannot dictate total core flow rates to PARET because PARET doesn't simulate the entire core; it only simulates a few representative fuel plates and their adjacent coolant channel. The user must directly tell PARET the coolant mass flow rate through the modeled coolant channel.

To determine an appropriate coolant channel flow rate to specify in the PARET MNR model, a portion of the analytical work completed for SOE document must be studied. This pertaining portion is shown in Figure 24, and expresses flow through various core components as a function of total core flow.

Both the MNR fuel plates modeled in PARET are from a standard 18 plate fuel assembly. Figure 24 is used to determine the coolant flow rate through the 18 plate fuel assembly as a function of total core flow. The assembly flow is divided by the number of coolant channels in a standard assembly to obtain the per channel flow.

Figure 24 predicts the flow through a standard 18 plate fuel assembly for any given total core flow, assuming 25 bypass flow holes are open in the core. Bypass holes allow pool water to flow around the outside of the fuel assemblies, but contribute to the loss of flow through coolant channels since minimum total core flow is equal to the sum of total coolant channel flow plus all flow which doesn't pass through the coolant channels. The administrative limit for number of open bypass holes is 24, and the PARET model of MNR would assume this number of holes are open; however, no resource makes predictions for fuel assembly flow in a core with exactly 24 holes open [Sec.6.1,6]. Using the flow values for 25 open holes will make a conservative estimate of the 24 hole case in PARET trip map analysis.

There are a number of flow uncertainties which have been considered in the MNR model. When the reactor operator sets the total core flow to be the nominal value, e.g. $1900\,GPM$, there is some uncertainty in the flow measuring instrumentation. SOE analysis has used an uncertainty of 5%, and the same uncertainty is used in the PARET model [Sec.3.3,9].

Once flow through a standard fuel assembly has been estimated flow variability within fuel assemblies, between coolant channels, must be accounted for. Figure 25 shows that the outermost coolant channel is expected to have the lowest flow compared to average channel flow, 94%. Given this outermost plate is associated with the highest plate-to-plate peaking factor (see Figure 17), the combination of the two conditions create the most likely place for boiling to occur, the most conservative case for analysis and the conditions that are used in the PARET model of MNR. However, the outermost coolant channel in the standard 18 plate fuel assembly is heated by only a single fuel plate which makes the PARET model conservative. The very outermost plate is not fuelled, and therefore generates zero heat, while PARET models the coolant channel as if it is heated on both sides.

The following summarizes how coolant flows for the PARET MNR model are derived:

The SOE document developed the minimum flow requirements according to power, and these recommendations are given in the OLC document as [9,6]:

Power Range	100kW → 2MW	2.01MW → 3MW	3.01MW → 4MW	4.01MW → 5MW
Min. Flow	900Usgpm	1200Usgpm	1600Usgpm	1900Usgpm

Operating MNR with flow set to these above nominal flow rates is subject to 5% flow measurement error, which means the following rates may be the actual flow total core flow rates [Sec.3.3,9] :

Power Range	100kW → 2MW	2.01MW → 3MW	3.01MW → 4MW	4.01MW → 5MW
Min. Flow	855Usgpm	1140Usgpm	1520Usgpm	1805Usgpm

Using Figure 24, the flow through the standard 18 plate fuel assembly as a function of the above minimum total core flow when 25 bypass holes are open is:

Power Range	100kW → 2MW	2.01MW → 3MW	3.01MW → 4MW	4.01MW → 5MW
18p Flow	0.95 lpm	1.24 lpm	1.63 lpm	1.93 lpm

Taking 94% of the 18 plate flow to account for channel-to-channel inter-element flow uncertainties (see Figure 25), dividing by 17 to obtain per channel flow values and then converting appropriately to obtain the required kg/m^2s units, the flow used in the model is [Fig.6.14,16]:

Power Range	100kW → 2MW	2.01MW → 3MW	3.01MW → 4MW	4.01MW → 5MW
Coolant Flow	262 kg/m^{2}s	342 kg/m^{2}s	449 kg/m^{2}s	532 kg/m^{2}s

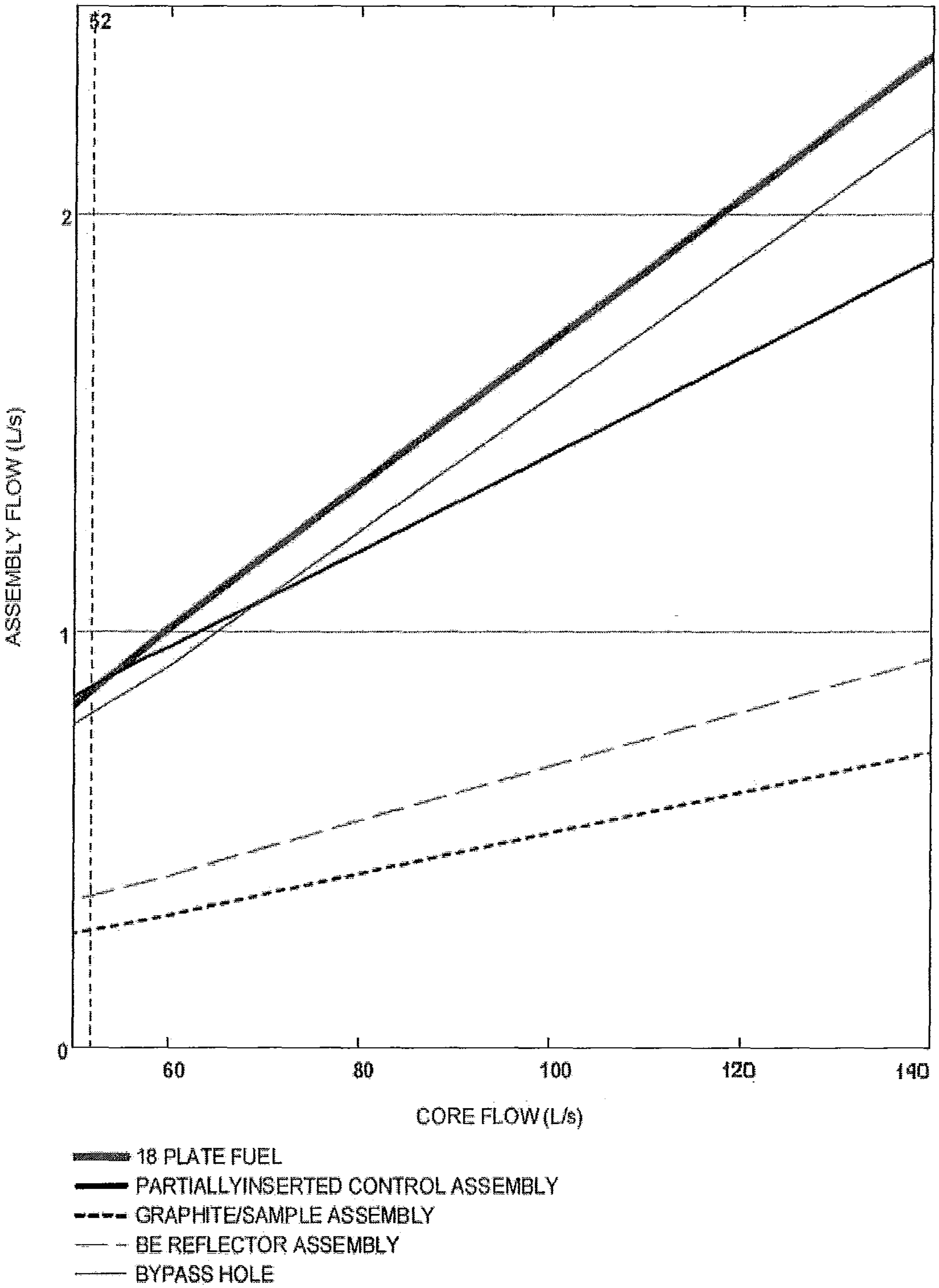

Figure 24. Flow Through Assemblies at Various Total Core Flow Rates [The figure in the reference is incorrect, the author supplied the correct version shown above, Pg.7,Appendix I,9]

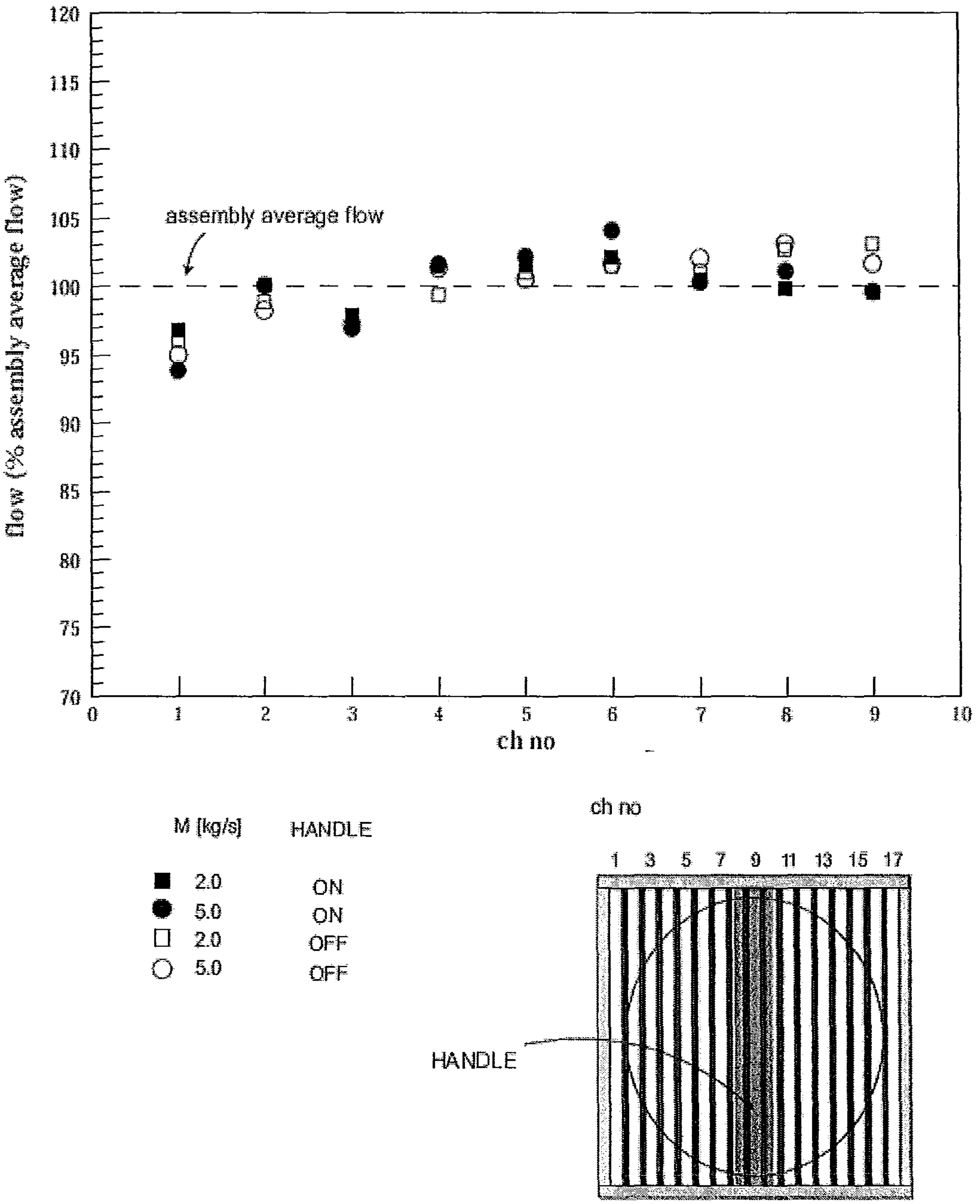

Figure 25. Channel-to-Channel Flow Distribution of 18 Plate Fuel Assembly [Fig.6.14,16]

3.7 Miscellaneous Model Considerations

For all transients modeled at high power, >0.1 MW, it is assumed the two uncompensated ion chambers, the neutron flux detecting devices of the two 125% HF safety channels, have been appropriately adjusted in position relative to the core to be trip capable at the nominal reactor power level. At lower reactor powers (say 1 MW) these chambers need to be closer to the core than for relatively higher powers (say $3\,MW$). Moving these chambers is not a routine task, and operators only move the chambers' position when the reactor is going to operate for a long period of time at a new power level [29].

If MNR is to operate at a nominal power level of $3\,MW$ for a long period, the safety channels are configured to trip at 125% HF, $3.75\,MW$. Thus, every morning during startup when reactor power passes between $1\,W$ and $3\,MW$ during the approach to nominal power, the safety channels are set to trip at $3.75\,MW$.

Low power operation ($<0.1\,MW$ with natural convective coolant flows) of MNR is not as common as high power operation, but its occurrence is common enough the SAR chose to evaluate the trip capabilities within this power range [10]. The compensated ion chambers, which are the neutron flux detecting devices for the Log N and Lin N channels, are functional at low power; therefore, the $<30\,s$ period inhibition, $<10\,s$ period reverse and $<3.8\,s$ period scram are always effective at low power and the +7% LSE reverse is effective at low powers during automatic control [Table8-1,3]. It is assumed for all simulations at high and low powers, unless otherwise noted, that operation is in automatic mode. It is assumed the Log N chamber is never moved to enable the 110% HF reverse at low powers.

Because the neutron flux is too small for the uncompensated ion chambers to monitor, the safety channels are not effective at low power operation [Sec.8.2.3,3]. Therefore, when simulating low power operation it must be assumed the two 125% HF safety channels will induce a trip at the high power settings the reactor is then tailored for. For example, if MNR is operating for a few hours at low power while it otherwise operates at $3\,MW$ the safety channels and the 110% HF will signal a scram/reverse at $(3)*(1.25)=3.75\,MW$ and $(3)*(1.1)=3.3\,MW$, respectively. To be conservative then, for all low power simulations it must be assumed the safety channels and the 110% HF reverse are configured for the largest licensed high power operation allowable, $5\,MW$, and will then signal a scram at 125% of $5\,MW$, $6.25\,MW$, and a reverse at 110% of $5\,MW$, $5.5\,MW$.

When developing the PARET MNR model, uncertainties in the coolant flows were incorporated into the model in a conservative manner. Similarly, one additional uncertainty needs to be considered, that of the core thermal power. The core power is calculated for MNR operators by measuring the coolant outlet temperature and accounting for the heat capacity. The variance of the temperature measuring device means nominal core power may be off by as much as 10% [Sec.3.4,9]. Therefore, anytime a nominal reactor power is simulated it needs to include an additional 10% when modeled in PARET. For example, modeling a transient with a nominal initial power of $5\,MW$, is simulated at $5.5\,MW$ and the overpower trip set points also include the 10% uncertainty, so the 125% HF trip is set at $(1.25)(5.5)=6.875\,MW$.

4 Accident Event Categories

The document Summary of Reactor Trip Coverage for Accidents Analyzed in MNR SAR 2002 predicts the effective trip coverage for all the postulated initiating events (PIE) analyzed in the SAR [10,1]. For each PIE discussed in SAR 2002, the previous SAR trip evaluation illustrates which engineered safety systems are and aren't thought to be effective in preventing the progression of power transients [10]. The SAR also lists the trips in the chronological order in which they are predicted to occur during the course of a transient, and are numbered as such within each PIE.

In order to develop further confidence in the accuracy of the SAR trip assessment, the CNSC has requested further analysis of the effectiveness of these safety systems. Running reactor transients with a benchmarked software package known to be capable of simulating power transients, such as PARET, is a way to satisfy this requirement. The information contained within the SAR guide trip map development for MNR, and trip map categories are organized in the same classification as those developed in the SAR trip analysis [10]. Each trip map category, like the categories from SAR Table 1, is named after the major phenomenon which initiates the transient, the PIE [10].

There are many accident event categories analyzed in the SAR assessment and each one is capable of adding reactivity to the reactor. However, PARET does not have the ability to model all of the PIE cases, such as those categories which require modeling of the secondary coolant circuit, or of the pool itself; PARET doesn't model these systems and it is impossible to have the PARET model a trip on low pool water level, for example. As a result, trip maps are only developed for the following categories capable of being modeled in PARET: Loss of Regulation Rod Control from High and Low Power, Irradiation Sample Handling Accidents, Withdrawal of Shim Safety Rods from High and Low Power and Fuel Handling Accidents. All categories can be considered reactivity insertion accidents (RIA).

This section discusses the assumptions made in each postulated initiating event accident category, in addition to those assumptions of the general PARET MNR model discussed previously. The range of initial power levels, reactivity insertion rate and max reactivity inserted for each trip map category are defined based upon the extreme or limiting expectations of each category.

The general PARET model of MNR, detailed previously, is utilized in all PIE categories. It should be noted that in all categories, compounding accident event scenarios are generally not considered and it is assumed the operational administrative limits in the OLC document are being met – except that the only shutdown system active is the one being examined. In practice, all shutdown systems are made available before criticality occurs and the result is layered trip coverage in most operating conditions.

4.1 Loss of Regulation Rod Control at High Power

During normal reactor operation the single regulating rod is actively controlling the criticality of the reactor. The control system withdraws the rod to add positive reactivity and inserts the rod to absorb neutrons and add negative reactivity. The loss of the regulating rod control is the postulated initiating event. It is assumed in this RIA that the motor which normally drives the regulating rod up and down to control power in the reactor malfunctions and drives the regulating rod entirely out of the core, causing reactor power to rise.

The high power description of this category requires that the trip map be developed between initial reactor powers of $100\,kW$ and $5\,MW$. These two values form the range of the trip map's ordinate axis for this PIE category. Nominal reactor powers above $100\,kW$ require forced convective cooling, and this area is colloquially named high power [Sec.6.2.2,6].

Since an administrative regulation limits operating the reactor to regulating rod positions between 20% and 80% withdrawn, the limiting maximum reactivity insertion case is withdrawing the regulating rod from 20% withdrawn [Sec.17,3]. Therefore, this limiting case is applied in all simulations of this category. The modeled reactor is critical at the beginning of all simulations, $\rho = 0$, and the regulating rod is at 20% withdrawn before the transient begins and the regulating rod is driven out of the core.

The reactivity worth of the regulating rod is administratively limited to between 3.5 and $6\,mk$ [Sec.17.3.2.2,3]. Modeling a regulating rod to be worth $6\,mk$ tests the simulations with the maximum bounding case; when the rod is driven from the core, the maximum amount of reactivity will be inserted. No rod profile worth a total of $6\,mk$ is available, therefore, the $6\,mk$ regulating rod worth profile is modeled by scaling up the regulating rod profile from the historical core arrangement 54A [17]. The regulating rod from core 54A is worth $3.77\,mk$, and its profile is scaled by a factor of 6/3.77=1.59 to obtain the profile shown in Figure 26 [17].

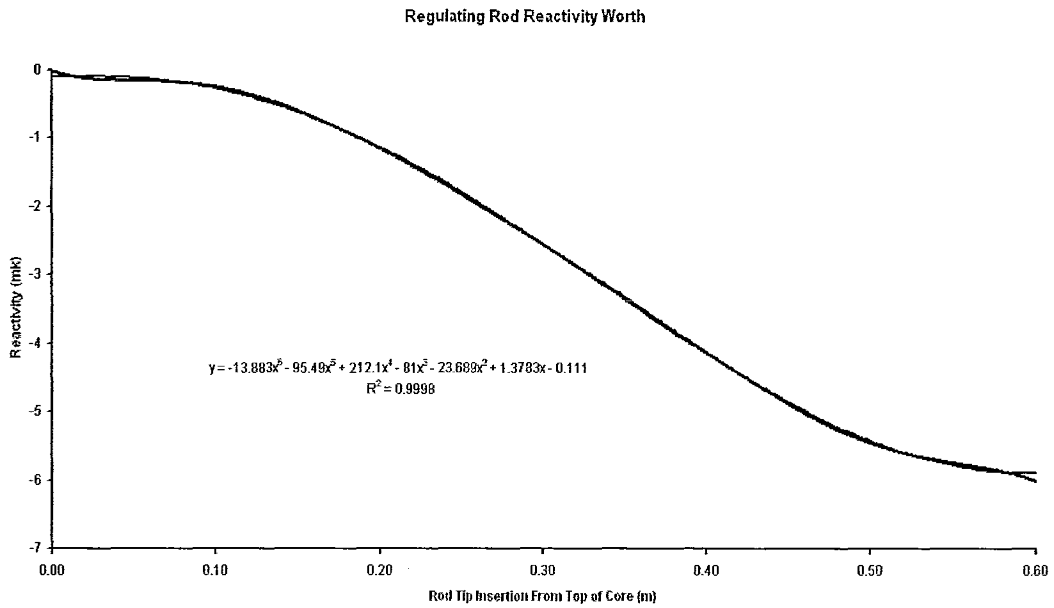

Figure 26. Regulating Rod Reactivity Profile for PARET MNR Model – Creating by Scaling Rod Worth of Core 54A [17]

According to the polynomial in Figure 26, the reactivity worth of the modeled $6\,mk$ rod at the 20% withdrawn position (rod tip $0.48\,m$ from top of core) is $-5.25\,mk$. Therefore, totally withdrawing this $6\,mk$ rod from the core, starting at the 20% withdrawn position inserts $5.25\,mk$; this is the maximum inserted reactivity limit for any rate of reactivity insertion within this loss of reactivity control category. If two transients are simulated in this category, one with a reactivity insertion rate of $0.1\,mk/s$ and the other with $10\,mk/s$, for example, both rates only insert reactivity until $5.25\,mk$ has been inserted – which would take $5.25/0.1=52.5\,s$ and $5.25/10=0.525\,s$, respectively.

To determine the range of the abscissa of this trip map category, plausible reactivity insertion rates should be examined. Knowing the active height of the core to be $600\,mm$, and that the rod is driven at a speed of $1.13\,cm/s$, it would take $60\,cm/1.13\,cm/s=53.1\,s$ to withdraw the rod from full insertion [Sec.05,3]. For a $6\,mk$ rod this corresponds to an average reactivity insertion rate of $6\,mk/53.1\,s=0.113\,mk/s$. Withdrawing the rod from 20% withdrawn position would take $48\,cm/1.13\,cm/s=42.5\,s$, giving an average insertion rate of $5.25\,mk/42.5\,s=0.124\,mk/s$.

Obviously each incremental distance the rod is withdrawn (or inserted) from the core is worth a different amount of reactivity than the one before it, so a variable reactivity insertion rate would be expected upon rod withdrawal, but these average values (0.113 and $0.141\,mk/s$) serve as points of interest when estimating the rates of insertion which need to be tested with this accident category. The trip maps created for this category include these average reactivity insertion rates within its range.

Examining the modeled $6\,mk$ regulating rod in Figure 26, the largest incremental reactivity insertion rate at a drive speed of $1.13\ cm/s$ is approximately $0.18\ mk/s$ and the minimum is approximately $0.01\ mk/s$. Therefore, the trip maps created for this category include the range of 0.01 and $0.18\,mk/s$.

To reiterate, none of the values developed above are expected to be sustained over the course of a regulating rod withdrawal, but are expected reactivity insertion rate extremes and form conservative bounds for the rates which are transient tested on the PARET MNR model for trip effectiveness. Presumably, if the rod profile in Figure 26 was scaled down to be worth a total of $3.5\ mk$ (the administrative low limit for regulation rod worth), a smaller incremental reactivity insertion range could be found, however, $0.01\,mk/s$ is already a very small value compared to what is plausibly expected for this accident category.

So far it has been assumed that the regulating rod drive mechanism only moves at its designed $1.13\,cm/s$ drive speed. As discussed previously, this trip map development study generally doesn't assume compounding accident event scenarios – in this accident category the single scenario is the loss of regulating rod control. However, out of interest, this trip map category is developed beyond the plausible range of 0.01 and $0.18\,mk/s$ and up to $10\,mk/s$. The only way to obtain reactivity insertion rates as high as $10\,mk/s$ during a loss of regulating rod control accident is for the drive mechanism to increase its drive speed during the primary loss of control event – a compounded accident event scenario assumption made out of interest simply to test the PARET MNR model up to $10\,mk/s$. These expanded reactivity insertion rates still observe the maximum $5.25\,mk$ total reactivity insertion.

4.2 Loss of Regulation Rod Control at Low Power

Like the previous category, this PIE involves the loss of the regulating rod control. However, this category examines the ability of the shut down systems to arrest a power transient in the low power range of $1\,W$ to $100\,kW$. Within this power range, the MNR Operating Limits and Conditions document allows the reactor to be run without forced convection and the pool becomes the primary heat sink [Pg.11,6]. The flow is therefore dictated by buoyancy forces and the mass coolant flow rate through the coolant channels tends to increase as the power of the reactor increases.

The trip maps in this category include the same 0.01 to $0.18\ mk/s$ reactivity insertion range as the Loss of Regulation Rod Control at High Power since the same mechanism is expected to be capable of inserting this reactivity rate. All reactivity insertion rates stop adding positive reactivity once $5.25\,mk$ has been inserted.

4.3 Irradiation Sample Handling Accidents

Because MNR is frequently used to irradiate objects directly within the core, the capability of the trips to arrest this accident need to be examined. The nature of this reactivity insertion is non-mechanical because objects are frequently placed into position within an irradiation core site by hand.

The pool water, which also moderates the neutrons, is displaced locally when an object is placed into the core area. Since irradiated objects are usually either effective neutron absorbers or neutron transparent, their presence in the core is worth negative reactivity. A water displacement event within the core will locally remove moderator and add negative reactivity; this is assuming the water displacing object is neither made of fissionable material nor an effective moderator. Upon removal of the typical in-core object, moderating water is no longer displaced and positive reactivity is inserted; this is the reactivity insertion event which may cause a transient.

An administrative restriction places a $2\,mk$ limit on the reactivity worth of any single in-core experiment, and this is therefore the maximum reactivity insertion limit for this transient category; reactivity inserted at different rates, insert a maximum of $2\,mk$ total [Sec.7.2,6].

To develop reasonable reactivity insertion rates, it is assumed that a sample of any size couldn't be withdrawn from the reactor core manually any faster than one tenth of a second. Given that this category is meant to model momentary inadvertent operator movements rather than malicious intent, this speed should be adequate given that the placement and removal of core objects is normally done with attentive care. $2\,mk$ of reactivity worth inserted with this speed is equivalent to the maximum $20\,mk/s$ insertion rate expected in this category. The chosen minimum reactivity insertion rate of $0.2\,mk/s$ is the product of withdrawing the $2\,mk$ sample in ten seconds. Sample withdrawal is typically done over a 10-30$\,s$ duration with close attention to instrumentation [29].

4.4 Withdrawal of Shim/Safety Rods at High Power

The PIE in this category is the loss of control of the entire shim/safety rod bank. This is an implausible event since there is a dedicated independent drive for all five SSR, and thus they are on separate circuits. The simultaneous withdrawal of all five shim safety rods can only be achieved through a set of compounding events, and compounding events are not otherwise being considered in this study; however, this is the manner this category has been analyzed in the SAR assessment [10].

This category requires one to assume that the same bank of SSR responsible for initiating the loss of reactivity control accident is also responsible for arresting it. This category requires the assumption of operator error to simultaneously drive all five motors. It is assumed the rods are driven out at the normal driving speed of $0.113\,cm/s$ [Sec.05,3]. It is assumed that these same rods being driven out of the core in an uncontrolled manner work properly when either a scram or reverse signal is sent by the reactor's instrumentation. It should be noted that the magnets which deactivate during a trip and cause the rods to drop do not depend on the proper operation of the drive motors.

As described in the SSR section of the PARET MNR model description, criticality cannot occur before the SSR position is 50% withdrawn. The limiting worst case scenario is withdrawing the shim safety rods from this 50% withdrawn position because from this position, the most amount of reactivity is available to be added upon withdrawal.

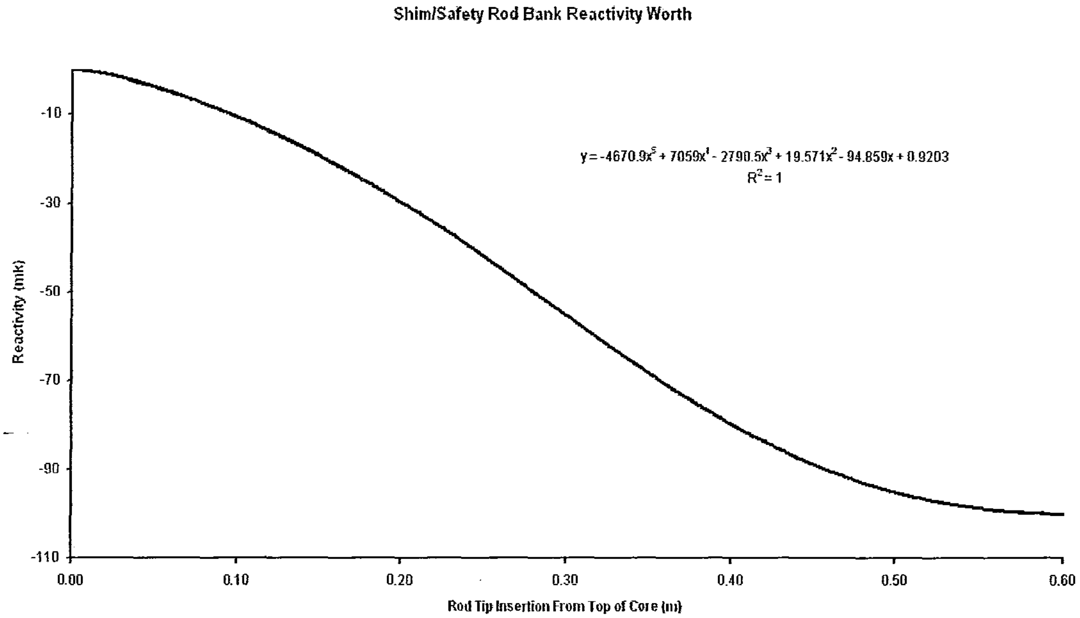

Figure 27. Shim/Safety Rod Bank Reactivity Profile Created by Scaling Rod Worth of Core 54A [17]

Expected extreme reactivity insertion rates can be determined by examining the polynomial on Figure 27 which shows a modeled -100 mk rod profile – the historical maximum rod bank worth is -100 mk. The modeled profile is obtained by scaling the historical 54A core rod bank worth up. Given a constant 0.113 cm/s rod drive speed, the largest incremental reactivity insertion the modeled profile from Figure 27 is 0.3 mk/s. The smallest is approximately 0.006 mk/s. These reactivity insertion rates bracket the envelope of rates tested in this trip map category.

If the bank of SSR were to completely withdraw from the 50% withdrawn position, according to the polynomial of the modeled profile in Figure 27, 55 mk would be inserted in 30 cm/0.113 cm/s =265.5 s - an average of 0.21 mk/s. The only time all 55 mk will actually be inserted though, is if all trip mechanisms fail since the SAR documents assume a trip will stop the SSR withdrawal process when the same rods move into the core following a scram or reverse [10].

MNR has various instrument channels which can induce an inhibition [Table 3,6]. An inhibition disables the ability of the SSR drive motors to drive the rods out of the core. Because the SSR are operated manually, an inhibition to all other RIA would have no transient arresting effect. This accident category is the only postulated accident an inhibition would have an effect upon, however, the SAR assumes the inhibitions are unavailable and therefore are not credited [10].

One of the conservative assumptions made for the PARET MNR model is that the amount of negative reactivity that would be inserted during a scram or reverse would be equal to the scaled curve shown in Figure 23. The curve in Figure 23 is based upon the assumption that the total SSR worth is only -75 mk - the smallest reactivity worth expected based upon historical core measurements, as discussed. So for this accident category, the driving mechanism behind the transient is a SSR worth of $-100\,mk$, but the same bank of rods are assumed to be worth only -75 mk upon a scram or reverse. Clearly, this situation is not physically possible; however, this is the result of making conservative assumptions for an idealized core.

4.5 Withdrawal of Shim/Safety Rods at Low Power

The accident scenario postulating the withdrawal of shim/safety rods during low power reactor operation is identical to that of the high power case except reactor core cooling is achieved by natural circulation and initial reactor power in the PARET simulations is between $1\,W$ and $0.1\,MW$.

Rod drive speed is identical to the high power case, and the shim/safety rod bank reactivity profile is still that as shown in Figure 27; therefore the same 0.006-0.3 $mk\,/\,s$ reactivity insertion range is expected to be plausible.

4.6 Fuel Handling Accidents

As with any other reactor, the MNR fuel assemblies need to be changed periodically. This process is done by hand, whereby the operators stand above the core and manipulate the core assemblies with a long hooked tool which reaches into the pool [29]. All fresh and used fuel assemblies are moved across the top of the core at some point in the fuel changing procedure. The fuel handling accident category postulates dropping a fuel assembly into the core during the fuel changing procedure.

Fuel handling operations are only conducted when the reactor is shutdown in a subcritical state [18]. The fact that this postulated accident can only occur at shutdown power levels negates simulating these transients in the MNR PARET model at various powers; it also makes developing a trip map for this category impossible since trip maps require multiple initial power levels for a vertical axis. Nonetheless, transients are still modeled in PARET from a single shutdown power level.

When the reactor is in a shutdown state, the entire bank of SSR is not to be inserted completely into the core, but rather be inserted enough into the core to induce subcriticality and have an amount of negative reactivity remaining above the core, poised for further insertion. This position is called the Safety Bank position. The SAR states that the SSR should be poised such that a "substantial amount of reactivity remains to be inserted" [Pg.1-13,3]. No document specifies a specific minimum value of reactivity to be available above the core for shutdown while in Safety Bank position, however, the operators have been using -30 mk in practice [29].

Since the MNR PARET model assumes the SSR are worth -75 mk total, positioning these rods with -30 mk above the core in reserve would require the rods to be 47% withdrawn (rod tips 0.318 m from top of core), according to the polynomial describing the shutdown rods worth in Figure 23. At the 47% withdrawn position, the rods have inserted -75+30=-45 mk into the core. Since rules restrict the reactor from going critical before rods are withdrawn 50% (rod tips 0.3 m from top of core), at which position the in-core rods are worth -41.3 mk, the modeled reactor cannot become critical until 45-41.3=3.7 mk is added. In other words, with the SSR at Safety Bank position, the PARET MNR model core is 3.7 mk subcritical.

The worst postulated fuel handling accident is dropping a fresh (0% burnup)18 plate fuel assembly into the central grid location 4C, which is worth +43 mk [19]. Obviously, for grid location 4C to be vacant, the burned up 18 plate fuel assembly must be removed. Removing the used fuel assembly adds -27 mk to the -3.7 mk subcritical core [19].

To simulate this conservative case in the MNR PARET model, the point kinetics of the fuel assembly addition must be considered to develop an equivalent model since PARET is not able to model anything but a critical core. The model cannot be made -27-3.7=-30.7 mk subcritical at time zero of the transient, before positive reactivity (which represents the dropped fresh fuel assembly) is added. Therefore, to model this accident, the PARET model is made critical at time zero. Adding the fresh assembly to the 4C location adds 43-(27+3.7)=12.3 mk. The SAR analysis assumes this assembly drops into the empty grid location upon mishandling in 2 s, giving an insertion rate of 12.3 mk /2 s =6.15 mk/s on average [19].

Since the PARET model cannot begin the transient as subcritical, the model is assumed to be critical at an extremely low initial power of 1 W at the time the transient is initiated.

5 Results

5.1 Introduction

This section summarizes the results of simulating the postulated accident event categories with the PARET MNR model and examining the ability of each engineered safety system to avoid the thermal limits developed for this trip coverage analysis. As discussed previously the thermal limits for this analysis are the onset of bulk boiling, film boiling, transient boiling or $450\,^{o}C$ clad surface temperatures. The fuel temperatures were monitored to assess the study in the context of this safety limit ($450\,^{o}C$).

It should be noted that to develop these results hundreds of simulations were run on the PARET MNR model. Of these many transients, none reached $450\,^{o}C$ fuel temperatures; the maximum fuel centerline temperature reached in any successfully arrested accident transient was $145\,^{o}C$ - significantly below the thermal limit of $450\,^{o}C$ clad surface temperatures.

If during a simulated transient a safety system failed to prevent the onset of a thermal limit it was regarding the onset of one of the boiling regimes. Most transients progressed slow enough that bulk boiling was induced before DNB.

The results are presented as a single trip coverage map for each engineered safety system within each postulated accident event and then the individual safety system trip maps are superimposed to create a cumulative trip coverage map for each accident event category. Many sample transients are plotted to show the physics of reactor power, fuel/coolant temperatures and shutdown systems within a PARET transient.

Throughout the discussion of the simulation results, the powers discussed as well as the powers plotted on the trip coverage maps are nominal (do not include the additional 10% uncertainty). All PARET simulations were run with the 10% uncertainty and the data used for the transient plots come directly from these simulations, therefore the transient plots include the 10% power uncertainty at transient time zero.

Unless specifically noted otherwise, all discussion of fuel, clad and coolant temperatures are in the hottest Channel of the PARET MNR model. As discussed in the development of the model, two parts of the core are being modeled, the hottest expected fuel plate and associated coolant channel (Channel 1) as well as the average expected fuel plate and coolant channel (Channel 2). As expected, in no transient did the average power channel ever reach a thermal limit before the hottest channel.

5.2 Steady State Power Boiling

Before presenting and discussing the transient inducing accident categories, steady state boiling in the PARET MNR model is investigated to aid discussion in later transient analysis.

As discussed in the coolant flow description of the PARET MNR model, there is a minimum core coolant flow rate which must be met according to the operating nominal power range of MNR. Each minimum coolant flow rate was prescribed by the SOE document to avoid bulk boiling [9]. Table 1 shows the steady nominal reactor power necessary to induce bulk boiling in the hottest coolant channel of the MNR PARET model at the administrative minimum core flow rates. Powers listed are nominal powers, meaning they are simulated with an additional 10%.

Under natural convection conditions, the PARET MNR model estimates bulk boiling will not occur in the hottest coolant channel until steady state power reaches $2.4\,MW$. At a coolant channel mass flux of $262\,kg/m^2s$ (the best estimate for coolant channel mass flux based upon a $900\,USgpm$ core flow rate with 25 open bypass holes) the PARET MNR model induces bulk boiling at $3.3\,MW$. And as should be the case, power required to induce boiling increases when the coolant channel mass flux increases. When MNR is operating within the 4.01 - $5\,MW$ range, operators are required to set total core flow at a minimum of $1900\,USgpm$ (which is estimated to equal a coolant channel mass flux of $532\,kg/m^2s$ when 25 bypass holes are open) and this flow requires $6.8\,MW$ before bulk boiling will set in. Table 1 shows the PARET MNR model agrees with the SOE document analysis because when core flow rates are set according to the reactor power specific SOE recommendations, bulk boiling is avoided.

Power Range	1 W → 100 kW	100 kW → 2 MW	2.01 MW → 3 MW	3.01 MW → 4 MW	4.01 MW → 5 MW
Minimum Total Core Flow	Natural Convection	900 USgpm	1200 USgpm	1600 USgpm	1900 USgpm
In Channel Coolant Flow	-	262 kg/m^{2}s	342 kg/m^{2}s	449 kg/m^{2}s	532 kg/m^{2}s
Bulk Boiling Inducing Power	2.4 MW	3.3 MW	4.4 MW	4.8 MW	6.8 MW

Table 1. Steady State Power Required to Induce Bulk Boiling in PARET MNR Model

The steady state powers required to induce bulk boiling shown in Table 1 will be referred to in later transient discussions to show how the onset of bulk boiling under transient conditions can occur at different power levels according to the PARET MNR model. As discussed previously, there is some questioning the applicability of codes utilizing thermalhydraulic correlations developed with steady state data for transient conditions [P.200,20]; transient simulation comparisons to Table 1 are therefore of value for discussion.

5.3 Loss of Regulation Rod Control at High Power

During a loss of regulation rod control accident from high reactor powers, the SAR trip evaluation credits the +7% LSE reverse, 110% HF reverse, both 125% HF scram channels, the manual scram and the self limiting shutdown as being capable of preventing fuel damage [10]. The SAR does not credit the $<10\,s$ period reverse nor the $<3.8\,s$ period scram because the authors were uncertain the reactivity insertion rates would be large enough to force a short reactor period [Note1,10].

All trip coverage maps and sample transient plots for this category are shown in Figure 28 through Figure 42. The PARET MNR model predicts the $<10\,s$ period reverse, the $<3.8\,s$ period scram, manual scram and self limiting shutdowns are unlikely to prevent bulk boiling in the hottest coolant channel during a loss of regulation rod control accident from high power. The PARET MNR model predicts the +7% LSE reverse, 110% HF reverse and both 125% HF scrams would prevent the onset of bulk boiling. These findings are based upon simulations using linear reactivity insertion rates.

Each trip coverage map in this accident category highlights the expected reactivity insertion range which is based upon regulating rod worth and drive speed (the 0.01 and 0.18 mk/s range) as explained in the Accident Event Categories section of this report.

Further details related to each individual safety system response and the resulting cumulative trip coverage-map associated with this accident category are given in the following sections.

5.3.1 Reverse on <10 Second Period

Figure 28 shows the trip coverage map for the $<10\,s$ period reverse, it shows the PARET MNR model predicts the trip is capable of preventing boiling in only a small area of the expected range of insertion rates, between 0.01 and $0.18\,mk/s$.

There is no trip coverage at insertion rates less than $0.10\,mk/s$ because reactivity is not being inserted fast enough to achieve reactor periods $<10\,s$; $0.10\,mk/s$ is the minimum insertion rate which gives periods $<10\,s$ for an initial reactor power of $0.1\,MW$.

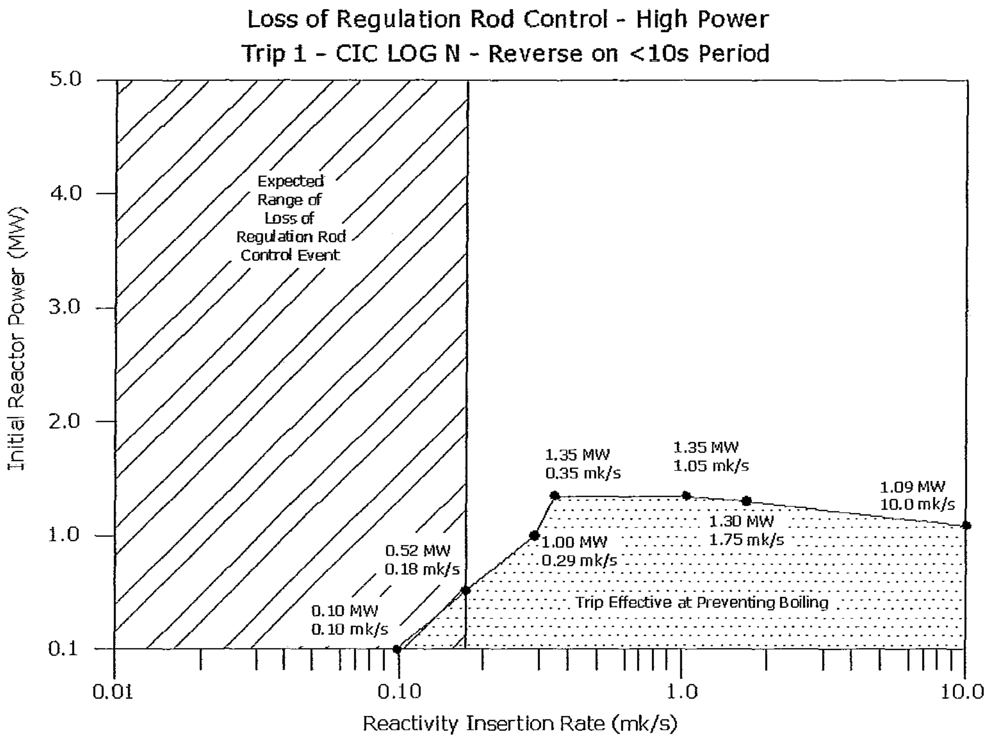

Figure 28. Trip Coverage Map – Loss of Regulation Rod Control HP – Trip 1

Figure 29 shows a single transient simulation from the $<10\,s$ period reverse trip coverage map. This sample simulation is taken from the $<10\,s$ period reverse trip boundary line on Figure 28; therefore, at this initial reactor power level, inserting less than $0.18\,mk/s$ is not enough to force reactor periods $<10\,s$. Initial reactor power is nominally $0.52\,MW$ and is simulated at an initial power which includes the 10% uncertainty, $1.1{*}0.52\,MW = 0.572\,MW$. Reactivity is linearly inserted at a rate of $0.18\,mk/s$ to a maximum of $5.25\,mk$, which takes $5.25\,mk/0.18\,mk/s = 29.2\,s$.

At $17\,s$ reactor power begins growing at a fast enough rate the $<10\,s$ period instrument signals a reverse, and immediately afterwards the SSR begins inserting enough reactivity to counteract the $0.18\,mk/s$ still being added and reduces total reactivity. Power grows until $29.2\,s$ where it reaches a maximum of $2.0\,MW$ before being reduced due to the SSR insertion. Maximum reactor power is well below the nominal steady state $2.4\,MW$ expected to produce boiling (as predicted by Table 1). A change in the reactivity slope is clear at $29.2\,s$; this is the point where the regulating rod has fully withdrawn and can no longer add positive reactivity.

Note the fuel and clad temperature are constantly separated by only a few degrees - a result of the thin fuel plates and high fuel material conductivity. On the scale used in Figure 29 their temperatures are plotted very close together. The maximum fuel temperature is $100\,^{o}C$ at the peak reactor power, far below the $450\,^{o}C$ thermal limit and too low to induce even nucleate boiling at the clad surface. The peak coolant temperature is 83 ^{o}C - well below the 117 ^{o}C saturation temperature.

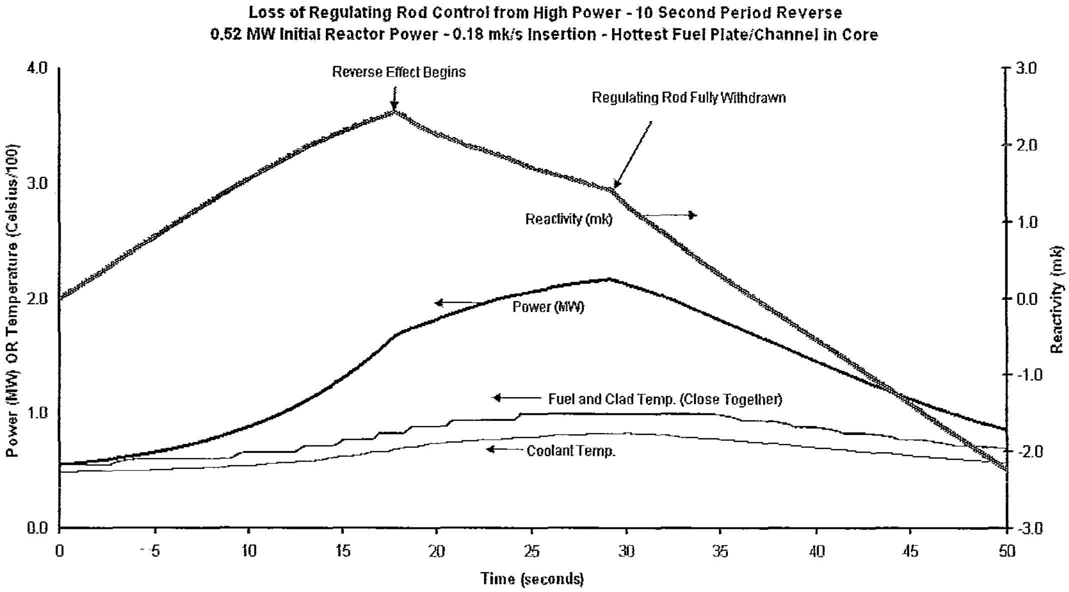

Figure 29. Transient from Simulation on <10s Period Reverse Map

5.3.2 Scram on <3.8 Second Period

Within the expected reactivity insertion rate range for this accident event category, *i.e.* between 0.01 and $0.18\,mk/s$, the PARET MNR model predicts the $<3.8\,s$ period scram would not be effective at preventing bulk boiling. Out of interest, the $<3.8\,s$ period scram coverage map, Figure 30, shows considerably more coverage over the high rate range (*i.e.* 0.1 to $10.0\,mk/s$) than does the $<10\,s$ period reverse (Figure 28). This is due to the faster SSR insertion upon scram compared to the reverse.

Large positive reactivity insertion rates are required to induce periods in the $<3.8\,s$ range. Figure 30 shows the slowest reactivity insertion rate capable of inducing a $<3.8\,s$ period scram is $0.28\,mk/s$ - as compared to the $0.10\,mk/s$ which is the smallest rate capable of forcing a $<10\,s$ reverse, as in Figure 28.

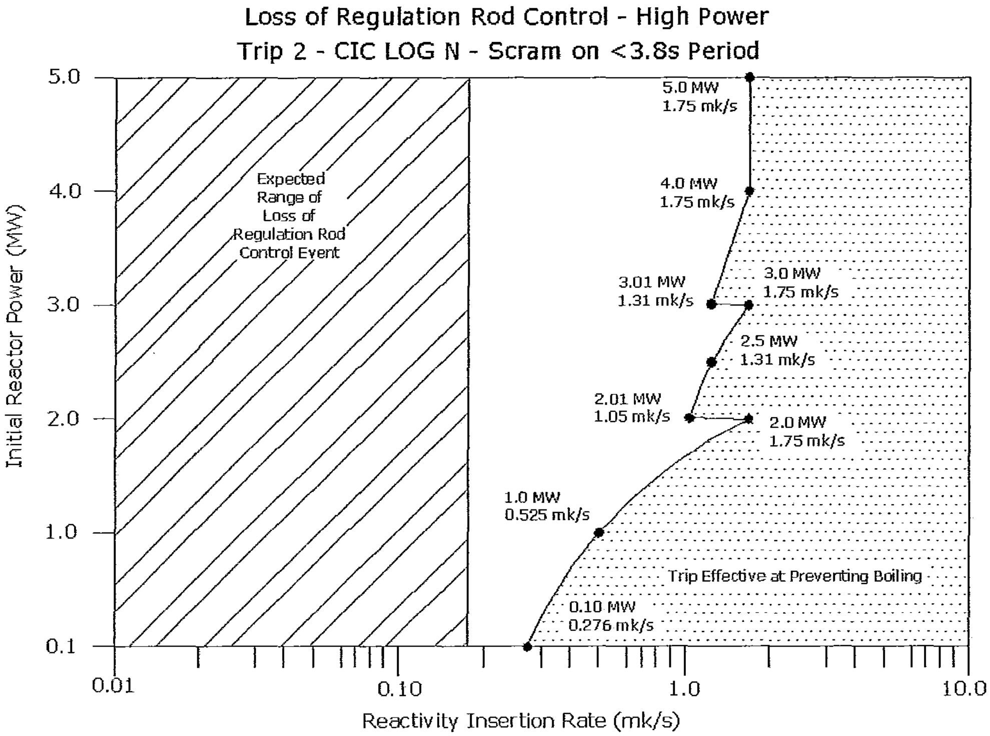

Figure 30. Trip Coverage Map – Loss of Regulation Rod Control HP – Trip 2

Just as the $<10\,s$ reverse is essentially non-effective within the expected reactivity insertion rate range, the $<3.8\,s$ scram is also not effective at preventing bulk boiling within this same range. However, the $<3.8\,s$ scram coverage up to $10.0\,mk/s$ is greater than the $<10\,s$ reverse because the SSR are moved into the core at a much faster rate during a scram than during a reverse. Not only is the $<3.8\,s$ scram effective in the lower power range of the 0.1-2 MW $262\,kg/m^2s$ flow bracket like the $<10\,s$ reverse, but it is also effective in all the power ranges of all flow brackets above $1.75\,mk/s$.

To illustrate the effectiveness of the $<3.8\,s$ period scram, a single PARET simulation (not shown) of $5\,MW$ initial power, with a step insertion of $5.25\,mk$ was run and the $<3.8\,s$ period scram was still capable of preventing bulk boiling; this step insertion with a simulation time increment of $0.001\,s$ is equivalent to an insertion rate of $5.25\,mk/0.001\,s = 5250\,mk/s$, a rate far beyond any realistic postulated value. Increasing the step insertion limit of $5.25\,mk$ to some larger value would challenge the instrument's ability to prevent boiling.

The abrupt changes in allowable insertion rates near 2.0 and $3.0\,MW$ of Figure 30 result from the changes in the minimum allowable flow rates. The $<3.8\,s$ trip coverage boundary generally shows an increase in the minimum reactivity insertion rates required to induce periods $<3.8\,s$ as power increases. As initial reactor power increases with constant flow (*e.x.* between 0.1 and $2.0\,MW$) more reactivity is required to create periods $<3.8\,s$ because the greater reactor power creates greater changes in coolant density and thus creates more reactivity feedback.

This increase of the minimum effective reactivity rate is especially large between 0.1 and 2.0 MW because negligible amounts of feedback reactivity are generated near 0.1 MW ; with no negative feedback, small amounts of inserted reactivity can create small periods. A transient starting from 0.1 MW has low fuel, clad and coolant temperatures because the thermal power of the core is dissipated throughout the core volume - even doubling the energy contained within the core will not significantly increase the fuel temperature. A reactor already at high power, which increases in power by even a small amount, is going to have an effect upon the core temperatures and induce reactivity feedback. In other words, a 10% increase in power at 5 MW is more noticeable than at 0.1 MW .

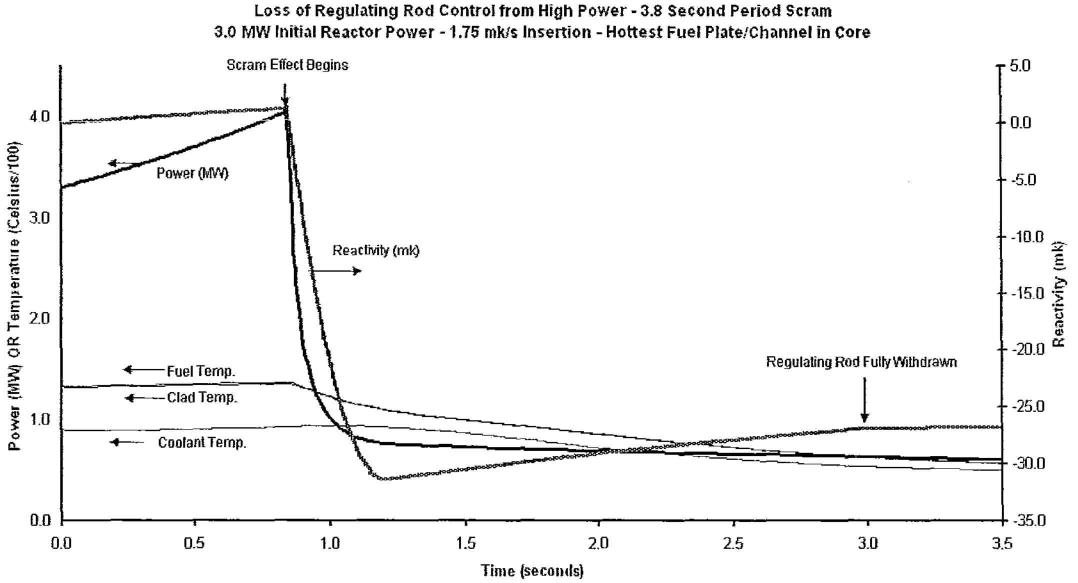

Figure 31. Transient from Simulation on <3.8s Period Scram Map

Figure 31 shows a transient from the boundary of the Figure 30 map that is successfully arrested before onset of bulk boiling by the <3.8 s period scram. Compared to the <10 s reverse transient shown in Figure 29, the power drops very quickly as a result of the scram's fast SSR insertion. The transient shown in Figure 31 takes $5.25\,mk/1.75\,mk/s=3.0\,s$ to withdraw the regulating rod fully; this rate is an order of magnitude larger than the maximum expected rate. The effect of the withdrawing regulating rod can be seen in the reactivity curve; following the scram reactivity continues to increase until 3.0 s as a result of the SSR withdrawing but the reactor remains deeply subcritical.

5.3.3 Reverse on +7% Large Servo Error

The first trip instrument predicted by the SAR to prevent bulk coolant boiling within this accident category is the +7% LSE reverse [10]. The PARET MNR simulations predict this instrument is able to prevent bulk boiling within all the expected reactivity insertion ranges and its trip coverage map is shown in Figure 32.

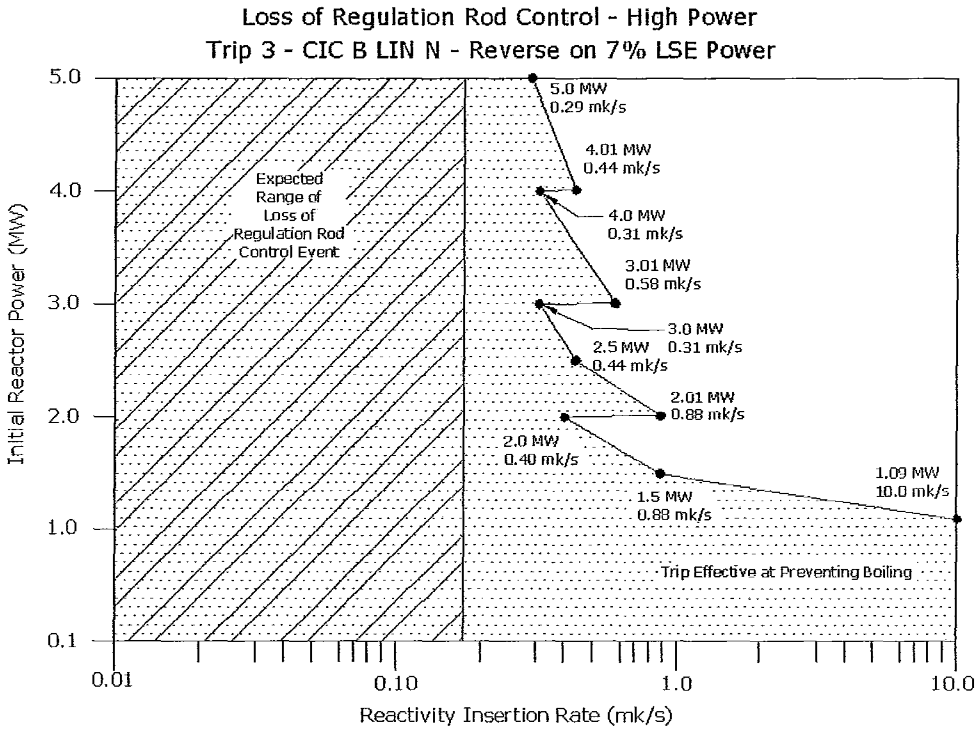

Figure 32. Trip Coverage Map – Loss of Regulation Rod Control HP – Trip 3

As with any other instrument set to trip on high power, a transient not restrained by feedback will always trigger the trip. What needs to be determined though is if the safety system trip occurs early enough and then inserts negative reactivity fast enough to prevent encountering a thermal boundary – bulk boiling in this case.

The +7% LSE reverse is effective on the lower (and expected) reactivity rate side of the trip coverage map boundary, as shown in Figure 32. Faster insertion rates, beyond what is expected to be possible, overcome the slow SSR insertion rate of the reverse. In contrast, the trip initiated by rate instruments, as in Figure 28 and Figure 30 are effective on the higher reactivity rate sides of their map boundaries, rather than the lower side since small power periods are not generated with small insertion rates.

As with the <3.8 *s* period coverage maps, the +7% LSE reverse has sudden allowable reactivity rate jumps around 2.0, 3.0 and 4.0 *MW* because the minimum allowable coolant flow rate changes at these nominal powers; these differences in flow alter the negative reactivity feedback characteristics of the reactor response. The +7% LSE reverse instrument is much more effective at higher rates in the lowest 0.1 to $2.0\,MW$ power range because the power margin to boiling is so large.

A sample transient from the boundary of Figure 32 is shown in Figure 33. Fuel temperature reaches a peak of $142\,^{o}C$ at $7.4\,MW$ and the hottest clad section at the same reactor power is $138\,^{o}C$ just prior to reactor power reduction. Note that the rate of positive reactivity insertion is larger than the rate of negative reactivity insertion between 2 and $18.1\,s$. At $18.1\,s$ the regulating rod has fully withdrawn and slowly inserting SSR bank reduces the total reactivity.

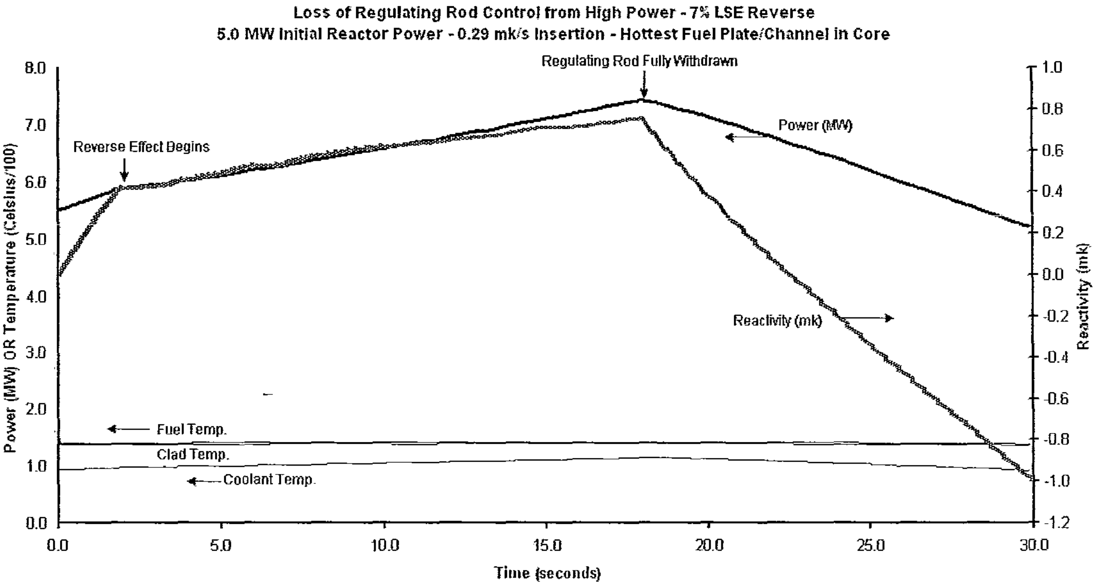

Figure 33. Transient from Simulation on +7% LSE Reverse Map

5.3.4 Reverse on 110% High Flux

Because the high power set points are so close together, and both invoke reverses of the SSR, the trip coverage map for the 110% HF reverse (Figure 34) looks almost identical to that of the +7% LSE reverse (Figure 32). As an example, for an initial

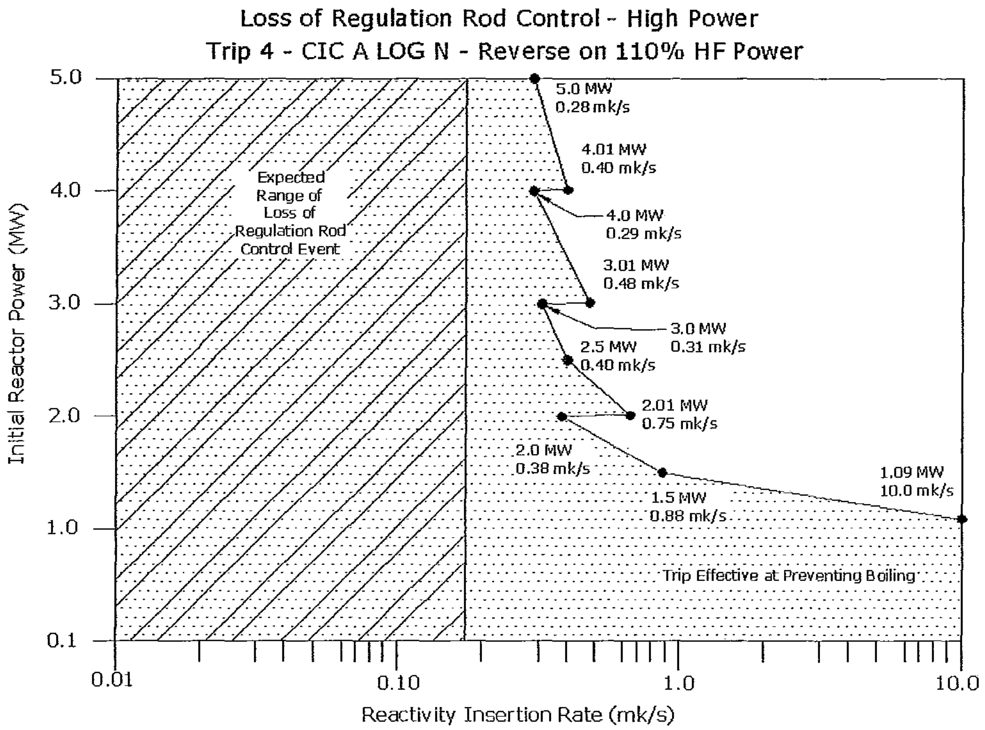

Figure 34. Trip Coverage Map – Loss of Regulation Rod Control HP – Trip 4

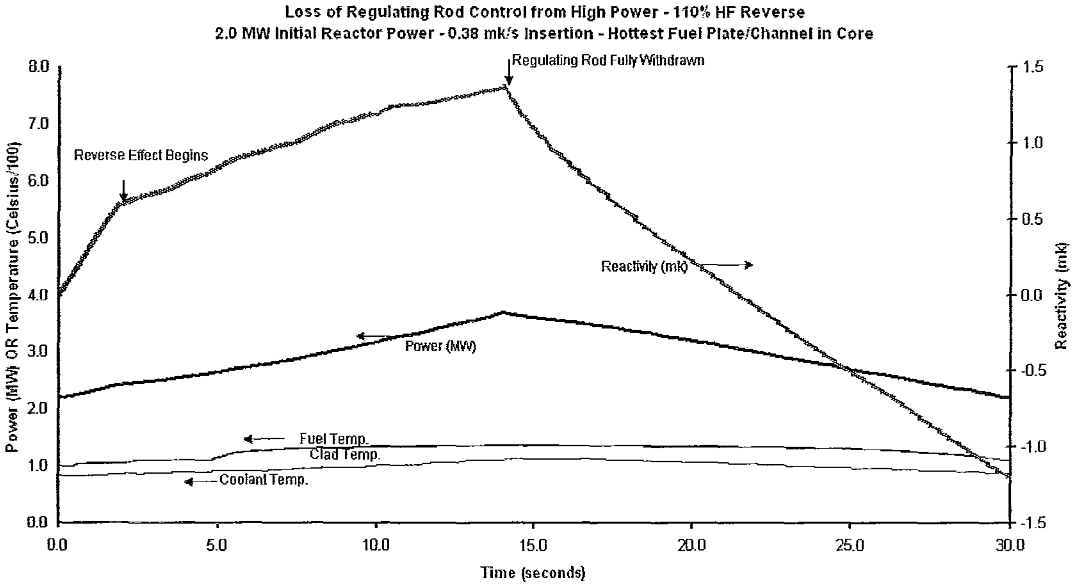

Figure 35. Transient from Simulation on 110% HF Reverse Map

nominal power of 1 MW, the 110% HF channel trips at 1.1 MW and the +7% HF channel trips at 1.07 MW. All allowable reactivity insertion rates are slightly lower for the 110% HF compared to the +7% LSE because the set power trip is 3% higher; thus the 110% HF has a smaller power margin to the onset of bulk boiling than the +7% LSE instrument.

A transient from the boundary of the Figure 34 110% HF reverse map is shown in Figure 35. The peak fuel temperature is 137 ^oC and the hottest clad section is 136 ^oC. This transient displays the same slow reduction in power as does the +7% LSE reverse in Figure 33.

5.3.5 Scram on 125% High Flux

The most capable instrument trip in the loss of regulation rod control event from high power is that of the 125%HF scram safety channel. Slow reactivity insertion rates eventually push power to trip power levels and are easily overcome by the subsequent fast inserting SSR. This capability extends completely through the entire range of examined reactivity insertion rates.

MNR has two safety instrument channels, UIC 1 SA and UIC 2 SA which are both 125% HF scram channels each monitoring a signal generated by an uncompensated ion chamber. Figure 36 shows a plot of the coverage map for the UIC 1 SA 125% HF scram channel, and is identical to the trip coverage map for the UIC 2 SA 125% HF scram. The PARET MNR simulations further support the SAR assertion that the 125% HF scram is effective at preventing fuel damage [10].

The fast acting 125% HF scram in Figure 37 reduces reactor power from a peak of 7.1 MW to approximately 1.4 MW in about 0.5 s. The reverses (as in Figure 33) take much longer to achieve similar reduction in reactor power. The peak fuel temperature prior to the scram in Figure 37 is 142 ^oC and the hottest clad temperature is 139 ^oC. The scram signal is generated at 0.17 s when reactor power reaches (5 MW)*(1.1)*(1.25) =6.875 MW. The power continues to rise in the delay between when the scram signal is generated and enough negative reactivity has been inserted to lower power, near 0.21 s.

The transient in Figure 37 avoids bulk boiling. Table 1 says bulk boiling will occur at the 5.0 MW power flow range (flow is set according to initial power) at nominal 6.8 MW which is (1.1)*(6.8)=7.48 MW.

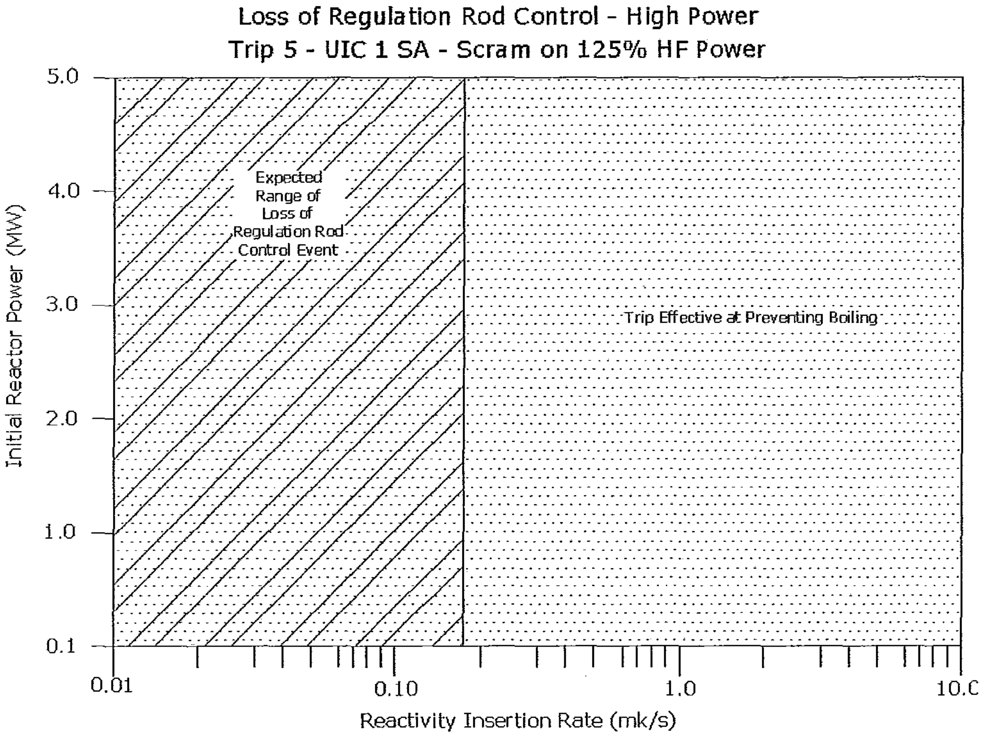

Figure 36. Trip Coverage Map – Loss of Regulation Rod Control HP – Trip 5

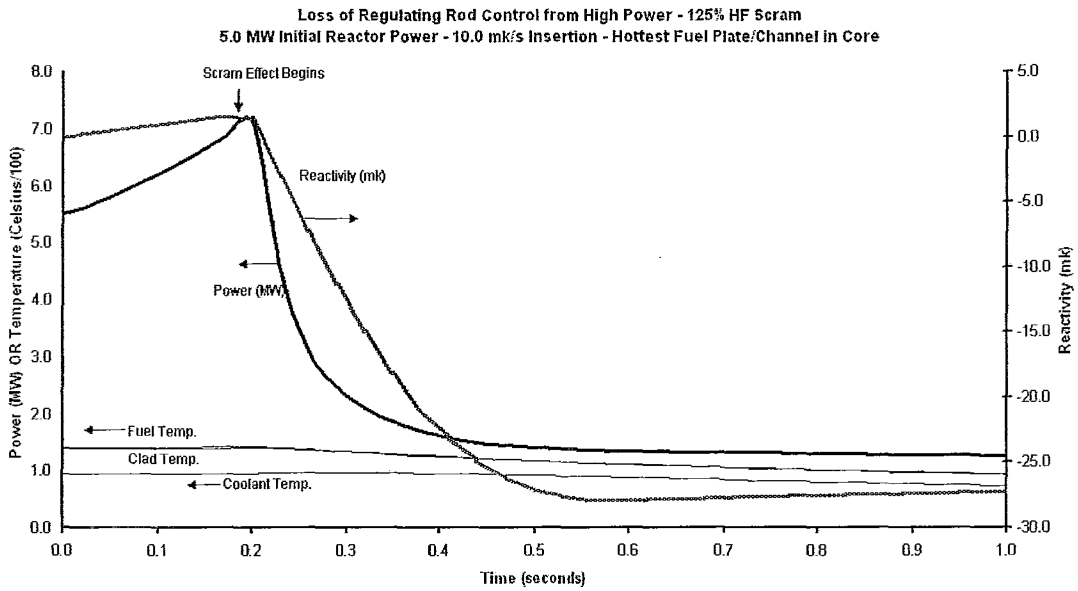

Figure 37. Transient from Simulation on 125% HF Scram Map

5.3.6 Manual Scram on Alarms

The SAR trip assessment gives full credit to manual scram in preventing fuel damage under loss of regulation rod control at high power [10]. According to the PARET MNR model, for operator intervention to be capable of preventing bulk boiling in the single hottest MNR channel, the reactivity insertion rate must be extremely small. Given an initial reactor power of $0.1\,MW$, a reactivity insertion rate of $0.0103\,mk/s$ is the largest insertion rate allowed if the +7% LSE audible alarm is to give at least the assumed minimum $300\,s$ of notice to the operator before boiling occurs (see Figure 38). Reactivity insertion rates larger than $0.0103\,mk/s$ result in faster power increases and an earlier onset of bulk boiling.

A successful manually arrested transient plot is shown in Figure 39. The plot shows where, at $21\,s$, the +7% LSE would first start an audible alarm. The alarm sounds at $21\,s$ because the reactor power has reached (1.07)*(initial power). The alarm continues to sound until $300\,s$ has elapsed; the operator is then credited with shutting the reactor down with a manually triggered scram at $321\,s$. The manual scram uses the same SSR as does any other instrument trip, and drop into the core with the same speed as an instrument triggered scram.

Reactor power in the transient in Figure 39 reaches a maximum of $3.7\,MW$ before the scram drops power. The model claims ONB occurs at $252\,s$; the hottest clad surface temperature at this time is 120^oC. When this particular transient is simulated without a manual scram, bulk boiling is predicted by the PARET MNR model to begin in the last axial node of the hottest coolant channel at $321.3\,s$.

The self limiting PARET MNR model simulations are similar to the manual scram runs, in that no instrument overpower or period trip is given credit; however, in the self limiting case neither is operator action. Instead, in a self limiting shutdown simulation the transient is allowed to continue until bulk boiling or some other thermal limit is reached (and the self limiting shutdown is declared ineffective) or power stabilizes to a steady state before reaching thermal limits (and the self limiting shutdown is considered effective at preventing transients from reaching thermal limits).

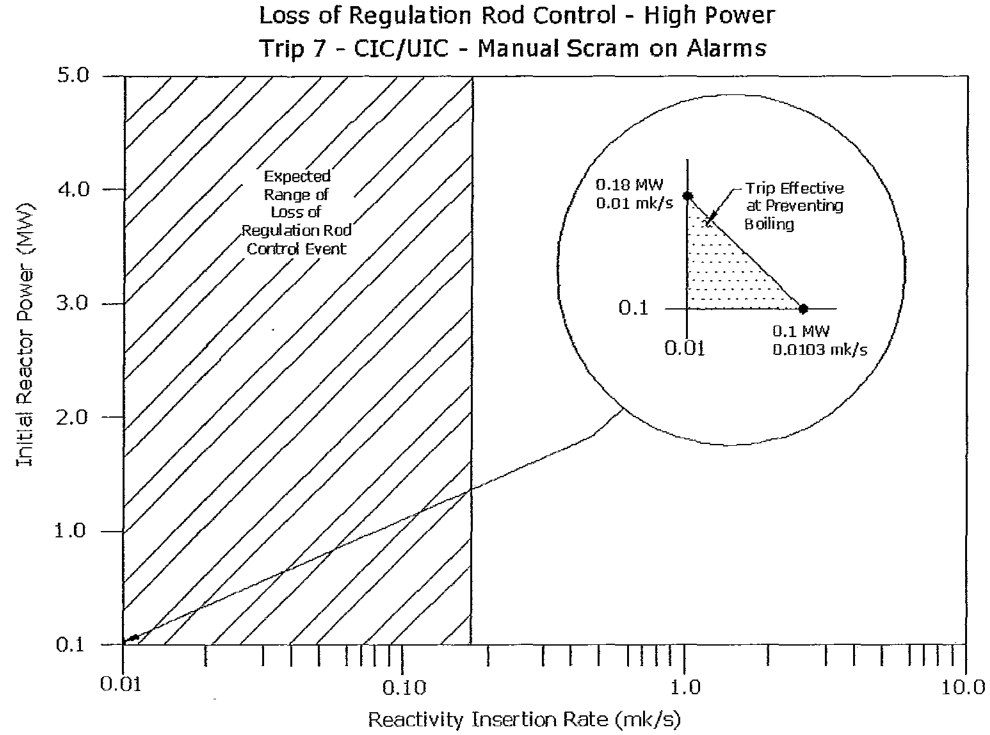

Figure 38. Trip Coverage Map – Loss of Regulation Rod Control HP – Trip 7

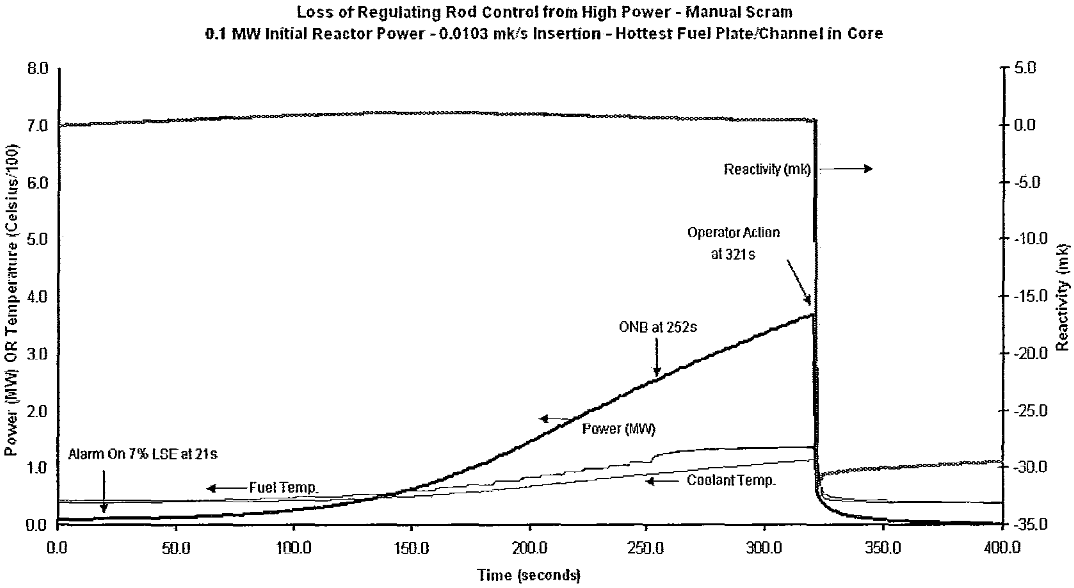

Figure 39. Transient from Simulation on Manual Scram Map

5.3.7 Self Limiting Shutdown

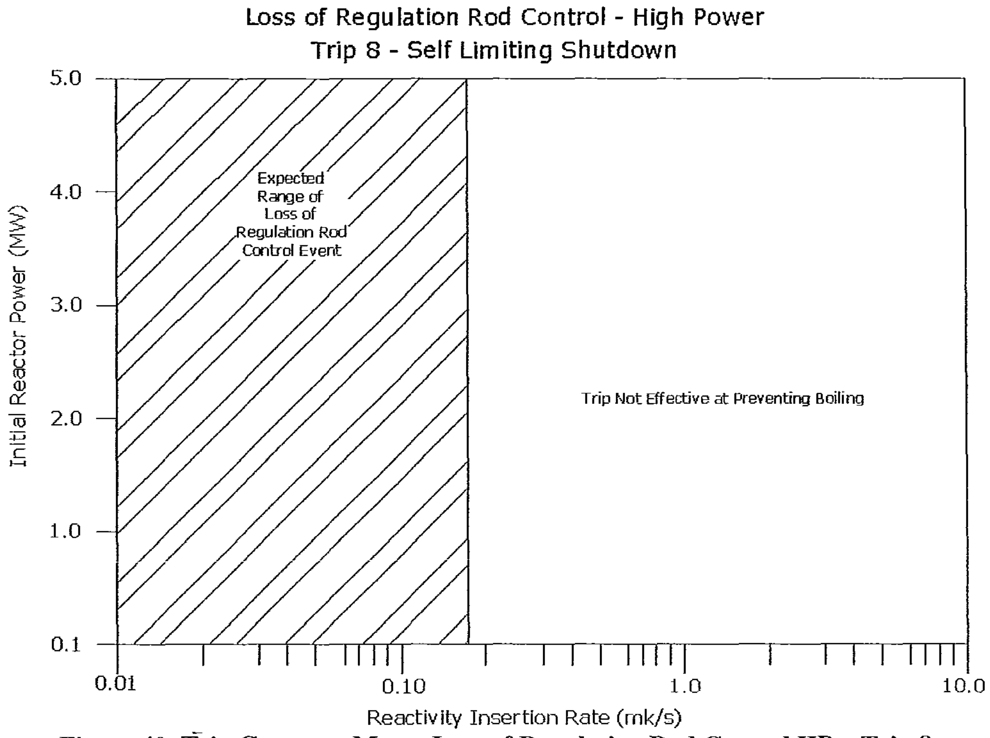

Figure 40. Trip Coverage Map – Loss of Regulation Rod Control HP – Trip 8

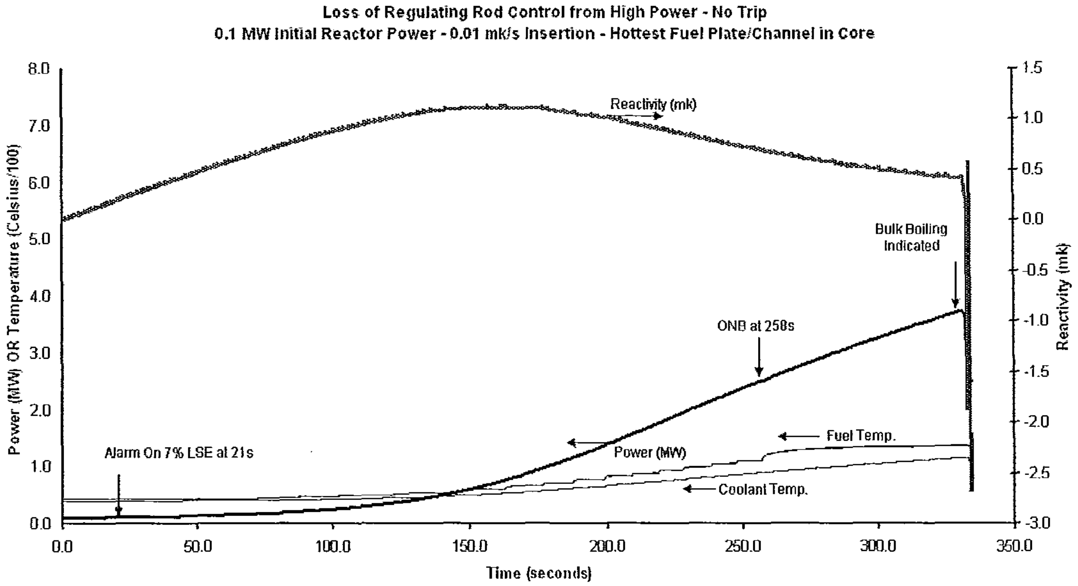

Figure 41. Transient from Simulation on Self Limiting Shutdown Map

According to the PARET simulations, within the conditions tested, negative feedback generated during a transient in this accident category is not large enough to limit transient power before bulk boiling. The trip coverage map for self limiting shutdowns in this accident category has no boiling protection coverage, and is shown in Figure 40.

An unsuccessful self limiting transient plot, in terms of preventing bulk boiling, is shown in Figure 41. The plot terminates at $340\,s$ where the PARET simulation crashes when its incompressible model produces asymptotic values as a result of boiling induced void creation.

The effect of feedback on the reactivity profile is apparent once reactor power reaches levels which begin to raise fuel, clad and coolant temperatures. The reactivity plot starts to decrease after approximately $160\,s$ due to the coolant and fuel temperature feedback effects. Prior to significant bulk boiling, the feedback effects are not strong enough to halt the reactor power growth. As with every other instrument trip tested in this accident category, a maximum of $5.25\,mk$ is inserted. Were this reactivity limit to be some lower value, the transient would indeed be self limited – see the discussion of self limited shutdowns in the irradiation sample handling accident category.

In the example transient, ONB first appears in the hottest axial clad section at $258.5\,s$ when reactor power is $2.53\,MW$, the fuel centerline temperature at the axial section experiencing ONB is $121.3\,^{o}C$ and the associated clad surface temperature is $120.5\,^{o}C$. Bulk boiling occurs in the outlet of the hottest coolant channel at $329.3\,s$ when the hottest axial centerline fuel temperature is $137\,^{o}C$ and the hottest clad surface temperature is $135.8\,^{o}C$.

5.3.8 Loss of Regulation Rod Control at High Power – Cumulative Trip Coverage Map

During MNR operation all instrument trips are active. The PARET simulations conducted to develop the trip coverage maps allowed only a single instrument to be active during a transient. To show the simultaneous and layered capacity of all the instruments to prevent transients from reaching the chosen thermal limits, the cumulative trip coverage map is shown in Figure 42.

Each instrument trip is numbered 1 thru 8 as they are in the SAR trip evaluation [10]. A vertical line at $0.18\,mk/s$ indicates the largest expected reactivity insertion rate associated with the loss of regulating control accident. The most probable 0.01-0.18 mk/s range is actively prevented from reaching thermal limits by at least four separate safety system responses.

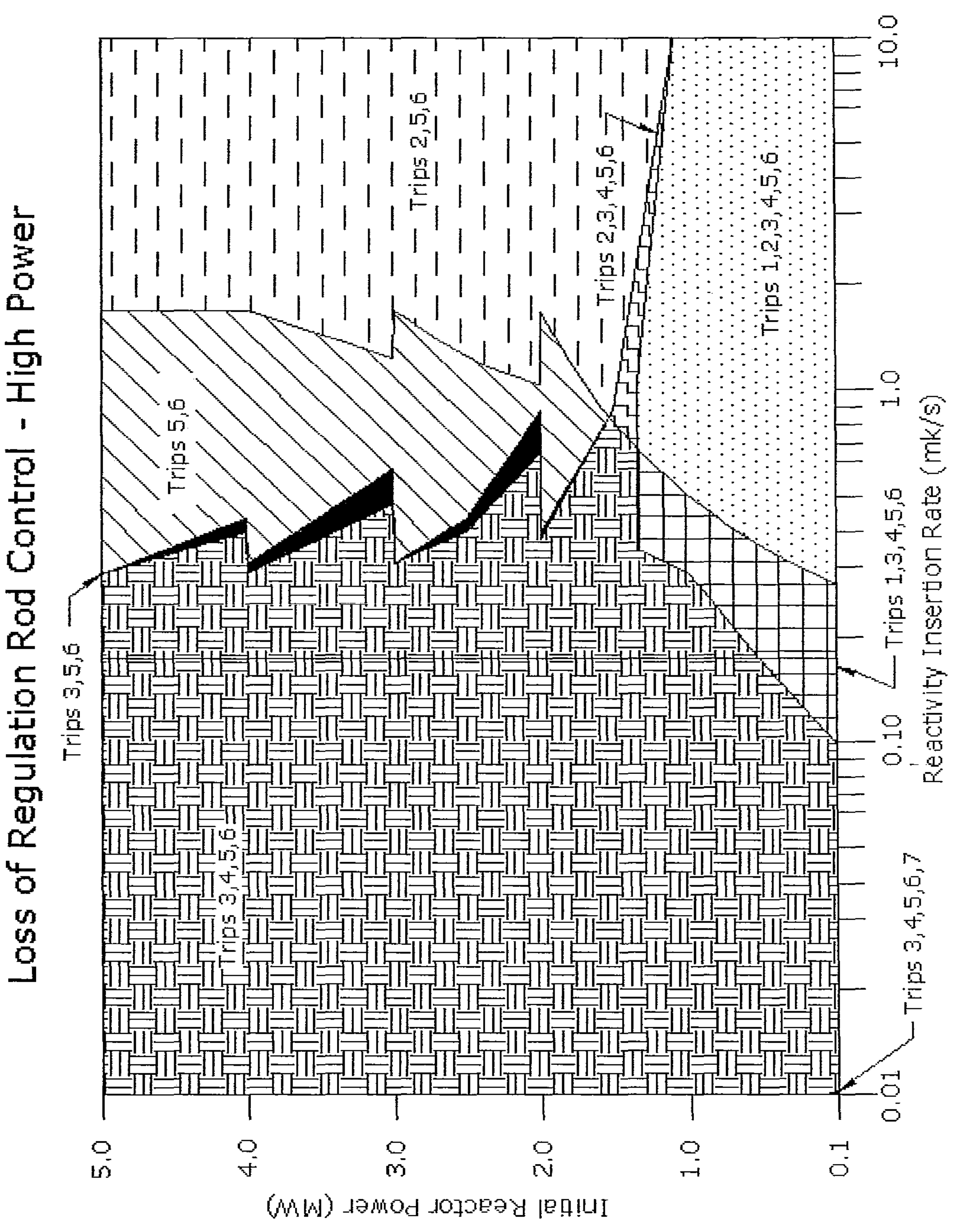

Trip 1 - CIC LOG N - Reverse on <10s Period
Trip 2 - CIC LOG N - Scram on <3.8s Period
Trip 3 - CIC B LIN N - Reverse on 7% LSE Power
Trip 4 - CIC A LOG N - Reverse on 110% HF Power
Trip 5 - UIC 1 SA - Scram on 125% HF Power
Trip 6 - UIC 2 SA - Scram on 125% HF Power
Trip 7 - CIC/UIC - Manual Scram on Alarms
Trip 8 - Self Limiting Shutdown

Figure 42. Loss of Regulation Rod Control at High Power - Cumulative Trip Coverage Map

5.4 Loss of Regulation Rod Control at Low Power

Low power operation in MNR is considered to be $0.1\,MW$ and below. At these powers, natural convection flows are allowed by the Operating Limits and Conditions [6].

The SAR trip evaluation credits the same instrument trips as being capable of fuel damage prevention during a loss of regulation rod control at low power as at high power: the +7% LSE reverse, 110% HF reverse, both 125% HF scrams, the manual scram and the self limiting shutdown [10]. Credit is not given to the $<10\,s$ period reverse nor the $<3.8\,s$ period scram because the SAR authors were unclear whether the reactivity insertion rates are large enough during loss of regulation rod control to force a short reactor period [Note1,10].

All trip maps and sample transients for this accident category are shown in Figure 43 through Figure 51. Each trip coverage map at the low power level spans the expected reactivity insertion rates developed in the Accident Event Categories description of the loss of regulation rod control at low power section, $0.01\,mk/s$ to $0.18\,mk/s$.

The loss of regulation rod control during low power postulated accidents are modeled to insert the same maximum $5.25\,mk$ as the high power accidents.

5.4.1 Reverse on <10 Second Period

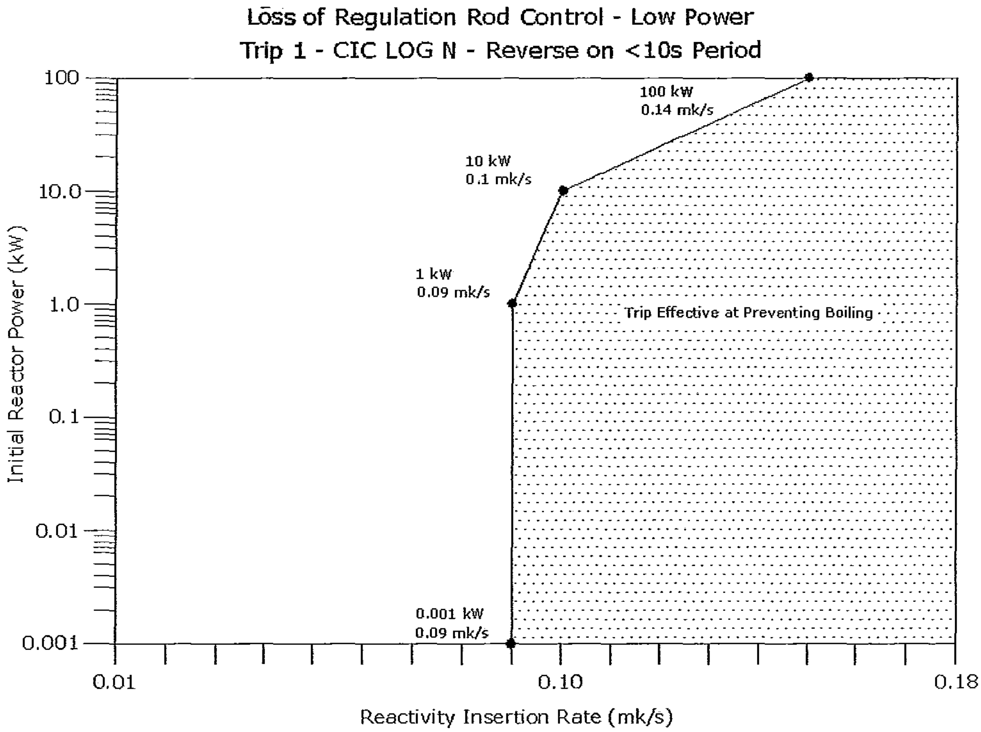

Figure 43. Trip Coverage Map – Loss of Regulation Rod Control LP – Trip 1

The $<10\,s$ period reverse at high powers is predicted to not be completely effective at preventing boiling within the $0.01\,mk/s$ to $0.18\,mk/s$ range, as Figure 28 shows; this is a result of the reverse's slow negative reactivity insertion rate. Figure 43 shows that the $<10\,s$ period reverse at low reactor powers has comparatively more coverage within the $0.01\,mk/s$ to $0.18\,mk/s$ range than the high power reverse map shown in Figure 28; this difference is attributed to the fact that transients initiated from low powers have a large power margin to grow before producing bulk boiling, giving more time for the reverse to arrest the transient once tripped. As is shown in Table 1, bulk boiling under steady state natural convective flows doesn't occur until approximately $2.4\,MW$, thus the reverse has more time to act than at higher initial reactor powers.

The $<10\,s$ period trip map boundary, shown in Figure 43, is constantly $0.09\,mk/s$ between $1\,W$ and $1\,kW$ because feedback effects become noticeable at higher powers – requiring larger reactivity insertion rates at higher powers to induce a reverse. Lower reactivity insertion rates are able to induce $<10\,s$ periods at lower reactor powers. If feedback effects were more powerful, faster reactivity insertion rates would be required to induce $<10\,s$ periods. The lowest reactivity insertion rate capable of inducing a $<10\,s$ period during high power operation is $0.10\,mk/s$ (see Figure 28).

The $<10\,s$ period trip coverage map predicts this instrument channel may not arrest transients within the entire expected range for a loss of reactivity rod control scenario, when the reactivity is inserted linearly.

5.4.2 Scram on <3.8 Second Period

The $<3.8\,s$ period instrument channel (Figure 44) has a trip coverage boundary at higher reactivity insertion rates than that of the $<10\,s$ period (Figure 43) since more reactivity is required for smaller reactor periods. Figure 44 shows the minimum insertion rate required to induce a $<3.8\,s$ period is $0.14\,mk/s$ as compared to the minimum $0.09\,mk/s$ required to induce a $<10\,s$ period.

At high power loss of regulation rod control the $<3.8\,s$ scram is predicted to have no ability at preventing bulk boiling within the expected $.01\,mk/s$ to $0.18\,mk/s$ range (see Figure 30). Comparatively, within the same range from low powers as shown in Figure 44, the $<3.8\,s$ period scram is predicted to have some coverage.

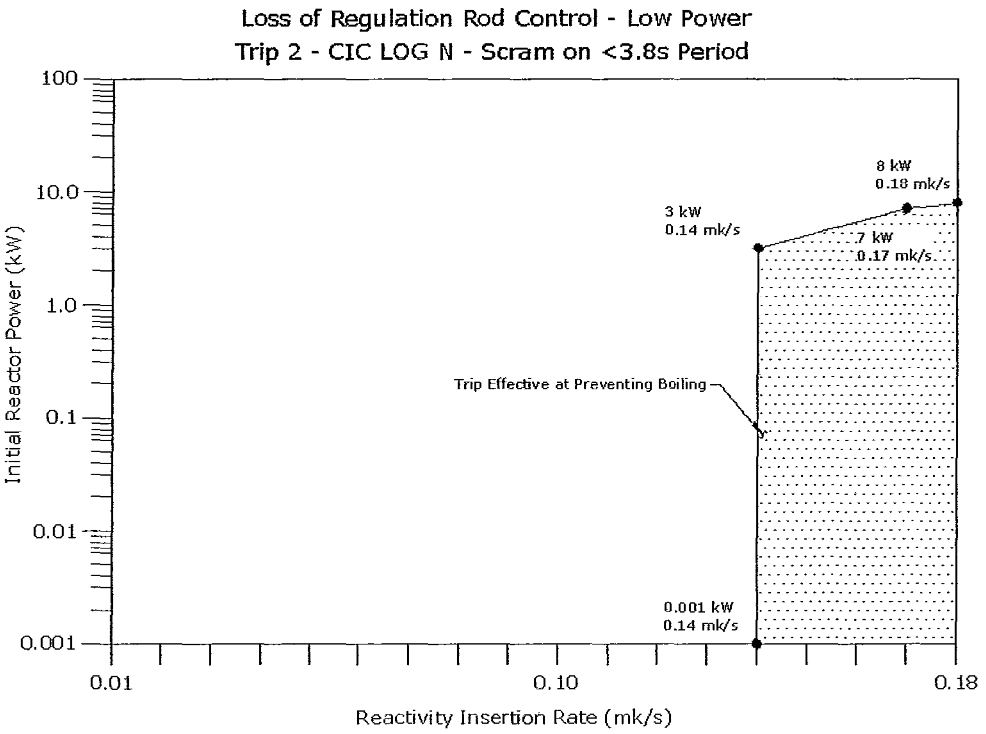

Figure 44. Trip Coverage Map – Loss of Regulation Rod Control LP – Trip 2

5.4.3 Reverse on +7% Large Servo Error

Just as the +7% LSE reverse is predicted effective in the high power loss of regulating rod accidents, it is also predicted to be effective in the 0.01 mk/s to 0.18 mk/s insertion rates during low power loss of regulating rod events at preventing boiling. This is dependent upon the reactor being operated in the automatic setting since the +7% LSE reverse is not active during manual operation. The trip coverage map for this instrument and event is shown in Figure 45.

This +7% LSE reverse is a power trip and is more effective than the <3.8 s period scram and the <10 s period reverse because the reactivity insertion rates being tested are relatively small. A power trip does not require a specific amount of reactivity to be inserted before signaling a trip.

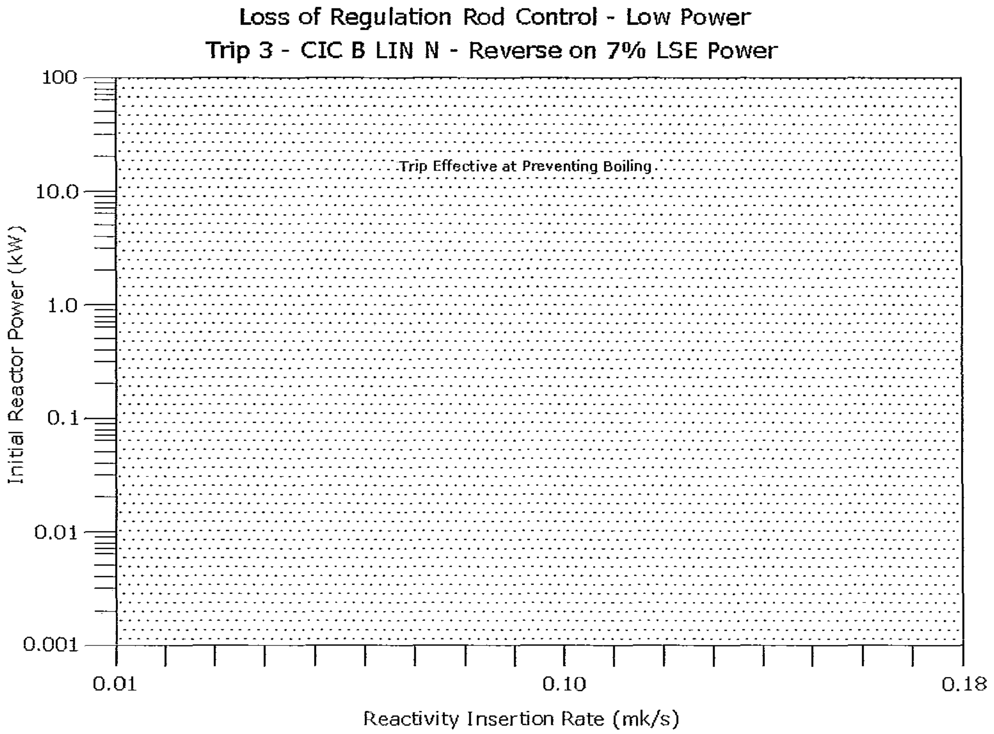

Figure 45. Trip Coverage Map – Loss of Regulation Rod Control LP – Trip 3

5.4.4 Reverse on 110% High Flux

The 110% HF reverse is predicted to be completely ineffective at preventing boiling because of a conservative assumption that was made in the development of the PARET model of MNR. The trip coverage map for this instrument is shown in Figure 46. As discussed in Chapter 3, for low power operation the 110%HF reverse trip point is assumed to be set at $(1.1)*(5\ MW)=5.5\ MW$ since configuring the Log N channel for low power operation is not practical for MNR operators in most cases.

Because the reverse trip power point is at $5.5\,MW$ and according to Table 1 under natural convection conditions bulk boiling sets in at a steady state power of $2.4\,MW$, bulk boiling occurs before power reaches the trip-inducing $5.5\,MW$. If the ion chamber and instrumentation associated with the trip were reconfigured by MNR for all low power operation of MNR, the 110% HF reverse would likely be effective in the $0.01\,mk/s$ to $0.18\,mk/s$ range of this accident category as it was in the high power category (Figure 34).

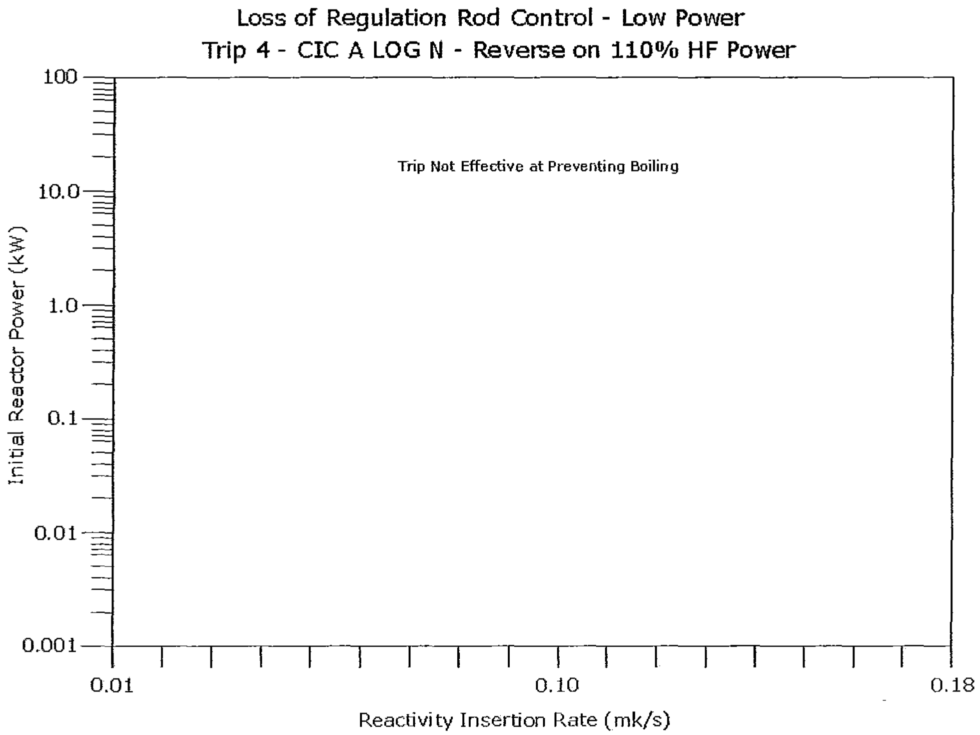

Figure 46. Trip Coverage Map – Loss of Regulation Rod Control LP – Trip 4

5.4.5 Scram on 125% High Flux

For the same reason the 110% HF reverse is predicted to be completely ineffective at preventing boiling, so are both 125% HF scram channels in this low power operation category. The trip coverage map for UIC 1 is shown in Figure 47, and is identical to the other safety channel UIC 2. The uncompensated ion chambers used to generate a flux proportional signal for the 125% HF scram channel are not configured by MNR operators to be effective during low power operation. Therefore, it has to be conservatively assumed that the trip set point is $(1.25)*(5\,MW)=6.25\,MW$.

As the reactor power grows it reaches bulk boiling power before $6.25\,MW$. Both safety channels are predicted to be extremely functional in the high power loss of regulation rod control category and would be for this low power operation as well if MNR operations felt the need to configure the UIC to be effective at low powers. It should be noted that investigations have not been conducted in this study to determine if these ion chambers are even capable of low power signal generation.

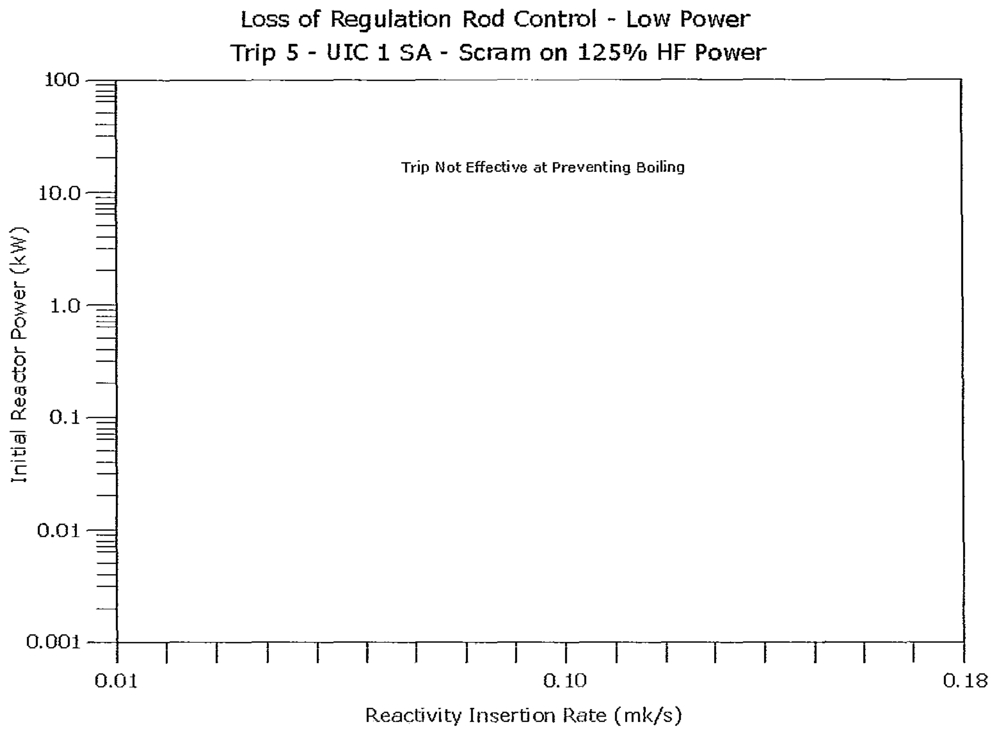

Figure 47. Trip Coverage Map – Loss of Regulation Rod Control LP – Trip 5

5.4.6 Manual Scram on Alarms

The PARET MNR model predicts the manual scram from low power will have some bulk boiling protection coverage in transients caused by linear reactivity insertion from low initial powers (see Figure 48). The range of coverage is larger than that of the manual scram in the high power loss of regulating rod control case (see Figure 38) because the margin to onset of boiling ($2.4\,MW$) is larger and provides for additional operator response time. Just as in the high power loss of regulating rod postulated accidents, the +7% LSE audible alarm is given credit for alerting reactor operators in all transients simulated for Figure 48.

The boundary in the manual scram trip coverage map has coverage on its lower reactivity insertion rate side because rates larger than the boundary induce bulk boiling before the +7% LSE audible alarm gives the operators $300\,s$ of notice.

As noted in the MNR PARET model development, the biggest difference between low and high power MNR operation is that low power operation is allowed to be cooled by natural convective flows. Figure 49 shows a successfully arrested low power transient taken from the boundary of the Figure 48 trip

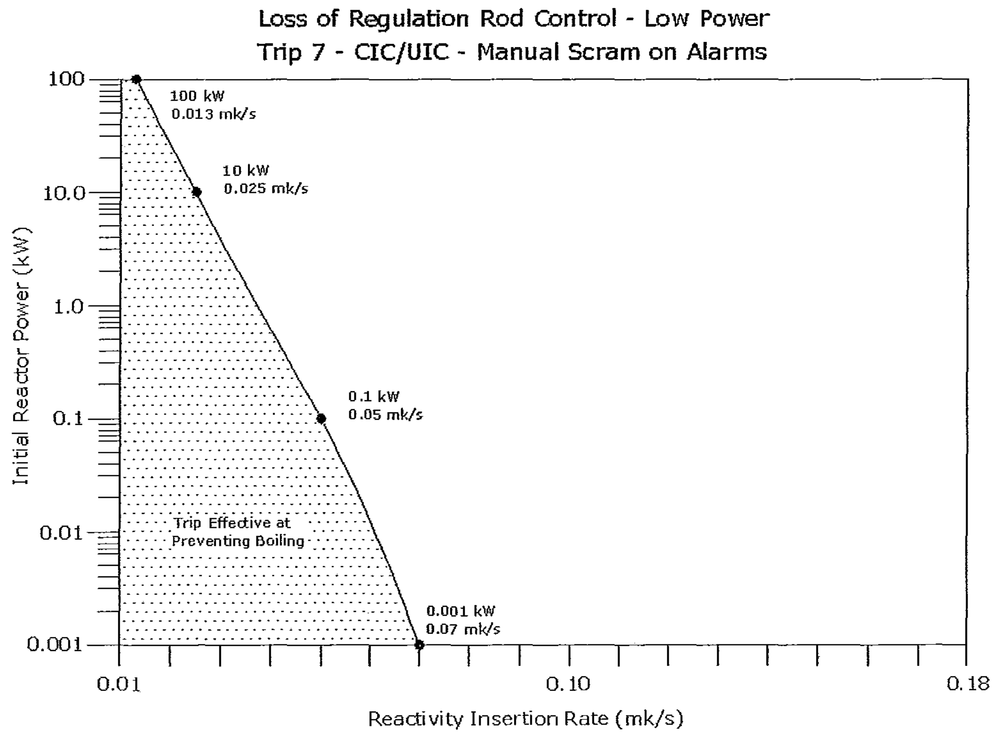

Figure 48. Trip Coverage Map – Loss of Regulation Rod Control LP – Trip 7

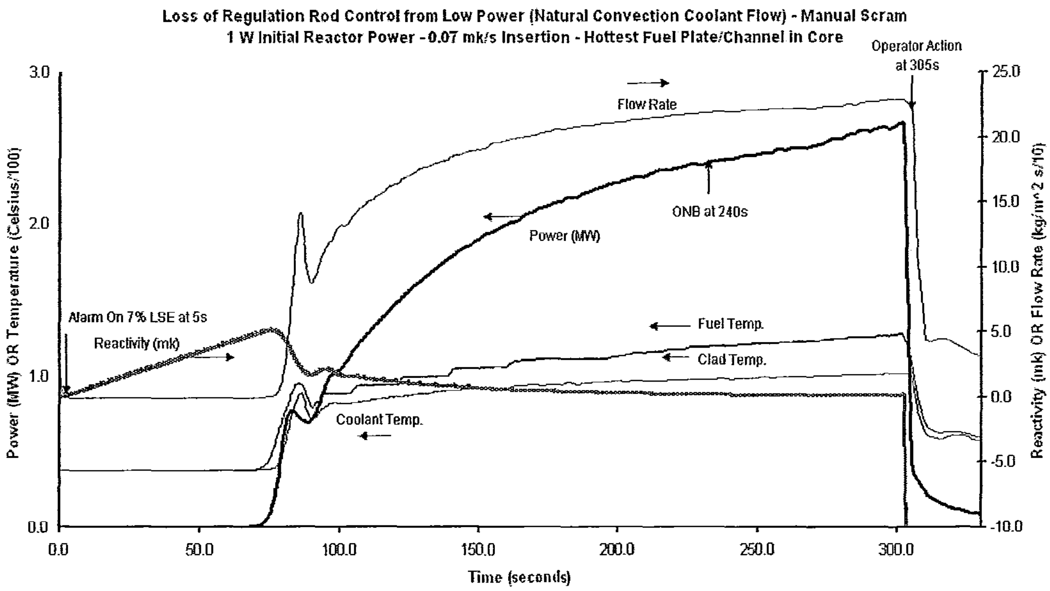

Figure 49. Transient from Simulation on Manual Scram Map

coverage map in which the buoyancy induced flow clearly increases as reactor power increases.

At an initial power of $1\,W$ the reactor fuel and cladding temperatures are the same as the coolant temperature, $38\,^{o}C$. The energy density at extremely low power levels is so small there isn't enough energy to noticeably heat fuel plates or cladding above that of the ambient pool temperature.

The reactivity inserted in the Figure 49 transient is a mild $0.07\,mk/s$. Nonetheless, this reactivity causes reactor power to grow. Although the power scale shown in Figure 49 is ill-suited to show the details in the first $65\,s$ of the transient, power is growing rapidly during this time from a very low initial power of $1\,W$.

Not until $65\,s$ does reactor power reach levels which are large enough to register on the power scale shown. Note that zero reactor feedback is generated until power grows to macroscopic levels; the total reactivity is a linear line until $65\,s$ when negative reactivity generated by feedback reduces the total reactivity. External reactivity is inserted linearly until $5.25\,mk / 0.07\,mk/s = 75\,s$. Between 0 and approximately $65\,s$ the total reactivity is equal to the externally inserted reactivity because no feedback effects are present.

Coincidentally, at $75\,s$ when external reactivity is no longer being added, reactor power is also high enough to create significant feedback effects; there is a sharp drop in total reactivity and momentarily in power before power continues to increase again due to the net positive reactor reactivity.

It takes only $5\,s$ to elapse before the +7% LSE signals an audible alarm. Power then grows to $2.6\,MW$ in the following $300\,s$ before a manual scram arrests the transient at $305\,s$. Nominal steady state power of $2.4\,MW$ (from Table 1, which is $2.64\,MW$ with reactor power uncertainties) is enough to induce boiling in the core when cooled by natural convection. The manually arrested transient in Figure 49 doesn't reach the $2.64\,MW$ required to induce bulk boiling according to the PARET MNR model.

At $305\,s$ with reactor power at the peak $2.6\,MW$ the maximum fuel temperature is $127\,^{o}C$ and maximum clad temperature is $126\,^{o}C$; the coolant channel outlet temperature is $100\,^{o}C$. The flow direction in these natural convection cases is upwards of course, and the coolant mass flow rate reaches a maximum of $227\,kg/m^2s$ when reactor power is at its peak. The Figure 49 transient confirms the PARET model considers natural convection coolant flow rate as dependant upon reactor power.

5.4.7 Self Limiting Shutdown

The trip map for the self limiting shutdown is shown in Figure 50. The trip coverage map predicts MNR is not capable of creating enough negative feedback to limit the transient initiated by the insertion of $5.25\,mk$ before the onset of boiling – just as in the high power case. It is clear (see discussion of the role of boiling in MNR transients in Chapter 2) that extensive bulk boiling will generate more than -5.25 mk in feedback, but that is the subject for another study examining post-boiling transient consequences.

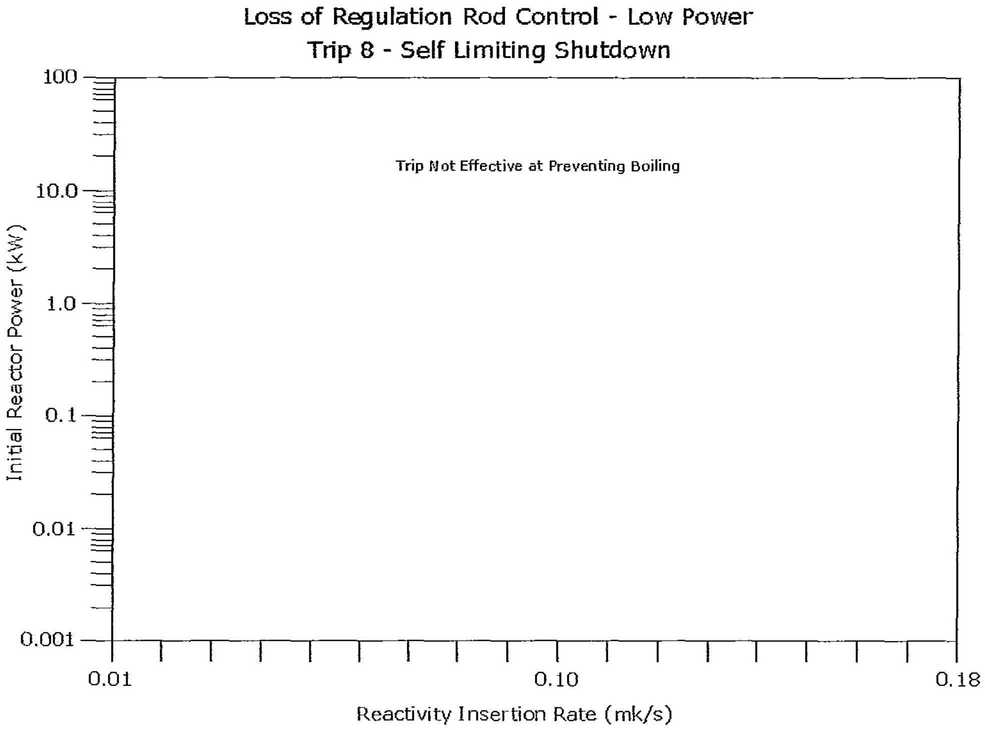

Figure 50. Trip Coverage Map – Loss of Regulation Rod Control LP – Trip 8

5.4.8 Loss of Regulation Rod Control at Low Power – Cumulative Trip Coverage Map

The cumulative trip coverage map for the loss of regulating rod control from low initial reactor powers is shown in Figure 51. Compared to the cumulative map for the high power accident (Figure 42) there are less instruments predicted by the PARET MNR model to be capable of preventing the onset of bulk boiling in the 0.01 mk/s to 0.18 mk/s range. The difference is primarily because of lack of coverage by the 125% HF scram and 110% HF reverse channels at low (<0.1 MW) MNR powers.

A significant area of the expected range is covered by a single safety response, the +7% LSE reverse. The remainder of the map is covered with dual and triple coverage due to the <3.8 s period scram, the <10 s period reverse and the manual scram.

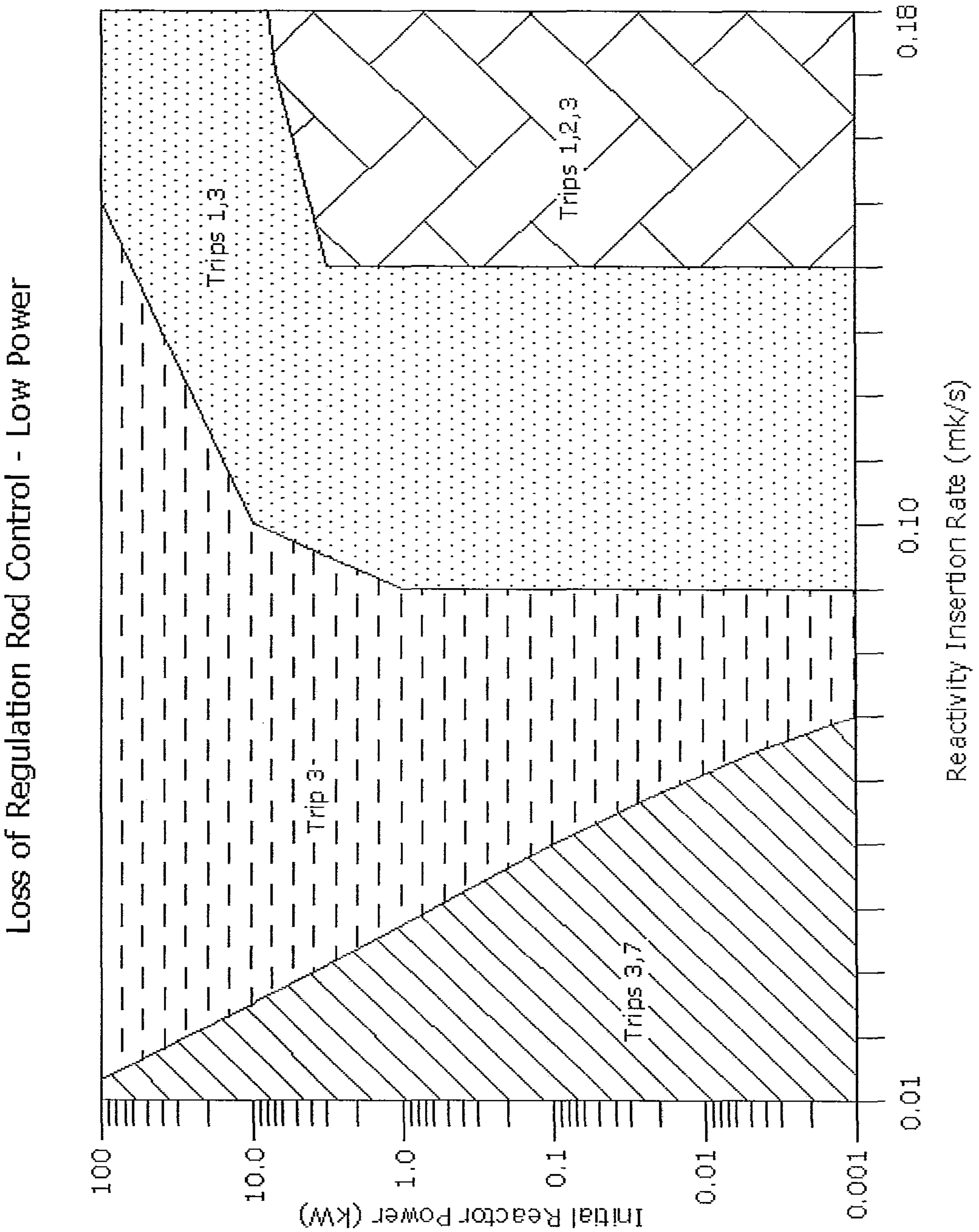

Trip 1 - CIC LOG N - Reverse on < 10s Period
Trip 2 - CIC LOG N - Scram on <3.8s Period
Trip 3 - CIC B LIN N - Reverse on 7% LSE Power
Trip 4 - CIC A LOG N - Reverse on 110% HF Power
Trip 5 - UIC 1 SA - Scram on 125% HF Power
Trip 6 - UIC 2 SA - Scram on 125% HF Power
Trip 7 - CIC/UIC - Manual Scram on Alarms
Trip 8 - Self Limiting Shutdown

Figure 51. Loss of Regulation Rod Control at Low Power - Cumulative Trip Coverage Map

5.5 Irradiation Sample Handling Accidents

Within this accident category the SAR credits the $<10\,s$ period reverse, +7% LSE reverse, 110% HF reverse, both 125% HF scrams, the manual scram and the self limiting shutdown as capable in preventing fuel damage [10]. The SAR does not credit the $<3.8\,s$ period scram because it was unclear whether the reactivity insertion rates would be large enough to force a short reactor period [Note7,10].

The trip coverage maps developed with PARET simulations predict the +7% LSE reverse, 110% HF reverse and both 125% HF scrams are able to prevent the onset of bulk boiling over the entire tested reactivity and initial power ranges. The $<3.8\,s$ period scram, the $<10\,s$ period reverse, the manual scrams and the self limiting shutdown are predicted to have partial trip coverage.

The trip coverage maps and sample transients for the instruments in this accident category are shown in Figure 52 through Figure 60.

The overpower trips (+7% LSE reverse, 110% HF reverse and both 125% HF scrams) are all effective because the rates of insertion tested are not so massive as to induce boiling before the SSR have a chance to insert significant amounts of negative reactivity. Just as the trip maps for the +7% LSE reverse and the 110% HF reverse in the loss of regulation rod control accident categories showed overpower trips are unable to prevent bulk boiling during some large reactivity insertion rate, in Figure 32 and Figure 34, it is expected that there safety instruments would fail to prevent bulk boiling at some rate of reactivity insertion larger than $20\,mk\,/\,s$.

This accident category inserts a maximum of $2\ mk$; the previously discussed loss of regulating rod accidents inserted a maximum of $5.25\,mk$. The consequences of this difference are most apparent in the differences between the self limiting transient simulations of the two accident cases, and are discussed in detail later.

The $<3.8\ s$ period scram and the $<10\ s$ period reverse display abrupt changes in coverage boundary near 2.0, 3.0 and $4.0\,MW$ as was observed in loss of regulation rod control maps. As discussed previously, these changes are a result of the administrative minimum flow rates which change at these power levels. Both rate trips have extensive coverage throughout the maps, but as discovered in other accident categories the slowest reactivity insertion rates tested do not have the capabilities to induce small reactor periods.

5.5.1 Reverse on <10 Second Period

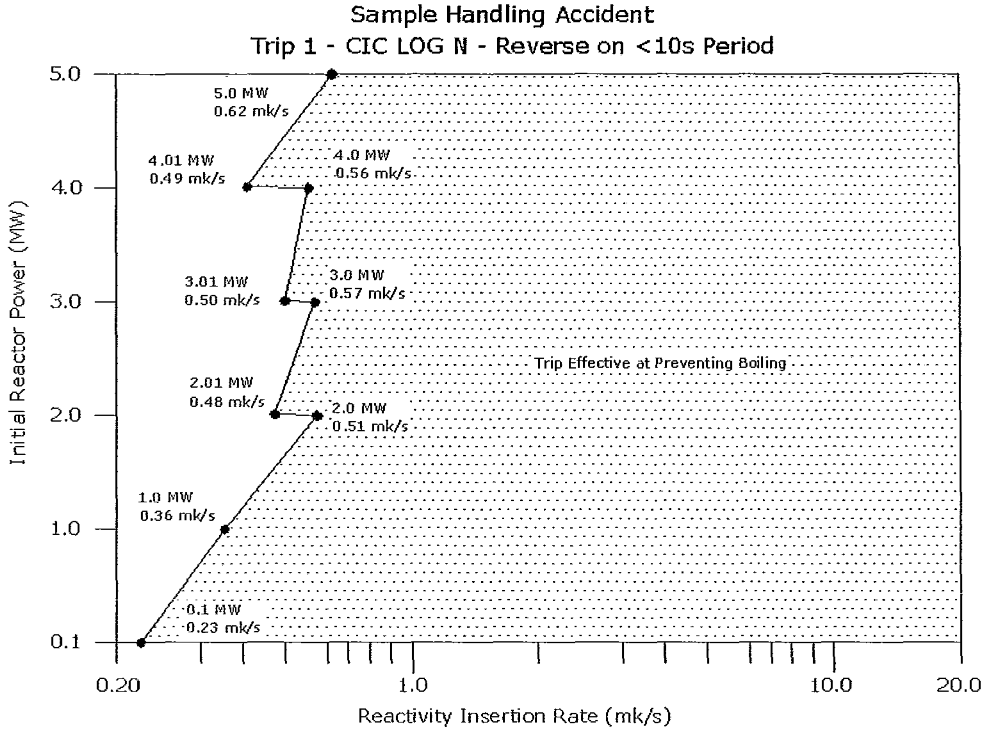

Figure 52. Trip Coverage Map – Sample Handling Accident – Trip 1

5.5.2 Scram on <3.8 Second Period

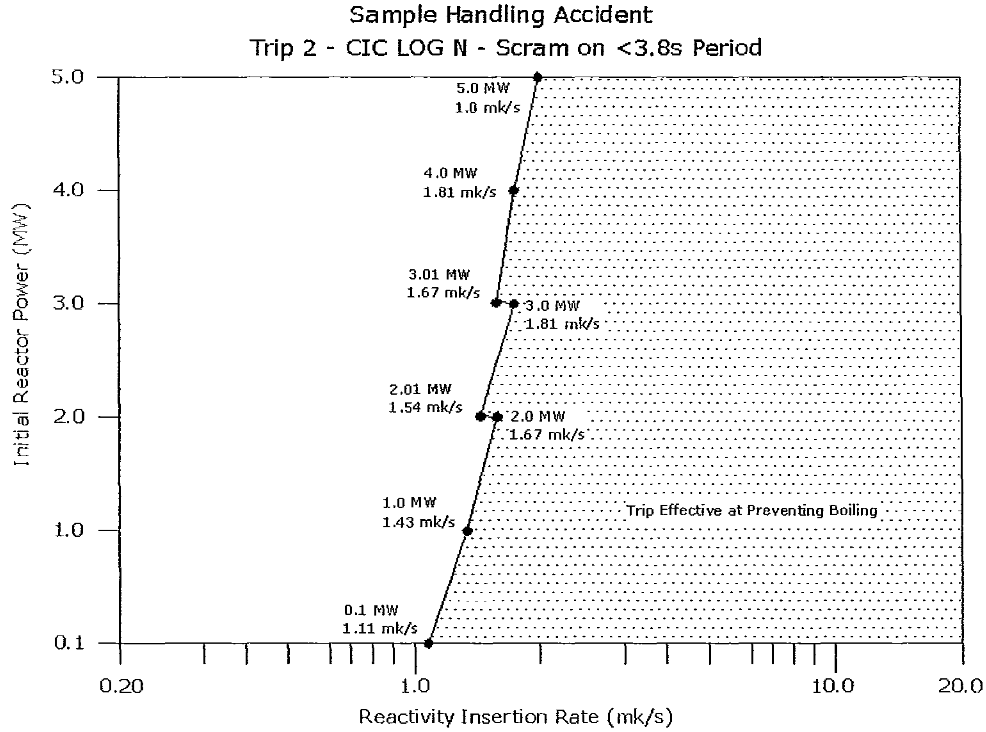

Figure 53. Trip Coverage Map – Sample Handling Accident – Trip 2

5.5.3 Reverse on +7% Large Servo Error

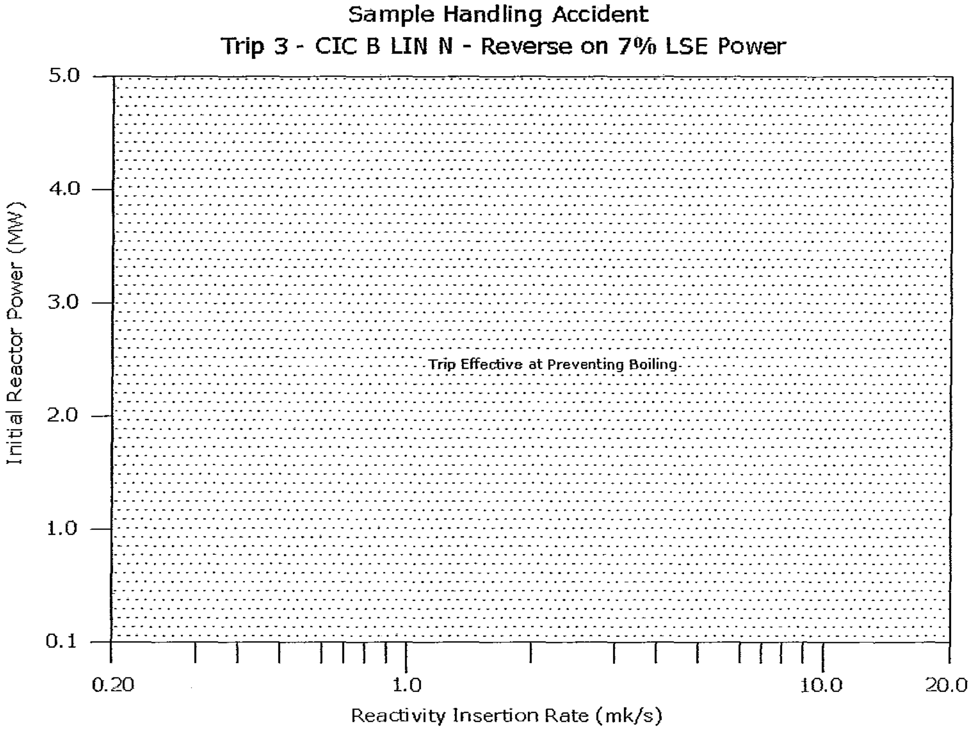

Figure 54. Trip Coverage Map – Sample Handling Accident – Trip 3

5.5.4 Reverse on 110% High Flux

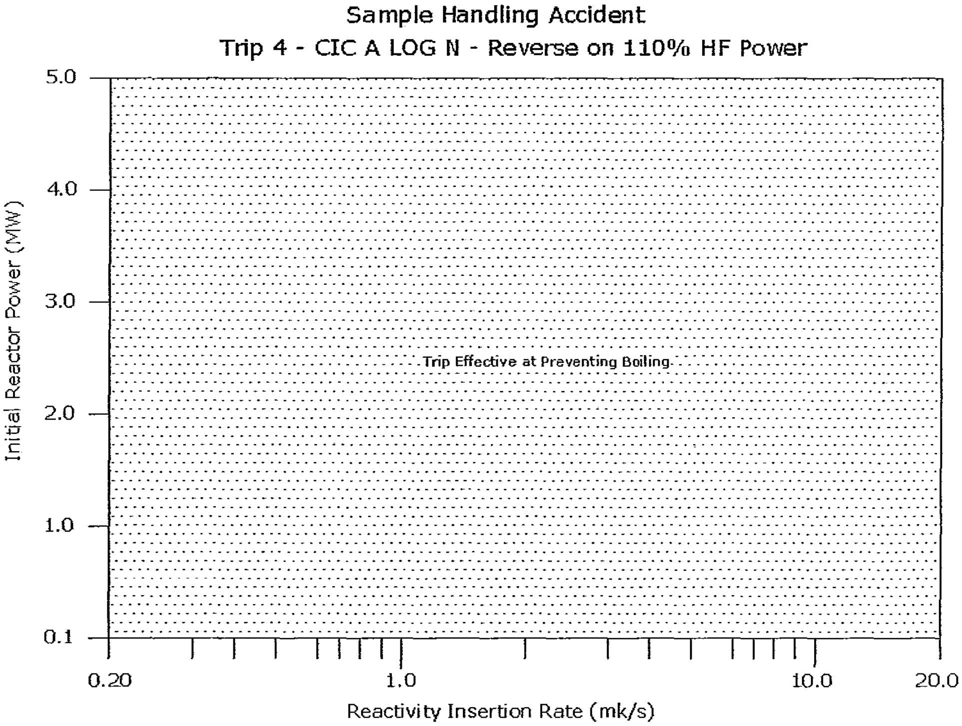

Figure 55. Trip Coverage Map – Sample Handling Accident – Trip 4

5.5.5 Scram on 125% High Flux

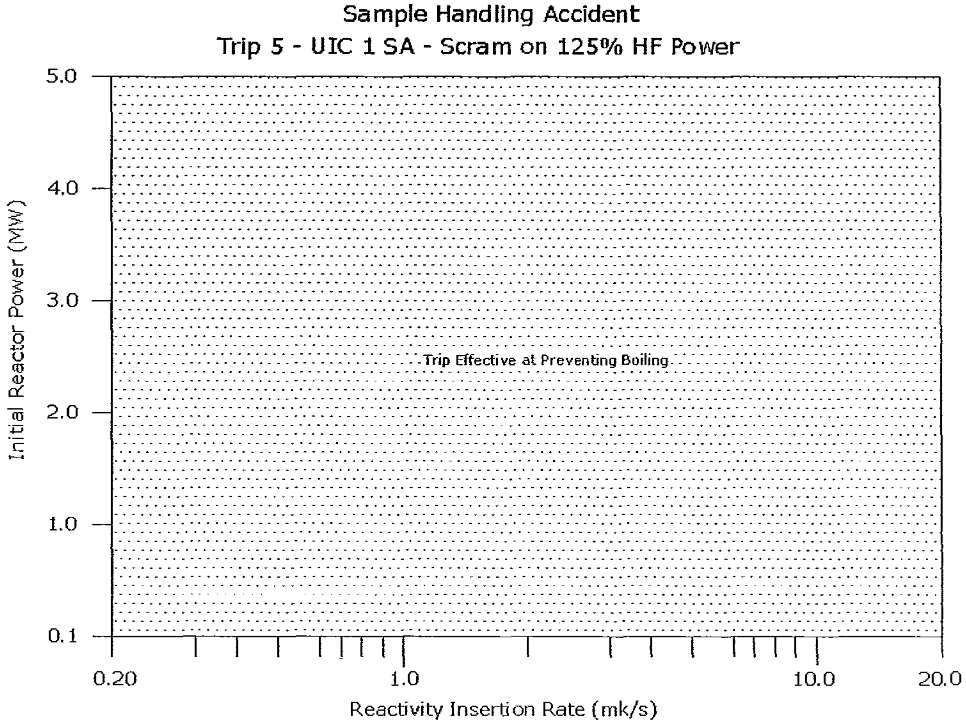

Figure 56. Trip Coverage Map – Sample Handling Accident – Trip 5

5.5.6 Manual Scram on Alarms

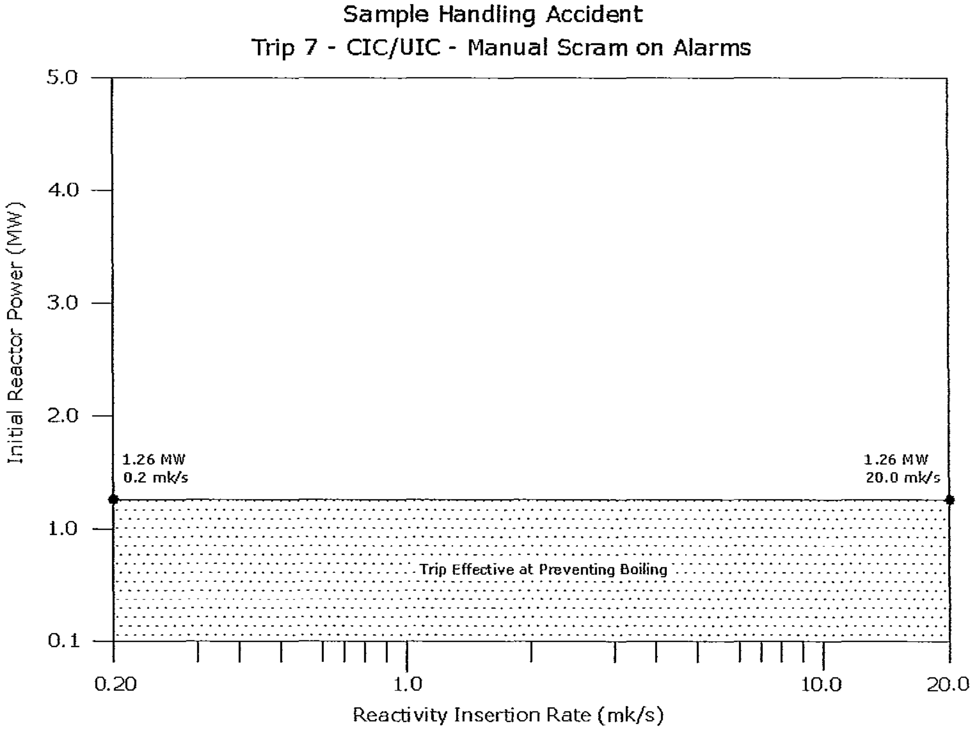

Figure 57. Trip Coverage Map – Sample Handling Accident – Trip 7

5.5.7 Self Limiting Shutdown

Unlike the high and low power loss of reactivity control accident categories which are not self limited from any initial power levels (see Figure 40 and Figure 50), sample handling initiated transients are predicted to be self limiting in some cases, see Figure 58. The sample handling accident category inserts a maximum of $2\,mk$, whereas the loss of reactivity control category inserted a maximum of $5.25\,mk$; this is the reason why comparatively, the PARET MNR model is able to prevent boiling in one case and not the other.

Enough negative feedback is generated during a transient to counter the $2mk$ added, no matter its speed of addition between 0.2 and $20.0\,mk/s$, when initial power is below $0.8\,MW$. Somewhat larger initial reactor powers are allowed at higher reactivity insertion rates because the faster insertion rates seem to provide more feedback than do the slower rates.

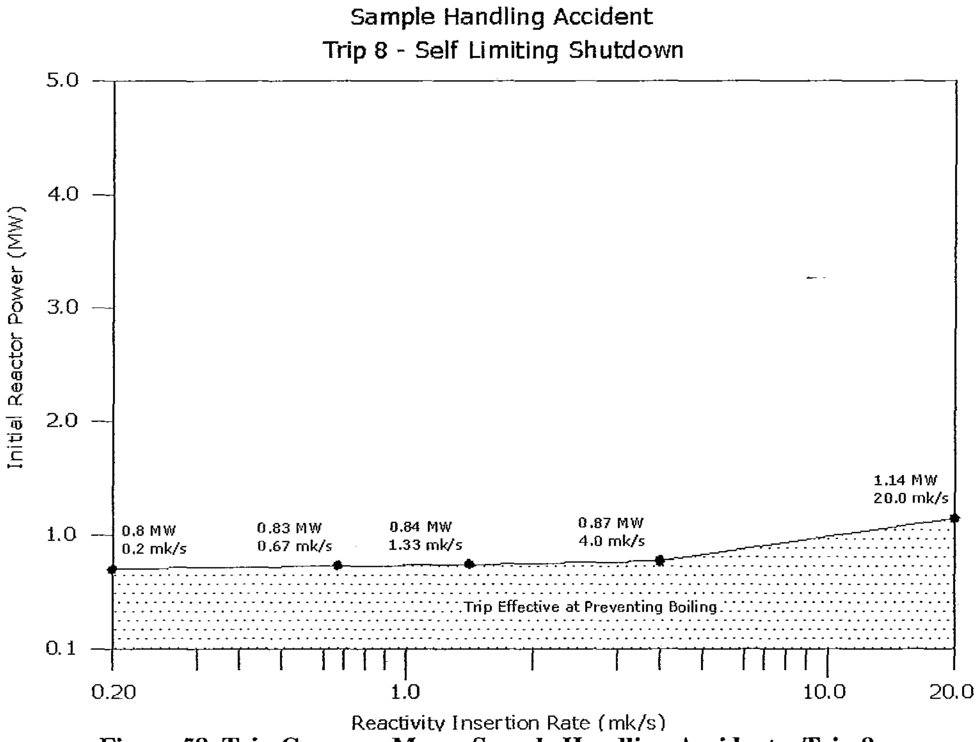

Figure 58. Trip Coverage Map – Sample Handling Accident – Trip 8

Figure 59 shows a single self limiting transient from the trip coverage boundary. On the time scale selected the reactivity insertion isn't clearly visible because it occurs in $2\,mk/20.0\,mk/s = 0.1\,s$. This fast insertion rate is responsible for raising the reactor power and generating the negative feedback which gradually inserts $-2\,mk$ of reactivity. After approximately $300\,s$ it is apparent the transient has become stable at $3.5\,MW$ (nominally $3.5\,MW/1.1 = 3.18\,MW$), far below the steady state $3.4\,MW$ nominal power required to induce bulk boiling according to Table 1.

Referring to Figure 15 which characterizes the fuel temperature reactivity feedback of MNR, fuel temperature would have to grow to $210\,^{o}C$ from an initial (pre-transient) fuel temperature of $80\,^{o}C$ to generate $-2\,mk$ of feedback. This assumes Doppler feedback to be the only source of feedback which is not the case; coolant density changes also contribute to feedback. In conjunction with coolant density feedback effects, fuel temperatures reach a maximum of $136\,^{o}C$ during the transient shown in Figure 59.

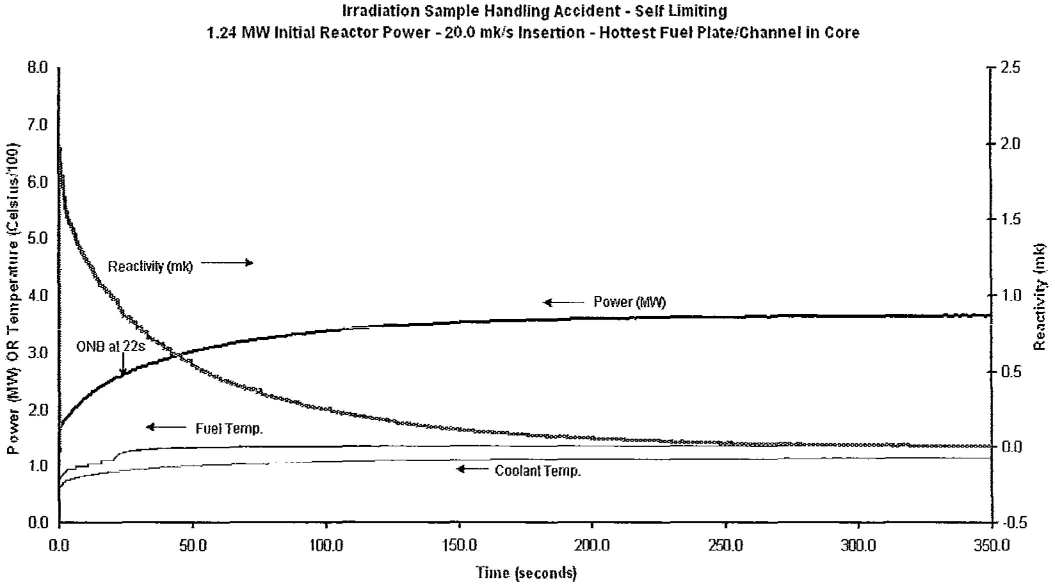

Figure 59. Transient from Simulation on Self Limiting Shutdown

5.5.8 Sample Handling Accident – Cumulative Trip Coverage Map

The cumulative trip coverage map for the modeled sample handling accident category is shown in Figure 60. Sample Handling Accident – Cumulative Trip Coverage Map. It shows PARET simulations of MNR predict there to be at least four independent instrument trips capable of preventing transients from reaching thermal limits (bulk boiling) within the simulated ranges.

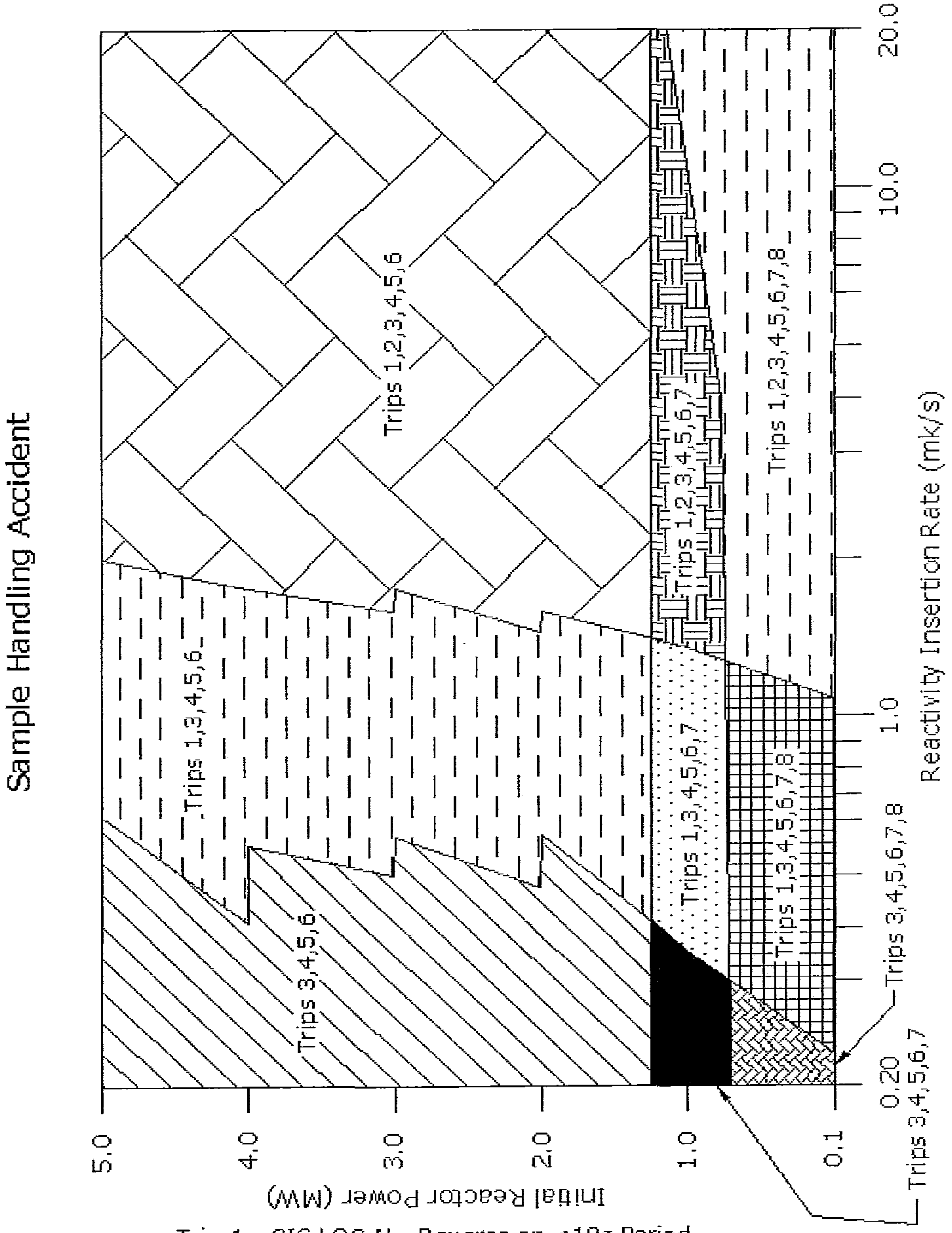

Trip 1 - CIC LOG N - Reverse on <10s Period
Trip 2 - CIC LOG N - Scram on <3.8s Period
Trip 3 - CIC B LIN N - Reverse on 7% LSE Power
Trip 4 - CIC A LOG N - Reverse on 110% HF Power
Trip 5 - UIC 1 SA - Scram on 125% HF Power
Trip 6 - UIC 2 SA - Scram on 125% HF Power
Trip 7 - CIC/UIC - Manual Scram on Alarms
Trip 8 - Self Limiting Shutdown

Figure 60. Sample Handling Accident – Cumulative Trip Coverage Map

5.6 Withdrawal of Shim/Safety Rods at High Power

The simultaneous withdrawal of all five SSR from the 50% withdrawn position inserts a very large amount of reactivity; the PARET MNR model predicts 55.1 mk to be inserted. Given this accident scenario has large reactivity insertion capability, the SAR does not credit self limiting shutdown for this accident category [10]. In order of occurrence, the SAR does credit the 110% HF reverse, both 125% HF scrams, the <10 s period reverse, the <3.8 s period scram and the manual scram [10].

It should be noted that the two rate trips, the <10 s period reverse and the <3.8 s period scram are credited by the SAR only because it is thought these instruments will trip "...by flow/power oscillations which arise in this accident if the reactor is not tripped prior to onset of boiling [Note11,10]." These two rate trips are nonetheless simulated with the PARET MNR model.

The +7% LSE reverse is not credited by the SAR because this accident category is postulated to occur under manual operation, and this instrument is capable of inducing a reverse when the reactor is set in automatic control [Note10,10]. The SSR can be driven out of the core manually when the reactor is under either manual or automatic control – assuming manual operation and the unavailability of the +7% LSE reverse for this analysis is the conservative assumption. The +7% LSE audible alarm does not operate under manual operation either [29].

The MNR Lin N instrument channel has an additional trip fully capable of arresting an inadvertent withdrawal of the SSR, a <30 s period inhibition. An inhibition is the disabling of the SSR drive mechanism's ability to withdraw the SSR [Sec.8.3.4,3]. However, the <30 s period inhibition is not given credit by the SAR because it is simply assumed to be unavailable. This inhibition has not been credited in any other accident category either since simply halting possible withdrawal of the SSR does nothing to arrest other accident categories which are driven by other positive reactivity sources (such as the regulating rod withdrawal, an in-core sample withdrawal or fuel assembly addition to the core).

As their trip coverage maps show, the 110% HF reverse channel (Figure 61. Trip Coverage Map – Withdrawal of SSR HP – Trip 2) and both 125% HF scram channels (Figure 62) are effective at preventing bulk boiling in PARET simulates within the estimated insertion rates. These instrument channels are effective because, as high power trips, all transients eventually bump into their power ceiling and trigger a trip; also, the subsequent insertion of the SSR is quick enough to prevent bulk boiling.

Although this accident category has the potential to insert a very large amount of reactivity, the SSR drive speed is a very slow 0.113 cm/s and this slow drive speed prevents all insertion rates tested from inducing a rate trip in the <3.8 s period scram channel (see Figure 64). Referring to Figure 63, only the largest reactivity insertion rates tested manage to achieve reactor transients with periods <10 s and are successfully

5.6.1 Reverse on 110% High Flux

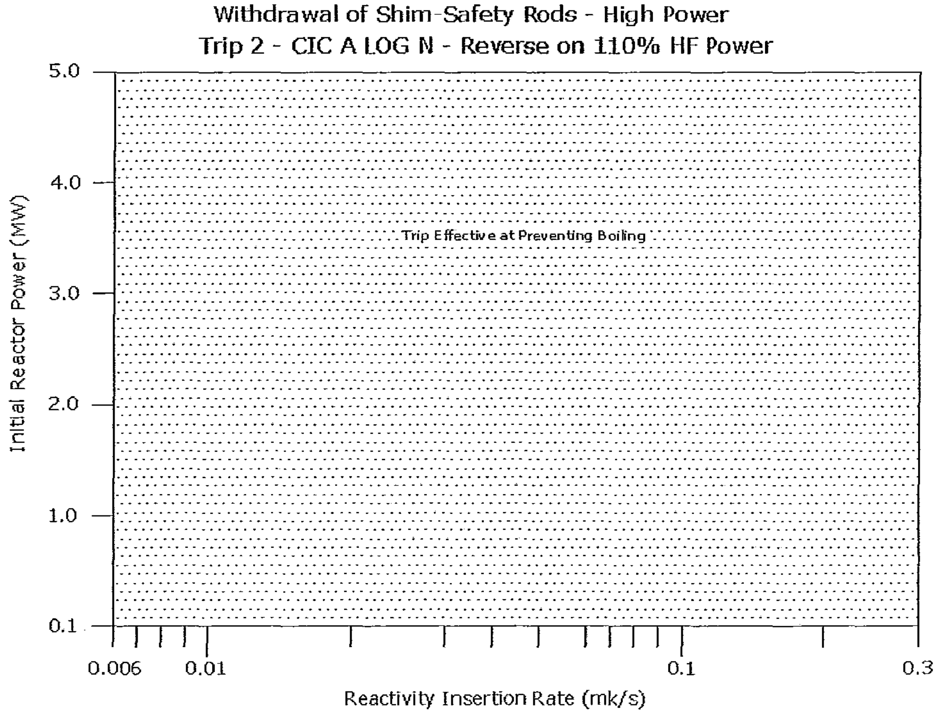

Figure 61. Trip Coverage Map – Withdrawal of SSR HP – Trip 2

5.6.2 Scram on 125% High Flux

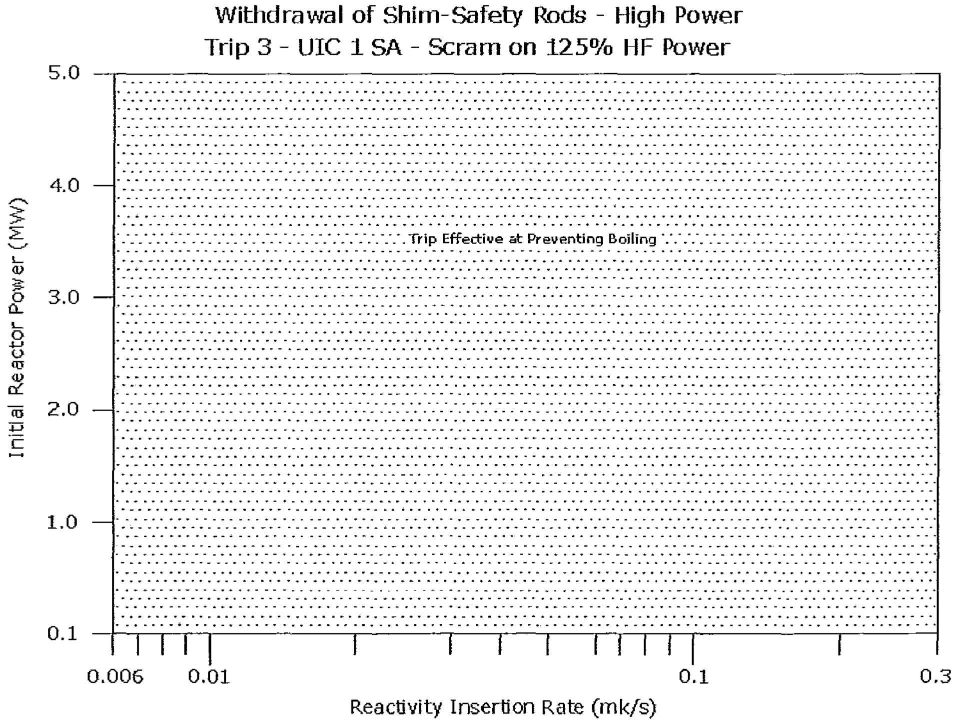

Figure 62. Trip Coverage Map – Withdrawal of SSR HP – Trip 3

5.6.3 Reverse on <10 Second Period

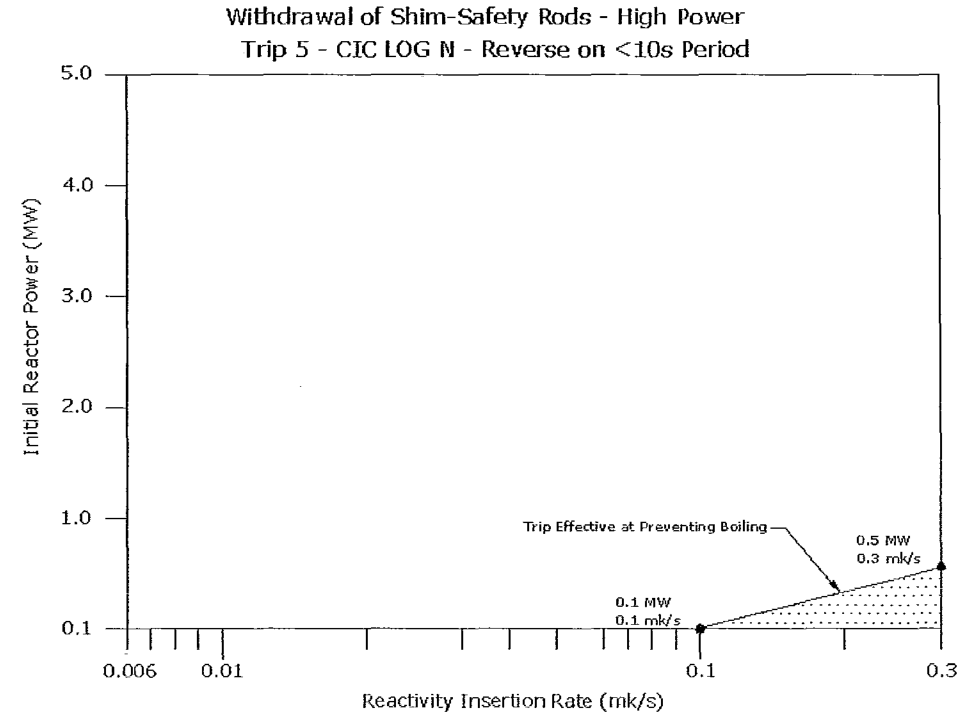

Figure 63. Trip Coverage Map – Withdrawal of SSR HP – Trip 5

5.6.4 Scram on <3.8 Second Period

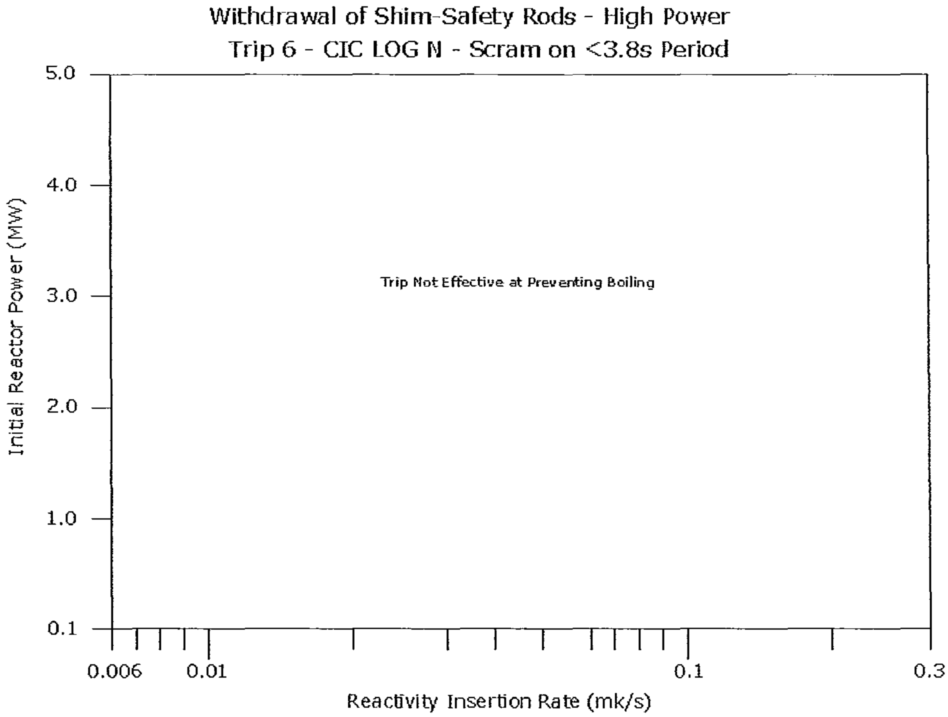

Figure 64. Trip Coverage Map – Withdrawal of SSR HP – Trip 6

arrested by the resulting reverse. Most reactivity insertion rates are just too slow to cause reactor power to build fast enough to signal a rate trip; this essentially confirms the SAR assumption that rate trips may only trip due to post-boiling power fluctuations.

5.6.5 Manual Scram on Alarms

Like the manual scrams in the other accident categories, a manual scram in the loss of SSR accident can only be effective at preventing bulk boiling during very small insertion rates, see Figure 65. The maximum reactivity insertion rate which gives the operator at least $300\,s$ to act is $0.009\,mk/s$ at $0.1\,MW$; at this rate of reactivity insertion it would take $55.1\,mk/0.009\,mk/s = 6110\,s$ to fully insert $55.1\,mk$.

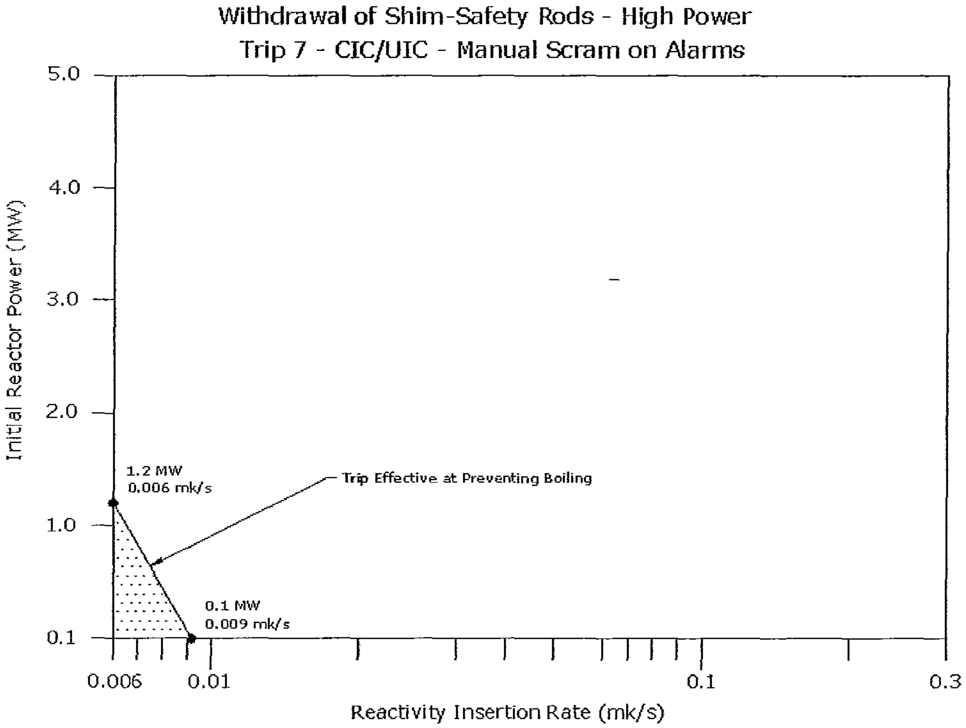

Figure 65. Trip Coverage Map – Withdrawal of SSR HP – Trip 7

A successful manual scram transient from the boundary of the Figure 65 map is shown in Figure 66. Reactivity in this transient is a very slow $0.009\,mk/s$.

Most other manual scrams simulated could assume the +7% LSE activates an audible alarm; however, this audible alarm is not available under manual operation. This category must depend upon the 110% HF audible alarm. Initial power is nominally $0.1\,MW$ and the audible alarm begins at $8.9\,s$ when power reaches $(1.1)(0.11\,MW) = 0.121\,MW$. At $308.9\,s$, after an elapsed $300\,s$, the operator is given credit for manually shutting the reactor down.

At the time of manual scram the reactor power has reached a peak of $3.05\,MW$. Throughout this transient the peak axial fuel temperature in the hottest fuel plate is predicted to be $133.4\,^{o}C$, peak clad temperature $132.7\,^{o}C$ and coolant at the channel outlet reaches only $99.8\,^{o}C$.

The defining characteristic of the SSR withdrawal accidents is the slow drive speed and large capacity for reactivity insertion. At $308.9\,s$ the SSR have withdrawn to insert only $2.829\,mk$ of the $55.1\,mk$ which could be inserted upon full SSR withdrawal. Upon scram the SSR stop inserting reactivity and drop into the core.

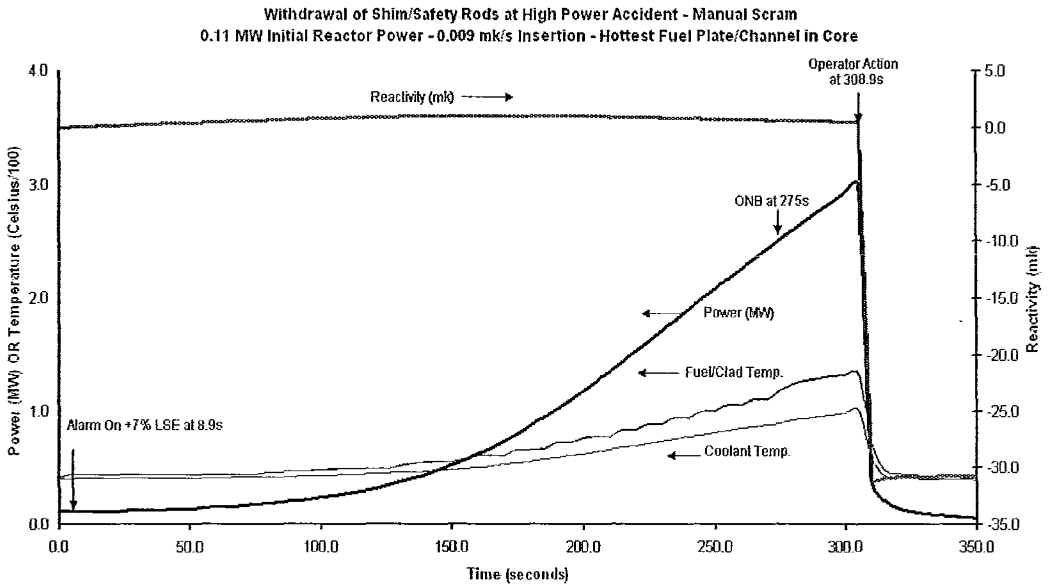

Figure 66. Transient from Simulation on Manual Scram Map

5.6.6 Withdrawal of Shim-Safety Rods at High Power – Cumulative Trip Coverage Map

The cumulative trip coverage map is shown in Figure 67. The PARET MNR simulations predict at least three instruments to be capable of preventing bulk boiling over the reactivity insertion ranges simulated.

The Lin N $<30\,s$ period inhibition channel was not simulated because the SAR trip evaluation assumes the instrument to be unavailable. Since the $<10\,s$ period reverse (Figure 63) is predicted to have some coverage over the parameters simulated, it is likely an instrument activated by a $<30\,s$ reactor period would have relatively more coverage.

Under automatic MNR operation, presumably the +7% LSE reverse would have a significant amount of additional coverage over the tested range. The +7% LSE reverse would halt the insertion of additional reactivity insertion upon a trip signal and would do so at an early point of seven percent above the initial reactor power.

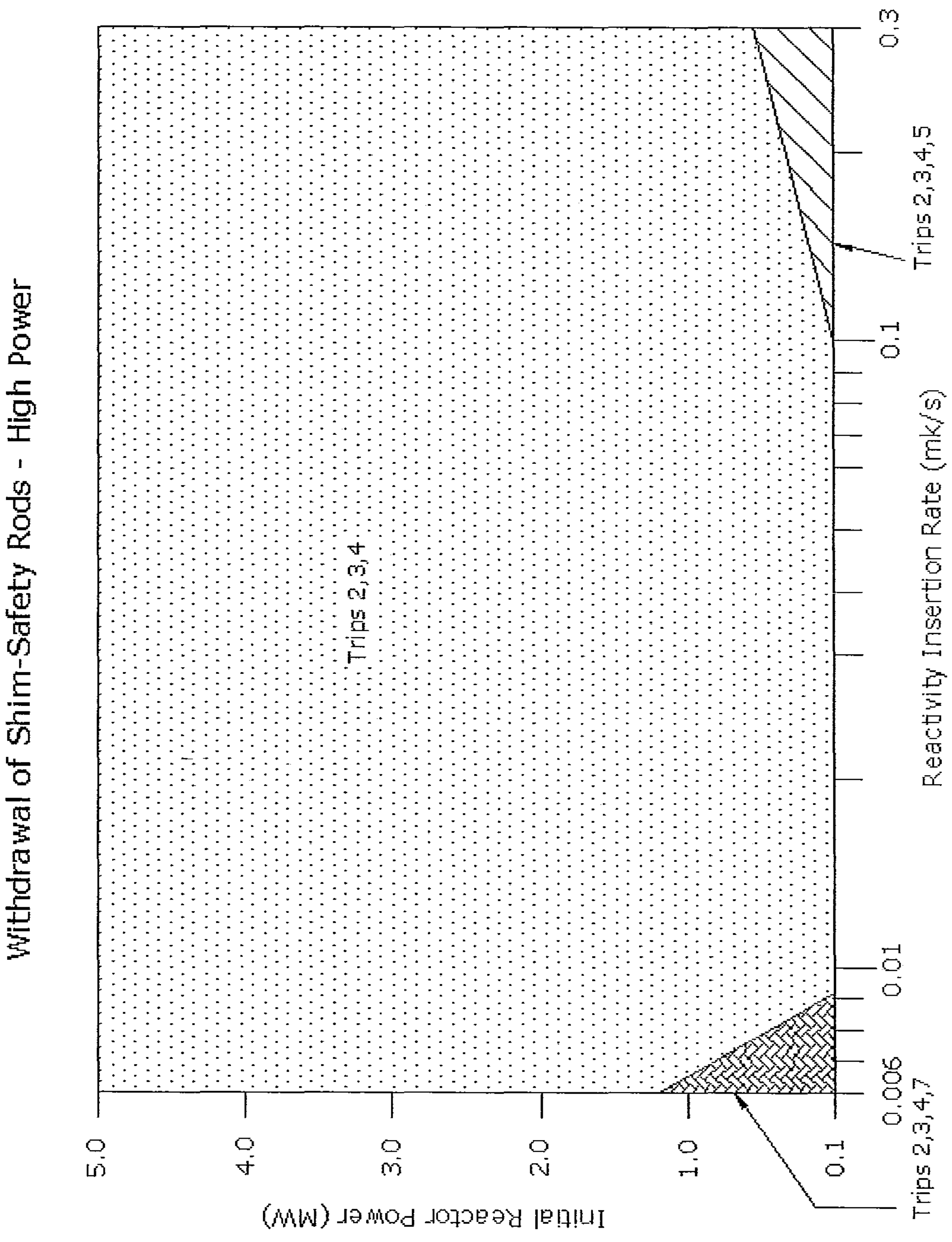

Trip 1 - CIC B LIN N - Reverse on 7% LSE Power
Trip 2 - CIC A LOG N - Reverse on 110% HF Power
Trip 3 - UIC 1 SA - Scram on 125% HF Power
Trip 4 - UIC 2 SA - Scram on 125% HF Power
Trip 5 - CIC LOG N - Reverse on <10s Period
Trip 6 - CIC LOG N - Scram on <3.8s Period
Trip 7 - CIC/UIC - Manual Scram on Alarms

Figure 67. Withdrawal of Shim/Safety Rods at High Power – Cumulative Trip Coverage Map

5.7 Withdrawal of Shim/Safety Rods at Low Power

Like the high power withdrawal of SSR accident cases, the SAR does not give credit to the <30 s period inhibition (because it is assumed unavailable) or to the +7% LSE reverse (because MNR operation is assumed to be in manual mode) during low power SSR withdrawal [10].

Compared to the high power withdrawal case, both the rate trips provide more coverage at powers below 100 kW. The feedback effects produced at higher powers subtract from the externally inserted positive reactivity and reduce its effect; unmitigated insertions at low powers achieve shorter reactor periods and induce trips while the same insertion rate at higher powers are somewhat arrested by reactor feedback; compare the high power <10 s period reverse in Figure 63 and the low power equivalent in Figure 68, as well as the completely ineffective high power <3.8 s period scram in Figure 64 and the partially effective low power equivalent in Figure 69.

The 110% HF reverse and both 125% HF scram channels are completely ineffective at preventing bulk boiling in this accident category (these trip coverage maps are not shown). They are ineffective because under low power operation their trip set points, 5.5 and 6.25 MW, are far above the power required to induce boiling; these conservative set point assumptions are identical to those made in the low power regulating rod withdrawal category.

The manual scram in this accident category is also ineffective at preventing boiling (trip coverage map not shown). The reason manual scrams are not effective is due to the fact that two of the three audible alarms normally depended upon to alert the operators of a transient are not available. The +7% LSE does not give an audible alarm when the reactor is in manual operation, the 110% HF alarm does not signal until a post-boiling 5.5 MW. Only the <10 s period alarm is capable of alarming during a transient, but periods of this size do not give the operator the required 300 s to react before coolant reaches saturation temperatures.

As a result of so many safety instruments being assumed unavailable and having reactor power trip set points assumed to be high, the cumulative trip coverage map for this accident category has no instruments capable of preventing bulk boiling under some conditions, see Figure 70.

5.7.1 Reverse on <10 Second Period

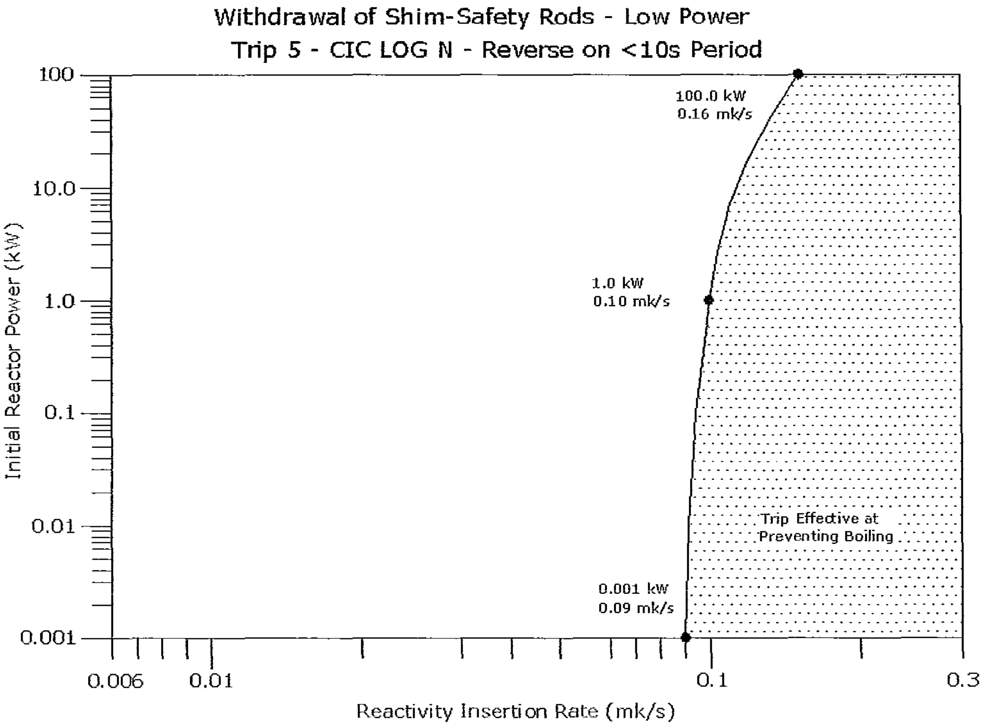

Figure 68. Trip Coverage Map – Withdrawal of SSR LP – Trip 5

5.7.2 Scram on <3.8 Second Period

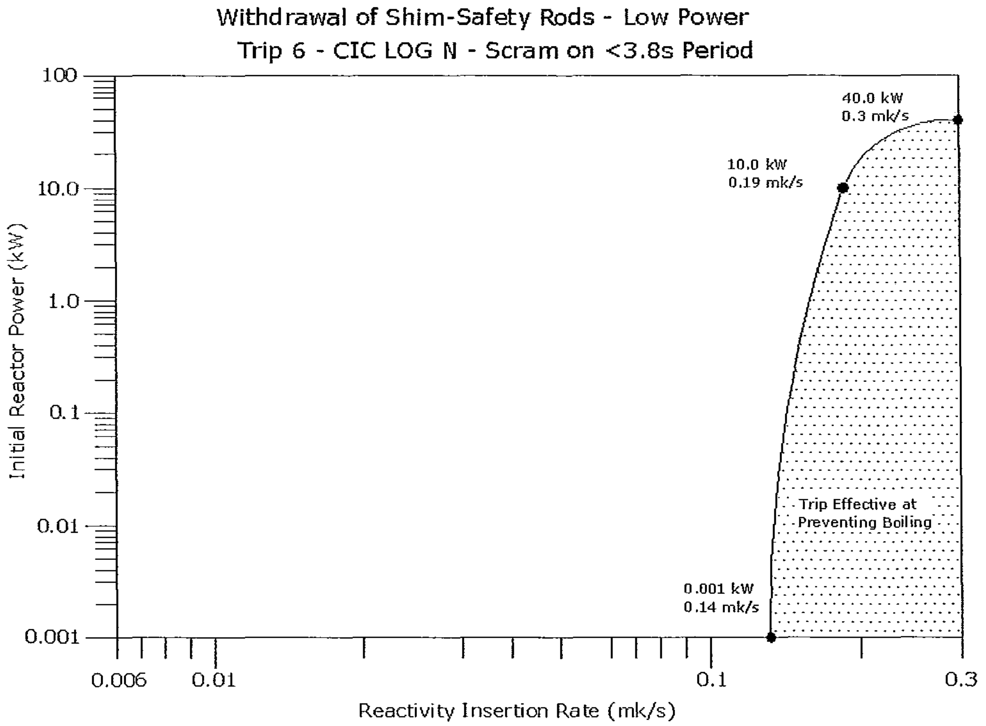

Figure 69. Trip Coverage Map – Withdrawal of SSR LP – Trip 6

5.7.3 Withdrawal of Shim-Safety Rods at Low Power – Cumulative Trip Coverage Map

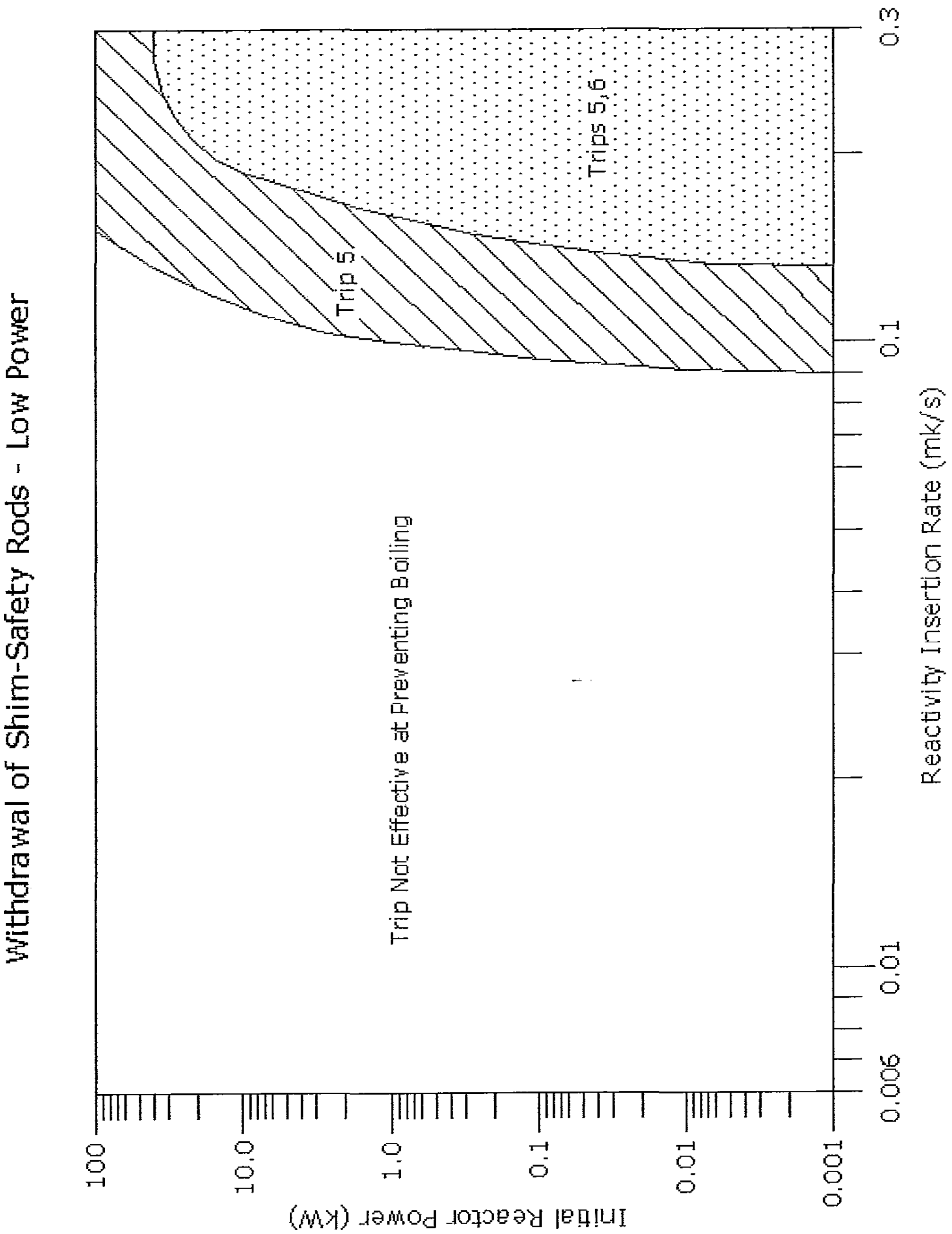

Trip 1 - CIC B LIN N - Reverse on 7% LSE Power
Trip 2 - CIC A LOG N - Reverse on 110% HF Power
Trip 3 - UIC 1 SA - Scram on 125% HF Power
Trip 4 - UIC 2 SA - Scram on 125% HF Power
Trip 5 - CIC LOG N - Reverse on <10s Period
Trip 6 - CIC LOG N - Scram on <3.8s Period
Trip 7 - CIC/UIC - Manual Scram on Alarms

Figure 70. Withdrawal of Shim-Safety Rods at Low Power – Cumulative Trip Coverage Map

5.8 Fuel Handling Accidents

The SAR gives credit to the <3.8 s period scram, both 125%HF scrams and the self limiting shutdown for preventing fuel damage in this accident category [10]. Fuel handling occurs when the reactor is in a shutdown state under manual operation, consequentially the +7% LSE reverse cannot be assumed available.

This postulated accident scenario adds large amounts of reactivity in a short amount of time therefore the <10 s period and 110% HF reverses are not given credit by the SAR for their limited negative reactivity insertion capabilities [10]. The manual scram is not given credit by the SAR for fast reactivity insertion rates [10]. Based upon running many simulations of these transients in other accident event categories, these are judged to be reasonable assumptions and these instrument channels have not been simulated with PARET and are assumed ineffective at preventing bulk boiling within this accident category.

Figure 71 shows the modeled fuel handling accident scenario where $12.3\,mk$ is inserted in $2\,s$ at a rate of $6.15\,mk/s$. The transient is successfully arrested by the <3.8 s period scram before reaching any thermal limit. As soon as the transient begins the period reaches very small values (reactor period is approximately 0.55 s over the first 0.1 s of the transient) and the instrument scrams at 0.1 s. These transient simulations examine reactor power every 0.1 s, if power over any 0.1 s interval has grown to a value larger than it would have with a 3.8 s period, the instrument trips; in other words the <3.8 s period instrument presiding over the transient in Figure 71 tripped at the first opportunity, 0.1 s.

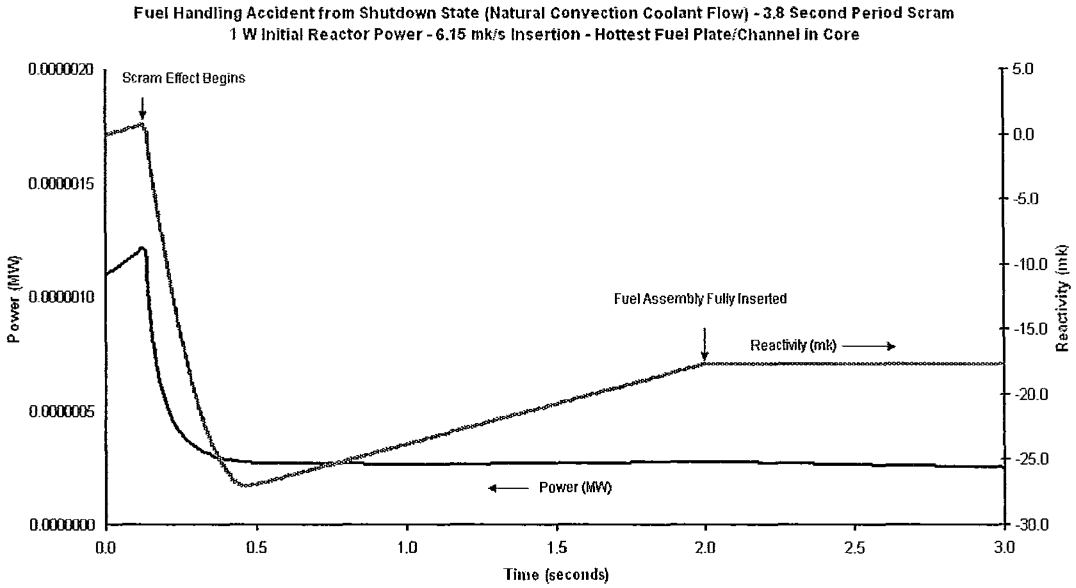

Figure 71. Transient from Simulation on CIC Log N <3.8s Period Scram

Initial reactor power is $1.1\,W$, and all fuel, cladding and coolant in the channel at transient time zero is $38\,^oC$. The PARET MNR model predicts power to reach a peak of $1.22\,W$ at $0.127\,s$ if a trip signal is generated at $0.1\,s$, before negative reactivity insertion begins to reduce power. The PARET MNR model has a $0.025\,s$ delay between trip signal and SSR movement, during which time reactor power continues to grow.

The transient is arrested before power grows beyond negligible values and thus fuel, clad or coolant temperature (which are not plotted in Figure 71) all remain at the pool temperature of $38\,^oC$. The dropped fuel assembly continues to add reactivity after the scram until $2.0\,s$; the depth of the scram shutdown is enough to keep the reactor deeply subcritical after the transient time $0.13\,s$ when total reactivity goes from positive to negative.

Figure 72 shows the fuel handling transient being successfully arrested by the 125% HF scram. The scram set point for both 125% HF channels is set at $6.875\,MW$; the transient reaches this set point and the instrument trips at $1.719\,s$. Reactor power peaks at $33.4\,MW$ at $1.763\,s$ before the insertion of the SSR drops reactor power. At the moment of peak reactor power the maximum fuel temperature is $90.8\,^oC$ - from $1.763\,s$ onwards the reactor power drops but fuel temperature continues to rise until $1.818\,s$ when fuel temperature reaches a peak of $130.0\,^oC$. The average reactor period between 0 and $1.763\,s$ is $0.1\,s$.

Although reactor power in this transient is much higher than encountered in any previous PARET MNR transient, the fuel and clad temperatures are still within allowable operating ranges. The short duration of time spent at high powers in this transient doesn't release enough energy to significantly heat the fuel, clad or coolant.

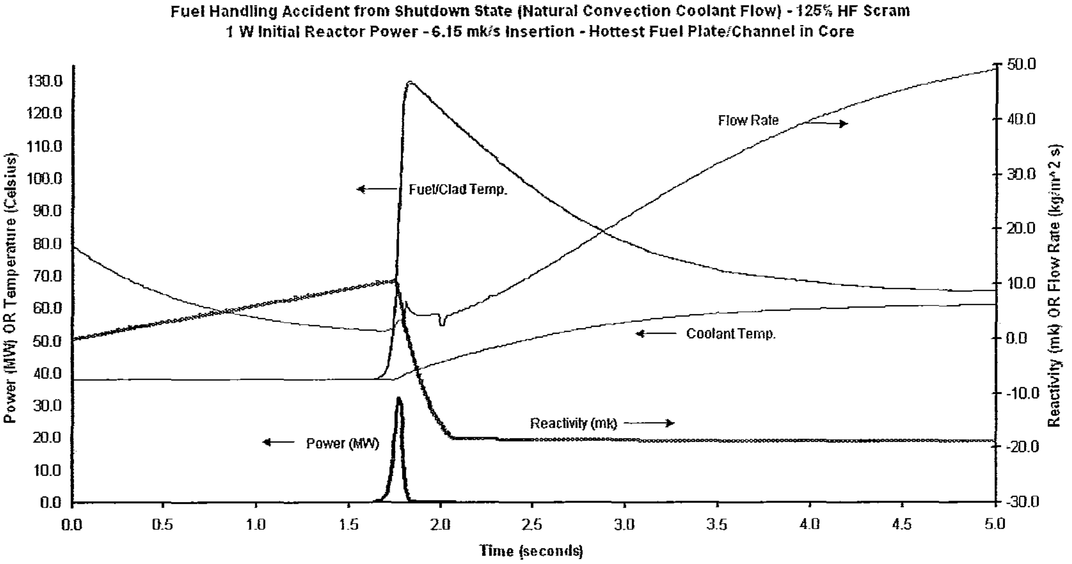

Figure 72. Transient from Simulation on UIC 1 and 2 SA 125% HF Scram

Bulk boiling is avoided throughout the transient, and ONB occurs at $1.788\,s$ when clad surface temperature reaches $119\,^{o}C$. The coolant flow rate in Figure 72 grows in magnitude as the energy generated in the fuel moves into the coolant.

The SAR credits the self limiting shutdown during a fuel handling accident because the "Administrative limit on the minimum negative reactivity margin is in effect, which avoids fuel damage in case of an unprotected reactivity insertion by any fuel handling accident [10]." This is interpreted to mean the SAR analysis presumed the reactor to be so deeply subcritical at time zero of the transient that fuel damage would be avoided upon an addition of positive reactivity created by a postulated fuel handling accident.

A PARET MNR simulation of the fuel handling accident scenario with no trip was run and the reactor feedback generated fails to prevent the onset of bulk coolant boiling. The PARET simulation predicts power to reach $242\,MW$ at $1.807\,s$ and maximum fuel temperature is $430\,^{o}C$ at $1.814\,s$ before the simulation crashes. DNB is predicted to occur at $1.784\,s$ when clad surface temperature is $159\,^{o}C$. As has been experimentally determined in other MTR-type reactors, this significant void generation may induce power oscillations, but this phase of the transient analysis is beyond the scope of this particular study [13].

6 Concluding Remarks

This chapter briefly summarizes the results discussed in Chapter 5. These conclusions may be used by MNR staff to enhance their understanding of the capabilities of the instrument shutdown systems, and as a reference to estimate early consequences of postulated power excursions.

Before concluding statements are made, suggested work topics which may be undertaken in the future to enhance the accuracy of this study are discussed. These suggested work topics address limitations in the concept of using PARET for MNR trip map development and limitations in the assumptions made during the development of the PARET MNR model.

Throughout the discussion of this report's conclusions, it should be kept in mind that this trip map development used conservative parameters to estimate the ability of the instrument shutdown systems to prevent the onset of bulk boiling within the context of film boiling and the $450^{o}C$ clad surface safety limit – as outlined in the Chapter 2 section Boundaries of MNR Trip Maps. The predicted failure of a shutdown system to preventing bulk boiling, film boiling or $450^{o}C$ clad temperatures does not necessarily lead to fuel melting [13].

6.1 Recommendations for Future Work

Throughout the trip map development process, it has been noted the boiling regime prevalent within a coolant channel is dependent upon the mass flow rate of the coolant. The PARET model of MNR depended upon past hydraulic studies (see Appendix B) to conservatively estimate the coolant flow rates within the fuel elements; Figure 24 gives flow rate information for the standard fuel assembly in a convenient form and was the key SOE document used in the development of the PARET MNR model.

The SOE document discusses at length the fact that no hydraulic study of the MNR core is certain of the flow rates through the bypass holes in the grid plate [9]. Since the bypass hole flow is a component of total core coolant flow (an operational variable which directly effects core cooling) it would be very useful if bypass hole flow could be directly measured. An actual measurement of bypass core flow would eliminate the need for the SOE (and by extension the PARET model) to make what are probably extremely conservative estimates of bypass flow.

Trip map development is extremely dependent upon the capabilities of the instrument safety systems – trip maps are a direct examination of their abilities. In this report, models of instrument abilities and behavior were developed in what is believed to be a conservative manner; however, the general assumptions could be reviewed by personnel familiar with MNR instrumentation to confirm the PARET model is not overly simplistic.

Particularly, a study should be undertaken to determine what duration of time the MNR period needs to be below a trip value (for example $<3.8\,s$, $<10\,s$ or $<30\,s$) before the instrument channels recognize the small period. Based upon conversations with MNR operating staff, duration of 0.1 s is believed to be conservative and is used in the PARET model as a sampling time [29].

The SAR credits rate trips in various accident categories with effective transient arrest after being tripped by the large power oscillations induced by the onset of large amounts of in-core boiling [10]. This trip map development study did not give credit to post boiling rate trips nor to rate trips simulated to occur beyond the first $30\,s$ of transient simulation. If an examination of the boiling induced power oscillations revealed these power oscillations to be quite fast, it is possible all the rate trips would be effectively triggered and offer effective transient protection against fuel damage.

Discussion of post onset of saturation boiling leads to another topic which may be studied for transient safety analysis - that of modeling late-stage power transients. As discussed in Chapter 2 PARET is not capable of modeling cores with significant amounts of vapor generation. A validated code capable of modeling the MNR core up to the onset of fuel melting temperatures would be of obvious value.

Although Woodruff shows the updated convective heat transfer correlations in PARET perform acceptably, a review of these correlations deemed by Woodruff to be "appropriate for research reactors" found some were not originally developed specifically for conditions in plate fuel or MNR typical flow rates and Reynolds numbers [20]. One can find various heat transfer coefficient, ONB and DNB empirical relationships in literature which would presumably be better suited to modeling MNR (and other research reactor) operation. For example, Cubillos-Moreno et.al. propose an ONB correlation empirically developed from flow observations in simulated plate fuel with a $3\,mm$ coolant channel [45].

PARET users wonder how accurate the variables they use to describe the core model need to be. After completing hundreds of PARET simulations a user develops a feel of the sensitivities of the most commonly changed variables, however, a formal study outlining the transient consequences resulting from variable perturbations would be useful.

6.2 List of Conservatisms

During the development of the MNR PARET model, various uncertainties were considered. Additionally, conservative assumptions were required to safely generalize the model for various reactor configurations and event categories.

Readers who briefly examine only the results of this study may not understand the magnitude of the conservatisms unless the remainder of the report is reviewed. Therefore, the major conservative assumptions and uncertainty allowances made throughout the report are summarized here for convenience in appropriate categories:

General Conservatisms

1. The stabilizing control of the regulating rod is completely ignored in the PARET model. PARET assumes reactivity to be zero at time zero of a simulated transient and the user inserts the desired amount of transient inducing reactivity. In MNR, positive or negative reactivity insertions of small enough size would be compensated for by the control system and the movement of the regulating rod.
2. All simulations account for the reactor power uncertainty by adding 10% to the nominal reactor power.
3. Because the core arrangement and power peaking factors for the PARET model were taken from the Reference Core and Power Peaking Factor reports, the model inherited all the associated conservatisms [1,11].
4. When simulating a transient with a rate trip instrument active (*i.e.* $<3.8\,s$ period scram or the $<10.0\,s$ period reverse) reactor period needed to be below 3.8 or $10.0\,s$ over a time span of at least $0.1\,s$ before the trip is signaled. For example, if reactor power grows significantly over a $0.001\,s$ time span during a simulation, the rate trip is not credited.

Coolant Conservatisms

1. The pool water is assumed to be $38\,^oC$ for all transients; this is the administrative maximum allowable temperature for pool water.
2. The lowest coolant channel flow in a standard assembly occurs in the outermost coolant channels. The highest power fuel plate in the 4C fuel assembly is the outermost fuelled plate. In the PARET model, the lowest coolant flow is dictated to cool the highest power fuel plate; the model assumes on the opposite side of the channel a similarly powered fuel plate is present. In reality the outermost coolant channel cools only one fuel plate – but the PARET model is not conservative by a factor of two since the second-outermost coolant channel cools two fuel plates with close to the same power density.
3. Operationally, the limit is 24 open coolant core-bypass flow holes. The PARET model assumes 25 holes to be open because the hydraulic reference document conducted analysis for 25 instead of 24 open holes [9].

4. The magnitude of flow assumed to pass through each bypass hole uses the same conservative factor as is used in the Flow Characteristics of MNR Core Components document [43].

Absorber Rod Conservatisms

1. In the development of the reactivity insertion rates for the loss of regulating rod control accidents, the maximum administrative rod worth limit was used, -6 mk.
2. In the development of the reactivity insertion rates for the shim/safety rod bank withdrawal accidents, the total rod bank was assumed to be worth the maximum of its historical range, -100 mk
3. Upon scram or reverse, the PARET model inserts a reactivity corresponding to the shim/safety rod bank's smallest historical worth value, -75 mk.
4. The shim/safety rods at time zero of all transients are assumed to have a position of 50% withdrawn. Therefore, upon shim/safety rod insertion on scram or reverse, the initial rod position is 50% withdrawn. This is a conservative approximation for the total amount of available negative reactivity.

6.3 Conclusions

Every reactivity initiated accident will eventually trigger overpower trip set points if allowed to progress and if the transient is not self limited by feedback. However, overpower instruments are not effective in the case of fast reactor transients which generate temperatures beyond thermal limits before safety systems take effect and mitigate the transient. For example, the coverage maps boundaries for the +7% LSE and 110% HF reverses are shown in Figure 32 and Figure 34; these boundaries show that reverses are more suitable for arresting transients driven by slow reactivity insertion rates.

When considering the same reactivity insertion rates, as in Figure 36, power trips which initiate scrams are more capable of arresting fast moving reactor transients since the SSR insert at a faster rate.

Rate trips are useful in that a fast moving transient can be detected as soon as it begins. When considering MNR power transients prior to progression to the creation of significant void, slow moving transients may not trigger a rate trip instrument, as is shown by the trip coverage maps in Figure 28 and Figure 30 which show a minimum effective reactivity insertion rate.

The PARET MNR model developed for this project is consistent with the analysis contained in the MNR SOE document, which defines minimum flow rates for various power set points based on an avoidance of bulk boiling; the recommended administrative minimum flow rates are predicted by the PARET

MNR model to be adequate in preventing saturated bulk boiling [9]. Table 1 summarizes these findings and illustrates bulk boiling inducing powers for all recommended flow rates are predicted by PARET to be appropriately high.

The conservative PARET model predicts MNR to have, at minimum, single instrument trip coverage against the onset of bulk boiling, film boiling and $450\,^{o}C$ clad surface temperatures during loss of regulating rod control, sample handling accidents and loss of shim/safety rod control, when initiated from reactor powers between $0.1\text{-}5.0\,MW$. These findings are based upon PARET transient simulations and are shown in the respective cumulative trip coverage maps of high power accident scenarios in Figure 42. Loss of Regulation Rod Control at High Power - Cumulative Trip Coverage Map, Figure 60. Sample Handling Accident – Cumulative Trip Coverage Map and Figure 67. Withdrawal of Shim/Safety Rods at High Power – Cumulative Trip Coverage Map. At a minimum, single instrument trip coverage is also expected during the loss of regulation rod control at powers below $0.1\,MW$, as is shown by the cumulative trip coverage map in Figure 51.

While assuming the +7% LSE reverse and the <30 s reverse are unavailable, the PARET model predicts some transients induced by the withdrawal of SSR during low power operation ($<0.1\,MW$) may not prevent the onset of saturated boiling in the single hottest fuel channel of MNR. These findings are summarized in the cumulative trip coverage map shown in Figure 70.

The fuel handling accident transient case modeled by PARET predicts the $<3.8\,s$ period scram and both 125% HF scram channels are effective at preventing the onset of saturated bulk boiling, as in Figure 71 and Figure 72. The maximum fuel centerline temperature reached in any successfully arrested accident transient is $145\,^{o}C$ - well below the thermal limit of $450\,^{o}C$ clad surface temperatures.

References

[1] Day, S.E., "MNR Reference Core for SAR", MNR Technical Note 010705, 5 July 2001.

[2] Pasuta, R., "MNR Fuel Management Procedure FM-2211; Critical Experiments: An Overview," Rev.98-11, Nov.16, 1998.

[3] "McMaster Nuclear Reactor Safety Analysis Report," MNR Document, 2002.

[4] Woodruff, W.L., Smith, R.S., "A Users Guide for the ANL Version of the PARET Code," Argonne National Laboratory, Argonne, ILL, USA, 2001.

[5] Obenchain, C.F., "PARET – A Program for the Analysis of Reactor Transients," U.S. Atomic Energy Comission, ID, USA, 1969.

[6] "MNR Operating Limits and Conditions," McMaster Nuclear Reactor Document AP-1111 Rev.6, June 8, 2007.

[7] - Open Source Freeware Engineering, Excel Engineering "X Steam Tables for MATLAB," Download from <http://www.x-eng.com/XSteam_Matlab.htm>, Jan.08.

[8] Olson, A.P., "A Users Guide to the PARET/ANL V7.4 Code," Argonne National Laboratory, Argonne, ILL, USA, May 22, 2009.

[9] Pasuta, R., "Safe Operating Envelope of McMaster Nuclear Reactor," McMaster Nuclear Reactor Document TN-2001-01, Rev. 4, April 30, 2007.

[10] Day, S.E, Blahnik, C., "Summary of Reactor Trip Coverage for Accidents Analyzed in MNR SAR 2002," McMaster Nuclear Reactor Document TN 2005-04, Rev. 0, January 2005.

[11] Day, S.E., "Power Peaking Factors in MNR," McMaster Nuclear Reactor Document Technical Report 1999-07, Rev.1, February 17, 2002.

[12] Duderstadt, J.J., Hamilton, L.J., "Nuclear Reactor Analysis," John Wiley & Sons, 1976.

[13] Dietrich, J.R., Layman, D.C., "Transient and Steady State Characteristics of a Boiling Reactor. The BORAX Experiments," United States Atomic Energy Commission, AECD-3840, Argonne National Laboratory, Illinois, 1953.

[14] Day, S.E., MNR JAN04 Data Set, Microsoft Excel File "mnr-JAN04-SED_REBUS-coolant-reactivity-details_090305.xls"

[15] Blahnik, C. "MNR Flow Summary Report, D2 (Draft)," MNR Document (Unpublished), 2007.

[16] Ha, T., "Hydraulic Studies of the 18-Plate Assembly in the McMaster Nuclear Reactor," M.Sc. Thesis Engineering Physics, McMaster University, April 2002.

[17] MNR Data Set, JAN04 Dataset, Provided by Day, S.E., Microsoft Excel File "Core 54A Reactivity Data and Tables.xls," March 2008.

[18] Butler, M., "MNR Fuel Management Program," MNR Document FM-2100, Rev 98-11, Issued Nov.23, 1998.

[19] Day, S.E., Private Note, Feb.20/2009, Fuel Handling Accident Scenarios, Excerpts from "McMaster Nuclear Reactor Safety Analysis Report," MNR, 2002.

[20] Woodruff, W.L., "A Kinetics and Thermal-Hydraulics Capability for the Analysis of Research Reactors," Nuclear Technology, Vol.64, Pg.196-206, Feb.1984.

[21] International Atomic Energy Agency, "Research Reactor Core Conversion Guidebook," LEU Delayed Neutron Data 10MW Benchmark Reactor, IAEA Tecdoc-643, April 1992.

[22] MNR Data Set, JAN04 Dataset, Provided by Day, S.E., Microsoft Excel File "mnr-sed_kinetics-parameter-summary_090219.xls," March 2008.

[23] MNR Data Set, JAN04 Dataset, Provided by Day, S.E., Microsoft Excel File "MNR-physics_SED_MTR-fuel-thermal-properties_r0.xls," March 2008.

[24] MNR Data Set, JAN04 Dataset, Provided by Day, S.E., Microsoft Excel File "MNR-JAN04-SED_REBUS-power-dist-results.xls," March 2008.

[25] MNR Data Set, JAN04 Dataset, Provided by Day, S.E., Microsoft Excel File "MNR-JAN04-RC_SED_power-dist-results.xls," March 2008.

[26] Blahnik, C., "Hydraulic Properties of MNR Core Components," McMaster Nuclear Reactor Document Technical Report TN 2001-03, July 7, 2001.

[27] Housiadas, C., "Simulation of Loss-of-Flow Transients in Research Reactors," Nuclear Engergy, 27, 2000, Pg.1683-1693.

[28] Olson, A.P., Argonne National Laboratory, Private Email, May 4, 2009.

[29] Personal conversations with R.Pasuta - MNR Operations, M.Butler - MNR Operations, March 2009.

[30] International Atomic Energy Agency, "Safety Assessment of Research Reactors and Preparation of the Safety Analysis Report," Safety Series No. 35-G1, Vienna Austria, 1994.

[31] Kreith, F., Bohn, M.S., "Principles of Heat Transfer," 6th Edition, Brooks/Cole, USA, 2001.

[32] Lamarsh, J.R., Baratta, A.J., "Introduction to Nuclear Engineering," 3rd Edition, Prentice Hall, New Jersey USA, 2001.

[33] Chart of the Nuclides, National Nuclear Data Centre, Brookhaven National Lab, Website <www.nndc.bnl.gov>, June 2009.

[34] Personal conversations with R.Pasuta - MNR Operations, M.Butler - MNR Operations, June 2009.

[35] Luxat, J., "EP 713 Nuclear Safety Analysis & Reactor Accidents," Course Notes (Unpublished), McMaster University, 2007.

[36] Luxat, J., "EP 4NE3 Advanced Nuclear Engineering," Course Notes (Unpublished), McMaster University, 2008.

[37] Reduced Enrichment for Research and Test Reactors, Website <http://www.rertr.anl.gov/>, Jan.15, 2008.

[38] Rosenthal, M.W., Miller, R.L., "An Experimental Study of Transient Boiling," ORNL-2294, 1957.

[39] Morgan, R.P., "A Review and Discussion of Literature Concerning Transient Heat Transfer and Steam Formation," IDO-17226, Idaho National Engineering Lab, 1967.

[40] Collier, J.G., Thome, J.R., "Convective Boiling and Condensation," Third Edition, Clardendon Press, 2001.

[41] Matos, J.E., Pennington, E.M., Freese, K.E., Woodruff, W.L., "Research Reactor Core Conversion Guidebook," IAEA, Volume 3: Analytical Verification, IAEA-TECDOC-643, 1992.

[42] Blahnik, C., "Flow Characteristics of MNR Core Components", MNR Technical Note 2001-07, 15 July 2001.

[43] Blahnik, C., "Hydraulic Properties of MNR Core Components", MNR Technical
Note, 7 July 2001.

[44] Rummens, H.E.C., "Thermalhydraulic Studies of the McMaster Nuclear Core,"
McMaster University, M.Sc. Thesis, 1988.

[45] Cublillos-Moreno, E., Belhadj, M., Aldemir, T., "Validation and Extension of a Correlation for Predicting Onset of Nucleate Boiling in Plate-Type Research Reactors," Journal of Nuclear Technology, Vol.98, June 1992.

Appendix A – MNR Flow Analysis

There are a number of MNR hydraulic studies which have analyzed the MNR coolant core flow and attempt to estimate the total coolant channel flow and the bypass flow (that is, flow not moving through the coolant channels) as a function of the total core flow. The SOE document is the authoritative document and is the document from which the OLC document takes its minimum flow recommendation. A short discussion follows of the foundational work used by the SOE document.

The SOE document "defines the combinations of reactor power, core flow and coolant temperatures which avoid laminar flow and/or [saturated] boiling in any channel of any fuel assembly [Pg.1,9]." Laminar flow is of concern "because the transition from turbulent to laminar flow cannot be reliably evaluated" and presumably because cooling in a laminar regime is not as effective as in a turbulent regime when the boundary layer is much smaller [Pg.1,9].

Based upon the results of an older experimental study of flow through MNR fuel assemblies, the SOE document states flow through a standard fuel assembly should be a minimum 1 liter per second to avoid laminar flow [Pg.2,9].

Knowing flow per standard assembly is to be above 1 liter per second and allowing the maximum outlet coolant temperature to equal saturation temperature, the SOE calculates minimum allowable flow rates based upon possible ranges of inlet (pool water) temperatures, reactor powers and number of open bypass holes [Pg.2,9]. To do this analysis a number of other hydraulic study documents were consulted.

Using the hydraulic resistances of each core component from the Hydraulic Properties of MNR Core Components report [43] and an estimated bypass hole flow from the report Thermalhydraulic Studies of the McMaster Nuclear Core [44] the core component flows as a function of plenum box pressure is developed, as shown in Figure 73. Throughout this analysis, a large bypass hole flow uncertainty is acknowledged as is shown in Figure 74; to make the work conservative each bypass hole flow is assumed to equal 92% of the flow through a standard fuel assembly.

The Hydraulic Properties of MNR Core Components report developed detailed resistance of all core assemblies such as the one shown in Figure 75 [43].

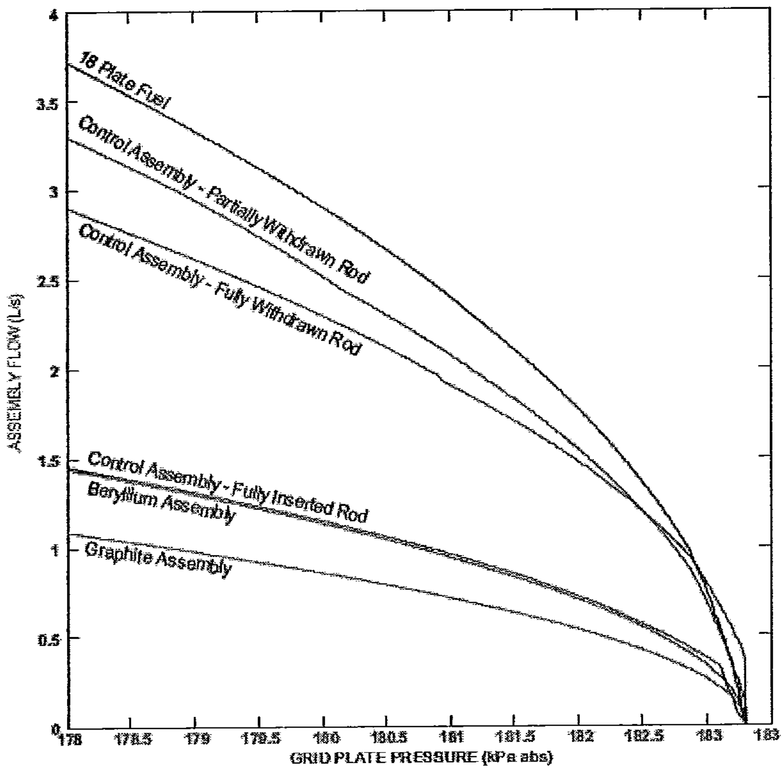

Figure 73. Flow Through Core Assemblies as Function of Plenum Box Pressure [42]

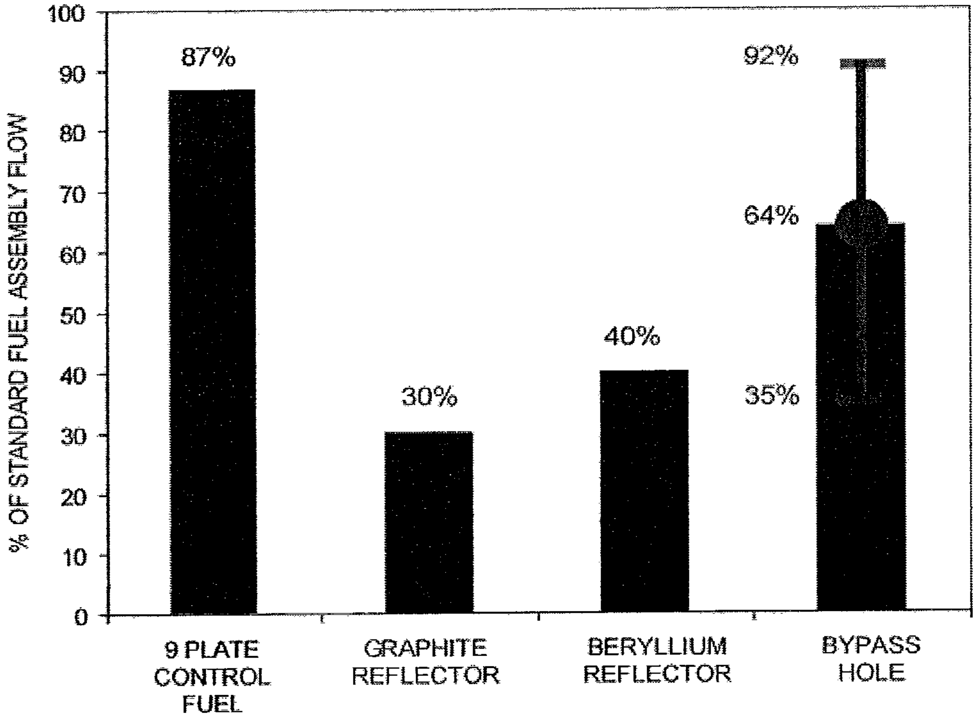

Figure 74. Component Flow Relative to Standard Fuel Assembly Flow [42]

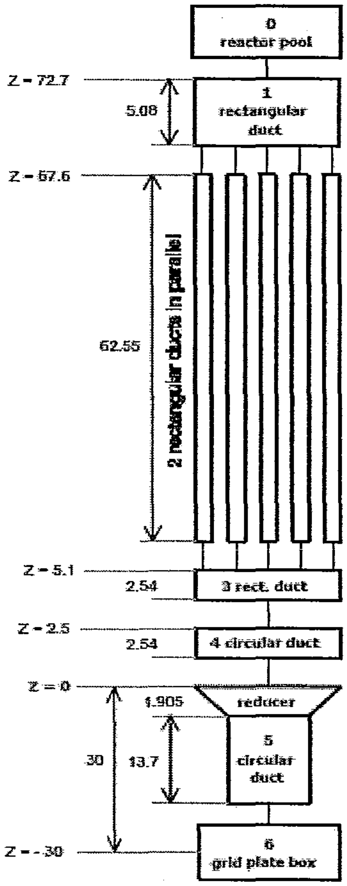

#	N	A (cm^2)	ΣA (cm^2)	Pe (cm)	D_h (cm)	ψ	ς	κ	X	ΔZ (cm)	L (cm)
0										72.7	
1	1	48.99	48.99	28.2	6.949	1	0.5	0.1	0.6	72.7	5.1
2	17	2.09	35.45	14.01	0.595	22.1	0.14	0	0.14	67.6	62.5
3	1	48.99	48.99	28.2	6.949	1	0.08	0	0.08	5.1	2.5
4	1	30.88	30.88	19.7	6.27	1	1.18	0	1.18	2.5	2.5
5	1	20.27	20.27	15.96	5.08	1	0.07	1	1.07	0	15.6
6										-30	

Figure 75. Flow Parameters for the 18 Plate Standard Fuel Assembly [43]

Appendix B - PARET Input File Preparation and Output File Reviewing

While creating the trip maps, it became apparent that not all of the information required to run PARET effectively was included in W.L. Woodruff and R.S. Smith's manual [4]. The new manual for PARET Version 7.4, which is based upon Woodruff and Smith's original and which was obtained later in the trip mapping process, has additional details added by A.P. Olson which confirmed some of the lessons already learned through hours of troubleshooting [8]. However, the manual for PARET V7.4 is still lacking in certain details and doesn't explain some things especially well, which can make operation of PARET confusing for the first time user. This Appendix is meant to supplement the official PARET manual to save future users time and to document the variable values used in the McMaster Nuclear Reactor PARET simulation input files.

Each PARET input file contains the variables the program requires to define the nature of the reactor and the conditions under which the simulated reactor is to operate. The manual lists each of the variables with a short explanation. For consistency, each variable is labeled here with the same item number and variable name as is used in the latest PARET manual written by A.P. Olson along with any additional details which will add to the understanding of the variable. Obenchain's original manual contains more detail about some of the program variables, and should be consulted in conjunction with this document for complete variable descriptions or historical understanding of the PARET development [5].

For most of the MNR transient simulations, the vast majority of the variables defined in the PARET input files do not change. For example all the runs completed in this study were completed on the MNR Reference Core arrangement. The geometric and kinetic variables which defined this core did not change from run to run, usually only the transient variables which describe the core's operating conditions such as initial power, reactor time step, flow and reactivity insertion rate changed.

Since it would not be practical to supply all the input files created during the trip mapping process (of which there are hundreds), the variables entered here will simulate MNR under a reactivity insertion of 2 *mk* in 1 *s* during 5MW operation, and should do the job of illustrating how the input files are created.

The input file preparation references the source of each thermalhydraulic, neutronic, geometric and operational parameter. Each parameter or variable is listed along with a discussion explaining any procedures or assumptions used to obtain a specific numerical value for the relevant variable.

The appropriate value to assign to some variables is not apparent, or it was impossible to define the variable specifically for the MNR model. In either of these cases, variable values are taken from an appropriate Woodruff sample input file, usually that of the 10MW IAEA Benchmark Reactor in the Woodruff manual [Pg.40,4]. At the very least then, MNR simulations use variables that were benchmarked by Woodruff.

The desired unit set for this case is SI, so input and output values will be stated in the units $s, m, kg, J, MW, Pa, {}^{o}K$ unless noted otherwise.

6.4 Input File Format

The entire PARET input file can be prepared in a text editor such as Notepad. Throughout the input file a standard spacing and line format is used. Each line of the input file begins with a card number. Each line of the input file defines specific variables, the card number identifies each line and PARET expects specific variables to be defined after each card number.

The card number is a four or five digit number followed immediately with a comma. The card number needs to be left justified and will occupy either four digits, a comma and a space or five digits and a space – six character columns total.

Each input file line has a defined width of 78 character columns, so no characters or spaces can be exist outside of this window. The first six character columns of each line are occupied by the card number discussed above and then contain a maximum of 12 numbers which define variables.

The maximum line containment of 12 defined variables is possible only if each variable is an integer (no decimal points allowed). In this special case the input line would have six character columns to define the card number and 12 windows six character column wide, for a total of 78 character columns. Each of the 12 variables must be contained entirely within its six character width window, which limits the size of the integer to six digits.

Rather than having an input line made entirely of integers, it is more likely that the variables will be defined with floating point numbers. A floating point number is basically a number containing a decimal (i.e. 0.01234 or 1.234-2 in scientific notation). Unlike integers, floating point numbers are defined in windows12 character columns wide, giving a maximum of 11 significant digits plus decimal or a maximum of 9 significant digits, a decimal, either a – or a + and a exponential digit for the scientific notation. Therefore, an input line containing only floating point numbers would contain six character columns to define the card number and six 12 character column sized windows, for a total of 78 character columns. Just as is required for integer windows, all pertaining characters can exist outside the respective window.

For input lines which contain a mixture of integers and floating point numbers, the manual provides sufficient further instruction. [P.29,30,8].

A useful tip to those using PARET is to justify each variable to the far right or left of its 6 or 12 character field window. This aligns the entire input file page into columns of numbers which is easy on the eyes and allows the user to spot any spacing irregularity. Also, take special notice of the spacing format required of the 5000 series cards; this is discussed at length in the input description of these cards as well as in the manual.

6.5 Discussion of Sign Convention

When the PARET code was originally written, it was to simulate the SPERT reactor tests. Many of those tests utilized natural convection (upward) coolant flows and subsequently the PARET convention simulates upwards flow when the 10000 series table coolant flow values are positive. It logically follows that negative values in the 10000 series table dictates flow is to be from the top of the reactor down. The acceleration of gravity (dictated in 1000 series cards under variable name GRAV) pulls the fluid down the channel no matter what the direction it flows in, and the sign convention reflecting this action in PARET is to make GRAV positive – all specifications of gravity in PARET runs used in this report dictated gravity as positive.

All simulations conducted for this study assumed that no matter what direction the flow is in, the axial nodes dictated by the user in the 4000 series cards are always numbered from bottom of the reactor to the top. So, in the case of positive flow (upward), the first axial node on the bottom of the reactor is at the inlet end of the coolant channel, and in the case of negative flow (downward) the last axial node NZ (dictated in the 1000 series cards) is at the inlet end of the channel. In other words, the inlet when flow is positive is the bottom of the coolant channel and the top of the coolant channel when flow is negative. Because the MNR uses forced convection at high power which pushes fluid through the top of the reactor, down through the coolant channels and out of the bottom of the core, all MNR forced convection runs in PARET have a negative flow. On the other hand, at low powers, MNR is allowed to run on natural convection flows, from the bottom of the core upwards and is positive flow in PARET.

The user must have a clear picture of channel and flow orientation when constructing the simulated reactor in PARET because there are consequences for other variables and the simulation results. Determining the appropriate sign convention without instructions is difficult because only subtle changes occur amongst the voluminous output files when experimenting with the possible sign combinations.

The user should be aware, that for unknown purposes it is possible to simulate the acceleration of gravity as pulling the coolant upwards by entering the acceleration variable, GRAV, as a negative value. The consequence of this confusing feature is that each reactor can be simulated in two ways. For example, a reactor with negative forced flow (downwards) and positive gravity (pulling fluid down the channel) can also be simulated correctly as having positive forced flow (upwards) and negative gravity (pulling the fluid up the channel) as long as the variables PFQ(84), VOICDVC(84), DOPPLR(84) and TEMPC(84) in the 5000 series cards are also reversed.

6.6 List of Variables

Item Variable Value

1000 Series Cards

1 NCHN -2

This is the number of channels to be modeled in PARET, up to 50. Negative value indicates SI units are to be used in the simulation. Two channels are being used here, the hottest and an average. See discussion in the 5000 series cards about how the axial source descriptions for the hot and average channel were obtained.

Each of the fuel channels modeled by PARET are assumed to have identical geometry, and differ from each other only by some operational parameter such as power level or coolant flow.

2 NZ 21

Number of heat source axial nodes in the channels, up to 97. See the 4000 series cards discussion for a larger explanation. Woodruff's benchmark work is based upon the older versions of PARET, therefore 21 nodes will be used as in the IAEA 10MW HEU sample file value [Pg.40,4]. Also see [Pg.199,20] .

3 NR 7

Number of radial node points – up to 44. As used by Woodruff [Pg.199,20].

4 IGEOM 0

Geometry code: 0 for slab, 1 for cylindrical geometry.

5 IPROP 1

The operation code: 0 for power level specified and 1 for reactivity specified (reactivity insertion is dictated in 9000 series cards). If a power specified problem is required, the Delayed Neutron Information (6000 series table) must be deleted.

6 IRXSWT 1

Vapor fraction and quality option. A zero indicates the assumption that subcooled R=X=0 where R and X are the void fraction and quality, respectively. An entry of 1 allows the code to calculate values of R and X in both the sub-cooled and saturation regions. Same as Woodruff's IAEA 10MW HEU sample file value. This toggles the subcooled voiding model on and off [Pg.200,20].

7 IPOP 0

Moderator pressure code: 0 for the inlet pressure level being specified (see item 15, 1000 series cards), and 1 for outlet pressure level being specified. Notice that switching the flow in table 10000 to positive and negative will change which end of the coolant channel is the inlet and which is the outlet – PARET automatically knows the inlet is the bottom of the reactor when flow is positive and the top when flow is negative.

8 KINTS 0

Kinetics time step parameter, see Woodruff's user manual for more details. An entry of 0 reduces and expands the time step. Same as Woodruff's IAEA 10MW HEU sample file value [Pg.40,4].

An entry of 1 and 2 was also tried, with apparently no difference to the transient. An entry of 2 is supposed to be used for "slow transients where poor stability in the power may be observed" – this entry made no apparent difference in the unstable power of a slow transient (tried with one case, and multiple time step arrangements).

9 IDLYGP 6

The number delayed neutron groups – up to 15. Same as the LEU sample file value [21].

10 KINPRT -1

Kinetics print parameter. Prints time, reactor power, reactivity, max outlet flow, average reactor period over time step. -1 gives printout by TRANSS. TRANSS cannot be found, must be referring to a subroutine name.

11 ISUPPR 0

Average temperature printout option. 0 yields no average temperature printout in the PARET output file. This is simply a matter of formatting preference.

12 MAXHCC 10

The maximum number of iterations through the heat transfer calculations at each axial node at any given time node. Same as Woodruff's IAEA 10MW HEU sample file value [Pg.40,4].

13 POWER 5.5 *MW*

Initial reactor power, in megawatts. This variable changes with almost every run. An additional 10% was added to the nominal power (i.e. $5\,MW$ nominal simulation is run as 5.5 MW) n each case as discussed in the description of the PARET MNR model to account for core power uncertainty – the same as is done in the SOE document [Sec.3.4,9].

14 PF 9.57-3 m^3

Total volume of fuel in the core. Assuming "volume of fuel" means sum of the fuel meat volumes. Using fuel dimensions in SAR, and knowing there are 28 standard and 6 control fuel elements in the reference core [Table5-2,Sec.05,3]:

$$\text{stdvolume} = (28)(16\,plates)(0.51mm)(62.3mm)(600mm) = 8.5406x10^{-3}\,m^3$$

$$\text{controlvolume} = (6)(9\,plates)(0.51mm)(62.3mm)(600mm) = 1.0294x10^{-3}\,m^3$$

$$\text{PF} = controlvolume + stdvolume = 9.57x10^{-3}\,m^3$$

15 PRESUR 7

Operating pressure. Item 7 (1000 series cards) for this case, has been selected to dictate that this pressure refers to the reactor inlet pressure. Same pressure used as in Appendix A of SOE Document [9]. The minimum allowable pool height above core during natural convection (inlet at bottom of core) is approximately equal to the height of the core, therefore the same inlet pressure is used for both natural convection and forced convection cases.

16 ENTHIN -38 ^oC

Enthalpy of inlet moderator. Or the inlet moderator temperature (in Celsius) may be used in lieu of its enthalpy by entering the negative of that temperature. 38 ^oC is the maximum allowable inlet temperature according to MNR OLC [Sec.7.6,6]. Item 32 (1000 series cards) depends upon this temperature as well.

17 RS 6.35-4 m

Fuel pin radius or plate half-thickness (including clad). Using fuel dimensions in SAR [Table5-2,Sec.05,3]:

$$\text{RS} = [(0.51mm) + (2)(0.38mm)]/2 = 6.35x10^{-4}\,m$$

18 RF 2.55-4 m

Fuel half-thickness. Using fuel dimensions in SAR [Table5-2,Sec.05,3]:

$$\text{RF} = (0.51mm)/2 = 2.55x10^{-4}\,m$$

19 RC 2.55-4 m

The half-distance to the inner surface of the clad. This is the same as item 18 (1000 series cards) unless another material lies between the fuel and clad.

20 PW 7.14-2 m
Plate width. SAR width is $71.4\,mm$ [Table5-2,Sec.05,3]. Each fuel plate is curved with a $139.7\,mm$ radius of curvature to control the direction of thermal expansion. PARET can model cylindrical fuel geometry, but does not have the capacity to model the fuel plate curvature. Since the curvature is slight, the fuel plates are modeled as simple slab elements – as did Woodruff [Pg.40,4].

21 FW 6.23E-2 m
Fuel width. Fuel meat width is $62.3\,mm$ [Table5-2,Sec.05,3] .

22 AL 0.6 m
Active fuel length. Must be in agreement with the axial description given on the 4000 series lines. Fuel meat length is $600\,mm$ [Table5-2,Sec.05,3].

23 ALDDIN 1.275-2 m
This and item 24 (1000 series cards) are the inlet and outlet non-fueled section length, respectively. These have been set to half the difference between the fuel meat length and the fuel plate length, $12.75\,mm$. SAR 17 states that the manufacturing tolerance of the fuel is such that this measurement will never be less than $8\,mm$, so it is expect such a value is a lower limit [3]. Item 23 and 24 need to be considered in 1d and 2d of 1114 series cards.

24 ALDDEX 1.275-2 m
See description of item 23, 1000 series cards.

25 BBEFF 0.00767
This is the effective delayed neutron fraction, β. For LEU Reference Core (a) [22].

26 EL 65.1-6 s
Prompt neutron generation time, Λ. For the LEU RC (a) [22].

27 GRAV -9.80664 m/s^2
Acceleration due to gravity. The negative value indicates moderator downflow. See section Discussion of Sign Convention.

28 QW 0.00664

Heat source description for moderator. This parameter is the fraction of the heat generated in the moderator multiplied by the ratio of the fuel meat volume PF (item14, 1000 series cards) to the moderator volume.

Referring to item 4, 3000 series cards, the fraction of heat generated in the fuel is 0.955 and in the cladding, 0. Therefore, the fraction of heat generated in the moderator is 1-0.955=0.045.

To begin calculating QW, the volume of moderator volume in the core needs to be calculated by simply multiplying the total amount of flow area *PSUBC* (item 1a, 1111 cards) by the reactor height. Reactor height is the sum of fueled and nonfueled channel lengths (items 23 and 24, 1000 series cards):

$$\text{core height}=(\text{active fuel length},AL)+(\text{inlet nonfueled section},ALDDIN)$$
$$+(\text{outlet nonfueled section},ALDDEX)$$
$$\text{core height}=(0.6m)+(1.275x10^{-2}m)+(1.275x10^{-2}m)$$
$$\text{core height}=0.6255m$$
$$\text{moderator volume}=(\text{moderator flow area},PSUBC)(\text{core height})$$
$$\text{moderator volume}=(0.10365m^2)(0.6255m)=0.064833m^3$$

$$QW=\left(PF/_{\text{moderator volume}}\right)(0.045)=\left(9.57x10^{-3}m^3/_{0.064833m^3}\right)(0.045)$$
$$QW=0.00664$$

29 TRANST 10 s

Transient time to be run in the simulation. This is the total reactor time interval to be simulated and changes for every simulation based upon the users needs.

30 RXXCON 0.8

A constant, unitless, in the void volume generation equation 11 from Obenchain's user manual. Same as Woodruff's IAEA 10MW HEU sample file value [Pg.40,4].

31 RXXEXP 1.0

An exponent, unitless, in the void volume generation equation 11 from Obenchain's user manual. Same as Woodruff's IAEA 10MW HEU sample file value [Pg.40,4].

32 RHOFEF 993.0 kg/m^3

Moderator reference density. This represents the density of the moderator at the initial reactor conditions. This density is based upon the 1000 series cards item 15 (operating pressure of 1.733+5 Pa) and item 16 (inlet or outlet enthalpy or temperature 38 ^oC). Density obtained with reference water properties program XSteam [7]. This value is used in the 10000 series cards to determine mass velocity.

33 GAMMA 0 -7.93E-1 $\$/{}^oK$

Items 33-37 are coefficients for the fuel temperature feedback (Doppler broadening) equation 46 and 49 the Obenchain manual [5]. The coefficients are all obtained from the Kinetics Parameter Summary document which was created with REBUS simulations [22]. The Kinetics Parameter Summary contains a plot titled MNR Fuel Temperature Reactivity Change – LEU RC, on which two fuel temperature dependent reactivity change plots are shown, see Figure 15.

The plot with the least amount of negative reactivity inserted per ^oK (i.e. the most conservative case for a reactor transient case) has the following polynomial equation, where temperature is in ^oK:

$$\text{reactivity}(mk) = -4.351x10^{-9}T^3 + 1.404x10^{-5}T^2 - 2.451x10^{-2}T + 6.082$$

PARET requires reactivity to be inserted in \$, so the mk units are converted to decimal values of reactivity by dividing by 1000 to obtain:

$$\text{reactivity}(decimal) = \delta k = -4.351x10^{-12}T^3 + 1.404x10^{-8}T^2 - 2.451x10^{-5}T + 6.082x10^{-}$$

Then units of dollars are obtained by dividing the equation by effective delayed neutron fraction, β (item 25, 1000 series cards):

$$\text{reactivity}(\$) = -5.673x10^{-10}T^3 + 1.831x10^{-6}T^2 - 3.196x10^{-3}T + 7.93x10^{-1}$$

By convention of equation 46 from Obenchain, GAMMA0 thru GAMMA3 are equal to the coefficients of this equation. However, the signs of the coefficients need to be reversed since equation 51 gives the total reactivity feedback a negative value [5].

Page 2 and Page 8 of reference [4] state GAMMA4 should be equal to -273.15 if T is to be in units of ^oC. Since the fuel temperature feedback polynomial uses ^oK, GAMMA4 is not required to convert units. DOPPN is set equal to the highest power of the independent variable in the polynomial.

34 GAMMA 1 3.196E-3 $\$/{}^oK$

See item 33 description.

35 GAMMA 2 -1.831E-6 $\$/{}^oK^2$

See item 33 description.

36 GAMMA 3 5.673E-10 $\$ / {}^oK^3$
See item 33 description.

37 GAMMA 4 0
See item 33 description.

38 DOPPN 3.0
See item 33 description.

39 EPS 0.001
Upper limit for kinetics time step test (unitless). Recommended in appropriate section to be set at 0.001 in [4].

40 DNBQDP 0.0
Transient DNB heat flux. If a value of zero is entered here, the code uses steady-state DNB heat flux values calculated internally to the code for each axial node at each time node. Refer to the discussion in the report about how ONB and DNB are determined by the correlations contained in PARET.

41 TAUUNB 0.0005 s
Nucleate boiling bubble collapse time. Woodruff recommends 0.0005 s [Pg.202,20]. The manual for PARET V7.4 recommends using 0.001 s as recommended by the SPERT-III (higher pressure and temperature) tests [Pg.200,20]. Woodruff's recommendation is used.

42 TAUUTB 0.001 s
Transition boiling bubble collapse time. Value is as recommended by Woodruff [Pg.202,20]. Same value also recommended by the manual for PARET V7.4.

43 ALAMNB 0.03
Fraction of the clad surface heat flux which is utilized in producing vapor in the sub-cooled nucleate boiling region. Woodruff recommends 0.03 s [Pg.202,20]. The manual for PARET V7.4 recommends using 0.05 s by the SPERT-III (higher pressure and temperature) tests [Pg.200,20]. . Woodruff's recommendation is used.

44 ALAMTB 0.05
Analogous to item 43, 1000 series cards, except that it applies to transition boiling. Value is as recommended by Woodruff [Pg.202,20]. Same value also recommended by the manual for PARET V7.4.

45 ALAMFB 0.05

Analogous to item 43, 1000 series cards, except that it applies to film boiling. Same as Woodruff's IAEA 10MW HEU sample file value [Pg.40,4].

46 HTTCON 1.4

Natural convection heat transfer constant number 1. Same as Woodruff's IAEA 10MW HEU sample file value [Pg.40,4]. This transient deals only with forced convection.

47 HTTEXP 0.33

Natural convection heat transfer constant number 2. Same as Woodruff's IAEA 10MW HEU sample file value [Pg.40,4]. This transient deals only with forced convection.

Further discussion of variables 41 through 47 by Woodruff [Pg.200,20].

1111 Series Cards

1a PSUBC 0.10319 m^2

A note in the PARET V7.4 manual says this item is no longer used within PARET. Despite this, it will be defined in all input files since its presence is likely required for format, and it was being defined as shown before V7.4 was used [8].

Total cross sectional area of all flow channels in core. From fuel dimensions in SAR, the fuel plate width is $71.4\,mm$ and is embedded into the side plates $2.5\,mm$ on each side; each coolant/moderator channel width is $3\,mm$; each standard fuel assembly has 17 coolant channels and each control assembly has 7 [Table5-2,Sec.05,3].

$$\text{channelwidth} = 71.4mm - (2)(2.5mm) = 66.4mm$$

$$\text{PSUBC} = (3mm)(66.4mm)(28std)(17) + (3mm)(66.4mm)(6cntrl)(7) = 0.10319m^2$$

This value is used in the 10000 series cards to determine mass velocity.

2a FACT2(2) 1.0 1.0

Flux weighting factor, one for each channel. To quote [Pg.20,4]: "This factor is used with the reactivity feedback weighting factor (item 5a, 5000 series cards) of the coolant energy and coolant energy removed which are outputs on the header page of major edits. FACT2(2) has no other affect on code calculations or results. Its physical significance is not clear and has been taken as unity in ANL calculations."

1112 Series Cards

These cards dictate the thermalhydraulic models to be used by PARET. The phenomenon to be modeled by the correlation is listed along with the name of the correlation selected. See discussion in report about the recommendations of Woodruff regarding which correlations gave the best results; Woodruff's benchmark recommendations are followed [20].

1b IONEP 1
Single phase correlation flag. Seider-Tate.

2b ITWOP 1
Two phase correlation flag. McAdams.

3b IMODE 1
Transient two phase scheme. Transition model.

4b ICHF 0
Original DNB.

5b IHT 0
Single phase heat transfer subroutine use. Original.

6b QAVE 4.035+5 W/m^2
Average heat flux used with ICHF=3&4. Since ICHF selected is not item 3 or 4, this variable is of no consequence; however, it will be set at the same value used in Woodruff's IAEA 10MW HEU sample file [Pg.40,4].

7b ETA 25.0
Bubble detachment parameter for ICHF=3. Default 25.

8b CP 1.0 $J/kg\,^oK$
Specific heat used with ICHF=3&4. Default 1.0.

1113 Series Cards

1c RDRATE -1.0

This variable flags the 18000 series cards to dictate rod worth according to position or elapsed time. If rod insertion according to position is desired, the speed of insertion is to be dictated here. If rod insertion according to elapsed time is desired -1.0 is dictated here. See 18000 series cards for more discussion on the PARET MNR model.

Knowing the active height of the core is 0.6m, and that it takes a minimum of 0.75 s for the rods to drop completely, the velocity could be dictated as [Pg.17-4,Sec17,3]:

$$\text{RDRATE} = 0.6m / 0.75s = 0.8m/s$$

2c   TDLAY   0.025 *s*

Delay time before rod starts in after the trip. SAR states this value to be $25\,ms$ [Pg.8-10,Sec.08,3].

3c   POWTP   6.5 *MW*

Overpower trip point, in megawatts. This value will depend upon the individual transient being modeled.

4c   FLOTP   95 %

Low flow trip point, in percent. SAR states trip will occur at any value less than the nominal coolant flow set point, i.e. no flow reduction is allowed, FLOTP=100% [Table17-3,Sec.17,3]. However, in order to avoid trips for small variations in flow rates during the simulation, 95% will be used for most forced convection runs. Note that under all forced convection simulations conducted, the dictated flow value didn't deviate significantly, this trip setting is then useful for buoyancy induced flow only.

5c   OPT   0.5 *days*

Previous operation time of reactor, in days – used in decay heat level after scram. Assume transient occurs after 0.5 days of operation. Transient which don't alter the core geometry will enable natural convection to continue to cool the core at all normally encountered decay heat levels. Decay heat levels generated in all simulations were negligible compared to cooling capacity of natural convection.

6c   POW0

Previous operating power of the reactor, in megawatts. Leaving this blank defaults the value to the initial power input of transient.

1114 Series Cards

1d   HNCTOP   1.275-2 *m*

Height above reactor for natural convection effects. Must include non-fueled section length 23, 1000 series cards, and any plenum length. Knowledge of this geometric area in the PARET model is nil, therefore only the non-fueled section length is being used here.

2d   HNCBOT   1.275-2 *m*

Height below reactor for natural convection effects. This length must include non-fueled section length 24, 1000 series cards. Knowledge of this geometric area is nil, therefore only the non-fueled section length is being used here.

Woodruff's own IAEA 10MW HEU sample file made 1d and 2d values zero, despite the reactor likely having a non-fueled length and a plenum length. Woodruff himself didn't know of a "plenum" definition [Pg.199,20].

A few PARET runs were made with very large "plenum" lengths. The operating pressure became large, indicating the program assumes "plenum" may consider it similar to water column – as does Woodruff who treated it as distance from top of core to pool water level (outlet side of SPERT reactors) [Pg.199,20]. MNR's outlet is the bottom of the core, so distance from pool water level to top of core has no relevance here.

3d REL_T 2300.0

Lowest Reynolds number for laminar to turbulent transition. 2300 by default.

4d RET_T 6000.0

Hightest Reynolds number for laminar to turbulent transition. 6000 by default.

5d FINF 1.0

Fin heat transfer enhancement factor. Set to 1.0 by default.

6d PHI 0.67

Laminar flow friction factor correction factor. Use 2/3 for flat plates.

1500 Series Cards

1e PERTP 10 *s*

Period trip time. This trip applies to positive periods and triggers when the simulated reactor period becomes less than this value. This feature has been commented out of the input files because it leads to spurious trips – period changes largely from time step to step, but over a larger time period maintains an accurate period. Using this period trip causes PARET to trip on periods which may occur for a very small amount of time.

See discussion of Perl program written to detect period trips in the Output File Reviewing section.

2e PTDLAY 0.025 *s*

Delay time before rod starts in after the trip. Since the period trip is not being utilized with this mechanism, this variable isn't relevant to the simulation, however, if it were to be used it would have the same value as TDLAY. SAR states this value to be $25\,ms$ [Pg.8-10,Sec.08,3].

2000 Series Cards

2001 $\alpha_1, \alpha_2, \alpha_3, \alpha_4, \alpha_5$

α_n (n=1,2...4) are the fuel meat thermal conductivity coefficients of the polynomial equation shown in section d) on P.43 [P.43,8]. α_5 is used as a conversion for units into ^oC (not required in this case). The thermal conductivity of 18 plate LEU U2SI2-Al (1997) fuel is constant over a wide temperature range at 78 $W/m^2\,^oK$ [23]. Therefore:
$\alpha_1 = 0, \alpha_2 = 0, \alpha_3 = 78\ W/m^2\,^oK, \alpha_4 = 0, \alpha_5 = 0$

2002 $\beta_1, \beta_2, \beta_3, \beta_4, \beta_5$

β_n (n=1,2...4) are the fuel meat volumetric heat capacity coefficients of the polynomial equation shown in [4 also 8]. α_5 is used as a conversion for units into ^oC (not required in this case). The volumetric heat capacity of 18 plate LEU U2SI2-Al (1997) fuel is 0.41193 $J/g\,^oK$ at $40\,^oC$ and 0.53073 $J/g\,^oK$ at $600\,^oC$ [23]. To convert these two points into a linear relationship of units into $J/m^3\,^oK$, the fuel meat density needs to be calculated first [23]:

$\text{density} = (0.041\,\textit{fraction})(0\,g/cm^3) + (0.33\,\textit{fraction})(12.2\,g/cm^3) + (1-(0.041+0.33))(2.7\,g$

$\text{density} = 5.724\,g/cm^3$

Now we can convert the $40\,^oC$ (313 ^oK)point:

$= (0.41193\,J/g\,^oK)(5.724\,g/cm^3)(1x10^6\,cm^3/m^3) = 2.358x10^6\,J/m^3\,^oK$

and the $600\,^oC$ (873 ^oK) point:

$= (0.53073\,J/g\,^oK)(5.724\,g/cm^3)(1x10^6\,cm^3/m^3) = 3.038x10^6\,J/m^3\,^oK$

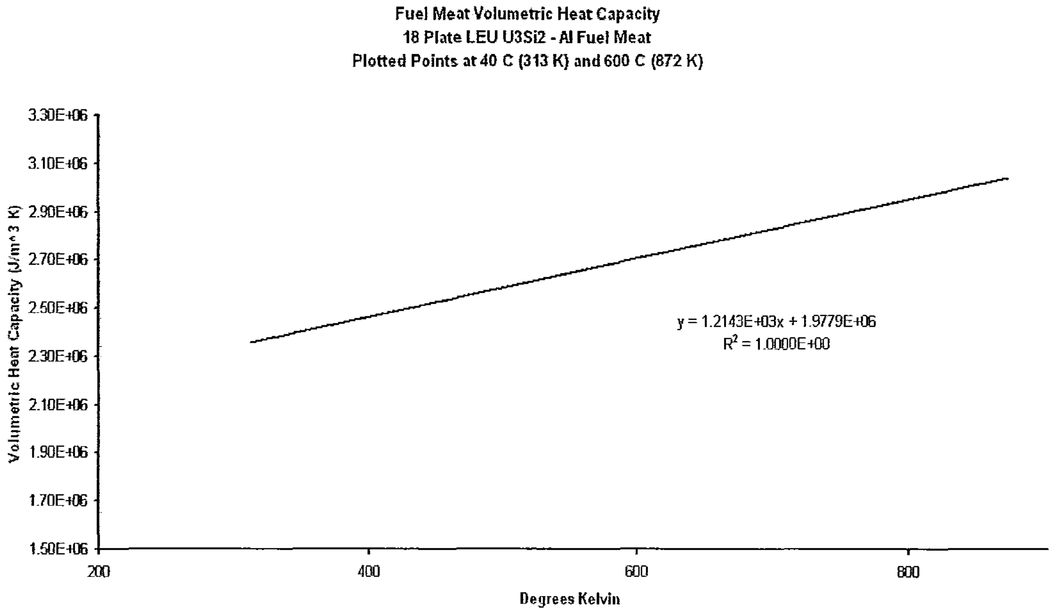

Figure 76. Fuel Meat Heat Capacity

The equation of the line formed between these two points (using the ^{o}K units) is:

$cp = 1214.3T + 1.978x10^{6}$ (see Figure 76)

therefore, the coefficients are:

$\beta_1 = 0, \beta_2 = 1214.3, \beta_3 = 1.978E6, \beta_4 = 0, \beta_5 = 0$

2003 $\alpha_1, \alpha_2, \alpha_3, \alpha_4, \alpha_5$

α_n (n=1,2...4) are the cladding thermal conductivity coefficients of the polynomial equation shown in reference [P.43,8]. α_5 is used as a conversion for units into ^{o}C (not required in this case). The thermal conductivity of AG3NE (CERCA) aluminum cladding is constant over a wide temperature range at 130 $W/m^2\,^{o}K$ [23]. Therefore:

$\alpha_1 = 0, \alpha_2 = 0, \alpha_3 = 130\ W/m^2\,^{o}K, \alpha_4 = 0, \alpha_5 = 0$

2004 $\beta_1, \beta_2, \beta_3, \beta_4, \beta_5$

β_n (n=1,2...4) are the cladding volumetric heat capacity coefficients of the polynomial equation shown in reference [4 also 8]. α_5 is used as a conversion for units into ^{o}C (not required in this case). The volumetric heat capacity of AG3NE (CERCA) aluminum to be 0.91040 $J/g\,^{o}K$ at $40\,^{o}C$ and $1.168\,J/g\,^{o}K$ at $600\,^{o}C$ [23]. Knowing the density

of the aluminum to be 2.7 g/cm^3 these units can be converted into $J/m^3\,{}^oK$. The 40^oC (313 ^oK) point:
$=(0.9104J/g\,{}^oK)(2.7g/cm^3)(1x10^6cm^3/m^3)=2.458x10^6\,J/m^3\,{}^oK$
and the 600^oC (873 ^oK) point:
$=(1.168J/g\,{}^oK)(2.7g/cm^3)(1x10^6cm^3/m^3)=3.15x10^6\,J/m^3\,{}^oK$

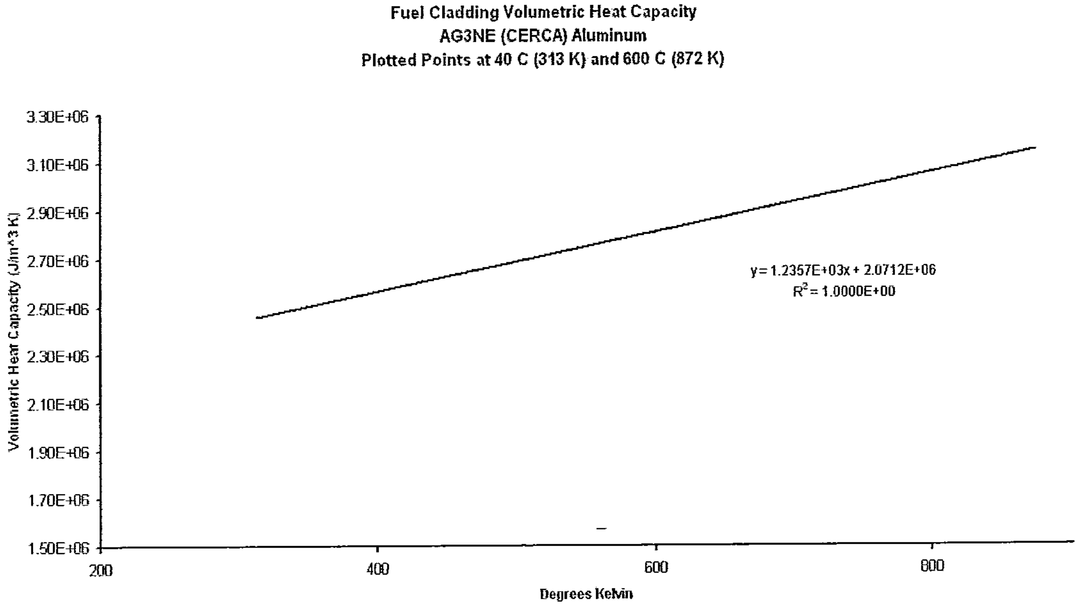

Figure 77. Clad Heat Capacity

The equation of the line formed between these two points (using the ^oK units) is:

$$cp = 1235.7T + 2.071x10^6 \text{ (see Figure 77)}$$

therefore, the coefficients are:

$\beta_1 = 0, \beta_2 = 1235.7, \beta_3 = 2.071E6, \beta_4 = 0, \beta_5 = 0$

3000 Series Cards

3001 AINCR(1), KK(1), ICOMP(1), QR(1)

For this specific run, the 3001 line refers to the half fuel meat thickness (material composition code ICOMP(1)=1 for the fuel meat). AINCR(1) is the radial node spacing of the nodalized fuel and will be 6.375E-5 m, the same as Woodruff's IAEA 10MW HEU sample file value. This nodal increment will allow 4 even spaces between 5 nodes on the 2.55E-4 m fuel half thickness, where node 1 and node 5 are on the half thickness fuel meat edges. Therefore, KK(1) – the radial node number up to which AINCR(1) spacing applies – must be 5.

QR(1) is the radial source description. This is the fraction of heat generated in the fuel material. Woodruff's IAEA 10MW HEU sample file uses QR(1)=0.955 and the same will be used here [Pg.40,4]. Note that item 28, 1000 series cards uses the complementary fraction of heat generated in the moderator, 0.045. Which when summed with 0.955 equals unity.

3002 AINCR(2), KK(2), ICOMP(2), QR(2)

For this specific run, the 3002 line refers to the fuel clad (material composition code ICOMP(2)=2 for the cladding). Woodruff's IAEA 10MW HEU sample file value uses an AINCR(2) of 1.9E-4 m for the clad which allows for 2 nodal spaces between three nodes [Pg.40,4]. Radial node 5 would be on the fuel clad edge, node 6 in the clad center and node 7 on the moderator side edge therefore KK(2)=7. Using the Woodruff convention, it is assumed zero heat is generated in the clad, so QR(2)=0.

4000 Series Cards

See Appendix C - PARET Power Instability Report for extensive discussion of this variable and optimum axial node selection.

5k00 Series Cards

These cards need to be dictated for each channel. Unless notes are made on the variable descriptions below, the variable value applies to both channels. Variable names with a (50) in their name simply indicate that they would need to be defined up to 50 times if 50 channels were used in the simulation. Special notice of the formatting in this card series needs to be taken because the second card entry DELP(50) can be either an integer or a floating point number depending on the corresponding IFLOW(50) setting.

1a k

Dictates channel number. Channel 1 is the hot channel, k=1. Channel 2 is the average channel, k=2.

2a IFLOW(50) 1

Flow parameter, 1 indicates this simulation is flow forced (as dictated by 10000 series cards). A flag of 4 is used here for buoyant forced flow MNR problems. No matter what flag is used this variable must always be placed in the first field of 6 spaces – despite the fact the formatting for the rest of the card line changes depending upon if a flag of 1 or 4 has been chosen.

3a DELP(50) 0

This variable is set to zero if IFLOW(4) is 1.

If set to zero (when IFLOW =1) this variable must be in the second field of 6 spaces. If this value is to be nonzero (when IFLOW = 4) it must be in the second field of 12 spaces i.e. a blank field of 6 spaces between IFLOW and DELP. If this condition is not met, for some reason PARET will not recognize the presence of DTMP (the coolant temperature feedback coefficient) and will not even inform the user of this issue, but rather, just set DTMP equal to zero – likely a bug in the system when DTMP was added to PARET.

When IFLOW(4) is set to flag 4 (indicating buoyancy induced flow in channel) DELP(4) is "not used but a zero value should not be specified." A value of 1.0 made no difference to a test transient compared to a value of 1000.0 – confirming DELP(4) is not used when IFLOW(4) is 4.

Notice that this number needs to be made negative if the buoyancy induced flow transient starts off with a negative (i.e. top down) flow. When flow from table 10 is negative, this value also must be negative, or PARET will see the table 10 value as positive

SEE THE TABLE 10 VALUE AS NEGATIVE, EVEN IF THE TABLE 10 VALUE IS ENTERED AS A POSITIVE NUMBER. THE VALUE OF THIS DELP(50) HAS NO EFFECT ON THE TRANSIENT.

4a RN(50) 2.135-3 m

RN94) is the radial distance from the center of the pin to the node in the center of the water channel. The coolant channel width is $3\,mm$, so half width is $1.5\,mm$. RN(4) is equal to the half fuel plate width (item 17, 1000 series cards, 6.35-4m) plus $1.5\,mm$.

5a BM(50) 0.03187 for Channel 1, 0.96813 for Channel 2

This is the reactivity feedback weighting factor for each channel. It is recommended to set this number equal to the volume fraction of the core represented by each channel [4]. The sum of the MB(4) values must be unity. To see how these values are used in the program, refer to the reactivity feedback equations in reference [5].

To determine the weighting factor for Channel 1, it should be recognized that the Channel 1 is meant to simulate the hottest assembly in the core, therefore, Channel 1 models 1 out of the 28 standard and 6 control assemblies. Knowing the total volume of fuel in the core is 9.57-3m^3 (item 14, 1000 series cards), and the individual fuel plate:

$$\text{high power volume}=(1 assembly)(16 plates)(0.51mm)(62.3mm)(600mm)$$

$$\text{high power volume}=3.0502x10^{-4}m^3$$

$$\text{BM(1)}={3.0502x10^{-4}m^3}\Big/{9.57x10^{-3}m^3}=0.03187$$

The average powered assemblies then make up the remaining core volume and weighting factor. Even though no fuel assembly is actually running at exactly total core power divided by number of fuel assemblies, this PARET model has only two channels and the second must make up the difference in the weighting factor, and:

BM(1)=1-0.03187 = 0.96813

6a ALOSCN(50) 0.14

This is the unrecoverable loss coefficient for abrupt changes in the area at the inlet to the channel. 0.14 is taken from the Hydraulic Properties of Core Components Document [Fig.1,26]. Resistance leaving the coolant channels is only flow resistance considered.

7a ALOSCX(50) 0.00001

Analogous to 6a, and refers to the outlet. Reference gives this value to be zero (i.e. resistance is non existent), however, PARET doesn't allow a zero value to be entered here – a very low value is used instead [Fig.1,26]. Resistance leaving the coolant channels is only flow resistance considered.

8a SIGIN(50) 1.0

The inlet area ratio of the channel area to the area of the associated inlet plenum. Unity value is the same as Woodruff's IAEA 10MW HEU sample file [Pg.40,4].

9a SIGEX(50) 1.0

The outlet area ratio of the channel area to the area of the associated inlet plenum. Unity value is the same as Woodruff's IAEA 10MW HEU sample file [Pg.40,4].

10a DVOID(50) 2.22-1

Overall density void coefficient. Up to 50 values can be entered here, one for each channel, however, following the standard set by Woodruff the same coefficient will be used here for both channels.

At each node, the product of DVOID(50) and the appropriate nodal value of VOIDVC(84) in 5kXX series cards is the value of the local coolant temperature coefficient at axial node XX of channel k. The units of the local density void coefficient needs to be $\$/\%void$, and since VOIDVC(84) is a unitless weighting factor, DVOID(50) needs to be in units of $\$/\%void$. The weighting factor VOIDVC(84) is discussed in detail in section 5kXX.

When the moderator (i.e. coolant) temperature increases, its density reduces. A "void" fraction associated with the temperature change can then be calculated by dividing the change in density by the initial reference density. Even though no actual void has been created, this procedure is used to find this density void coefficient, DVOID(50).

The program REBUS was used to determine reactivity effects in MNR resulting from changes in moderator temperature changes. REBUS was able to determine the overall combined reactivity effects due to temperature and density changes as well as effects due to temperature changes only. The effect due to density changes only is then equal to the difference between the combined effect and the temperature effect. The REBUS simulations were all run with a reference coolant/moderator temperature of $20\,^{o}C$. Most PARET runs will be using $38\,^{o}C$ as the inlet coolant temperature.

See the plot of void reactivity feedback in Figure 13. The slope of the coolant density reactivity change plot, $2.2\text{x}10^{-1}\,\$/\%$ is the value given to DVOID(50) for both channels. The slope of the plot is negative (meaning the reactor has a negative coolant void coefficient of reactivity, i.e. reactor power goes down when coolant void goes up), however, an examination of equations 43, 50 and 51 of [5] show that PARET requires DVOID(4) to be positive to model a negative coolant void coefficient of reactivity. Obenchain's equation 43 defines the total reactivity feedback at each time step r_{MD}^{m}:

$$r_{MD}^{m} = \frac{100}{V_{MOD}\beta_{eff}\overline{\rho}_{ref}} \sum_{k=1}^{k} x_{k2} \sum_{j=1}^{NZ} c_{j,k}[(V_{MOD})_{j,k}][\overline{\rho}_{ref} - \overline{\rho}_{j,k}^{m}] - r_{MD}^{o}$$

Reading Obenchain's description of the formula will explain all the variables in the equation [5]. Most important to this discussion is that the term $\overline{\rho}_{ref} - \overline{\rho}_{j,k}^{m}$ is positive when void increases (relative to the reference density) and gives r_{MD}^{m} a positive value. In the case of MNR one may think that because MNR has a negative coolant void coefficient of reactivity DVOID(4) (ultimately introduced into Obenchain's equation 43 as $c_{j,k}$) should be negative to make r_{MD}^{m} negative when $\overline{\rho}_{ref} - \overline{\rho}_{j,k}^{m}$ is positive. However, Obenchain's equations 50 and 51 subtract r_{MD}^{m} from the total reactivity $r(t^{m})$ at any given time therefore neglecting the need to make DVOID(4) negative. Equations 50 and 51 are respectively:

$$r_{c}^{m} = r_{rod}^{m} + r_{MD}^{m} + r_{Dop}^{m}$$

$$r(t^{m}) = r_{in}(t^{m}) - r_{c}^{m}$$

To check that the above interpretation of Obenchain's equations 43, 50 and 51 are correct, examining input files created for other MTR reactors with a negative coolant void coefficient of reactivity show that this DVOID(4) sign convention is correct. The coefficients presented by

Housiadas for another MTR type reactor, confirms that the magnitude of the density/void coefficient is roughly close to the one obtained for MNR [Table2,27].

It should be noted that Housiadas equation 14 paraphrases Obenchain's equations 50 and 51 [27]. The way in which equation 14 is presented may cause some confusion because the "changes of coolant density or void term" is added rather than subtracted to the total reactivity, however, Housiadas' term $\delta\overline{\rho_j}$ becomes negative when void increases and complements Obenchain's equations correctly [27].

11a DTMP(50) 1.314-2

This is the coolant temperature coefficient. Up to four values can be entered here, one for each channel, however, following the standard set by Woodruff the same coefficient will be used here for both channels.

At each node, the product of DTMP(50) and the appropriate nodal value of TEMPC(84) in 5kXX series cards is the value of the local coolant temperature coefficient at axial node XX of channel k. The units of the local coolant temperature coefficient needs to be $\$/{}^{o}C$, and since TEMPC(84) is a unitless weighting factor, DTMP(50) needs to be in units of $\$/{}^{o}C$. The weighting factor TEMPC(84) will be discussed in detail in section 5kXX.

This coolant temperature reactivity feedback was not available in the original version of PARET and therefore is not discussed in Obenchain [5]. A discussion can be found on Pg.7 of the Woodruff manual [4].

DTMP(50) is equal to the slope of the coolant temperature reactivity change plot see Figure 14, $1.314\text{x}10^{-2}\ \$/{}^{o}C$. This plot shows MNR has a negative coolant temperature coefficient of reactivity. For the same reason DVOID(50) was made positive despite modeling a negative coefficient of reactivity, DTMP(50) also need to be positive (see discussion in section 10a about Obenchain's equations 50 and 51, and for how the coolant temperature reactivity change plot was obtained). It should be noted that the magnitude of the coolant temperature coefficient obtained by Housiadas is very close to the value determined here for DTMP(50) with REBUS simulations [Table2,27].

5k01 Series Cards

All the values for variables 1-4b are taken from Woodruff's IAEA 10MW HEU sample file [Pg.40,4].

1b ALPPIN(50) 0

Represents the length of the inlet plenum, 0. Woodruff himself didn't know of a "plenum" definition [Pg.199,20]. Zero is being used here in all runs to eliminate any influence on the simulations.

2b ALPPEX(50) 0

Represents the length of the exit plenum, 0. Woodruff himself didn't know of a "plenum" definition [Pg.199,20]. Zero is being used here in all runs to eliminate any influence on the simulations.

See the discussion of "plenum" in the descriptions of variables 1d and 2d of 1114 Series cards.

3b DEEIN(50) 0.3048

Represents the inlet plenum equivalent diameter.

4b DEEEX(50) 0.3048

Represents the exit plenum equivalent diameter.

There are a number of other variables included on this card in PARET V7.4 which only apply if 1000 series card variable IGEOM=2 - this doesn't apply to MNR and thus these other variables won't be discussed here.

5kXX Series Cards

This series of cards defines four parameters at each of the NZ (item 2, 1000 series cards) axial nodes. Each of the four variables must be defined at each node, for each Channel 1 and Channel 2.

The four parameters defined in this card are: the axial source description, moderator density feedback weighting factor, Doppler feedback parameter and coolant temperature weighting factor.

Axial Source Description

See the discussion in the section Flux Profiles and Power Peaking Factors discussing how the axial flux profiles for Channel 1 and 2 were obtained.

The polynomial describing the flux profile in Channel 1, see Figure 21, is:

$$= 1.0x10^{-9}x^6 - 5.0x10^{-8}x^5 - 2.0x10^{-6}x^4 + 1.0x10^{-4}x^3 - 0.0015x^2 - 0.0785x + 3.291$$

where x dictates the axial assembly location between 0 and 30 cm, in either direction from the vertical center of the core.

The polynomial describing the flux profile in Channel 2, see Figure 22, is:

$$= 5.0x10^{-6}x^6 - 2.0x10^{-8}x^5 - 8.0x10^{-7}x^4 + 4.0x10^{-5}x^3 - 0.0006x^2 - 0.0295x + 1.2372$$

Knowing that there are NZ nodes (item 2, 1000 series cards) and are spaced according to the discussion in the 4000 series cards, the axial source descriptions for both Channels, are:

Node	Channel 1	Channel 2
j1	0.691	1.789
j2	0.850	2.201
j3	1.024	2.651
j4	1.182	3.062
j5	1.307	3.384
j6	1.388	3.596
j7	1.426	3.692
j8	1.422	3.683
j9	1.384	3.584
j10	1.320	3.418
j11	1.237	3.204
j12	1.145	2.965
j13	1.048	2.715
j14	0.952	2.467
j15	0.859	2.225
j16	0.769	1.991
j17	0.680	1.761
j18	0.590	1.529
j19	0.498	1.291
j20	0.402	1.042
j21	0.305	0.789

Notice the relative power in both Channels at the top nodes of the core (j21) is significantly less than the bottom of the core, due to the presence of the SSR penetrating the core top.

Weighting Factors

The Doppler feedback parameter is a variable from equation 46 in Obenchain [5]. For all nodes in both channels, this variable is set to unity because the polynomial equation using the variables GAMMA 0 thru GAMMA 4 (items 33 to 37, 1000 series cards) are capable on their own of numerically describing the fuel temperature feedback characteristics of the reactor. If a fraction of the feedback polynomial in equation 46 was required at some node, then the fraction would be entered here.

Regarding the moderator density and coolant temperature feedback weighting factors, Woodruff's IAEA 10MW HEU sample file value assigns non-unity weighting factors at each axial node to the moderator density and coolant temperature feedback [Pg.40,4]. However, these values presumably were developed with some analysis.

The weighting factors are meant to be used in conjunction with the coefficients 10a and 11a of the 5000 series cards. Since these coefficients 10a and 11a were obtained for MNR by simulating the entire reactor core in REBUS and are cumulative coefficients. Therefore, the individual nodes in PARET will not be weighted uniquely – each weighting factor will have a value of unity. Setting all VOIDVC and TEMPC values equal to unity was also recommended by Olson, stating: "...you can use variable VOIDVC as a relative axial weighting factor, if you know what that is from detailed neutronics analysis. Use 1.0 if you don't [28]." As well, Woodruff assumed uniform weighting in his benchmark work [Pg.203 and 199,20].

Sensitivity analysis shows that with all other variables being equal, a $2\,mk$ insertion in $1\,s$ from $5\,MW$ changes the transient negligibly between using Woodruff's IAEA 10MW HEU [Pg.40,4] weighting factors and making them all unity. Loss of coolant flow case was run with weighting factors equal to unity and compared to non unity case – with little change. Reactivity insertion case with unity weighting factors showed little change to non unity case as well.

6000 Series Cards

This card series specifies the delayed neutron fraction and delayed neutron decay constant for each IDLYGP (item9, 1000 series cards) delay group. The data is entered in pairs – there are IDLYGP pairs entered. The first number entered is the delayed neutron fraction, the second is the associated delayed neutron decay constant in s^{-1}.

For this value the Woodruff IAEA 10MW HEU sample file cannot be used, and instead the IAEA 10MW LEU sample file values are used [21].

Group1	Group2	Group3	Group4	Group5	Group6
3.8385-2	2.0862-1	1.8873-1	4.0722-1	1.2994-1	2.71-2
1.2727-2/s	3.1716-2/s	1.167-1/s	3.1214-1/s	1.3985/s	3.8521/s

This series of cards must be deleted entirely if the simulation is to be power level specified.

9000 Series Cards

Reactivity driven transients take the externally inserted reactivity from this table. The value of the reactivity inserted needs to be in $. Divide fractional units of reactivity δk (not mk) by β (item 25, 1000 series cards) to obtain reactivity in $. For example, a user wanting to insert $2\,mk$ (δk =0.002) would do the following conversion:

$$\$ = {\delta k}/{\beta} = {0.002}/{0.00767} = 0.26076$$

and then pair this value with the time associated with full insertion. PARET will interpolate linearly to insert this amount of reactivity between time zero and the dictated time. Multiple pairs can be used to vary the amount of external reactivity according to time. Inserted reactivity is not saved, a time/reactivity entry dictating zero reactivity after $2\,mk$, for example, has been inserted tells PARET the $2\,mk$ has been removed (i.e. -$2\,mk$ inserted). Maintaining a level of external reactivity inserted requires defining the reactivity quantity with time until desired transient is complete.

Note that this card must be defined for an amount of time greater than the total transient time dictated in item 29, 1000 series cards.

10000 Series Cards

Inlet mass velocity. For forced convection flow, this card allows reactor moderator mass flux velocity to be dictated at any time throughout the progress of the transient. In most flow forced simulations it is assumed that flow will be constant at the set flow rate. Note that this card must be defined for an amount of time greater than the total transient time dictated in item 29, 1000 series cards. Refer to the note at the beginning of this section regarding the flow, gravity and sign convention. In the MNR case the forced convective flow should be negative, buoyant driven flow should be positive.

See the report section discussing Coolant Flow in the PARET MNR model for specific values used according to power.

11000 Series Cards

If thermal expansion of the clad was significant, it would be entered here. Woodruff, in all his sample files, neglects thermal expansion and the same will be done for this example [Pg.40,4].

These values are used in equation 39 of Obenchain's manual to develop reactivity feedback due to fuel rod expansion [5].

12000 Series Cards

For transients (or individual channels) driven by moderator pressure drop, the pressure drop will be dictated here.

14000 and 16000 Series Cards

These cards dictate the simulation time step and printout time interval, respectively. How specific transients are reported in the output file is a user preference. How the time step interval is dictated may depend upon the transient – fast moving transients will require small time steps for any meaningful resolution.

Notice in Appendix C that a change in time step can change the reactivity within the simulation – a completely undesirable consequence. However, the effect is extremely small and essentially negligible, but the number of time step changes in a simulation should still be kept to a minimum.

A very small time step increases significantly the time duration required to complete a simulation. The smallest time step used for any transient was 0.0001 s.

17000 Series Cards

This card series is used when transients are driven by flow decay. See notes in A.P. Olson manual for general instructions of use [8].

This table is meant to dictate "pump" decay in fractions of initial flow. MNR doesn't have a pump forcing flow through the coolant channels, but uses hydrostatic head instead. This table can still be used for modeling flow decay. Note that if the user wishes to model pump decay to zero and subsequent natural convection flows, the last fraction entered into 17000 table needs to be zero. Natural convection buoyancy forces will not override the decayed forced flow, no matter how small the dictated decay flow becomes. Natural convection only occurs once "pump" flow is zero.

In MNR a flow reversal occurs in the coolant channel when a transition is simulated from forced convection flows (down) to natural convection flows (up).

18000 Series Cards

Rod reactivity worth of the SSR at specific positions are given here. This set of reactivity worth is used when the simulation scrams.

The reactivity worth needs to be stated in $. The individual SSR worth is not of concern here, but rather the entire bank worth, as the MNR model assumes the entire bank is moved at once upon reverse or scram. Refer to the discussion about the SSR in the PARET MNR model description, and to the -75 mk rod profile in Figure 27 and the associated polynomial used for describing the rod bank. PARET accepts a maximum of 20 pairs of rod position/worth dictations in the 18000 Series Cards and they will all be used for the interest of accuracy; PARET linearly interpolates between dictations.

Rod worth can be entered according to rod tip location or lapsed time from trip signal, according to how the flag RDRATE (item 1c, card 1113) is set. The PARET MNR model uses the same rods for two different "trips": scrams and reverses. Both involve moving the rods the same distance from the same position, under different time spans, therefore, rod worth is dictated according to time span. One set of dictations for scrams, another for reverses, both from 50% withdrawn and another scram dictation from safety bank position:

Scram		Reverse		Safety Bank Scram	
Time (s)	ρ($)	Time (s)	ρ($)	Time (s)	ρ($)
0.000	0.000	0.000	0.000	0.000	0.000
0.020	-0.410	13.950	-0.410	0.019	-0.378
0.039	-0.815	27.900	-0.815	0.037	-0.748
0.059	-1.210	41.850	-1.210	0.056	-1.104
0.079	-1.590	55.800	-1.590	0.074	-1.446
0.099	-1.953	69.750	-1.953	0.093	-1.768
0.118	-2.295	83.700	-2.295	0.111	-2.070
0.138	-2.613	97.650	-2.613	0.130	-2.350
0.158	-2.905	111.600	-2.905	0.148	-2.605
0.178	-3.169	125.550	-3.169	0.167	-2.836
0.197	-3.406	139.500	-3.406	0.185	-3.043
0.217	-3.614	153.450	-3.614	0.204	-3.224
0.237	-3.795	167.400	-3.795	0.222	-3.382
0.257	-3.950	181.350	-3.950	0.241	-3.818
0.276	-4.079	195.300	-4.079	0.259	-3.632
0.296	-4.186	209.250	-4.186	0.278	-3.726
0.316	-4.270	223.200	-4.270	0.296	-3.800
0.336	-4.331	237.150	-4.331	0.315	-3.854
0.355	-4.370	251.100	-4.370	0.334	-3.888
0.375	-4.381	265.000	-4.381	0.352	-3.898

Blank Space at Bottom of Input File

PARET will not run without a single blank row at the end of the input file. No edition of the manual makes reference to this, and it takes hours for a new user to determine their lack of a blank line is preventing PARET from running.

Output File Reviewing

PARET will produce a number of files each time a simulation is executed. The most important file for the user to review is the .out file. It contains the information which details the behavior of the reactor during the transient simulated.

Throughout the .out file are major and minor edits which appear at frequencies dictated by the 16000 series cards. Major edits contain various thermal and hydraulic information of each axial node of each channel, while minor edits contain only a couple lines of summary reactor status data. The 14000 and 16000 tables must work together to provide enough information in the output file to not skip over short events which may occur in the transient. Users must watch the output file for erratic or unexplained jumps in power, reactivity, temperature and flow to confirm that the reactor time steps selected and reported are judicious.

Checking the major output edits to confirm that the coolant temperature at the first axial nodes on the inlet end of the channel are at the temperature ENTHIN (1000 series cards) will confirm that the flow direction has been defined correctly.

Unfortunately PARET does not have the ability to plot data graphically, so users will have to spend time transferring text files into another program to gain the ability to view time dependent characteristics of the reactor. This must be done in order to check that PARET is behaving as expected (since the results of any computer code simulation should be checked against general rules of thumb and reconciled with governing principles) and often uncovers issues with input file preparation.

Users may find the channel Pressure Drop edits in the major edits confusing for its misleading nomenclature. One would expect that any positive number included in a set of numbers labeled Pressure Drop to indicate the magnitude of the pressure drop, and negative values to indicate the magnitude of a pressure rise. However, the label for these edits should be called "Pressure Change" since negative values for the Friction, Elevation, Spatial Acceleration, Transient Acceleration or Total labels indeed indicate pressure drops, as was determined by many investigative runs in PARET.

In the case of MNR, the PARET simulations have been conducted with coolant flow moving from the top of the core to the bottom of the core. The coolant channel can then be thought of as a vertical conduit, with flow from top to bottom. By applying Bernoulli's equation to an adiabatic, frictionless vertical conduit, one will find that the pressure at the bottom of the vertical channel is higher than whatever the pressure is at the top of the channel. It may seem counterintuitive to find that flow moves from low to high pressure when observing the pressure edits in PARET, but that is the effect the gravity head term in Bernoulli's equation has on the outlet pressure. If, however, frictional losses are taken into consideration, high enough flow values through the conduit will drop the outlet pressure, perhaps to pressures below that of the inlet pressure.

The output file labels and reports the Inlet and Outlet Pressures in the major output edits. PARET is able to distinguish, based upon the sign of the coolant flow, which end of the core is the inlet and which is the outlet. Keeping in mind that the axial nodes are always numbered from bottom-of-core to top-of-core, depending upon the direction of flow, the first axial node may or may not be at the inlet end of the core. The pressure edits given at each major edit time step list the pressure at each axial node. The user should note that there is usually a difference in pressure between the Inlet Pressure shown and the pressure at the node closest to the channel inlet. Similarly, there is usually a difference in pressure between the node closest to the outlet of the channel and the Outlet Pressure. Investigative runs in PARET determined that these differences in pressure depend completely upon the unfueled and plenum lengths dictated in the input files. Larger lengths increase the pressure difference between the inlet or outlet and the closest axial node.

A postprocessor is supplied with the PARET software and is very useful for parsing down the large amount of time step data from the output file to representative volumes for plotting. Importing the individual channel output files into a plotting program without parsing will require handling thousands of time step data. The directions supplied in the manual regarding the operation of the postprocessor are adequate, however, users will find the postprocessor's capabilities lacking in a few areas; there is no capability to process reactor period, channel pressures or boiling status of the channels.

The program Perl has been used to write a program to scan the major and minor edits for the information the postprocessor can't provide. By scanning the major edits of the .out file with Perl for nucleate boiling, bulk boiling, vapor and film boiling notifications one can monitor the status of boiling in the channels – usually a key signpost in transient analysis.

As discussed in the list of input variables, the period trip feature on PARET V7.4 (1500 series cards) will trip if the period drops below PERTP at any time step. While an in depth study could be conducted to determine if the MNR instrumentation is capable of detecting fast reactor power growths lasting only thousandths of a second, intuitively it seems that there must be some short time duration at which the instrumentation system will not detect a short period. A Perl program is used to monitor the reactor power from time step to step, and compare the power growth over a time span thought to be detectable by instrumentation to determine if power was growing at a rate faster than the period trip point. If Perl determined that indeed the power was growing at a rate fast enough that a trip should occur, a second run is performed with reactor power set at a power level appropriate to trip at the time the low period was observed. This is a very laborious process, but one that must be followed to simulate the reactor power decay after the trip on period. It is hoped that the period trip in future PARET versions allow the user to define the length of time the reactor period must be below PERTP before a trip occurs.

Appendix C – PARET Power Instability Report

During the process of becoming familiar with PARET's operation, using version 6.1, a core simulation was run in which no external source of reactivity was inserted. It was expected that the initial reactor power of $5\,MW$ would be maintained throughout the duration of the simulation. However, it was found that power did not remain at its initial power level. Upon investigation it was found that small amounts of positive or negative reactivity were being created by the feedback effects and the power changed as a consequence.

Numerous investigative PARET runs were made and various suspect variables in the input file were changed to examine their effect on the instability in an effort to minimize or eliminate the power instability.

No solution to the power instability was found until PARET V7.4 was obtained. The manual for V7.4 contained a discussion on optimizing the axial nodal spacing for each Channel within the model, and a discussion about a corrected error in the V7.4 code which helped reduce power drifting [Pg.7-11,8].

This section summarizes the results of implementing the optimized axial nodal spacing in V7.4 on the power instability as compared to the power instability investigation completed in V6.1. A significant improvement in stability is observed – almost entirely due to the corrected error in V7.4 rather than due to the optimized nodal spacing.

6.7 PARET V6.1 Power Instability Investigations

6.7.1 V6.1 Simulation 1

Input File

The first simulation is a PARET MNR run at $5\,MW$. No reactivity is inserted and forced convective flow is set very high at $-1100 kg/m^2 s$ to ensure vapor generation is precluded since it may be a complicating factor. Overpower and low flow trips are disabled, even though neither power nor flow is expected to deviate significantly. Time steps are set to $0.001\,s$ until $3\,s$ (transient time) has lapsed, where the time step changes to $0.01\,s$. Transient run for $10\,s$ duration. Inlet temperature (pool temperature) is set to $35\,^oC$.

Results

Power and reactivity are plotted in Figure 78. Reactivity dips to approximately -0.001$ by approximately $0.25\,s$ due to negative coolant void and temperature coefficients of reactivity. The PARET manual states time step 0 is used for calculating the steady reactor state, but this doesn't seem to occur [Item29,Pg.18,4]. The negative reactivity introduced immediately seems to be a result of heating the $35\,^oC$ pool water in the coolant channels.

Around $0.25\,s$ reactivity reverses, due to the power drop. At this point power has reduced by approximately 0.2% of full power. Reactivity becomes positive, peaking at approximately 0.005$ at 1 second before slowly approaching 0$ from the positive side (again likely due to the negative feedback coefficients).

At transient time $3\,s$ when the PARET simulation changes its time step (as dictated in the input file), reactivity steps downwards.

Over the $10\,s$ transient duration, power has increased by approximately 0.6% of initial power.

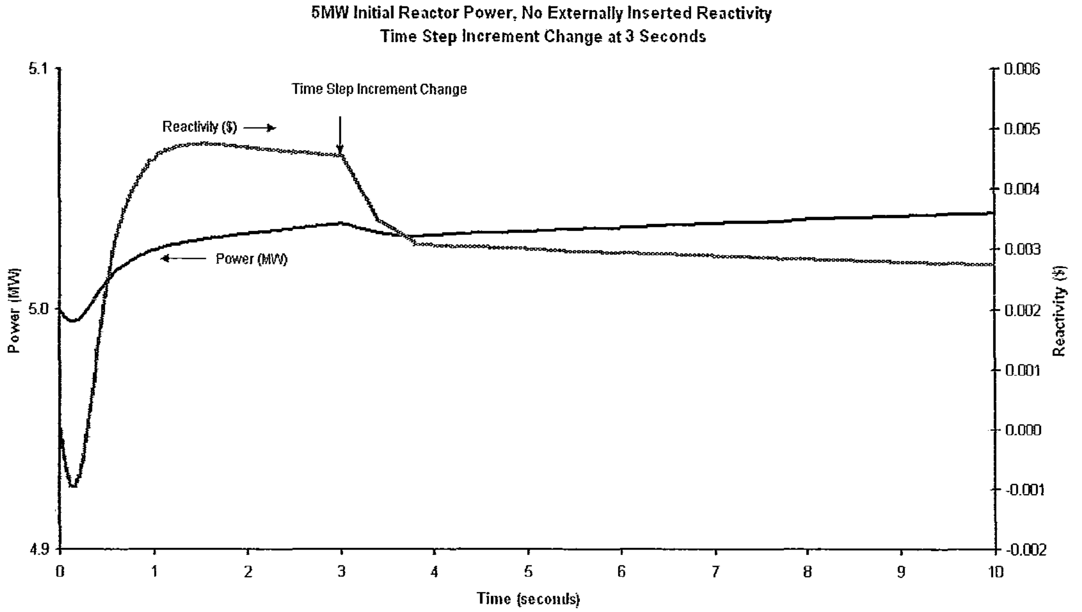

Figure 78. V6.1 Simulation 1

6.7.2 V6.1 Simulation 2

Input File

To test if the reactivity change observed at $3\,s$ is dependent upon the time step change, the time at which PARET changes its time step for Simulation 2 is at $8\,s$ instead of $3\,s$. All other variables are identical to Simulation 1.

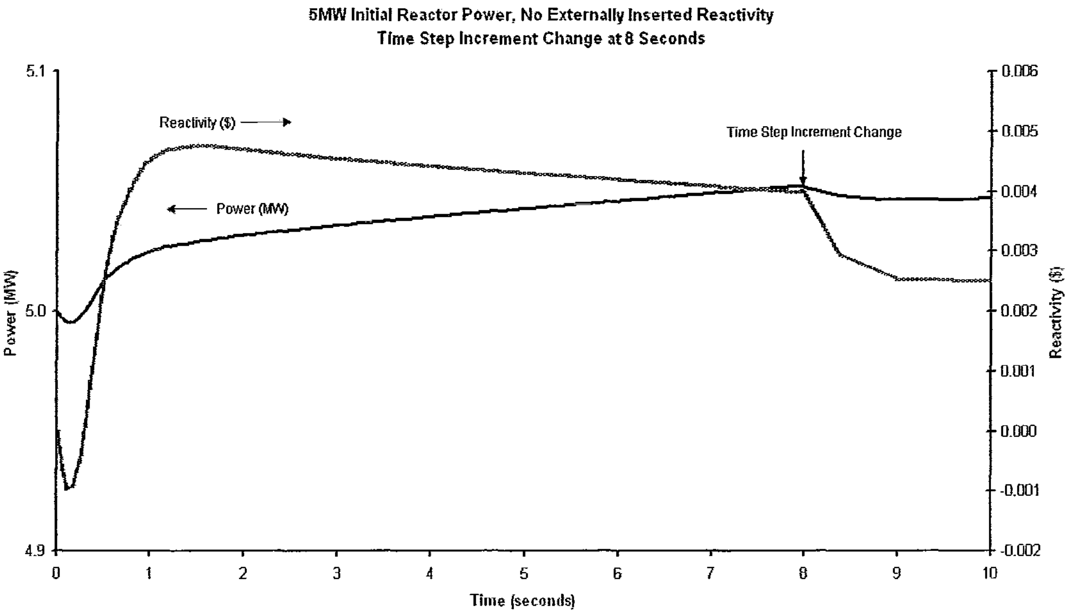

Figure 79. V6.1 Simulation 2

Results

Reactivity behaves in the same manner as the first simulation, however, the drop in reactivity previously observed $3\,s$ now occurs at $8\,s$, which indicated time step is directly responsible for the mild reactivity step. Magnitude of reactivity change due to simulation time step change in observed runs is approximately 0.0015$ (0.01 mk). This shouldn't cause large issues.

All other V6.1 simulations are based upon this Simulation 2 and have some variable perturbed to investigate the power instability sensitivity.

6.7.3 V6.1 Simulation 3

Input File

Input file identical to Simulation 2, except the coolant density and temperature feedback coefficients have been doubled in magnitude.

Results

The reactivity behavior pattern is as in Simulation 2, however, the magnitude of the fluctuations is larger; the lowest negative reactivity shown has increased by a factor of 1.5. The reactivity feedback effects are involved in at least a small way with the reactivity instability.

6.7.4 V6.1 Simulation 4

Input File

Reactivity feedback coefficients same as Simulation 2; initial power is lowered from $5\,MW$ to $4\,MW$.

Results

The magnitude of the reactivity fluctuation is smaller than the 5 MW Simulation 2, seeming to state that the instability is more pronounced at higher powers. This may simply mean that since the coolant is heated less, the reactivity feedback mechanisms have less of an influence.

6.7.5 V6.1 Simulation 5

Input File

Compared to Simulation 2, initial power is lowered from 4 MW to 1 MW.

Results

Peak maximum reactivity is smaller than the 4 MW case, again indicating higher power levels increase the reactivity instability.

6.7.6 V6.1 Simulation 6

Input File

Compared to Simulation 2, the flow has been lowered from -1100 kg/m^2s.

Results

Reactivity displays the same pattern of negative and then positive fluctuation, however, the magnitude of fluctuation is larger with the lower flow. For any given reactor power, lowering flow increases the peak coolant temperature, therefore, it should not be surprising the reactivity fluctuates more compared to Simulation 2. Further simulations using lower flow values confirm this theory, as their reactivity fluctuation is even larger. Lowering flow to -550 kg/m^2s shows a significant change in power – almost 4% over the short 10 s simulation.

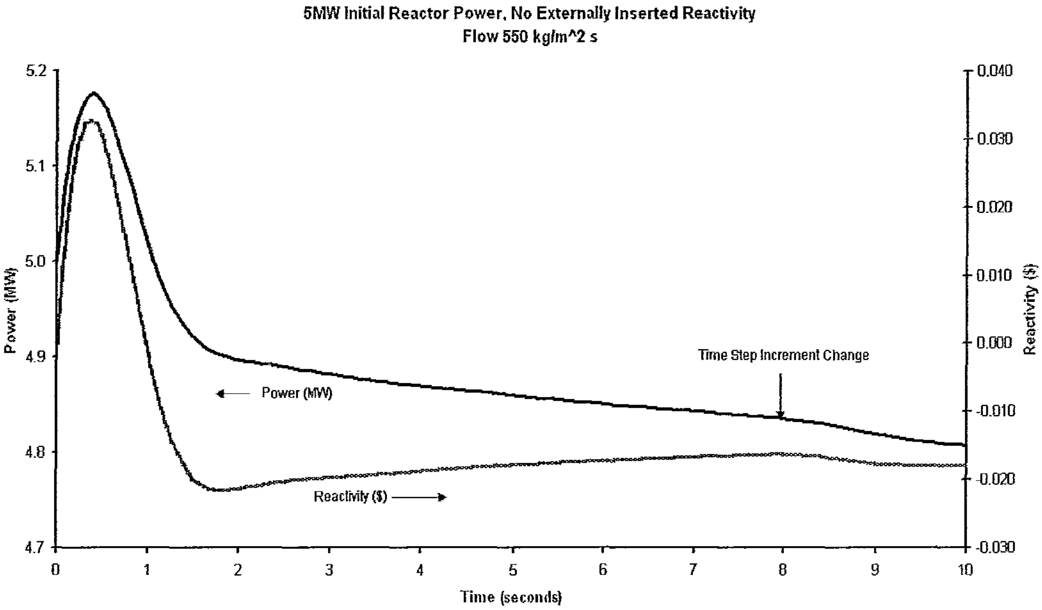

Figure 80. V6.1 Simulation 6

6.7.7 V6.1 Simulation 10

Input File

In order to check that the input file for MNR hasn't been prepared incorrectly in some manner, a SPERT IV D12/25 sample input file provided with the PARET software was run. The sample input file was changed only by eliminating the reactivity insertion and by making the initial power $5\,MW$ so it was comparable to the MNR cases, and customizing the 14000 table to provide good transient resolution.

Results

The same general reactivity instability is observed as in the MNR cases; therefore the preparation of the MNR model is not solely to blame.

6.8 Axial Node Optimization

The PARET manual for V7.4 contains a discussion on the inability for PARET to hold power at a constant value under reactivity specified simulations (by selecting IPROP for power level specified simulations, any power level can be maintained exactly, however, reactivity driven transients cannot then be simulated) [Pg.4,8]. The author suggests selecting the axial fuel nodes in such a manner that "residual errors" are reduced, and PARET may increase the ability to hold at constant power.

PARET has two sets of axial nodes. As illustrated in Figure 81, the user typically divides the $0.6\,m$ long active axial fuel length by specifying the number

(NZ) and spacing of the fuel axial elements DZ. PARET then uses the DZ spacing to create a second mesh group on which the coolant fluid properties are apparently defined. The number of fluid elements DELZ is always equal to NZ-1 as is best illustrated by Figure 81.

The manual suggests that instead of implementing 21 uniform axial fuel regions, the fuel regions be selected such as to force the fluid increments DELZ to uniformity, as is shown in Figure 81 [Pg.9-10,8].

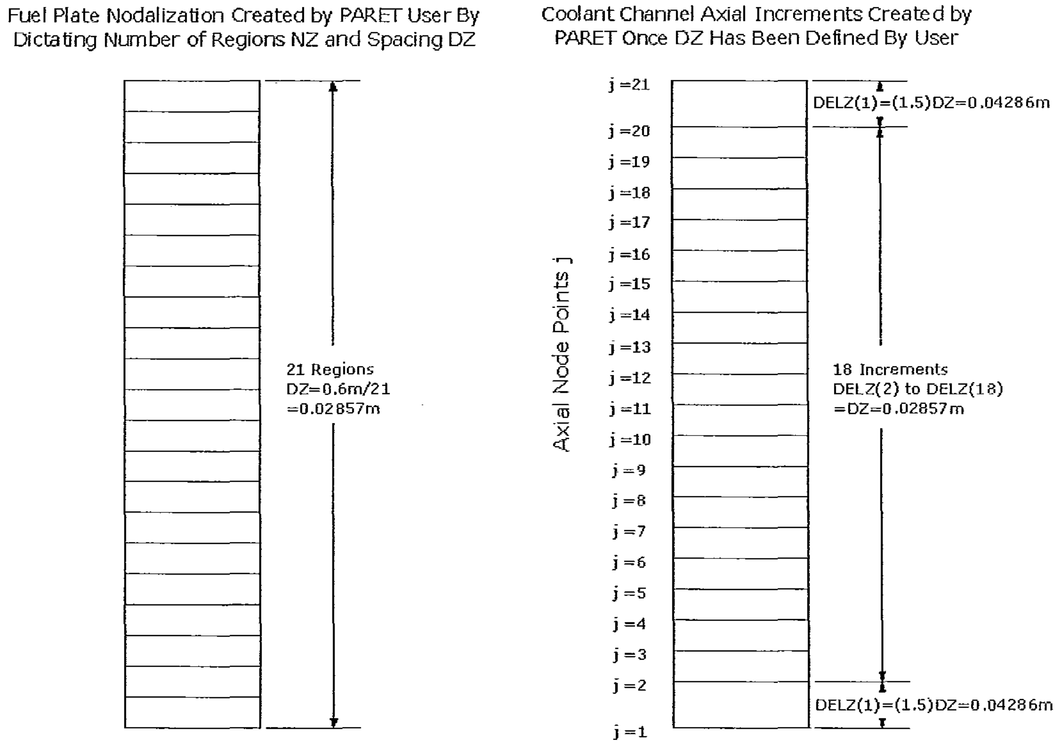

Figure 81. Woodruff Axial Node Convetion of NZ=21 and Making DZ Length Uniform - Used With PARET V6.1 Simulations

A V6.1 simulation was completed with these recommendations and they made no significant impact upon reducing the power instability. However, the change was left implemented for the entire trip map analysis since the author claims improved accuracy [Pg.10,8]. It should be noted that attempting to run PARET V7.4 without the "optimized" DZ spacing will result in the program changing to the recommended spacing automatically [Pg.11,8].

6.9 PARET V7.1 Power Instability Investigations

6.9.1 V7.1 Simulation 1

Input File

V7.4 manual discusses the discovery of an old and congenital error implemented in solving the energy balance equation [Pg.7,8]. V7.4 is the first version of PARET which is free of this subroutine error.

To test the power stability performance of V7.4, the input file used in V6.1 Simulation 1 was tested on V7.4.

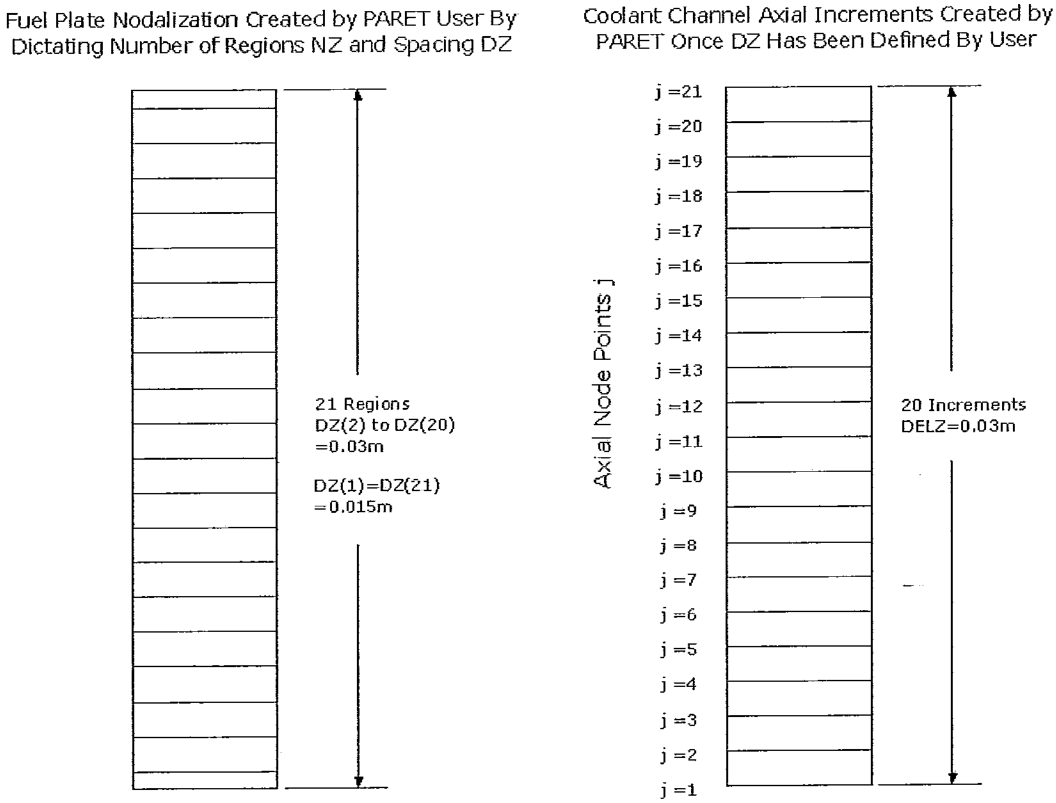

Figure 82. Olson Recommendation for Forcing DELZ to be Uniform - Used With V7.4 and PARET MNR Model [Pg.7-11,8]

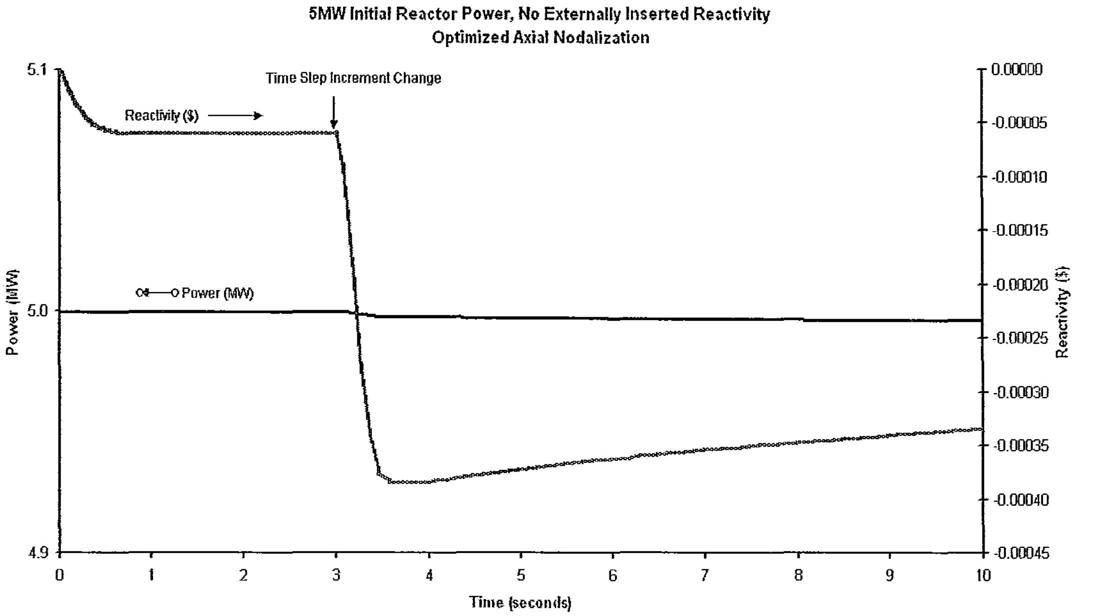

Figure 83. V7.4 Simulation 1 - Compare to V6.1 Simulation 1

Results

Comparing Figure 78 to that of Figure 83 shows a marked improvement in power stability. Effectively, the power instability is gone. The step in reactivity associated with the time step change, is still present albeit is an order of magnitude smaller than that found in the V6.1 Simulation 1.

6.9.2 V7.1 Simulation 2

Input File

As with V6.1 Simulation 2, the time step change was moved from 3 s to 8 s to check that the time step is still directly responsible for the reactivity step.

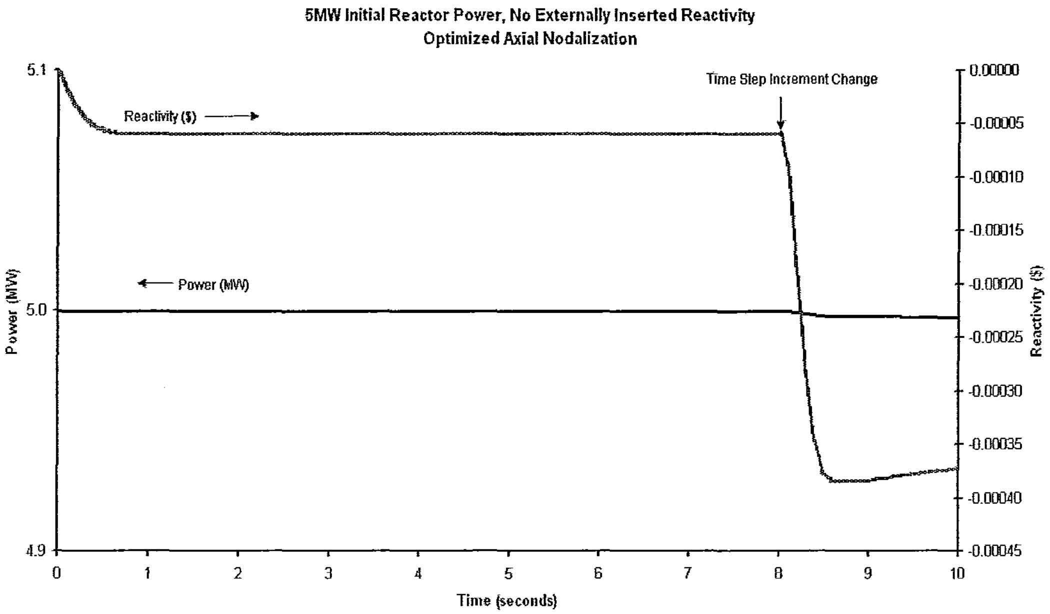

Figure 84. V7.4 Simulation 2 - Compare to V6.1 Simulation 2

Results

As is shown in Figure 84, the reactivity change moved exactly with the time step – the subroutine error corrected in V7.4 did not eliminate this behavior.

6.9.3 V7.1 Simulation 3

Input File

V6.1 Simulation 6 demonstrated the most drastic power instability of all the V6.1 simulations. This V7.1 simulation uses the same input file, to compare the improvement in PARET's ability to hold power constant.

Results

As is shown in Figure 85, the improvement is dramatic. The power loss is under 0.2% of initial power during the transient's first 10 s - the 4% power spike observed in V6.1 Simulation 6 is gone.

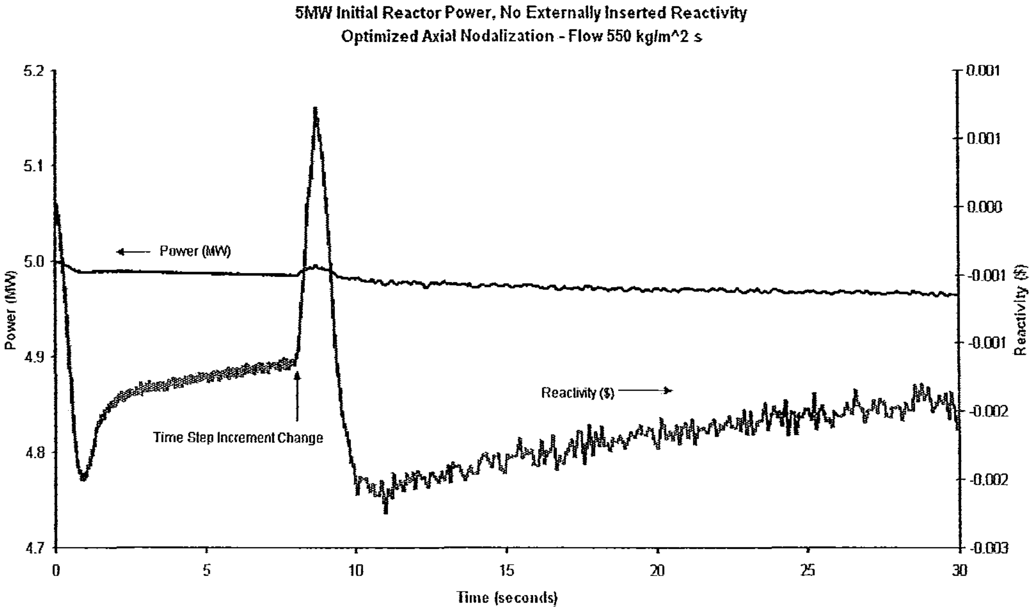

Figure 85. V7.4 Simulation 3 - Compare to V6.1 Simulation 9